

Post translational modification of Exo1 in *Saccharomyces cerevisiae*

Emily Elizabeth Barber Strong B.Sc. (Hons)

A thesis submitted for the degree of:

Doctor of Philosophy



May 2017

University of Sheffield

Department of Molecular Biology and Biotechnology

Post translational modification of Exo1 in *Saccharomyces cerevisiae*

Emily Elizabeth Barber Strong

Meiosis is the cell division that produces haploid gametes for the purpose of sexual reproduction. During this division it is essential for homologous chromosomes to be securely paired and segregated in order for the gametes to receive a single copy of each chromosome. An important protein in this process is the exonuclease Exo1.

Exo1 has two important and distinct roles during meiosis: resection of DNA at double-strand breaks (DSBs) exposing single stranded DNA suitable for strand invasion, and resolution of double-Holliday junctions (dHJs) as cross-overs. Exo1 also acts as a nuclease during DSB repair during mitosis. Previous studies have shown that Exo1 is phosphorylated in response to DNA damage in mitotically cycling cells. The role of this phosphorylation is yet to be definitively determined. This study aimed to test the hypothesis that Exo1 might also be phosphorylated in response to meiotic DSBs.

It was confirmed that Exo1 was phosphorylated in response to mitotic DNA damage by designing a tagged version of Exo1 in the *Saccharomyces cerevisiae* background SK1, a strain commonly used for meiotic experiments. Meiotic progression and spore viability appeared to be normal in cells with *exo1* mutated at the phosphorylation sites reported as active in mitosis.

In meiotic studies Exo1 was found to be phosphorylated during meiosis, and this phosphorylation was different to that seen in previous mitotic studies. It was found that this phosphorylation was transient during meiosis and that it reflected the presence of Spo11-DSBs and their repair.

Declaration

Declaration

Unless otherwise stated, the experimental data contained within this thesis are the result of the authors own research and have not been submitted for any other qualifications.

Signed: _____

Date: _____

Acknowledgements

A long and challenging PhD leaves me with an equally long list of people to thank:

A huge thanks to all of the Yeast Group here in Sheffield for your support, guidance and advice, especially when I wasn't even a member of your lab! Foremost I'd like to thank Alastair; through all of the struggles, academic and personal, you have provided unwavering support and guidance to get me through for which I will always be grateful. To Ta Chung and Tzu Ling, my first tutors in the lab, thank you for helping me find my feet and my smile when science wasn't going my way. Thank you to old members, Janet and the Adams, for passing on your wisdom, advice, and the highly sought after lucky lab chair. To Laura, for not being too angry when I ordered primer after primer right at the home bell, Bin for keeping me on track when I went off on a tangent, and to all members of E20; Yinka, Inam, Emad, Chris, Selina, Hassan and Julia, for making the lab a less lonely place. A special mention also to Niko, John, Simon and Jamie who have always made me welcome in their labs when I've needed help or advice, and Vicky who has looked after me more than I'd like to admit. I can only say I'd be nowhere without each of you.

Also thank you to all of my friends in the department, particularly Will Wood for never failing to make me laugh at lunch, Sam Barnett, my fellow explorer, James Morby for dragging me out of early morning labs for some well needed exercise and Amy Irvine for being a wonderful friend and outreach extraordinaire. To everyone from Hands on DNA and Atom Labs, thank you for reminding me why I love science, and why everyone else should too. Gus and Liam, thank you for taking me in as a homeless scientist. In particular, thank you to Claudine Bisson, for your immeasurable support both in and out of the lab, and for enjoying printing 3D nerdy things as much as me. Also to Hayley, Jason, Sam and Vic, who along with Claudine gave me games night, a reason to always make it to the end of the day and bring me back to Sheffield.

Acknowledgements

To all of my friends of the pre-PhD era, thank you for sticking by me when I've dropped off the radar and reminding me the world doesn't stop at the doors to Firth Court! To my new friends in medicine, thank you for making sure I was never alone too long, and giving me a light at the end of the tunnel. A special thanks to the wonderful Dan for all of the late night lifts, office picnics and armchair-psychology sessions. You've watched me go through every emotion during the last five years, and put me back together after many late night breakdowns. Your love and faith in me has kept me going, without it I wouldn't be where I am now.

Finally, to all my family near and far, for unwavering love and support, only ever being a phone call away and putting up with my impromptu dinner table lectures on science. If you all only read this far, I'll understand!

“To be confused is really a very exciting thing.”

“Science is the desire to remain confused.”

– Robin Ince & Brian Cox; *The Infinite Monkey Cage*

Abbreviations

AE	axial element
bp	base pair
BYTA	buffered yeast extract tryptone acetate
CE	central element
CTAB	hexadecyltrimethylammonium bromide
DAPI	4'6'-diamidino-2-phenylindoline
dH ₂ O	distilled deionised water
dHJ	double Holliday junction
DNA	deoxyribonucleic acid
dNTPs	deoxynucleotide triphosphates
DSB	double stranded break
DSBR	double strand break repair
DTT	dithiothreitol
EDTA	ethylenediaminetetraacetic acid
HJ	Holliday junction
HR	homologous recombination
hr	hour
HRP	horse radish peroxidase
IGEPAL	Octylphenoxypolyethoxyethanol
IP	Immuno precipitation
kb	kilobase
kDa	kiloDaltons
LB	lysogeny broth
LE	lateral element
LMP	low melting point (agarose)
MAT	mating type
mbar	millibar

min	minute
MI	meiosis I
MII	meiosis II
MMS	methylmethanesulphonate
mqH ₂ O	MilliQ™ filtered water
MRX	Mre11 – Rad50 – Xrs2 complex
MW	molecular weight
NHEJ	non-homologous end joining
NP40	nonylphenoxypolyethoxyethanol
OD _(wavelength)	optical density _(wavelength)
ORF	open reading frame
PCR	polymerase chain reaction
PFGE	pulsed-field gel electrophoresis
PEG	polyethylene glycol
PLB	protein loading buffer
PMSF	phenylmethylsulfonyl fluoride
PVP40	polyvinylpyrrolidone
RNA	ribonucleic acid
RNase	ribonuclease
RPA	replication protein A
rpm.	revolutions per minute
s	second
SC	synaptonemal complex
SC-	synthetic complete – (supplement) media
SCD	[Serine/threonine] glutamine cluster domain
SCE	sorbitol sodium citrate EDTA buffer
SDSA	synthesis-dependent strand annealing
SDS-PAGE	sodium dodecyl sulphate – polyacrylamide gel electrophoresis
SEI	single end invasion

SOC	super optimal broth with catabolite repression
SPHERO	sorbitol potassium phosphate EDTA buffer for spheroplasting
SPM	sporulation media
SSA	single strand annealing
SSB	single strand DNA break
ssDNA	single-stranded DNA
SSPE	sodium chloride-sodium hydrogen phosphate-EDTA buffer
TAE	tris-acetate-EDTA buffer
TBE	tris-borate-EDTA buffer
TBS	tris-buffered saline
TBS	tris-buffered saline plus TWEEN
TCA	trichloroacetic acid
TEMED	tetramethylethylenediamine
TF	transverse filament
TFB	transformation buffer
T _m	melting temperature of a primer
TWEEN20	sorbitan mono-9-octadecanoate poly(oxy-1,2-ethanediyl)
UV	ultra violet
VDE	<i>VMA1</i> -derived endonuclease
W/V	weight/volume
YPAD	yeast extract peptone dextrose with adenine
YPD	yeast extract peptone dextrose
YPG	yeast extract peptone glycerol

Nomenclature

Dominant genes are referred to in uppercase italics, e.g. *EXO1*.

Mutant genes are referred to in lowercase italics, e.g. *exo1-4S::E*.

Proteins are referred to in lowercase with the first letter capitalised in non-italics, e.g. Exo1.

Full Latin names of organisms are italicised e.g. *Saccharomyces cerevisiae*. Following the first use of the full Latin name, organisms are abbreviated to the first initial of their genus followed by their species, e.g. *S. cerevisiae*.

Contents

SUMMARY	I
DECLARATION	II
ACKNOWLEDGEMENTS	III
ABBREVIATIONS	VI
NOMENCLATURE	IX
CONTENTS	X
LIST OF FIGURES AND TABLES	XIV
1. INTRODUCTION	1
1.1 MEIOSIS	1
1.2 <i>S. CEREVISIAE</i> AS A MODEL ORGANISM	6
1.3 CHROMOSOME PAIRING AND SYNAPSIS	13
1.3.1 SISTER CHROMATID COHESION	14
1.3.2 HOMOLOGUE PAIRING	15
1.3.3 SYNAPSIS	20
1.4 MEIOTIC DOUBLE STRAND BREAK FORMATION AND PROCESSING	23
1.4.1 DSB SITE SELECTION	23
1.4.2 THE DSB FORMING COMPLEX	24
1.4.3 FORMATION AND EARLY PROCESSING OF DSBs	25
1.5 RECOMBINATION AND CROSSOVER FORMATION	29
1.5.1 REPAIR TO YIELD CROSSOVERS	32
<i>Recombinases</i>	33
<i>Template choice</i>	34
<i>Resolvases</i>	34
1.5.2 REPAIR TO YIELD NON-CROSSOVERS	35
<i>Synthesis-dependent strand annealing (SDSA)</i>	36
<i>Single-strand annealing (SSA)</i>	36
1.5.3 CONTROLLING GLOBAL DISTRIBUTION OF CROSSOVERS	37
<i>Recombination nodules</i>	37
<i>Crossover interference</i>	38
1.6 THE MEIOTIC CHECKPOINT NETWORK	39
1.7 EXO1 IN DETAIL	42
1.8 INITIAL AIMS OF THIS STUDY	46
2. MATERIALS & METHODS	47
2.1 MEDIA AND CHEMICALS	47
2.1.1 MEDIA	47
2.1.2 STOCK SOLUTIONS	51
2.2 MOLECULAR BIOLOGY TECHNIQUES	53
2.2.1 DNA RESTRICTION DIGESTS	53
2.2.2 DNA LIGATION	54
2.2.3 GIBSON ASSEMBLY	54
2.2.4 ETHANOL PRECIPITATION OF DNA	54
2.2.5 GEL PURIFICATION OF DNA	55
	X

2.2.6 POLYMERASE CHAIN REACTION (PCR)	55
2.2.7 PCR CLEAN-UP	56
2.2.8 COLONY PCR	57
2.2.9 SIMPLE EXTRACTION OF YEAST DNA	57
2.2.10 CTAB EXTRACTION OF YEAST DNA	58
2.2.11 MEASUREMENT OF DNA CONCENTRATION IN SOLUTION	60
2.2.12 NATIVE DNA GEL ELECTROPHORESIS	60
2.2.13 PULSED-FIELD GEL ELECTROPHORESIS	61
2.2.14 SOUTHERN BLOTTING	62
2.2.15 GENERATION OF ³² P-LABELLED PROBES	63
2.2.16 HYBRIDISATION OF PROBE TO MEMBRANE	63
2.2.17 SCANNING DENSITOMETRY	64
2.2.18 STRIPPING OF SOUTHERN BLOT FOR RE-PROBING	64
2.3 BIOCHEMISTRY TECHNIQUES	65
2.3.1 SOLUBLE PROTEIN EXTRACTION	65
2.3.2 TOTAL PROTEIN EXTRACTION	65
2.3.3 DETERMINATION OF PROTEIN CONCENTRATION	66
2.3.4 IMMUNOPRECIPITATION (IP) OF TARGET PROTEINS	66
2.3.5 PHOSPHATASE TREATMENT OF IMMUNO-PRECIPITATED PROTEIN	67
2.3.6 SDS-POLYACRYLAMIDE GEL ELECTROPHORESIS	67
2.3.7 WESTERN BLOTTING	68
2.3.8 IMMUNODETECTION OF BLOTTED PROTEINS	68
2.4 E. COLI TECHNIQUES	68
2.4.1 PRODUCTION OF DH5A CELLS CHEMICALLY COMPETENT FOR TRANSFORMATION	68
2.4.2 TRANSFORMATION OF CHEMICALLY COMPETENT <i>E. COLI</i> CELLS	69
2.4.3 SMALL-SCALE ISOLATION OF PLASMID DNA (MINIPREPS)	69
2.5 GROWTH AND CULTURE OF <i>S. CEREVISIAE</i>	70
2.5.1 GENERAL METHODS FOR PRODUCTION OF YEAST STRAINS WITH DESIRED PHENOTYPE	70
2.5.2 PRODUCTION OF SINGLE YEAST COLONIES	71
2.5.3 MATING OF HAPLOID YEAST COLONIES	71
2.5.4 CHECKING OF COLONY MATING TYPE & PLOIDY	72
2.5.5 STANDARD LIQUID CULTURES	72
2.5.6 STORAGE OF YEAST CLONES AT -80°C	72
2.5.7 CULTURE OF EXPONENTIALLY GROWING YEAST	73
2.5.8 LITHIUM-ACETATE HIGH EFFICIENCY TRANSFORMATION	73
2.5.9 BLEOMYCIN-INDUCED DNA DAMAGE OF CELLS	74
2.5.10 SPORULATION OF DIPLOID STRAINS (SOLID MEDIA)	74
2.5.11 TETRAD DISSECTION	74
2.5.12 SYNCHRONOUS SPORULATION OF <i>SACCHAROMYCES CEREVISIAE</i>	75
2.5.13 HARVESTING CELLS FOR DNA EXTRACTION	76
2.5.14 DAPI STAINING OF CELLS TO MONITOR NUCLEAR DIVISIONS	76
2.6 YEAST, PLASMIDS & PRIMERS	76
2.6.1 NOMENCLATURE OF DIPLOID STRAINS USED IN THIS STUDY	76
2.6.2 YEAST STRAINS USED IN THIS STUDY	77
2.6.3 PLASMIDS	77
2.6.4 PRIMERS	78

3. CHARACTERISATION OF EXOGENOUSLY EXPRESSED EXO1 MUTANTS	83
INTRODUCTION	83
RESULTS	84
3.1 HYGROMYCIN RESISTANCE MARKER INTEGRATION AFFECTS MEIOTIC PROGRESSION	84
3.2 SPORULATION DEFECT OF <i>EXO1Δ</i> IS PARTIALLY RESCUED BY TRANSFORMATION WITH EXO1 PLASMIDS	86
3.3 SPORE VIABILITY IS REDUCED IN <i>EXO1-4S::A</i>	88
3.4 DSB TURNOVER AT THE <i>ARE1</i> LOCUS IS NOT INFLUENCED BY THE EXO1 ALLELES TESTED	90
3.4.1 Redefining the base level of DSB turnover	90
3.4.2 DSB turnover in <i>Exo1</i> and phospho-mutants	91
3.5 CHROMOSOME-WIDE DSB TURNOVER MAY BE INFLUENCED BY EXO1 PHOSPHORYLATION	96
3.5.1 Analysis of DSB turnover for chromosome III in WT cells as a baseline	96
3.5.2 Analysis of DSB turnover for chromosome III in <i>exo1</i> mutant cells	98
DISCUSSION	100
4. CHARACTERISATION OF EXO1 PHOSPHORYLATION DURING MITOSIS	103
INTRODUCTION	103
RESULTS	104
4.1 TAGGING OF EXO1 FOR WESTERN BLOT ANALYSIS & INTEGRATION OF TAGGED EXO1 PHOSPHOMUTANTS	104
4.2 EXO1 AND <i>EXO1-4S::A-PK9</i> EXPRESSION IN MITOSIS CHANGES DURING THE RESPONSE TO BLEOMYCIN-INDUCED DNA DAMAGE	107
4.3 CONFIRMING EXO1 IS PHOSPHORYLATED IN RESPONSE TO BLEOMYCIN INDUCED-DNA DAMAGE	109
DISCUSSION	111
5. CHARACTERISATION OF EXO1 PHOSPHORYLATION DURING MEIOSIS	112
INTRODUCTION	112
RESULTS	113
5.1 EXO1 EXPRESSION VARIES THROUGH MEIOSIS	113
5.2 EXO1 IS PHOSPHORYLATED IN MEIOSIS	113
5.2.1 Analysis of <i>Exo1-PK9</i> extracted under denaturing conditions	113
5.2.2 Analysis of <i>Exo1-PK9</i> isolated under native conditions	117
5.3 EXO1 IS PHOSPHORYLATED DIFFERENTLY IN MEIOSIS THAN IN MITOSIS	119
5.3.1 Analysis of <i>Exo1-4S::A-PK9</i> extracted under denaturing conditions	119
5.3.2 Analysis of <i>Exo1-4S::A-PK9</i> isolated under native conditions	121
5.4 EXO1 PHOSPHORYLATION IS DEPENDENT UPON SPO11 NUCLEASE ACTIVITY	123
5.5 EXO1 IS PHOSPHORYLATED PRIOR TO STRAND INVASION	123
5.6 MEIOSIS IS NOT AFFECTED BY AN INABILITY TO PHOSPHORYLATE MITOTICALLY SIGNIFICANT RESIDUES	125
5.6.1 Spore viability is not altered by the inability of <i>Exo1</i> to be phosphorylated in a mitotic pattern	127
5.6.2 Meiotic progression is not affected by the inability of <i>Exo1</i> to be phosphorylated in a mitotic pattern	127
5.6.3 DSB turnover at <i>ARE1</i> is not significantly impacted by the inability of <i>Exo1</i> to be phosphorylated in a mitotic pattern	130
DISCUSSION	132

6. GENERAL DISCUSSION & FUTURE DIRECTIONS	136
GENERAL DISCUSSION	136
6.1 EXOGENOUS EXPRESSION OF EXO1 AND PUTATIVE PHOSPHOMUTANTS WAS NOT SUCCESSFUL FOR THE INVESTIGATION OF MEIOTIC EFFECTS	137
6.2 EXO1 IS PHOSPHORYLATED DURING MITOSIS IN THE SK1 BACKGROUND IN RESPONSE TO BLEOMYCIN-INDUCED DSB FORMATION	139
6.3 EXO1 IS PHOSPHORYLATED DURING MEIOSIS IN RESPONSE TO DSB FORMATION	139
FUTURE DIRECTIONS	142
CONCLUDING REMARKS	143
7. REFERENCES	144

List of Figures and Tables

FIGURES	<i>page</i>
FIGURE 1.1	2
FIGURE 1.2	9
FIGURE 1.3	11
FIGURE 1.4	12
FIGURE 1.5	21
FIGURE 1.6	27
FIGURE 1.7	30
FIGURE 1.8	43 & 44
FIGURE 3.1	85
FIGURE 3.2	87
FIGURE 3.3	89
FIGURE 3.4	92
FIGURE 3.5	94
FIGURE 3.6	95
FIGURE 3.7	97
FIGURE 3.8	99
FIGURE 4.1	105
FIGURE 4.2	107
FIGURE 4.3	110
FIGURE 5.1	114
FIGURE 5.2	115
FIGURE 5.3	118
FIGURE 5.4	120

List of figures and tables

FIGURE 5.5	122
FIGURE 5.6	124
FIGURE 5.7	126
FIGURE 5.8	128
FIGURE 5.9	129
FIGURE 5.10	131

TABLES	<i>page</i>
TABLE 1.1	40
TABLE 2.1	49
TABLE 2.2	52
TABLE 2.3	78
TABLE 2.4	79
TABLE 2.5	81
TABLE 2.6	81
TABLE 2.7	82

1. Introduction

1.1 Meiosis

Living organisms can be defined by their ability to grow, divide, and self-regulate in response to their environment, making them distinct from any other collection of molecules or organic material. They can be classified into three domains based on their cellular features; archaea - the most ancient organisms, eubacteria - true bacterial cells, and eukarya - the most recently evolved domain including fungi, plants and animals. From unicellular life forms to complex multicellular organisms, the tools for reproduction are highly conserved, indicating that this ability is key to survival success.

Cellular proliferation entails the replication of genetic information and subsequent division of this information, as well as cellular machinery and structural components. Eukaryotic cells, though varied in their form and function, can reproduce in two ways: mitosis or meiosis. Mitotic division, a form of asexual reproduction, consists of a single round of replication and division to yield two genetically identical offspring from a single parent cell. In contrast, meiosis is more time and resource-intensive, eventually producing four genetically distinct daughter cells each with half the amount of genetic information of the parent cell (Figure 1.1).

Eukaryotic cells contain nuclei, which house their genetic information on chromosomes. The total number of chromosomes in a set can vary between organisms. The number of complete sets of chromosomes is referred to as *ploidy*. A single set of chromosomes can be referred to as monoploid, two sets diploid, three sets triploid, and so on. Humans have 23 distinct chromosomes, carrying two versions (homologues) of each in somatic cells to give an overall total of 46, and so are described as diploid. Occasionally a cell may have an extra copy of one

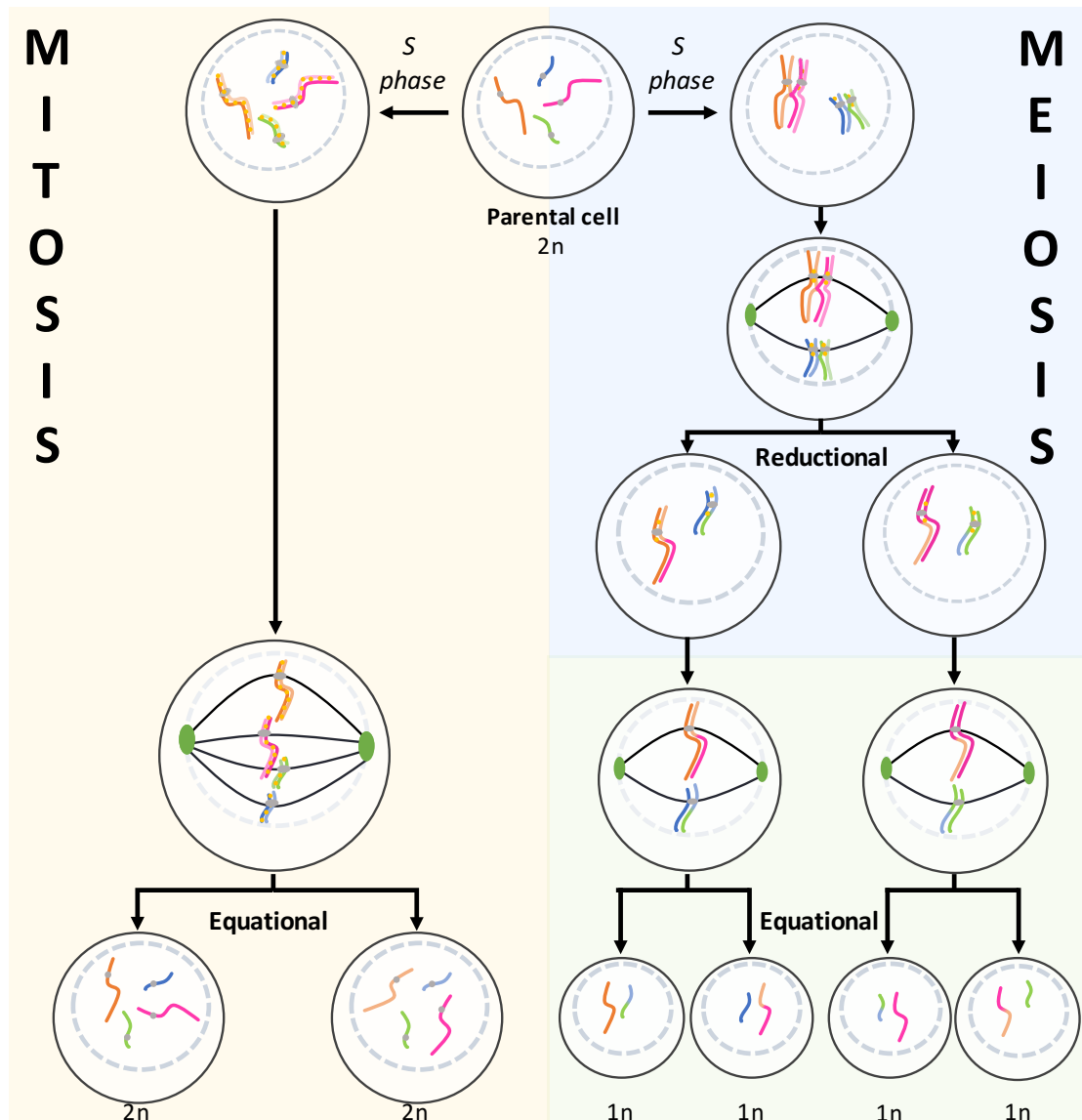


Figure 1.1 - Chromosome segregation in mitosis and meiosis

S-phase generates identical sister chromatids, associated through sister chromatid cohesion (yellow dots between sisters). In mitosis (left), sisters are associated along their length, and align along the equator during metaphase. In anaphase sister chromatids separate in an equational division, and two distinct new cells are formed. The products of mitosis are genetically identical to the parent cell and to one another. Meiosis (right) consists of two divisions instead of one, known as MI and MII. In MI, following meiotic S phase, homologues synapse. Sister chromatid cohesion is selectively degraded along the arms and crossovers are formed between homologues. Homologues align along the equator during metaphase I in the first meiotic division, and then divide. MI is reductional, as the number of distinct chromosomes is halved. Following MI, segregated homologues line up along the equator during metaphase II. Sister chromatid cohesion is degraded, and sisters separate in an equational MII division, similar to the division of mitosis.

or several chromosomes, or one or several chromosomes missing; the general term for this is aneuploidy.

Mitotic division maintains the ploidy status of the parent cell, whilst meiotic division halves the total number of chromosome sets (Figure 1.1). Therefore, the offspring of a meiotic division may be referred to as *haploid*, relative to the progenitor cell, rather than the absolute number of chromosome sets. Human gametes are haploid, containing a single set of 23 chromosomes. The ascomycete *Saccharomyces cerevisiae* (also known as brewer's yeast) has a set of 16 chromosomes and can exist as a diploid or haploid. Various other eukarya, particularly plants, can exist at higher levels of polyploidy, some with chromosome sets of over many hundreds (Faseena & Thoppil 2007).

Meiosis describes the process by which all sexually reproducing organisms produce haploid gametes, also known as germ cells. In mammals these haploid cells are spermatozoa or oocytes, in flowering plants pollen and ovules, or in fungi spores. By halving the number of chromosomes in this way these organisms ensure that, following fertilisation, offspring reconstitute a full diploid complement of chromosomes; half from the maternal cell line and half from the paternal. The process of meiotic division and subsequent fertilisation introduces genetic variation into offspring, potentially conferring advantage and increased fitness for survival in an unpredictable environment. This process continues through generations and introduces great variability within populations. In simple eukaryotes these haploid cells can proliferate mitotically, whereas higher eukaryotes such as plants and animals produce gametes specialised for sexual fusion. The ability of an organism to undergo meiosis and produce gametes capable of fusing to become a zygote usually requires the organism to exist as reciprocal genders. In humans and other higher eukaryotes this may be classified as male or female, or in the case of the unicellular *S. cerevisiae*, the opposite mating types a or α (Lindegren & Lindegren 1943).

Meiosis is not a proliferative form of cell replication, and is not considered a part of the cell-cycle like mitosis. However, much of the machinery for mitosis is employed in meiotic division, and the second of the two meiotic divisions closely

resembles a mitotic division. The first division of meiosis utilises various specialised mechanisms, important for the separation of homologues.

Prior to division, both processes begin with a round of synthesis (S-phase) where each chromosome is replicated. The duplicates are paired together and referred to as sister chromosomes, in contrast to the original two different versions of each chromosome referred to as homologues. In mitosis the sisters are then separated, so that each daughter cell contains a single copy of each homologue pair. In meiosis however, the homologues are secured together by crossover formation, and two distinct divisions succeed S-phase. The first (meiosis I or MI) is referred to as a reductional division, as the overall chromosome number is halved. In this division the secured homologue pairs are segregated, while the sisters remain paired together. Through this division and the dissolution of the crossovers holding homologues together, sections of chromosomes are exchanged between the homologues, creating new combinations of genes on each homologue. The next division (meiosis II or MII) is more similar to that of mitosis and is referred to as an equational division. The sisters are separated, and the process yields four gametes, each genetically distinct from one another. The proper segregation of homologues and sisters at each stage is essential to maintaining the proper ploidy and genetic integrity of the gametes. Should homologues or sisters fail to pair correctly, they cannot be located on the metaphase plate and separated from one another effectively. This can result in the placement of homologues or sisters into the same gamete, causing aneuploidy. Failure to segregate sufficiently is referred to as non-disjunction. Should this occur during MI, resulting in failed segregation of homologues, we refer to it as an MI non-disjunction. Failed segregation of sisters in MII is referred to as MII non-disjunction.

In unicellular organisms aneuploidy may occasionally be tolerated, such as in a diploid *S. cerevisiae* lacking one homologue of a pair (a monosomic diploid) or a haploid with two copies of a homologue (a disomic haploid). Higher organisms however are less able to tolerate aneuploidy. Very few aneuploidies can produce viable offspring in humans. Monosomy of any autosomal chromosome is inviable, except in instances comprising only partial loss such as Cri-du-chat syndrome

(loss of the short arm of chromosome 5). Trisomy of partial and whole chromosomes can be tolerated, but confers life-long learning and physical disabilities, bringing with them a consideration of social, emotional and economical costs. Down's syndrome (chromosome 21), Edwards syndrome (chromosome 18), and Patau syndrome (chromosome 13) each encompass the collection of symptoms associated with each autosomal trisomy. Sex chromosome aneuploidy may also be tolerated, as seen in Turner's syndrome (XO), Klinefelter syndrome (XXY), and Triple X syndrome (XXX). The severe developmental abnormalities seen in these syndromes, and the complete inviability of most aneuploidies, impress the importance of proper chromosome segregation in meiosis. Constitutional failure to control segregation in meiosis would rapidly lead to species extinction, and so tight regulation of this process has been evolutionarily conserved.

Chromosomes were first observed by light microscopy in 1842 by Karl Wilhelm von Nägeli, and their role in heredity described by Theodor Boveri and Walter Sutton at the turn of the twentieth century. Sutton was also the first to suggest chromosomes exist in pairs of maternal and paternal origin, and observed their separation during meiosis (Sutton 1903). Despite sufficient cellular microscopy and staining techniques, it was not until 1956 that Tjio and Levan determined the number of human chromosomes to be 46 (Tjio & Levan 1956), and following this the first aneuploidies were quickly discovered. The ground-breaking development of chromosome G and Q banding in 1969, as well as the earlier invention of the electron microscope, facilitated observation of chromosome movements, interactions (synapsis) (Fawcett 1956) and exchange of material between chromosomes (recombination) (Carpenter 1975). The field of molecular biology began to emerge throughout the 1950's, and by the 1970's the development of various new analytical techniques added new tools to the arsenal for the study of meiotic processes. Molecular probes facilitated a deeper understanding of the role of chromosome substructure in meiosis (Rockmill & Roeder 1998) and protein localisation (Wassarman & Fujiwara 1978). Methods for detecting protein::DNA interactions, known as chromatin immuno-precipitation or ChIP were established (Gilmour & Lis 1984). Tools for the manipulation of DNA such as restriction

enzymes, and the advent of PCR, led to the ability to engineer reporter cassettes for loci involved in meiosis (Keeney & Kleckner 1995). These methods introduced us to the molecular processes at work during meiotic recombination.

Whole genome sequencing has arguably provided the greatest development in the field of molecular genetics, and the genome of *S. cerevisiae* was the first eukaryotic genome to be sequenced (Goffeau et al. 1996). Multicellular organisms soon followed (Consortium 1998) and as the number of genomes sequenced rose, so too did the applications available. New technologies such as microarrays for genome-wide expression studies (Lashkari et al. 1997) facilitated the discovery of genes necessary for meiosis (Primig et al. 2000) (Rabitsch et al. 2001). Established methods such as ChIP combined with new micro-array technology benefited the field of meiotic study enormously, allowing investigations into protein::DNA associations, both temporally and spatially, by ChIP on chip analysis (Glynn et al. 2004)(Prieler et al. 2005). As the number of organisms whose genomes were sequenced has increased, it has become apparent that many proteins active in meiosis share homologues across species. Given that all organisms undertaking sexual reproduction divide in a way recognisable as meiosis, this is a logical finding, and one supportive of the use of model organisms during our continued efforts to understand meiosis.

1.2 *S. cerevisiae* as a model organism

Saccharomyces cerevisiae is a yeast of the phylum ascomycota, literally meaning sac (*ascos* – Greek) fungi (*-mycete*), as it is a spore-forming member of the fungi kingdom. Its genus and species name, “sugar-fungus beer” in Latinised-Greek, refers to the yeast’s ability to ferment sugars into alcohol under anaerobic conditions. *S. cerevisiae* exists in the wild on the surfaces of ripe fruits such as grapes and plums, and can be transmitted between fruit in the digestive tracts of social wasp species who provide an ideal environment for yeast mating and sporulation (Stefanini et al. 2015). For over 7000 years *S. cerevisiae* has been used for the making of wine (McGovern et al. 1996), beer (Meussdoerffer 2009), and bread, but it was only relatively recently that it was identified and domesticated as a model organism for use in scientific research (Pasteur 1872).

Model organisms are used in science in place of the organism of interest to overcome ethical and practical constraints associated with the target life-form, while remaining representative of the target and allowing the development of practical methods and analysis. As a small (5-10 μ m) unicellular organism that forms unordered spore asci, *S. cerevisiae* could not be fully exploited as a model organism for genetic research until the mid 20th century, and the rise of molecular biology. By the end of the twentieth century, the genome of *S. cerevisiae* was well characterised (Carle & Olson 1985) and sequenced (Goffeau et al. 1996).

Many qualities of *S. cerevisiae* make it an excellent model organism. It has a very short generation time; one cell cycle lasts around 90 minutes depending on the strain. This facilitates quick turnaround of generations, particularly for an organism in meiotic study. Yeast culturing is also relatively easy and inexpensive when compared to other meiotic model organisms, and as a unicellular organism it is innately easier to manipulate in terms of its genetics and expression. Many molecular tools exist for the efficient manipulation of yeast, giving researchers a set of reliable and useful methods for experimenting. This makes yeast an ideal candidate not only for primary research, but also as a screening tool for testing hypotheses before carrying out more complex experiments in higher eukaryotes (Karathia et al. 2011). The study of *S. cerevisiae* has led to the discovery of many of the genes involved in yeast and higher eukaryote meiosis, as well as furthered our overall understanding of the process. Many proteins involved in yeast meiosis have functional homologues in humans (Hochwagen & Amon 2006; Mimitou & Symington 2009), and some of those involved in the control double strand break formation and repair are listed in Table 1.1.

Saccharomyces cerevisiae exists as many genetically distinct strains (Schacherer et al. 2007). While maintaining many of the overall characteristics of the species, each strain has different alleles giving a slightly different background to the next, offering characteristics suitable to different types of experiment (Louis 2016). The most commonly used and first to be sequenced was S288C (Mortimer & Johnston 1986), a strain isolated in the 1960's, and the first isogenic strain available as either *a* or α mating type. S288C was selected to be non-flocculent (not clumping

in liquid culture) with minimal nutrient requirements. However this strain also showed limited sporulation efficiency (Deutschbauer & Davis 2005) and poor growth on some carbohydrate sources (Charron et al. 1986), restricting its relevance in certain fields. Another strain commonly used is W303, a strain with 85% genome sequence similarity to S288C, but differing in several key aspects of cell growth and maintenance (Ralser et al. 2012). Both S288C and W303 are commonly used in cell-cycle and other research of vegetatively growing cells.

The strain most commonly used for meiotic study is SK1 (Kane & Roth 1974). This strain shows substantial West African ancestry, with only distant genetic relatedness to S288C and W303 (Schacherer et al. 2007). SK1 is prone to more efficient and synchronous sporulation than S288C or W303, thanks to altered transcription regulation and better adaptation to a respiratory lifestyle (Deutschbauer & Davis 2005; Ben-Ari et al. 2006; Williams et al. 2002). This not only makes it easier to work with during meiosis from an experimental perspective, but may also enable clearer investigation of temporally distinct events during meiotic progression (Primig et al. 2000). While working with SK1 it is important to maintain these traits, in particular the strong respiratory component, as meiosis is a highly energy-dependent process. This can be achieved by selection on a non-fermentable carbon source such as glycerol.

As an established model organism, *S. cerevisiae* has pioneered much of our understanding of growth and cell cycle processes. Yeast grows optimally at 30°C with good aeration in a rich medium containing glucose as a carbon source, yeast extract and bactopectone to provide amino acids, and salts that supply nitrogen, phosphorus and trace metals. The cells will readily grow and divide mitotically as haploids or diploids (Figure 1.2). The cell cycle can be divided into several discrete events. An initial growth phase (G1) prepares the cell for the upcoming synthesis phase (S) in which the DNA is replicated. A second growth phase (G2) precedes mitosis (M) and cellular division during which the earlier prepared genetic material and cellular machinery are divided between the parent and daughter cell. The new cell physically dissociates from the parent by forming a bud that is pinched off. Entry into and progression of each stage is tightly controlled by many

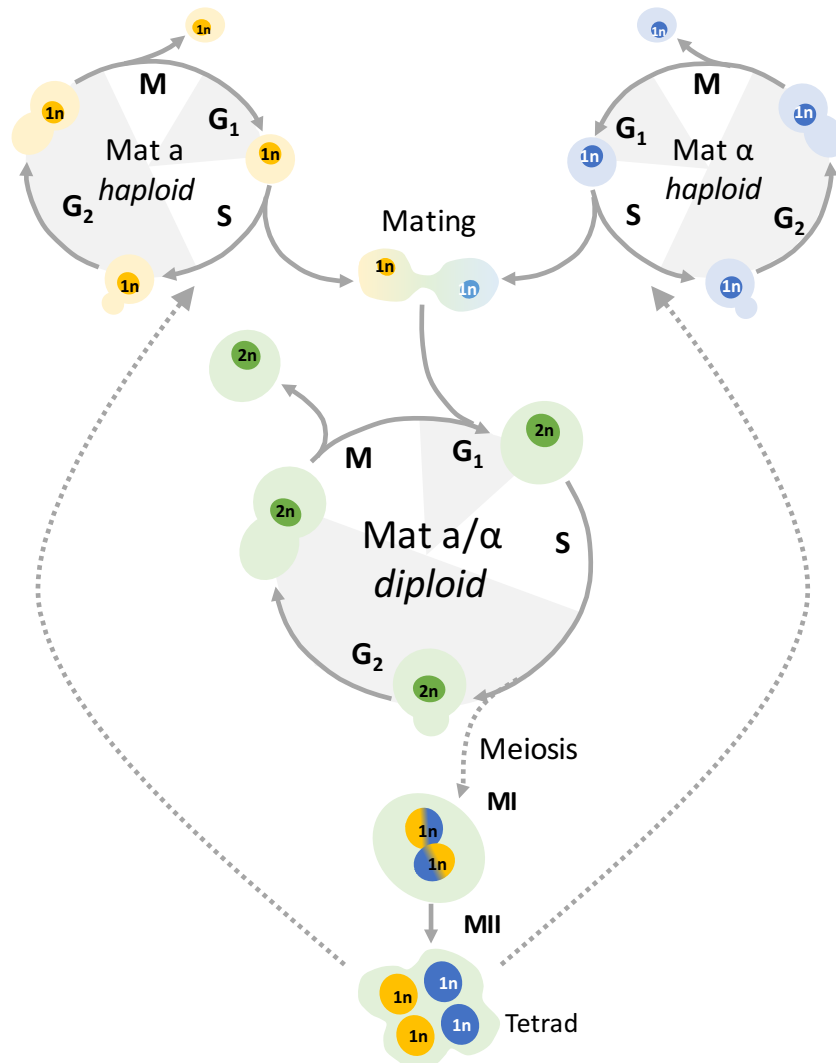


Figure 1.2 - The budding yeast life cycle

Yeast cells can grow mitotically as haploids or diploids. Two haploids of opposite mating type (a and α) can mate to form a zygote, and then a diploid cell. Diploids may undergo meiosis and sporulation to form four genetically distinct daughter cells that may either be mating type a or α. Tetrads may germinate spontaneously or following dissection, and will grow as haploid cells, completing the cycle.

check point proteins, responsible for monitoring the extracellular environment as well as the intracellular processes. The entire cycle usually lasts around 90 minutes. However, if starved of carbon and nitrogen sources diploid cells will readily undergo meiosis to form four genetically distinct haploid spores. Spores are determined to be viable if they can germinate and produce a colony when grown on a rich medium. Should a small molecule or mutation cause a breakdown of the normal processes contributing to the formation of balanced gametes, it is likely that one or more meiotic products of a tetrad will not be able to germinate. This is because the majority of non-disjunction events will lead to aneuploidies, most of which are lethal. Examining the pattern of viability allows the study of how variables impact upon meiosis (Figure 1.3).

DNA synthesis is an energy-intensive process and would oblige the cell to subsequently undertake mitosis, also relying further on environmental resources. Therefore, during G1 the cell must monitor its environment for nutrient availability before it commits to S-phase. Starvation conditions (the absence of glucose and a nitrogen source in the presence of a non-fermentable carbon source) trigger the activity of various transcription regulators (Smith & Mitchell 1989) so that S-phase is instead entered in to in a meiosis-specific manner. The machinery involved in pre-meiotic S-phase is the same as in the usual cell cycle, however the duration is two to three times longer (Williamson et al. 1983), possibly to allow for the more complex organisation of chromosomes necessary for meiosis (section 1.3.2). Recombination and the two divisions of meiosis follow S-phase, and a membrane forms separating the four nuclei (Figure 1.4 (i)).

Both meiotic divisions and the single mitotic division consist of 5 stages; interphase, prophase, metaphase, anaphase and telophase. These describe the cytological features associated with each phase (Figure 1.4 (ii)). While mitosis progresses through each stage once in a linear fashion, meiosis cycles through the five stages twice, the first cycle comprising MI and the second, MII. In *S. cerevisiae* the stages of meiosis are usually completed in one continuous process over a time period of 8-10 hours, unless check point activation causes arrest. In humans however, the timing of events is different. Human oocytes arrest normally during

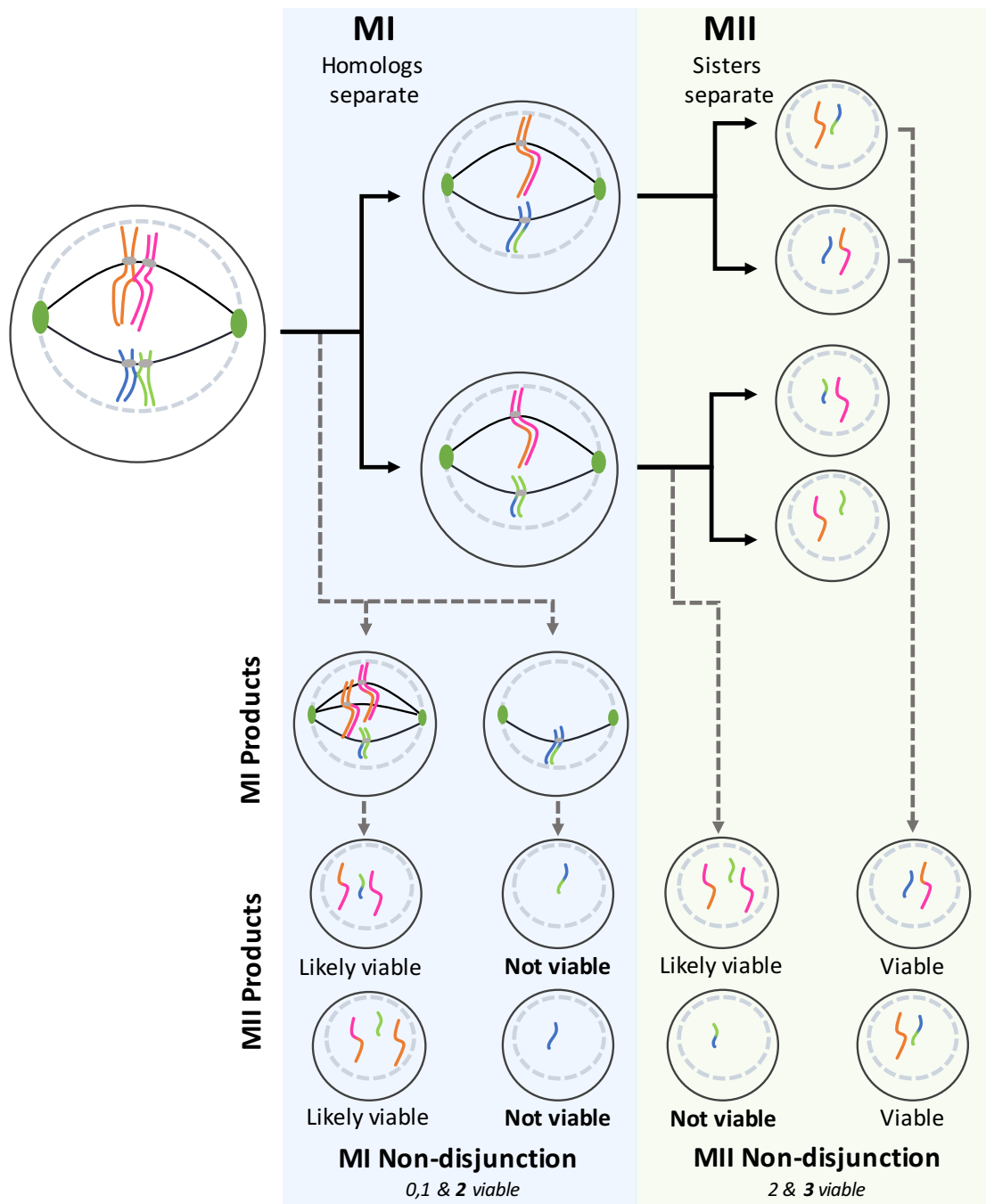


Figure 1.3 - Examples of non-disjunction leading to spore viability patterns

Following DNA replication and crossing over, homologues are separated in MI and sisters in MII. If a pair of homologues do not separate properly during MI then this will lead to all meiotic products being imbalanced; two products ultimately gain a sister and two lose a sister. Usually *S. cerevisiae* can tolerate an extra copy of a chromosome, but a loss is lethal. If a pair of sisters do not separate properly during MII then this will lead to two meiotic products being imbalanced, one product will gain a sister and the other lose a sister. The other two products would be unaffected. Multiple non-disjunctions can happen across different chromosomes, and so the above scenarios represent the likely viability with respect to an individual chromosome.

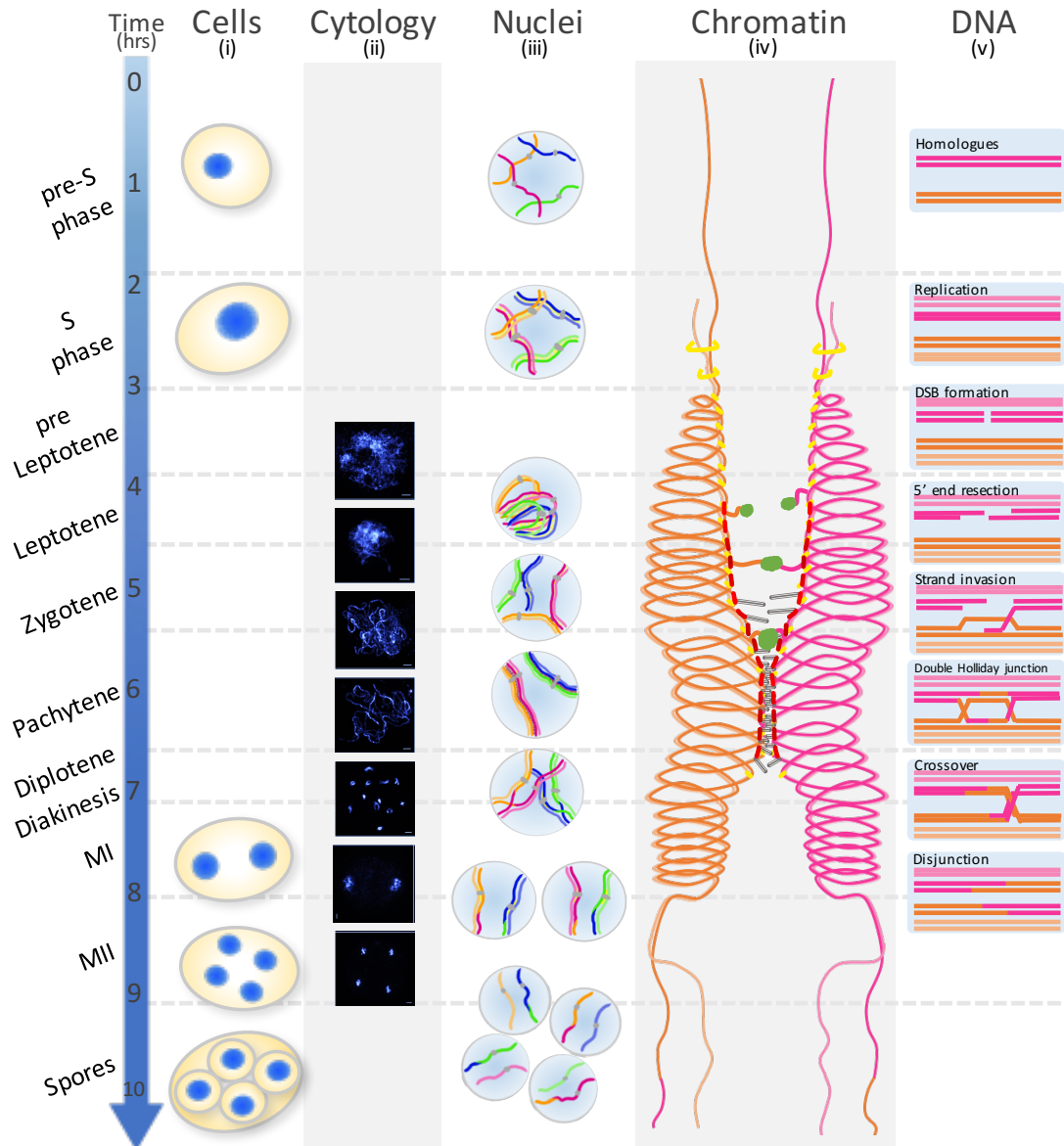


Figure 1.4 - Cellular features through meiosis

Changes in cellular morphology, chromosome organization, and DNA processing are illustrated through time.

- (i) During meiosis cells progress from mononucleate to binucleate, and finally tetranucleate.
- (ii) DAPI stained nuclear spreads of rice nuclei (*Oryza sativa*) illustrate the cytological changes.
- (iii) The chromosomal organization of two homologous pairs within the nucleus is shown schematically; following replication at S-phase, homologues transiently arrange in the bouquet formation before making early associations at regions of homology where synapsis is then initiated during zygotene. In pachytene the SC secures homologues before it disassembles, leaving chiasmata. The reductional division of MI is followed by the equational division of MII.
- (iv) During S-phase the DNA replicates and sister chromatids (orange and pale orange/pink and pale pink) are secured together by cohesin (yellow). The chromosomes begin to undergo compaction prior to leptotene, and lateral elements (red) assemble along the axis. Recombination nodules (green) begin to appear, and become established during zygotene. At this time the SC is formed between homologues by transverse filaments and central elements (grey) including Zip1. Following recombination, the SC is degraded and homologues dissociate ready for segregation. MI is followed by MII yielding chromosomes which may have exchanged genetic material during recombination.
- (v) DNA is shown at the molecular level. Replicated homologues (pink and orange) undergo DSB formation and 5' end resection of the pink homologue during leptotene. Strand invasion follows during zygotene and upon finding homology, a dHJ is formed. This may be resolved as a crossover to yield a chiasmata and following disjunction will result in reciprocal exchange of material between homologues.

(Own figure; drawn using Agarwal & Roeder 2000; Wang et al. 2009; Subramanian & Hochwagen 2015)

diplotene of prophase I while the female is still a foetus, until ovulation many years later stimulates further progression. The oocyte then continues until a second programmed arrest at metaphase II, and can only be triggered to complete MII in the event of fertilisation by a spermatozoon. Spermatocytes undergo the steps of MI and MII in a continuous manner, arresting prior to complete cytokinesis in telophase II to allow for synchronous maturation of the spermatozoa. The formation of spermatozoa takes roughly two months, while oogenesis can take several decades. This long period of arrest in oocytes increases the risk of non-disjunction of chromosomes. As women age, the stability of this arrested state is more likely to become compromised, accounting for the increased incidence of aneuploid offspring conceived by mothers over 35 years of age. *S. cerevisiae* mutants that are compromised at various stages of meiosis allow us to extrapolate the processes that may lead to failed meiosis in higher eukaryotes.

1.3 Chromosome pairing and synapsis

To halve the ploidy of diploid cells, meiosis relies on several key events.

1. During meiotic prophase I pairs of homologous chromosomes must complete recombination to yield crossovers, also known as chiasmata, securing homologues together.
2. Sister chromatids must each attach to opposite spindle pole bodies, so that they are segregated to each pole independently.
3. The interaction between sisters, known as cohesion, must be selectively degraded, to only leave centromeric areas associated.
4. S-phase must be suppressed between MI and MII to ensure the process is reductive.

Each of the pathways required for these steps is tightly controlled during meiosis, and the foundations for the first three measures are established in the way sisters and homologues interact with one another. Cells have established surveillance mechanisms to ensure each happens at the right time in the correct manner (section 1.6).

Entry into meiosis is suppressed in vegetatively growing cells, and can only be

normally induced in diploid cells. In diploid *S. cerevisiae* this process is induced by starvation. Entry into meiosis requires the transcription of genes regulated by Ime1 (initiator of meiosis) (Mitchell et al. 1990), a protein whose own expression is suppressed in haploid cells by the activity of Rme1 (repressor of meiosis) (Covitz et al. 1991). In diploid cells Rme1 is inhibited by the *MATa1* and *MATa2* gene products, allowing Ime1 to induce expression of early meiotic genes via interaction with Ume6 under starvation conditions (Rubin-Bejerano et al. 1996). The initiation of S-phase is differentially controlled in meiosis and mitosis, each requiring a different set of proteins, ensuring that entry to either is mutually exclusive.

1.3.1 Sister chromatid cohesion

Meiotic S-phase is up to three times longer than that of mitosis (Holm 1977). This lengthiness is hypothesised to support the development of inter-sister associations, called sister chromatid cohesion, that are sufficient for the more complex inter-homologue interactions required later on (Burgess et al. 1999) (Panizza et al. 2011). The machinery of replication is thought to likely be the same in both meiosis and mitosis, however the origins of replication chosen may vary in order to influence DSB formation (Wu & Nurse 2014).

Sister chromatid cohesion comprises a protein complex called cohesin, which loads on to the DNA in S-phase before replication and secures the newly synthesised sisters together. This structure ensures the sisters remain paired, and provides the tension and resistance necessary for spindle pole attachment. Key components of cohesin are Smc1 & 3 (structural maintenance of chromosome proteins) and a “kleisin” (Greek for closure) subunit Scc1 (Michaelis et al. 1997), which together form a ring that embraces the two sister DNA strands (Haering et al. 2002; Farcas et al. 2011). During early mitosis cohesin is protected by the protein securin (Pds1). Securin is an inhibitory chaperone of separase (Esp1), a proteolytic enzyme responsible for the cleavage of Scc1 (Cohen-Fix et al. 1996). Once microtubules are attached to sister kinetochores during metaphase the inhibition by securin is lifted, and cohesin is degraded in order to initiate

anaphase (Figure 1.4 (iv)).

In meiosis the role of Scc1 is carried out by the functionally analogous kleisin protein Rec8 (Klein et al. 1999). Cohesin is selectively maintained through meiosis until metaphase II, and the nature of this persistence is integral to ensuring proper segregation of sister chromatids during MII. While cohesin cleavage during meiosis is still via the activity of separase (Buonomo et al. 2000), the cleavage is carried out at two distinct stages (Salah & Nasmyth 2002). This complex stepwise degradation is a compromise; during MI it is important for cohesin to be degraded at the chromosome arms in order for chiasmata to resolve for homologue disjunction, while centromeric cohesin must persist until MII to maintain the stable association of sisters. This is achieved by localised inhibition of Rec8 processing. In MI Rec8 is targeted for separase degradation by phosphorylation (Brar et al. 2006), but centromeric Rec8 is protected from this by shugoshin (Sgo1) and so resists cleavage (Kiburz et al. 2005; Kitajima et al. 2006). The remainder is later cleaved by separase for anaphase II progression.

The attachment of microtubules, extending from the spindle pole bodies to the kinetochores, triggers the breakdown of cohesin. During mitotic metaphase each sister kinetochore associates with an opposing microtubule, known as bi-orientation, in preparation for an equational division. For meiosis to be reductional, sisters must first be segregated to the same pole during MI. This is achieved through preference toward mono-orientation of paired sister kinetochores, via the activity of a protein complex called monopolin (Toth et al. 2000; Petronczki et al. 2006) and the activity of Spo13 (Lee et al. 2002; Shonn et al. 2002; Katis et al. 2004). Spo13 is also active in maintaining centromeric cohesion during MI and is a member of the Meikin family of proteins involved in meiotic kinetochore maintenance (Kim et al. 2014). The later MII division is equational and resembles mitosis, assembling bi-oriented microtubules (figure 1.1).

1.3.2 Homologue pairing

After replication and the establishment of secure sister chromatid cohesion,

chromosomes must compact in order to be more manageable. To do this the DNA must transform from globular threads seen at the end of S-phase, into arrays of linear, elongated loops, without becoming crosslinked and entangled. This organisation is completed in the leptotene stage of prophase I. The functional unit of this process is condensin, a protein complex made up in *S. cerevisiae* of two Smc family proteins, Smc2 and Smc4, and non-Smc family proteins Brn1, Ycg1 and Ycs4 (Freeman et al. 2000). Condensins partake in a hypothesised process called loop extrusion (Nasmyth 2001). In this model, condensin complexes bind adjacently to one another on DNA and proceed to slide along the strand in opposing directions (Goloborodko et al. 2016). This causes the DNA to loop out behind the complexes as they slide, remaining coupled. Intermittent association of condensins along the chromosome at designated regions (Wang et al. 2005) creates an array of similarly sized consecutive loops. The bases of the loops, where condensins reside, accumulate along a central linear core with the loops radiating outward in a bottle brush configuration (Paulson & Laemmli 1977; Marko & Siggia 1997; Goloborodko et al. 2016). The yeast condensin, condensin I, is conserved throughout many eukarya, and has been shown to have a role in meiosis in several organisms. In mitosis cohesin and condensin assembly are followed by spindle attachment and anaphase progression. The role of condensin in meiosis is still not fully understood, and study is complicated by the existence of a second condensin, condensin II, in higher eukaryotes. Meiotic condensin I is thought to play a part in establishing synapsis between homologues, proper processing of double strand breaks, and proper orientation of sister chromatids on the MI spindle (Yu & Koshland 2003; Viera et al. 2007; Li et al. 2014; Brito et al. 2010).

For homologues to identify one another they must be brought into relative proximity, and organisms have developed various strategies to manage this process. Though the mechanisms and functional players vary, the general principles remain the same; (1) tentative coupling, mediated by centromeres, (2) genome tethering, mediated by telomeres and the nuclear envelope, and (3) chromosome movement within the nucleus, mediated by the cytoskeleton. This pattern can be observed in budding yeast, fission yeast, maize and mice, while two of the three steps are also seen in *C. elegans* and *D. melanogaster* (Klutstein &

Cooper 2014). The organisation of chromosomes in the nucleus is a dynamic and active process, and the movements involved can be mediated by the chromosomal architecture (autonomous) or be driven by the rest of the cell (non-autonomous) (Cowan et al. 2001). Autonomous behaviour is seen when chromosomes compact or centromeres associate, while non-autonomous behaviour would be telomere tethering and rapid movements orchestrated by microtubules extended from spindle pole bodies.

Tentative coupling, the first step in meiotic pairing, relies on the interactions of centromeres. During prophase I there are two kinds of centromeric associations; initial centromere *coupling* (between non-homologous chromosomes) in early prophase, and centromere *pairing* (between homologues) in late prophase (Obeso et al. 2014). Centromere coupling between non homologous chromosomes is dependent on Zip1, a component of the synaptonemal complex (SC) (section 1.3.3) (Tsubouchi & Roeder 2005) and its interaction with axis protein Rec8 (section (Bardhan et al. 2010)). Coupling is not universally conserved within meiosis or essential to later pairing (Falk et al. 2010), and so far its purpose remains a mystery. It has been proposed that perhaps couples repeatedly pair and dissociate to allow homology assessment of chromosome arms before establishing stable pairing, or else that random coupling helps to repress recombination at homologous centromeres. Coupling persists until the repair of DSBs is initiated, at which stage centromeres appear to quickly switch to homologous pairing (Falk et al. 2010). This switch is dependent on Spo11 (Obeso & Dawson 2010). Centromere pairing of homologues appears to be conserved, and is sufficient for disjunction of achiasmatic chromosomes (those that did not recombine) (Guacci & Kaback 1991). Again Zip1, or its murine functional homolog SYCP1, is required for this process (Newnham et al. 2010; Bisig et al. 2012). The mechanisms of centromere pairing may vary between organisms. In *S. cerevisiae*, the process is believed to be driven by an exclusion mechanism, in which remaining achiasmatic chromosomes pair with one another by necessity (Kemp et al. 2004). In *Drosophila*, homologous pericentric regions of heterochromatin and repetitious DNA may provide an epigenetic basis for pairing preference (Sun et al. 2003). Though these centromere interactions appear to be important for proper disjunction, the exact mechanism

and function are yet to be determined. As well as physically securing pairs, another use for centromere pairing may be to help orientate chromosomes properly on the meiotic spindle. Models for this mechanism suggest pairing may secure the chromosomes facing away from one another toward the spindles, or that pairing may help to produce tension when a bi-polar spindle attachment is made (Stewart & Dawson 2004; Kurdzo & Dawson 2015).

In early leptotene, alongside establishing centromere coupling, chromosomes physically move in relation to each other and become tethered (figure 1.4). This process is a non-autonomous behaviour of chromosomes, and is mediated by the interaction of chromosome telomeres with the nuclear periphery. A telomere is the region of DNA at the end of a chromosome, and differs from the rest of the chromosome in structure and function. The DNA itself is repetitive, and maintained by the enzyme telomerase. Yeast telomeres are around 300bp long and have a length of 3' single stranded DNA called a tail (Wellinger & Zakian 2012). Telomeres serve to protect the ends of chromosomes, by both physically capping them against degradation or end-to-end fusion, and by being non-coding, thereby preventing loss of information in the event of damage. This protective responsibility and their role in chromosome movement means that the integrity of telomeres is crucial, and this is maintained by surveillance with proteins related to DNA repair, such as check point proteins Mec1 and Tel1 (Bianchi & Shore 2007; Hector et al. 2012).

During vegetative growth chromosomes in cells may reside in discrete territories (Cremer & Cremer 2001) or be arranged in the nucleus in the Rabl orientation. In anaphase, chromosomes are mechanically pulled towards opposing poles by spindle microtubules attached to the centromeres, leaving the chromosome arms and telomeres trailing in their wake. Once the chromosomes become stationary they persist into interphase in this configuration, telomeres occupying one side of the nuclear periphery and centromeres the other (Dernburg et al. 1995). It has been postulated that this formation assists in spatial segregation of transcription or perhaps serves to maintain order between numerous large chromosomes (Manders et al. 1999; Cowan et al. 2001). The Rabl-

like positioning of chromosomes in *S. cerevisiae* interphase has been shown to rely upon centromere anchorage, telomere-telomere interaction and chromatin compaction (Bystricky et al. 2005). This arrangement of chromosomes loosely associates homologues at early stages of meiosis initiation, before the association is lost during S-phase and subsequently re-established during meiotic prophase (Weiner & Kleckner 1994). Early determination of transient unstable interactions may serve as a precursor for homologue pairing and synapsis in prophase I (Kleckner & Weiner 1993). It has been observed that homologous DNA molecules are capable of pairing together in the absence of auxiliary proteins, metal ions or crowding agents (Danilowicz et al. 2009). Therefore, this early arranging of homologous chromosomes in close proximity may increase the chances of initial physical pairing and subsequent stabilised interaction.

In meiotic prophase I, at the leptotene – zygotene transition, telomeres can be observed in a meiosis specific arrangement called the telomere bouquet, where the ends of chromosomes bind to the inner surface of the nuclear envelope and group within a localised area (Scherthan et al. 1996; Zickler & Kleckner 1998). This orientation is unique to meiosis and can be observed in many organisms, first described over a century ago. Bouquet formation coincides with that of synaptonemal complex establishment, and is morphologically opposed to the Rabl formation. Rabl formation chromosome movement is led by the centromeres, while the bouquet appears to rely on telomere-mediated tethering (Martínez-Pérez et al. 1999). The purpose of this arrangement has been debated; it may in itself serve to bring homologues closer together, or else simply be a morphological by-product of arranging the chromosomes ready for extensive nuclear movement.

Many organisms display oscillatory movements during meiotic prophase, the final step in preparing chromosomes for synapsis and recombination. Variations of these movements have been seen in mice spermatocytes, fission yeast (the “horse-tail” movement in *Schizosaccharomyces pombe*), budding yeast (rapid prophase movements in *S. cerevisiae*), and *C. elegans* (bursts of movement) (Scherthan et al. 1996; Klutstein & Cooper 2014). The budding yeast telomeric protein Ndj1 (Conrad et al. 1997) associates with nuclear envelope protein Mps3

(Conrad et al. 2007) in order to generate rapid telomere movements via interaction with Csm4 and the cytoskeleton on the exterior of the nucleus (Kosaka et al. 2008; Conrad et al. 2008). Deletion of Ndj1 leads to a delay in homologue pairing (Trelles-Sticken et al. 2000) and an increase in ectopic recombination (erroneous recombination between regions of homology on heterologues). This suggests that controlled mediation of homologue interaction may be necessary to limit recombination to between appropriate homologues (Goldman & Lichten 2000). The rapid movement generated at this stage of pairing may serve to disrupt weak interactions of non-homologous chromosomes, while retaining any associations formed between homologues, thus repressing ectopic recombination. Ndj1 is also shown to associate with the spindle pole body (SPB) and mediates the SPB interactions with the nuclear periphery via Mps3 and Mps2 (Li et al. 2015). This dual function of Ndj1 may help to coordinate SPB dynamics and telomere motility in preparation for metaphase I.

1.3.3 Synapsis

The alignment of homologues must be stabilised to maintain pairing. This stability is provided by the synaptonemal complex (SC), a zipper-like proteinaceous structure assembled in a highly organised manner, interconnecting the paired homologous chromosomes (Figure 1.5). The complex consists of a central element (CE) and lateral elements (LE), established from an axial element (AE) formed on each sister chromatid (Schmekel et al. 1993). Various proteins make up each of these elements, and build up sequentially to create the SC.

The SC assembles in stages during prophase of MI. Firstly during leptotene, the AE is formed along the base of each sister chromatid, via interaction with cohesin protein Rec8 (meiotic kleisin) (Watanabe & Nurse 1999; Klein et al. 1999; Llano et al. 2012). Proteins Hop1, Red1 and Mek1 act together to form the AE (Rockmill & Roeder 1990; Rockmill & Roeder 1991; Hollingsworth & Ponte 1997), and are required for the homologous interactions needed to produce viable spores in *S. cerevisiae* (Hollingsworth et al. 1995; Schwacha & Kleckner 1994). The AE proteins localise to the cores of meiotic chromosomes (Smith & Roeder 1997) in a specific stoichiometry necessary for normal progression of meiosis (Bailis et al.

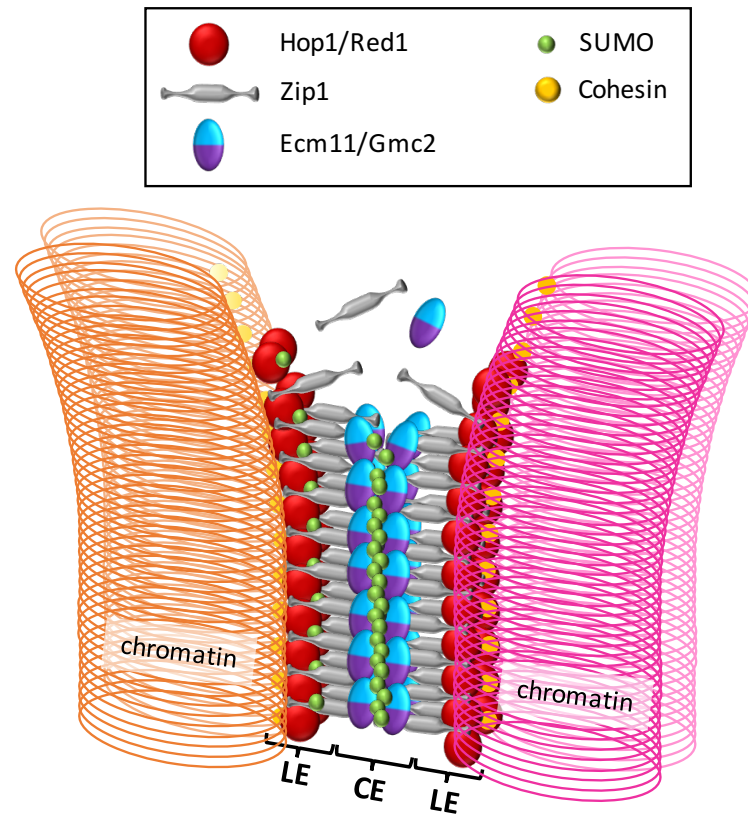


Figure 1.5 - Model of the structure of the synaptonemal complex

A hypothetical cross section of assembling synaptonemal complex (SC) is shown. The lateral elements (LE) and central element (CE) are highlighted. Assembly initiates with Red1/Hop1 association with cohesin component Rec8, forming the axis element (AE). Red1 is sumoylated by Zip3, priming it for Zip1 loading. Zip1 is also called the transverse filament. Following initiation of synapsis, central element proteins Ecm11/Gmc2 join Zip1 in loading the SC, and Ecm11 is sumoylated in a positive feedback loop, promoting further SC assembly. Transverse filaments from each AE interlock, “zipping up” the homologues. The region of overlap where Zip1 interlocks and Ecm11/Gmc2 associate forms the CE. The AE is now mature and forms the LE.

(Own figure drawn using Altmannová et al. 2012, Humphries et al. 2013 and Tsubouchi et al. 2016).

2000). Faithful assembly of the AE serves as a meiotic checkpoint. In the presence of Red1, Pch2 permits Hop1 phosphorylation by ATR/ATM homologues Mec1/Tel1 (Carballo et al. 2008; Lo et al. 2014). Phosphorylated Hop1 acts as a meiotic adaptor protein for Mec1/Tel1, mediating the activation of Mek1, a kinase responsible for suppressing inter-sister repair of DSBs during meiosis (Niu et al. 2005; Niu et al. 2007; Niu et al. 2009; Penedos et al. 2016). Together, these proteins provide a checkpoint mechanism, and help to establish inter-homologue bias needed for meiotic recombination (Joshi et al. 2009; Wu et al. 2010; Hayashi et al. 2010; Zanders et al. 2011). The assembly of the AE occurs simultaneously with the formation of DSBs (Padmore et al. 1991).

Following AE assembly, in zygotene, transverse filaments (TF) begin to assemble on to the AE. These filaments arrange themselves perpendicular to the AE. The *S. cerevisiae* TF is Zip1 (Sym et al. 1993), and functional analogues have been found in many organisms, such as mammalian SYCP1 (De Vries et al. 2005) and C(3)G in female *D. melanogaster* (Page & Hawley 2001). Zip1 is a member of the ZMM group, a collection of proteins critical for the formation of crossovers (Jessop et al. 2006) (section 1.5.3). Mek1 promotes the phosphorylation of Zip1, further establishing inter-homologue bias (Xiangyu Chen et al. 2015). For Zip1 to assemble efficiently a second ZMM protein, Zip3, sumoylates Red1 at discrete intervals along the AE (Chua et al. 1998; Eichinger & Jentsch 2010; Leung et al. 2015). These foci of Zip3 activity are thought to be the sites of synapsis initiation (Agarwal & Roeder 2000), and even in the absence of Zip1 these so called axial associations will still display homologous interaction (Rockmill et al. 1995; Chua et al. 1998). The formation of axial associations requires Hop2, a protein involved in the prevention of synapsis between non-homologous chromosomes (Henry et al. 2006). Once synapsis is initiated central element (CE) proteins Ecm11 and Gmc2 join Zip1 in loading the SC (Humphryes et al. 2013), and positive feedback of continued sumoylation maintains the process (Altmannová et al. 2012; Tsubouchi et al. 2016), progressively connecting the AEs. Transverse filaments from each AE interlock, “zipping up” the homologues. The region of overlap where Zip1 interlocks and Ecm11/Gmc2 associate forms the CE. The AE is now mature and

forms the LE. By pachytene the process of SC formation is complete.

1.4 Meiotic double strand break formation and processing

Accurate segregation of chromosomes during meiosis is ensured by secure pairing of homologous chromosomes prior to division. This secure interaction is achieved in most sexually reproducing organisms by the process of meiotic recombination, through the formation and repair of programmed DSBs. Mechanisms for DSB formation and repair exist across most eukaryotes, and have been extensively studied in various model organisms including *C. elegans*, *D. melanogaster*, murine models and fission yeast. The process is best characterised in *S. cerevisiae*, but many of the key components are conserved across species (de Massy 2013).

DSB formation occurs during leptotene, approximately 90 minutes after replication has completed (Borde et al. 2000). Temporal control of breaks is essential to recombination; too early and replication would be compromised, too late and segregation would be impaired. DSBs formation is therefore carefully coupled with the end of replication by controlling the expression of DSB machinery and association of accessory proteins (Henderson et al. 2006; Brar et al. 2006; Panizza et al. 2011).

1.4.1 DSB site selection

Rather than occurring sporadically throughout the genome, DSBs are distributed in a non-random fashion at specific loci termed recombination hotspots (Lichten & Goldman 1995; Gerton et al. 2000), where DSBs are more likely, but not guaranteed, to occur. Conversely there are also regions of DNA that receive relatively few DSBs, known as coldspots. Hotspots tend to locate to intergenic regions rather than intragenic, and commonly in promotor regions of genes, likely due to the more open configuration of chromatin at these loci (Wu & Lichten 1994). Coldspots are most likely to be found at the centromere and telomeres (Baudat & Nicolas 1997). Hotspots and coldspots have been mapped down to single-gene resolution and characterised regarding their levels of recombination (Gerton et al. 2000). No single rule governs the designation of

hotspot locations, instead sets of “gate-keeper factors” make their presence more likely (Lam & Keeney 2015; Cooper et al. 2016). These factors vary in number and significance across different organisms. Designation in *S. cerevisiae* depends upon GC content, methylated histone H3K4me3, intergenic promotor regions and regions of nucleolar depletion (Fan & Petes 1996; Nishant & Rao 2006; Pan et al. 2011). Contrastingly humans and *M. musculus* rely on a single factor for hotspot determination, the histone trimethyl-transferase PDRM9, responsible for H3K4me3 methylation (Berg et al. 2010; Grey et al. 2011). Hotspots show no sequence motif directly recognised by the DSB machinery, and so any locus that fulfils the requisite characteristics for recruitment of the machinery may become a DSB (Liu et al. 1995; de Massy et al. 1995). Indeed, cold spots may be induced to become hotspots if the DSB machinery is recruited synthetically (Pecina et al. 2002). The hotspots are found on the looped regions of chromatin, radiating out laterally from the axis of the condensed chromatin (the bottle brush formation described in section 1.3.2). This structure may ensure the hotspots are more accessible for processing by the DSB machinery (Pan et al. 2011).

1.4.2 The DSB forming complex

At least 10 proteins are known to be required for DSB formation in *S. cerevisiae*. These can be divided into subgroups based on their function and interactions: 1. Spo11-Ski8, 2. Rec102-Rec104, 3. Rec114-Mei4-Mer2, and 4. Mre11-Rad50-Xrs2 also known as the MRX complex (Malone et al. 1991; Galbraith & Malone 1992; Ivanov et al. 1992; Menees et al. 1992; Xu et al. 1995; Johzuka & Ogawa 1995; Keeney et al. 1997; Jiao et al. 2003; Arora et al. 2004; Li et al. 2006; Maleki et al. 2007).

In preparation for the formation of breaks Rec114-Mei4-Mer2 associate with chromatin in the axial region via the recruitment of Mer2 by Hop1 and Red1 (Panizza et al. 2011). Mer2 is phosphorylated by CDK and DDK, a pair of S-phase kinases, providing a link between replication and recombination (Henderson et al. 2006; Murakami & Keeney 2014). Phosphorylation of Mer2 leads to further enrichment of Rec114, Mei4 and Xrs2 at axes (Panizza et al. 2011). DSBs are formed at hotspots found on the looped regions of chromatin, radiating out from

the axis, while Rec114-Mei4-Mer2 and the other DSB forming complex proteins are associated with the axes. There must then be a means for the union of these two spatially distinct regions. Such a mechanism has been elusive, but recently a new function of the Set1 complex protein, Spp1, has been implicated as the missing link between hotspots and the axis. The Set1 complex promotes methylation of H3K4 (Dehé & Géli 2006). Trimethylation of this histone (H3K4me3) is promoted by Spp1 (Kirmizis et al. 2007), and is one of the strongly defining features of hotspots. Spp1 has now been found to interact with Mer2 as well as with H3K4me3, and is believed to bring the axis and loop regions together in order to activate DSB formation in the nearby nucleolar depleted regions (NDR) (Sommermeyer et al. 2013; Acquaviva, Drogat, et al. 2013; Acquaviva, Székvölgyi, et al. 2013).

Rec102-Rec104 act as a functional unit, and also localise preferentially to the axes (Panizza et al. 2011). Relatively little is known about the function of these proteins, but their interactions with Rec114-Mei4-Mer2 and Spo11-Ski8 suggest a role in bridging the two complexes (Arora et al. 2004; Maleki et al. 2007). Spo11 initially localises at pericentromeric regions along with Rec8 during S-phase, before redistributing along replicating regions and through Ski8 associating with Rec102-Rec104 at the axes (Arora et al. 2004; Sasanuma et al. 2007; Kugou et al. 2009). Mre11 begins to co-localise with Spo11 at replicating regions (Kugou et al. 2009), and is the last component of the DSB forming complex to assemble (Borde et al. 2004). This may be a precautionary measure, to ensure swift initiation of processing once DSBs are formed; Spo11 is the DSB-forming component (Keeney et al. 1997), while MRX is key in early resection of breaks (Neale et al. 2005; Borde 2007; Nicolette et al. 2010). MRX is thought to associate with the machinery via Xrs2 interaction with phosphorylated Mer2 (Arora et al. 2004; Borde et al. 2004).

1.4.3 Formation and early processing of DSBs

Once the DSB forming complex is assembled, break formation is initiated. DSBs are formed by the topoisomerase relative Spo11 (Keeney et al. 1997). Orthologues of Spo11 have been found in every sexually reproducing organism, and functional conservation is seen in other fungi, *C. elegans*, *D. melanogaster*, *M. musculus* and *A.*

thaliana (Dernburg et al. 1998; Mckim & Hayashi-hagihara 1998; Baudat et al. 2000; Celerin et al. 2000; Romanienko & Camerini-Otero 2000; Hartung & Puchta 2000; Steiner et al. 2002; Storlazzi et al. 2003; Bowring et al. 2006). Spo11 cleaves DNA as a dimer, each monomer sitting on one side of the DNA duplex and cleaving a single strand, together generating a DSB with a Spo11 monomer covalently bound to the 5' end (Figure 1.6) (Liu et al. 1995; Keeney et al. 1997; Keeney 2008). Spo11 catalyses DSB formation by nucleophilic attack of a phosphodiester linkage in the backbone of DNA. Catalysis relies upon tyrosine residue 135 and binding of magnesium ions; absence of either abolishes DSBs (Bergerat et al. 1997; Cha et al. 2000; Diaz et al. 2002).

Following DSB formation Spo11 must be liberated from the DNA for resection to proceed. Rather than hydrolysis of the covalent bond between Spo11 and the 5' end, Spo11 is released still covalently bound to a short oligonucleotide by endonucleolytic cleavage of the DNA (Neale et al. 2005). This processing is asymmetric, yielding two distinct species of Spo11-oligonucleotide complex of different molecular weights. The release of these complexes relies upon the MRX complex and endonuclease Sae2 (Hartsuiker, Mizuno, et al. 2009; Hartsuiker, Neale, et al. 2009; Milman et al. 2009; Gobbin et al. 2016).

Sae2, also known as Com1, was discovered in *S. cerevisiae* as part of a screen for mutants capable of sporulation in the absence of Spo11 (eleven) (McKee & Kleckner 1997; Prinz et al. 1997) and has orthologues in other organisms from fungi (Ctp1) (Limbo et al. 2007) to mammals (CtIP) (Sartori et al. 2007). Sae2 may show endonucleolytic activity, and along with the MRX complex is important in the removal of proteins from ssDNA associated with DSB ends in both meiosis and vegetative cells (Rattray et al. 2001; Lengsfeld et al. 2007; Puddu et al. 2015). In its inactive form it exists as insoluble oligomers of Sae2 monomers (Fu et al. 2014), and is phosphorylated to become active in a Mec1/Tel1 dependent manner (Baroni et al. 2004). It's activity at breaks is stimulated by the presence of the MRX complex (Lengsfeld et al. 2007). Sae2 Δ mutants allow formation of DSBs, but subsequently arrest without initiation of resection (Prinz et al. 1997).

The highly conserved MRX complex, or MRN in mammals, consists of three

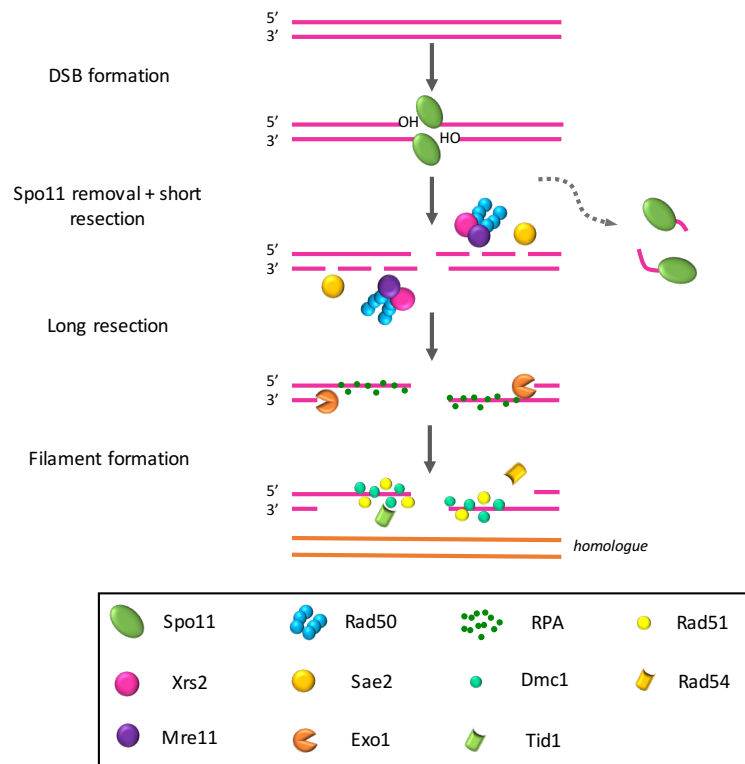


Figure 1.6 - Model for double strand break formation and processing

Spo11 cleaves DNA as a dimer, generating a DSB with a Spo11 monomer covalently bound to the 5' end by nucleophilic attack of the phosphodiester bond. Spo11 is released still covalently bound to a short oligonucleotide by endonucleolytic cleavage of the DNA, yielding two distinct species of Spo11-oligonucleotide complex of different molecular weights. Liberation is dependent upon the MRX complex (Mre11, Rad50 and Xrs2) and Sae2. As well as Spo11 release, Mre11 is believed to contribute to early resection by creating nicks in the DNA. DNA is resected in a 5' → 3' direction to expose long tracts of 3' single stranded DNA by Exo1 and other (as of yet) unknown nucleases. This long resection yields ssDNA, which is protected from enzymatic attack or secondary structure by the presence of RPA. Recombinase proteins Rad51 and meiosis-specific Dmc1 displace RPA to assemble a proteinaceous DNA filament capable of carrying out strand invasion of the homologue (orange). Tid1 and Rad54 are required for the loading of Dmc1 and Rad51 respectively.

proteins Mre11, Rad50, and Xrs2/Nbs1 (Ohta et al. 1998; Trujillo et al. 1998; Paull & Gellert 1999). It is active in response to various types of DNA damage (Symington 2014; Steininger et al. 2009). As well as being required for the formation of DSBs in *S. cerevisiae* (section 1.4.2) it is important in the resection of

DSBs (Garcia et al. 2011), homologous recombination (Bressan et al. 1999), and tethering the ends of DSBs together (Cassani et al. 2016). Distinguishing the roles of each component of MRX has proven difficult. Sequence analysis of Mre11 found 5 conserved motifs of phosphodiesterase enzymes (Sharples & Leach 1995), and the protein has demonstrated manganese dependent 3' → 5' dsDNA exonuclease and ssDNA endonuclease activity (Trujillo & Sung 2001). Loss of this nuclease activity renders cells more sensitive to DNA damage (Lewis et al. 2004). The dsDNA exonuclease activity is in the opposite direction to that expected for resection of the 5' strand. Therefore the nuclease activity of Mre11 is believed to contribute to early resection and the liberation of Spo11-oligonucleotides by creating nicks in the DNA (Neale et al. 2005; Gobbin et al. 2016), while another nuclease carries out the resection necessary for longer tracts of 3' ssDNA (Garcia et al. 2011). Rad50, an ATPase, interacts with Mre11 as a 2:2 complex (Raymond & Kleckner 1993; Hopfner et al. 2000; Hopfner et al. 2001; Lim et al. 2011). Rad50 ATPase activity regulates the nuclease activity of Mre11 (Williams et al. 2011; Möckel et al. 2012). Rad50 has a hook domain, allowing it to dimerise with other Rad50-Mre11 complexes, creating the bridges responsible for tethering DSB ends together (Hopfner et al. 2002). Both Mre11 and Rad50 are conserved in bacteria and archaea while Xrs2/Nbs1 is unique to eukaryotes, and is believed to be responsible for nuclear localisation of the complex and interaction with checkpoint protein Tel1 (Nakada et al. 2003; Tsukamoto 2004). Xrs2 may also have a role in unwinding of dsDNA (Paull & Gellert 1999).

Following release of the Spo11-oligonucleotide complex from the 5' strand DNA is processed in a 2-step process; after initial short resection of DNA by MRX nicking, DNA is resected in a 5' → 3' direction to expose long tracts of 3' single stranded DNA by a different exonuclease (Garcia et al. 2011; Hodgson et al. 2011). Exo1 and Dna2/Sgs1 are involved in the long resection of mitotic DSBs (Mimitou & Symington 2008; Hodgson et al. 2011). Exo1 is conserved across the eukaryotic domain and is thought to be one of the strongest candidates for meiotic resection (Tishkoff et al. 1997b; Qiu et al. 1999; Tsubouchi & Ogawa 2000). Dna2 as of yet has not been determined to be active in meiosis, and partner Sgs1 does not influence resection (Zakharyevich et al. 2010), however *exo1Δ* cells still show

some resection, suggesting a redundant nuclease is at work (Kirkpatrick et al. 2000; Zakharyevich et al. 2010). Trm2 has also been suggested as a potential candidate (Asefa et al. 1998; Choudhury, Asefa, Kauler, et al. 2007; Choudhury, Asefa, Webb, et al. 2007). Exo1 has 5' → 3' dsDNA exonuclease activity and 5' flap endonuclease activity (Lieber 1997). On average DSBs are resected by 800 nucleotides, and ~65% of this relies upon the nuclease activity of Exo1 (Zakharyevich et al. 2010). Overexpression of Exo1 partially rescues the DNA damage sensitivity of MRX mutants, suggesting some redundancy may also exist between Exo1 and the complex (Chamankhah et al. 2000). Phosphorylation of Exo1 has been observed in response to DNA damage of mitotically cycling cells (Engels et al. 2011). This modification is proposed to negatively regulate the activity of Exo1 in *S. cerevisiae* (Morin et al. 2008), while the effect in *H. sapiens* cells depends on the target residues (Bolderson et al. 2010; Tomimatsu et al. 2014). A more detailed account of Exo1 is outlined in section 1.8. As long resection proceeds an ssDNA binding protein, RPA (replication protein A), associates with the exposed ssDNA (Wold & Kelly 1988; Gasior et al. 1998), a role required for meiotic recombination (Soustelle et al. 2002). Variants of RPA exist across and within organisms, often tailored for ssDNA in specific circumstances, such as meiosis-specific MEIOB seen in some fungi and metazoans (excluding *S. cerevisiae*) (Souquet et al. 2013; Ribeiro et al. 2016). RPA and its paralogues stabilise the ssDNA, protecting it from aberrant processing and preparing it for recombinase recruitment.

1.5 Recombination and crossover formation

Repairing DSBs in meiosis can yield either a crossover (CO) or a non-crossover (NCO) (Figure 1.7). COs are the result of reciprocal exchange of chromosome arms flanking the break between homologues, while NCOs do not exchange and so maintain the parental configuration. Through the formation of COs homologues achieve secure pairing, necessary for normal disjunction of chromosomes in anaphase of MI. COs create a physical connection between homologues, and these

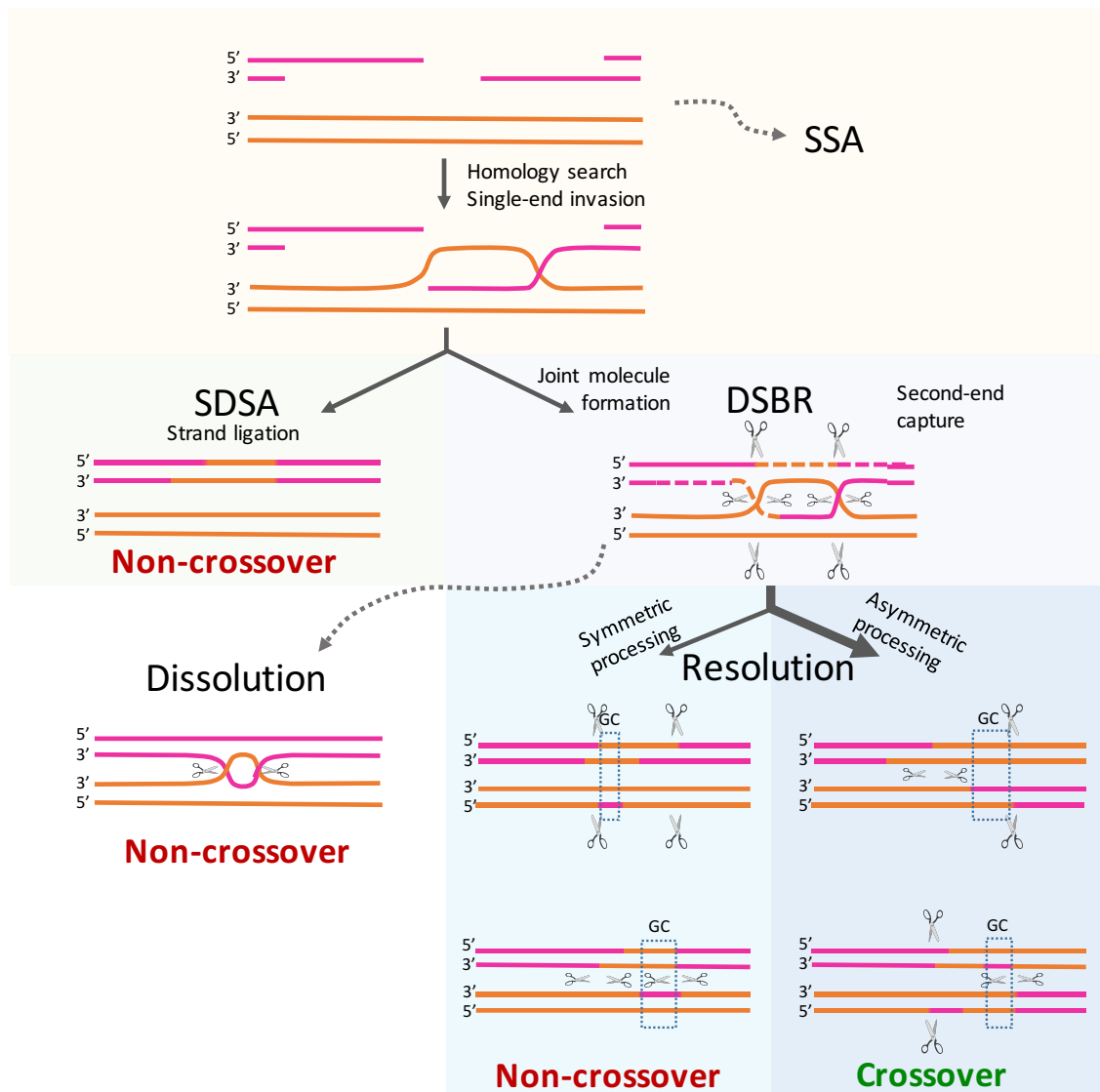


Figure 1.7 – Models of repair

Processed breaks yield ssDNA suitable for repair via several mechanisms. In the event of extensive resection across many kilobases, regions of homology within the donor may be used for repair by single strand annealing (SSA). Following resection of ~800nt, donor ssDNA coated with recombinase proteins Rad51 and Dmc1 invades the homologous DNA. The donor strand searches for homology, displacing the complementary strand of the recipient homologue, creating a D-loop. During this invasion and subsequent extension, the associations may be disrupted and displaced, in which case the invading strand will reanneal with the opposite side of the DSB and be repaired as a non-crossover event known as synthesis dependent strand annealing (SDSA). If the associations prevail, repair is hypothesised to proceed via the DSBR model. The second end of the donor is captured by the D-loop and a double Holliday junction (dHJ) is formed. dHJs can migrate toward each other and dissolve into a non-crossover event. Alternatively, dHJs are processed symmetrically or asymmetrically by resolvases to yield either crossovers or non-crossovers, and in yeast dHJs generally result in CO formation. Several resolvases have been proposed, and CO resolution is dependent upon various proteins, including Exo1 and Mlh1-Mlh3. Areas at which gene conversion can occur are highlighted in a dashed box and labelled 'GC'. (Own figure adapted from Gray & Cohen 2016)

are known as chiasmata. Models for the mechanism of recombination were first made possible following the discovery of the structure of DNA by Watson and Crick in 1953.

Fungi had long been a useful model organism for the study of genetics (section 1.2), and in particular *Neurospora crassa* proved most useful in the pursuit of a model for recombination due to its ordered tetrads reflecting the segregation pattern of each homologue. The understanding of genetic inheritance was underpinned by the work of Gregor Mendel, and his theory of Mendelian inheritance by which chromosomes segregate in a 2:2 fashion. However, study in *N. crassa* revealed that gene conversion, a non-reciprocal exchange event, could happen to cause non-Mendelian segregation (3:1) (Lindgren 1955; Mitchell 1955). Gene conversion is associated with a CO if the homologous chromosomes are heterozygous for the DSB locus region. During the process of CO formation (section 1.5.1) the resected strand of the DSB invades the homologue, and anneals with the reciprocal homologous region between two Holliday junctions. In the cases where heterozygous strands anneal together, the heteroduplex DNA is repaired using mis-match repair (MMR) mechanisms. This results in conversion of one of the two strands to the genotype of the complimentary strand (gene conversion) (Chen et al. 2007). In cases where MMR fails mismatched heteroduplex DNA persists, resulting in another type of non-Mendelian inheritance called post-meiotic segregation (PMS), resulting in various types of segregation patterns. In PMS, inheritance of heteroduplex DNA is corrected later after meiosis, creating colonies that have a segmented appearance due to their varying genotypes following repair (White et al. 1985). A model for recombination was then required to account for the various outcomes of meiosis, and the structure of DNA was integral to this understanding.

Early models struggled to reconcile the observations of segregation, but in 1964 Robin Holliday provided the first solution to account for the available data. Holliday proposed that COs were initiated by the formation of single-strand nicks, one on each homologue, that led to exchange of single strands. This accounted for heteroduplex DNA formation, and described a four-stranded intermediate now

known as a Holliday junction, that could be resolved to yield reciprocal exchange of homologues (Holliday 1964). Over time this model could not fully account for all non-Mendelian inheritance patterns, leading to many revisions by different groups over the coming decades. A mechanism in which DSBs initiated recombination was first proposed in 1976 (Resnick 1976), but it was not until the 1980's that the idea took hold. In 1983 Jack Szostak proposed the first iteration of the double-strand break repair (DSBR) model, which is currently accepted as the best model for recombination (Szostak et al. 1983). The best description of meiotic recombination over all arises from a model combining the principles of DSBR and an NCO pathway called synthesis-dependent strand annealing (SDSA) (section 1.5.2). This model is by no means complete, e.g. it does not reconcile the different activities of various nucleases and MMR-related proteins known to be necessary for subsets of COs within species, or the different requirements between species.

1.5.1 Repair to yield crossovers

The refined hypothesis of DSBR presents a model in which Spo11 forms DSBs at a hotspot in one homologue. The DSB is resected on each side in a 5' → 3' direction yielding a length of 3' ssDNA. One of the resected strands carries out strand invasion of the homologue, displacing the complementary strand to form a displacement-loop (D-loop) as it searches. The D-loop is caught by the second resected 3' strand. As each strand anneals to its reciprocal region of homology a Holliday junction is formed, and these two junctions together form a double-Holliday junction (dHJ) (Gilbertson 1996; Stahl 1996) (figure 1.7). Asymmetrical cleavage of the dHJ structure yields a crossover, while symmetrical cleavage yields a non-crossover (Manhart & Alani 2016). Cleavage of dHJs is carried out by enzymes known as resolvases. Resection and formation of joint molecules (JMs) can be detected by Southern blot, as each step of DSB formation and repair creates a corresponding sized species of DNA, supporting the DSBR model. Continuous resection over varying distances causes species of differing sizes, seen as a smear on Southern blots due to the various migrations during electrophoresis (Cao et al. 1990; Bishop et al. 1992). JMs, including dHJs and single-end invasions (SEIs) can also be seen as distinct species of specific molecular weights (Weiner & Kleckner

1994; Schwacha & Kleckner 1994; Hunter & Kleckner 2001). Resolution of dHJs seems to be the dominant pathway of CO formation in *S. cerevisiae*, but it is also possible to obtain COs from non-dHJ single end invasion (SEI) intermediates (Matos & West 2014).

Recombinases

Following resection of DSBs to yield 3' strands of DNA, proteins called recombinases bind to the ssDNA, forming presynaptic filaments (tracts of protein-coated DNA). Recombinases promote two key processes in recombination. First, the filaments invade and bind the complementary strand of the dsDNA, in a step called strand invasion. Next the paired region expands, displacing the complementary strand as it goes, in a step called DNA strand exchange. The two recombinases in *S. cerevisiae* are homologues of bacterial RecA: Rad51 and meiosis specific Dmc1 (Bishop et al. 1992; Shinohara et al. 1992; Ogawa et al. 1993; Hong et al. 2001). Rad51 is the principle recombinase in mitosis, while Dmc1 is exclusive to meiosis. Rad51 is also required in meiosis to promote Dmc1 activity (Cloud et al. 2012). This supporting role for Rad51 is independent of its enzymatic activity, as Hed1 has been shown to inhibit Rad51 during meiosis in order to promote invasion of the homologous chromatid rather than the sister as in mitosis (Tsubouchi & Roeder 2006; Busygina et al. 2008; Busygina et al. 2012). RPA associated with the 3' ssDNA stabilises the strand and promotes nucleoprotein filament formation. Rad51 and Dmc1 also require Rad54 and Tid1 respectively for regulating their loading and activity during recombination (Petukhova et al. 1998; Shinohara et al. 2000; Shinohara et al. 2003; Holzen et al. 2006). Earlier study of Rad51 and Dmc1 foci in *S. cerevisiae* had suggested a model by which Rad51 and Dmc1 associate with opposing strands at the break as homofilaments through an asymmetric loading mechanism (Shinohara et al. 2000; Kurzbauer et al. 2012). This model did not account for a few key observations; Rad51 is required for Dmc1 assembly (Cloud et al. 2012), Rad51 is catalytically inactive though both strands are known to catalyse strand exchange (Oh et al. 2007), and there was no apparent control for mutually exclusive loading. More recent work in *S. cerevisiae*, using new super-resolution dSTORM microscopy, supports a model in which both Rad51 and Dmc1

load on to each DSB end together in a heterofilamentous fashion, over a short stretch of ~100nt (Brown et al. 2015).

Template choice

As meiotic DSB repair is a modified version of the mitotic HR repair pathway, it is important to ensure that it results in sufficient strand invasion of the homologue and not the sister chromatid. The mechanisms behind this bias may be direct, positively influencing inter-homologue (IH) invasion (Goldfarb & Lichten 2010; Terentyev et al. 2010), or indirect, creating a barrier to inter-sister-chromatid recombination (BSCR) (Niu et al. 2005; Niu et al. 2007; Niu et al. 2009). The meiosis specific kinase Mek1 has been shown to orchestrate many of the components required for IH bias (Niu et al. 2005; Niu et al. 2007; Niu et al. 2009; Penedos et al. 2016). As described in section 1.3.3, Hop1 phosphorylation by Mec1/Tel1 (Carballo et al. 2008; Lo et al. 2014) leads to activation of Mek1, helping to establish IH bias needed for meiotic recombination (Joshi et al. 2009; Wu et al. 2010; Hayashi et al. 2010; Zanders et al. 2011). Mek1 targets accessory proteins of Rad51 (Rad54 and Rdh54), blocking their interaction with Rad51 in order to decrease IS strand invasion (Niu et al. 2009). Mek1 hyper-activation by Hop1 also leads to meiotic arrest in the *dmc1Δ* cells, blocking progression in the absence of IH invasion (Penedos et al. 2016). Srs2, a DNA helicase with translocase activity, has also been shown to promote IH bias by dismantling Rad51 from nucleofilaments (Sasanuma et al. 2013). Not all IS recombination is inhibited however, suggesting a balance between IH and IS recombination may exist to ensure appropriate numbers of COs are formed (Goldfarb & Lichten 2010).

Resolvases

Joint molecule intermediates must be resolved appropriately to yield COs. The enzymes responsible for this step are known as resolvases, but identification of a eukaryotic HJ resolvase has proven to be a challenge. Bacterial resolvase RuvC is known to process HJs (Iwasaki et al. 1991), and has been used in in vitro experiments to study HJs in eukaryotic cells (Schwacha & Kleckner 1995). Early studies into eukaryotic resolvases revealed a role for Mus81 and Eme1, *S. pombe*

proteins important in the resolution of meiotic HJs (Boddy et al. 2001; Osman et al. 2003; Smith et al. 2003). However, in *S. cerevisiae* and mouse models this was not found to be the case (De los Santos et al. 2003; McPherson et al. 2004), perhaps because *S. pombe* meiosis tends to create COs through single HJ intermediates while *S. cerevisiae* and mice use dHJs (Cromie et al. 2006). Other candidates include mammalian Gen1 (Yen1 in *S. cerevisiae*) and mammalian Slx1/Slx4 (Y Ip et al. 2008; Fekairi et al. 2009; Svendsen et al. 2009; Sarbajna & West 2014). Resolvases of dHJs have been harder still to establish. DNA mismatch repair proteins Mlh1-Mlh3 (MutL γ) have been shown to promote CO formation in *S. cerevisiae* meiosis. Candidates for directing Mlh1- Mlh3 functions are Msh4-Msh5, Sgs1-Top3-Rmi1, and Exo1 (Zakharyevich et al. 2012; Manhart & Alani 2016). Originally believed to be a CO suppressor, RecQ helicase Sgs1 (human BLM homologue) has now been shown to promote CO formation along with Top3 and Rmi1 (Tang et al. 2015; Kaur et al. 2015). Zakharyevich et al demonstrated that interaction between Exo1 and MutL γ via Mlh1 is essential for normal levels of recombination in meiosis, in a mechanism independent of Exo1's nuclease function (Zakharyevich et al. 2010). Their findings suggest a model in which this interaction promotes nuclease activity of Mlh3, necessary for resolution of dHJs to yield COs. MutL γ appears to function at hotspots in a Hop1-dependent fashion, suggesting chromatin structure helps to influence meiotic CO resolution (Medhi et al. 2016).

1.5.2 Repair to yield non-crossovers

Not all DSBs are processed to yield COs. In *S. cerevisiae* 140-170 DSBs are estimated to be formed during meiosis (Buhler et al. 2007), and around 60% of these become COs (Mancera et al. 2008). At least one chiasma per chromosome is necessary for normal disjunction (the obligate crossover) (Page & Hawley 2003). A lot of time and energy is invested in this process of forming and repairing many breaks, perhaps as a safety measure to guarantee a CO is achieved rather than relying on the success of a single event. DSBs that do not become COs must still be repaired, and instead result in NCOs. NCOs may arise at any point prior to dHJ formation, as it has been demonstrated that all dHJs resolve to form COs (Hunter &

Kleckner 2001). If NCOs arose from a similar pathway to COs, it would be anticipated that both would appear contemporaneously. Indeed, when purified dHJs are treated with bacterial resolvase RuvC both CO and NCO products are formed (Schwacha & Kleckner 1995). Instead, *in vivo* evidence suggests NCOs appear first by about an hour, and preceding dHJ formation (Allers & Lichten 2001). No further NCOs are observed subsequently with the appearance of COs, supporting the hypothesis that the mechanisms behind each are mutually exclusive. Additionally, in the CO deficient *ndt80Δ* background, levels of NCOs are unchanged, implying that at this stage the two pathways have diverged, and the CO intermediates are unable to be reversed (Allers & Lichten 2001). While COs are accounted for by the DSBR model, SDSA is believed to be responsible for the formation of NCOs.

Synthesis-dependent strand annealing (SDSA)

Synthesis dependent strand annealing (SDSA) is the major pathway for formation of NCOs (Allers & Lichten 2001; Villeneuve & Hillers 2001; McMahon et al. 2007). In SDSA DSBs are processed as in the DSBR model, and strand invasion proceeds to the stage of D-loop formation, priming DNA synthesis from the SEI intermediate. At this point, rather than second end capture, the invading strand dissociates. The synthesized region of this strand anneals to the complementary single strand from the other side of the break, and the D-loop reanneals the duplex of the donor. The donor is not modified or cleaved, and so the end product is a non-crossover (Anderson & Sekelsky 2010) (Figure 1.7). The 3'→5' helicase Srs2 is believed to moderate the dissociation of the invading strand, by interfering with Rad51 filament formation (Dupaigne et al. 2008) and directing the heteroduplex towards DNA synthesis in a moving bubble, reducing stability of the intermediate compared to a D-loop and promoting SDSA (Miura et al. 2013).

Single-strand annealing (SSA)

Single-strand annealing (SSA) is an intra-chromosomal repair method used for repair of DSBs between two regions of repeated DNA without use of a template. Breaks initially undergo resection as in DSBR, however this resection usually

proceeds over many kilobases, much further than in DSBR. Exposure of the repeated DNA results in annealing of the complimentary regions of homology. Regions as small as 30bp can provide sufficient homology for SSA (Villarreal et al. 2012). The intervening sequence proximal to the break creates a flap, and is excised by Rad1-Rad10 resulting in deletion of the region (Schiestl & Prakash 1990). The resultant gaps are closed by DNA synthesis. This pathway is predominantly used in mitosis, as resection in meiosis does not proceed over sufficiently long distances. Some recent work by a PhD student in the Goldman Lab, Tzu Ling Tseng, demonstrated that in certain circumstances meiotic cells will carry out SSA (thesis).

1.5.3 Controlling global distribution of crossovers

In order to regulate the location and quantity of DSBs, cells have developed mechanisms to control the global distribution of DSBs and their repair products. It is important to form sufficient COs for effective pairing of homologues while also minimising the risk of surplus interactions that may secure them too tightly, as both too few or too many could cause non-disjunction events.

Recombination nodules

From leptotene of MI it is possible to observe regions of chromatin destined to become DSBs, known as recombination nodules (Carpenter 1975). Electron microscopy reveals these nodules in almost all sexual organisms, finding early nodules (EN) during late leptotene and zygotene, followed by late nodules (LN) observed in pachytene (Zickler & Kleckner 1999). The number of nodules corresponds to the number of DSBs formed, and the number of ENs that go on to become LNs corresponds to the number and distribution of COs formed and correlate with chiasmata, leading to the conclusion that LNs are likely DSB sites that have progressed to become COs, and the remainder are NCOs (Zickler & Kleckner 1999; Mancera et al. 2008). Before the discovery of proteins associated with crossing over, LNs were used to monitor chiasmata formation.

Crossover interference

Distribution of crossovers is governed by a phenomenon called interference, by which recombination events are spaced less closely than would be expected from a random distribution. The effect was first described more than a century ago, and has persisted through decades of further study. Several mechanisms have been proposed for how interference is established in the cell, most commonly the mechanical stress model, the polymerisation model, and the counting model, but one is still yet to be determined as the preferred explanation (Berchowitz & Copenhaver 2010). The mechanical stress model posits that the structure of meiotic chromatin exerts tension across the chromosome, leading to areas of increased stress which when broken (by a DSB) relieve the tension on the surrounding area, reducing the likelihood of further DSB formation (Kleckner et al. 2004). However this model makes it difficult to account for how COs would reduce tension differentially to DSBs resulting in NCOs. The polymerisation model proposes that early recombination machinery assembles at hotspots independently of other loci, and then subsequently initiate a polymerisation event along the axis, as ZMM proteins are known to help stabilise CO intermediates at the point of strand invasion (Lynn et al. 2007). The polymerisation of one region suppresses that of others nearby, and these sites of initiation progress to become LNs (King & Mortimer 1990). Experiments have shown that the SC machinery is dispensable for interference, and NCOs still form in the absence of ZMM components, contradicting this theory (Shinohara et al. 2008). The counting model suggests a more organised mathematical model, by which COs are interspersed between set numbers of NCOs, in a fixed proportion (Foss & Stahl 1995). This cannot fully account for crossover homeostasis, which allows for chromosomes to still attain the required number of COs in the presence of reduced DSBs (Martini et al. 2006). Each model has strengths and weaknesses with respect to the experimental findings, and further understanding of the interference process has been hindered by difficulties in isolating the proteins involved. The models described here all attempt to explain “cis interference”, that is how cells regulate to distribution of COs along the same chromosome. More recently attention has turned to potential mechanisms for “trans interference”, investigating how cells

prevent DSBs being instigated at the reciprocal site on the homologous chromosome (Zhang et al. 2011). Both classes of interference are dependent upon DNA damage response kinase Tel1, as abolishing Tel1 leads to DSBs forming at ranges expected by chance (Garcia et al. 2015).

1.6 The meiotic checkpoint network

For faithful meiosis yielding balanced gametes, cells rely on intricate surveillance mechanisms capable of signalling both normal progression and instances of abnormal recombination. These checkpoints create dependent relationships between otherwise independent processes, ensuring that conditions for each stage are correct (Roeder & Bailis 2000; Hochwagen & Amon 2006; Longhese et al. 2009; MacQueen & Hochwagen 2011; Gray & Cohen 2016). In occasions when cells deviate from their normal processes this surveillance permits a delay or termination of the cycle to protect the integrity of the population.

S. cerevisiae has 12 key proteins that are involved in signalling during meiosis (Table 1.1) all of which share homologues across the eukaryotic domain (Subramanian & Hochwagen 2015). The following is a brief consideration of the checkpoints and some key players involved in meiotic progression.

Meiotic replication – completing replication prior to DSB formation is necessary to ensure recombination only happens between complete chromosomes, and prevents conflicts between the different sets of machinery (Blitzblau & Hochwagen 2013). DNA repair kinase Mec1 (mammalian ATR) inhibits the expression of Spo11 (Blitzblau & Hochwagen 2013), and influences the localisation and activity of DSB machinery components Mer2 and Rec114 via Rad53.

Synapsis & asynapsis – in the absence of DSBs, synapsis formation is delayed, possibly via Zip3 (MacQueen & Roeder 2009; Serrentino et al. 2013). Failure to synapse also leads to activation of Dot1, a silencing protein capable of triggering pachytene arrest via epigenetic histone modifications influencing Pch2 (Cavero et al. 2016).

<i>S. cerevisiae</i>	Mammals	<i>C. elegans</i>	<i>S. pombe</i>	<i>Drosophila</i>	Function	Checkpoint
Mec1	ATR	ATL-1	Rad3p	Mei-41	PI3 ^a kinase-like kinase	Meiotic replication, DSB processing & failure, inter-homologue bias, prophase exit
Tel1	ATM	ATM-1	Tel1p	Atm	PI3 kinase-like kinase	DSB levels, DSB processing & failure, inter-homologue bias
Ddc1	RAD9A	HPR-9	Rad9p	Rad9a	PCNA ^b -like clamp (9-1-1 complex)	Pachytene checkpoint
Rad17	RAD1	MRT-2	Rad1p	Rad1	PCNA-like clamp (9-1-1 complex)	Pachytene checkpoint
Mec3	HUS1	HUS-1	Hus1p	Hus1	PCNA-like clamp (9-1-1 complex)	Pachytene checkpoint
Rad53	CHK2	CHK-2	Cds1p	Mnk	Protein kinase with FHA ^c domain	DSB processing & failure
Mek1			Mek1p			Inter-homologue bias, prophase exit
Cdc5	several	PLK-2	Plo1p	Polo	Protein kinase	Pachytene exit
Hop1	HORMAD1	HTP-1	-	-	Chromosomal HORMA-domain proteins	Inter-homologue bias
Red1	SYCP3	HTP-3	Rec10	C(2)M	Chromosome axis component	Inter-homologue bias
Sir2	several	SIR-2	Sir2p	Sir2	NAD-dependent deacetylase	DSB site regulation,
Pch2	TRIP13	PCH-2	-	Pch2	AAA+ ATPase ^d	Synapsis & asynapsis, DSB processing & failure,

^aPhosphoinositide 3-kinase.

^bProliferating cell nuclear antigen.

^cFork-head associated domain.

^dATPases associated with diverse cellular ATPase.

Table 1.1 – Meiosis checkpoint network proteins and their homologues. (Table adapted from Subramanian & Hochwagen 2015)

DSB levels – as previously discussed in section 1.5.3, cis- and trans-interference is important for the distribution of DSBs. DNA repair kinase Tel1 (ATM) is thought to inhibit repeated formation of superfluous DSBs at the same loci both inter and intra-chromosomally. Rec114 may serve as the target for Tel1, as mimicking phosphorylation by Mec1/Tel1 causes a notable decrease in DSBs (Carballo et al. 2013).

DSB processing & failure – DSB formation is activated by processes downstream of CDK and DDK (section 1.4.2) and Mec1 exerts positive feedback through inhibition of Ndt80 (Medhi et al. 2016). The MRX complex senses DSB formation and activates Tel1, which in turn signals the initiation of end resection (Usui et al. 2001; Cartagena-Lirola et al. 2008). Mec1 is also activated in response to DSBs and further influences resection (Cartagena-Lirola et al. 2008). Various checkpoints are also activated in response to defective DSB processing, including the Pch2 protein involved in DSB formation and responsible for arrest of cells at pachytene if DSBs remain unrepaired (Farmer et al. 2012; Lo et al. 2014).

IH bias – Tel1/Mec1 phosphorylation of axis protein Hop1 leads to activation of meiosis specific kinase Mek1, which influences choice of template by inhibiting the recombinase activity of Rad51 via Rad54 (Carballo et al. 2008). Other unconfirmed targets of Mek1 are thought to be involved in this process (Niu et al. 2009; Terentyev et al. 2010).

Suppression of ectopic recombination – a poorly characterised pathway for the prevention of non-allelic recombination and protection of DSB ends that is believed to be influenced by the checkpoint mechanisms via Rad54 (Shinohara & Shinohara 2013).

Meiotic prophase exit – exit is controlled by transcription factor Ndt80. In the case of defective synapsis or DSB repair, Mec1 activates Mek1 which in turn inhibits CDK via the action of Swe1 (Acosta et al. 2011). Surveillance mechanisms also inhibit nuclear export of Ndt80, preventing transcription of genes necessary for prophase exit (Tung et al. 2000). This arrest is rapidly reversible should the cell be rescued.

1.7 Exo1 in detail

Exo1 is a nuclease with 5' → 3' dsDNA exonuclease activity and 5' flap endonuclease activity (Lieber 1997), that functions in DNA metabolism processes including mismatch repair, homologous recombination, telomere maintenance, replication and checkpoint signalling (Szankasi & Smith 1995; Fiorentini et al. 1997; Tran et al. 2004; Bertuch & Lundblad 2004; Morin et al. 2008; Zakharyevich et al. 2010). In the absence of Exo1 mitotically cycling cells are more sensitive to DNA damaging agents such as camptothecin (Morin et al. 2008), and show a reduction in spore viability from ~98% to ~80% following meiosis (Fiorentini et al. 1997). Conversely, increased expression of Exo1 leads to hyper-resection of DNA, and this can suppress sensitivity to DNA damaging agents (Tsubouchi & Ogawa 2000; Moreau et al. 2001). It was first identified in *S. pombe* as a nuclease expressed during meiosis (Szankasi & Smith 1992), and subsequently described in *S. cerevisiae* as a nuclease important in recombination (section 1.4.3) (Fiorentini et al. 1997; Tishkoff et al. 1997b). It is part of a wider family of nucleases active in DNA damage responses, including Rad27 (Fen1 in humans/Rad2 in *S. pombe*) and Rad2 (Xpg1 in humans/Rad13 in *S. pombe*), and homologues have been found across eukaryota, including in *H. Sapiens*, *M. musculus*, *C. elegans* and female *D. melanogaster* (Digilio et al. 1996; Tishkoff et al. 1998; Lee et al. 1999; Lemmens et al. 2013). *S. cerevisiae* also has a paralogue of Exo1, Din7, that arose from the gene duplication event (Mieczkowski et al. 1997). Din7 is induced by DNA damage, however it is restricted to the mitochondria (Fikus et al. 2000).

S. cerevisiae Exo1 (702 residues) and *H. sapiens* hExo1 (846 residues) show variable protein sequence similarity along the length of the protein (NCBI Blast 2016) (Figure 1.8). The N-terminal regions have 62% sequence similarity across the first 300 residues, reflecting conservation of the N- and I-nuclease domains. The only other stretch of significant similarity (43%) spans ~80 residues encompassing the MIP box, a conserved motif for Mlh1 binding. The remaining regions of the C-terminus flanking this MIP region show no sequence conservation. The structure of the first half of hExo1, incorporating the nuclease domains, has been solved using X-ray crystallography (Orans et al. 2011). These studies have helped to illustrate the mechanism by which Exo1 binds with and

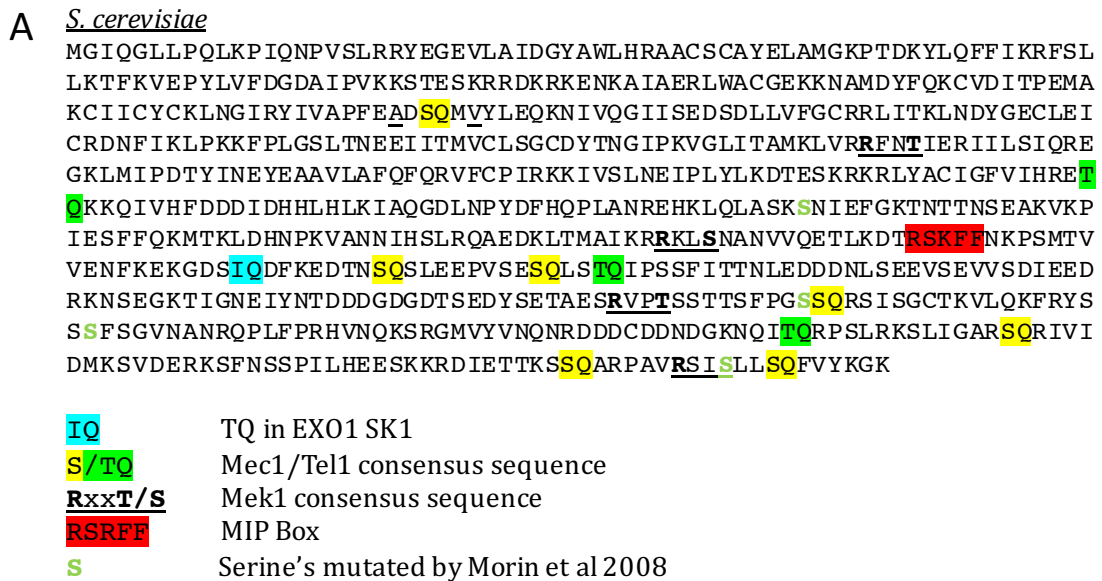
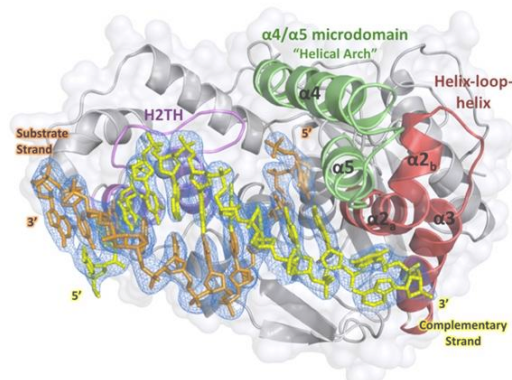
**B**

Figure 1.8 – Sequence analysis of *S. cerevisiae* Exo1 and comparison to *H. sapiens* sequence

A – Amino acid sequence of *S. cerevisiae* Exo1, highlighting those residues identified by Morin et al. as phosphorylated and motifs known to be potential kinase targets. All but one of the sites identified are located within the latter half of the sequence, of which little is known in terms of structure and function compared to the well characterised N-terminal nucleolytic domain.

B – Cartoon structure of *H. sapiens* N-terminal region of Exo1 bound to DNA obtained via x-ray crystallography. The 300 nucleotides identified as sharing significant similarity with *S. cerevisiae* constitutes this domain, which is responsible for the catalytic function of Exo1. (Figure from Orans et al. 2011)

C

Range 1: 1 to 299		Graphics		▼ Next Match ▲ Previous Match	
Score	Expect	Method	Identities	Positives	Gaps
219 bits(558)	4e-65	Compositional matrix adjust.	121/302(40%)	187/302(61%)	8/302(2%)
Query 1	MGIQGLLPQLKPIQNPVSLRRYEGEVL	AIDGYAWLHRAACSCAYELAMGKPTDKYLQFFI			60
Sbjct 1	MGIQGLL +K P+ +R+Y+G+V+A+D Y WLH+ A +CA +LA G+PTD+Y+ F +	MGIQGLLQFIKEASEPIHVRKYKQVAVDTCWHLHKGAIACAELKAKGEPTRDYYVGF			60
Query 61	KRFSLLKTFKVEPYLVFDGDAIPVKKSTESKRRDKRKENKAI	AERLWACGEKKNAMDYFQ			120
Sbjct 61	K ++L + ++P LVFDG +P KK E RR++R+ N ++L G+ A + F	KFVNMLLSHGIKPILVFDGCTLPSKKEVERSRRRERQANLLKKGQLLREGKVSEARECFT			120
Query 121	KCVDITPEMAKCIICYCKLNGIRYIVAPFEADSOMVYLEQKNI	VOGIISEDSDLLVFGCR			180
Sbjct 121	+ ++IT MA +I + G+ +VAP+EAD+Q+ YL + IVQ II+EDSDLL FGC+	RSINITHAMAHKVIKAARSQGVDCLVAPYEADAQLAYLNKAGIVQAIITEDSDLLAFGCK			180
Query 181	RLITKLNLDYGECLIEICRDNFIKLPKKFPLGSLTNEEII	ITMVC-LSGCDYTINGIPKVLIT			239
Sbjct 181	++I K++ +G LEI + +L LG + EE +C LSGCDY + + +GL	KVILKMDQFGNGLEI---DQARLGMCRQLGDVFTTEKFRYMCILSGCDYLSLRLGIGLAK			237
Query 240	AMKLVRRFNT--IERIILSIQREGKL--MIPDTYINEYEAAV	LAFQFQRVFCPIRKKIVS			295
Sbjct 238	A K++R N I ++I I K+ +P+ YIN + A F +Q VF PI++K++	ACKVLRLANNPDIKVIKIKIHYLKMNITVPEDYINGFIRANNTFLYQLVFDPIKRRKLI			297
Query 296	LN 297				
	LN				
Sbjct 298	LN 299				

Range 2: 430 to 507		Graphics		▼ Next Match ▲ Previous Match ▲ First Match	
Score	Expect	Method	Identities	Positives	Gaps
20.0 bits(40)	0.52	Compositional matrix adjust.	18/81(22%)	35/81(43%)	3/81(3%)
Query 368	LASKSNIEFGKTNNTNSEAKVKPIESFFQKMTKLDHNPKVANNI	HSLRQAEDKLTMAIKR			427
Sbjct 430	L S+ ++ F K NS K + + L + P ++ + + +K ++R	LLSQYSLSPFKTKKNSSEGNKSLSFSEVFPDLVNGPTNKKSVSTPPRTRNKPFATFLQR			489
Query 428	RKLSNANVVQETLKDTRSKFF	448			
	+ + VV + TRS+FF				
Sbjct 490	KNEESGAVV---VPGTRSRFF	507			

C – Screen grab of the alignment results of Exo1 from *S. cerevisiae* (query) and *H. sapiens* (subject). The MIP box conserved in the C-terminal region is highlighted in orange.

resects DNA, and demonstrate that Exo1 is capable of interacting with DNA in the absence of over half of its sequence.

Exo1 has a second role in meiosis in addition to its nuclease activity, as part of the machinery responsible for resolving crossovers following recombination (Zakharyevich et al. 2010). These two roles are distinct from one another both in timing and in their mechanism, as the nuclease function of Exo1 is not required for its resolvase activity. This role relies on interaction with MutLγ complex proteins, Mlh1 and Mlh3 (Zakharyevich et al. 2010). Absence of Exo1, Mlh1/Mlh3, or loss of their interaction, leads to a dramatic reduction in crossover formation. It has been previously demonstrated that phosphorylation plays a role in the regulation of Exo1 in *S. cerevisiae* and mammalian models (Morin et al. 2008; Bolderson et al. 2010; Engels et al. 2011; Tomimatsu et al. 2014). Morin et al. identified four serine residues S372, S567, S587 and S692, that were phosphorylated in *S. cerevisiae* in response to DNA damage induction. They produced mutant alleles of *EXO1* that were either non-phosphorylatable (*exo1-4S::A*) or mimicked phosphorylation (*exo1-4S::E*). Examining sensitivity to DNA damage in these mutants has suggested that phosphorylation inhibits the activity of Exo1, as the non-phosphorylatable mutant *exo1-4S::A* is less sensitive to DNA damage than its wild type or phospho-mimetic counterparts. In addition to these experimental findings, sequence analysis of Exo1 shows potential targets for phosphorylation by Mec1/Tel1. Mec1/Tel1 homologues ATR/ATM preferentially target serine or threonine residues followed by a glutamine (S/TQ) (Kim et al. 1999). At least 3 of these motifs clustered within 100 residues is known as an SCD (Traven & Heierhorst 2005), and SCDs have been identified in over half of all investigated ATM/ATR target proteins (Matsuoka et al. 2007). Exo1 exhibits 3 potential SCDs, and has one stringent SCD (containing more than 3 motifs within 50 residues) (Figure 1.8). Further potential sites of phosphorylation were identified in a search for Mek1 motifs, characterised by the consensus sequence RXXT/S (Mok et al. 2010), 4 of which were identified in Exo1, one including a serine residue mutated by Morin et al.

Early studies in human cells have further supported a role for phosphorylation

in the negative regulation of Exo1, perhaps as a mechanism for attenuating resection in preparation for recombinase loading (Bolderson et al. 2010). More recent findings have shown phosphorylation of other residues of human Exo1 promote recruitment and resection (Tomimatsu et al. 2014). Taken together these findings suggest that phosphorylation of Exo1 regulates its localisation and activity, and the direction of this influence is dependent on the residue modified. As of yet no studies into whether Exo1 is phosphorylated during meiosis have been published.

1.8 Initial aims of this study

The initial aims of this study were to:

- Investigate whether Exo1 is phosphorylated in response to meiotic DSB formation in *S. cerevisiae*.
- Investigate whether the Exo1 phosphorylation state differs between mitotic and meiotic cells.
- Investigate whether mutants of mitotic phosphorylation influence the activity of Exo1 in meiosis.

This thesis describes findings from experiments investigating whether mitotic phospho-mutants of Exo1 have an impact upon Exo1 activity during meiosis by examining meiotic progression, processes and products. By creating a tagged version of Exo1 and these mutants, protein levels and modifications can be studied to determine how Exo1 is expressed and if it is phosphorylated in response to DSBs during meiosis.

2. Materials & Methods

2.1 Media and chemicals

2.1.1 Media

All media were prepared using dH₂O (deionised water) except when stated. Solutions were autoclaved using a standard program: no free steam, 15 minutes' sterilization. In some cases, solutions were filter-sterilised instead of autoclaving, using 0.22µm filters (Sartorius Stedim Biotech) attached to either syringe or vacuum container, depending on the volume. Percentage concentrations given throughout are w/v solids and v/v for liquids.

YPAD

Standard yeast growth medium containing 1% Bacto™ yeast extract (BD), 2% Bacto™ peptone (BD), 2% D-glucose (Fisher chemical), 40mg/L adenine hydrochloride (Sigma), and for solid media 2% Bacto™ agar (BD).

Yeast strains with *KanMX* or *HphMX4* genes were selected on YPAD plates containing 200µg/ml G418-disulphide (Melfords) or 300µg/ml Hygromycin B (Duchefa) respectively. Both compounds were added to molten autoclaved YPAD agar after cooling to 55°C.

For plates containing methyl methanesulphate (MMS) (Sigma), MMS was added at 0.005-0.02% to autoclaved cooled YPAD. MMS is a volatile and hazardous chemical, and must be opened under laminar flow hood. The plates must be used within 12 hours of pouring.

YPG

Medium to select against petite yeast mutants ensuring healthy mitochondria: 15% glycerol (BD), 1% Bacto™ yeast extract (BD), 2% Bacto™ peptone (BD) and 2% Bacto™ agar (BD) for solid media.

Dropout Media (Synthetic Complete -)

Medium deficient in specific amino acids to screen for yeast auxotrophies: 2% D-glucose (Fisher chemical), 0.67% yeast nitrogen base w/o amino acids (BD), 0.87g/L dropout master mix (see Table 2.1 for composition) (for preparing SC-Thr or SC-Asp media, 0.54g/litre master mix was used), 200µl/L 10N NaOH (Fisher chemical) to obtain pH 5.5, and 2% Bacto™ agar for solid media. Synthetic complete medium contains all possible supplements.

5-FOA Media

Medium for selection of *ura*- auxotrophic yeast. Make 400ml yeast synthetic complete medium, add 1g 5-fluoroorotic acid (5-FOA) (ZymoResearch) and sterilise by filtration. Autoclave 600ml dH₂O with 20g Bacto™ agar (BD), cool to 55°C and add warmed SC + 5FOA medium. Mix and pour plates.

Minimal Media

Medium to test yeast ploidy using hAG55 (a) and hAG56 (α) (strain list Table 2.3): 2% D-glucose (Fisher chemical), 0.67% yeast nitrogen base w/o amino acids (BD) and 2% Bacto™ agar (BD) for solid media.

Potassium-Acetate Media (K-Ace)

Medium to induce sporulation of diploid yeast cells: 1% potassium acetate (Sigma-Aldrich), 0.1% Bacto™ yeast extract (BD), 0.05% D-glucose (Fisher chemical) and 2% Bacto™ agar (BD) for solid media.

Supplement	Mass in dropout master mix (mg)
Adenine	800
Arginine	800
Aspartic acid	4000
Histidine	800
Leucine	2400
Lysine	1200
Methionine	800
Phenylalanine	2000
Threonine	8000
Tryptophan	800
Tyrosine	1200
Uracil	800

Table 2.1 - Mass of each amino acid for making master mix for dropout media (synthetic complete -)

The relevant amino acid was omitted from the master mix to make the corresponding dropout media, e.g. ura⁻ media would omit the 800mg of uracil.

BYTA

Medium to pre-induce diploid yeast cells for synchronous sporulation: 1% Bacto™ yeast extract (BD), 2% Bacto™ tryptone (BD), 1% potassium acetate (Sigma-Aldrich) and 50mM potassium phthalate (Sigma-Aldrich).

SPM

For medium to synchronously sporulate pre-induced diploid yeast cells: 0.3% potassium acetate (Sigma-Aldrich) and 0.02% raffinose (Sigma Aldrich).

LB (Lysogeny Broth)

Standard medium used for growth of *Escherichia coli* (*E. coli*). The formulation can be varied for salt-sensitive antibiotics. Adjust pH to 7.4 using 10N NaOH (Fisher chemical).

LB – Miller Normal salt: 1% Bacto™ tryptone (BD), 0.5% Bacto™ yeast extract, 1% NaCl (Fisher chemical)

LB – Lennox Low salt (for salt-sensitive antibiotics such as Hygromycin B or Clonat): 1% Bacto™ tryptone (BD), 0.5% Bacto™ yeast extract, 0.5% NaCl (Fisher chemical)

For solid media 1.5% Bacto™ agar was added. For selection of replicating plasmids expressing resistance markers, antibiotics were added to sterile media cooled to 55°C at the following final concentrations: Ampicillin 50µg/ml (Sigma-Aldrich), G418 50µg/ml (Sigma-Aldrich) or Hygromycin B 100µg/ml (Duchefa). Plates containing antibiotics must be used within one month of pouring.

2TY (2 x Yeast extract and Tryptone)

Medium for cultivation of *E. coli* prior to treatment for chemical competency: 1.6% Bacto™ tryptone (BD), 1% Bacto™ yeast extract, 0.5% NaCl (Fisher chemical), adjusted to pH 7.4 using 10N NaOH (Fisher chemical).

SOC (Super Optimal broth with Catabolic repressor)

Medium for initial outgrowth of *E. coli* following heat-shock during the transformation of chemically competent cells. This medium is rich, contains Mg^{2+} to support growth at higher cell densities, and glucose as a catabolic repressor, preventing expression of recombinant proteins potentially damaging to normal cell physiology. Ready-made SOC media (NEB) was used.

2.1.2 Stock solutions

Amino acid and base stocks Stock solutions of amino acids (Sigma Aldrich for individual amino acid/base stocks) were made up as w/v (g/100ml) in dH₂O and filter sterilised to concentrations specified in Table 2.2. Stocks were stored at room temperature, histidine and tryptophan were stored in opaque falcon tubes to avoid light degradation.

Blocking buffer 5% w/v skimmed milk powder (Sigma Aldrich), 50mM Tris-HCl pH 7.5, 150mM NaCl.

Proteinase K 20mg/ml proteinase K in 10mM Tris-HCl, 2mM CaCl₂ and 50% glycerol (filter sterilised before addition of proteinase K, aliquoted and stored at -20°C).

PMSF 100 mM PMSF in isopropanol. Aliquot into 1.5ml eppendorf tubes and store at -20°C.

RNase 10mg/ml RNase A in 10mM Tris-HCl pH7.5 and 22.5mM NaCl (heated to 100°C for 15 minutes, slowly cooled to room temp, aliquoted and stored at -20°C).

Protein loading buffer (PLB) 250mM Tris-HCl (pH 6.8), 9.2% SDS, 40% Glycerol, 0.2% (w/v) bromophenol brilliant blue (Sigma Aldrich), and make to required volume with dH₂O. Solution was gently warmed and rolled to dissolve before storing at -20°C as 900µl aliquots. Immediately before first use 100mM DTT was added (100µl of a 1M stock) and stored at -20°C between uses for up to one month.

Amino acid	Stock concentration (w/v)	Final concentration in 1L normal medium (mg/L)	Final concentration in 1L sporulation medium (mg/L)
Adenine sulphate	0.2	20	5
L-Arginine HCl	1	20	5
L-Aspartic acid ¹	1	100	25
L-Glutamic acid	1	100	25
L-Histidine HCl	1	20	5
L-Isoleucine	1	30	7.5
L-Leucine	1	100	25
L-Lysine HCl	1	30	7.5
L-Methionine	1	20	5
L-Phenylalanine	1	50	12.5
L-Serine	8	400	100
L-Threonine ¹	4	200	50
L-Tryptophan	1	20	5
L-Tyrosine	0.2	30	7.5
Uracil	0.2	20	5
L-Valine	3	150	37.5

¹Store in opaque falcon tubes

Table 2.2 - Stock solutions and final working concentrations of amino acids for supplementation

Amino acids were dissolved in dH₂O and filter sterilised.

TAE buffer 50x 2M Tris-acetate, 50mM EDTA (all Sigma Aldrich; autoclaved and stored at room temperature).

TBE buffer 5x 445mM Tris-base, 445mM boric acid, 10mM EDTA-disodium salt (all Sigma Aldrich; autoclaved and stored at room temperature).

TBS buffer 10x 198mM Tris-base, 1.5M NaCl, to pH 7.6 with 10N HCl (all Sigma Aldrich; autoclaved and stored at room temperature).

TBS-T 0.1% 1x TBS with 0.1% TWEEN added immediately prior to use. Stored at 4°C for up to one month.

TE 10x 100mM Tris-HCl, 10mM EDTA (all Sigma Aldrich; autoclaved and stored at room temperature).

2.2 Molecular biology techniques

2.2.1 DNA Restriction digests

Purified DNA of genomic, plasmid or PCR origin was digested with restriction enzymes according to the conditions specified by the manufacturer and using sterile MilliQ™ filtered water (mqH₂O).

- For analysis of DNA double strand break (DSB) turnover by Southern blot, 1000-2000ng yeast genomic DNA was digested with 10 units of specified enzyme for 3 hours at 37°C in a reaction volume of 20µl.
- For confirmation of point mutations in amplified DNA, 5µl of purified PCR product was digested with 10 units of specified enzyme for 1 hour at 37°C in a reaction volume of 20µl.
- For diagnostic restriction of plasmids, 1µl of plasmid DNA was digested with 10 units of specified enzyme for 1 hour at 37°C in a reaction volume of 20µl.
- For restriction of plasmids to further use in cloning, 15µl of plasmid DNA was digested with 20 units of specified enzyme for 3 hours at 37°C in a reaction volume of 20µl.

- For double digests of DNA to further use in cloning, 30µl of purified DNA was digested with 10 units of each specified enzyme for 3 hours at 37°C. The optimum buffer was determined using the online New England BioLabs Double Digest Finder resource (NEB n.d.).

2.2.2 DNA ligation

Amplified DNA fragments and plasmids for cloning were restricted as described and subsequently purified using the Monarch™ PCR & DNA Clean-up Kit (NEB) according to the manufacturer's instructions. The concentration of fragments and linearised vector were determined using a NanoDrop™ Lite spectrophotometer (Thermo Scientific). The molar ratio of vector to insert required was 1:3, and the mass of each needed was calculated using the NEBioCalculator™ v.1.5.0 online resource. The required volume of vector and insert were ligated using T4 DNA Ligase (NEB) according to the manufacturer's instructions. Ligation reactions were then transformed into chemically competent Alpha-Select Silver Efficiency cells (Bioline) for cloning.

2.2.3 Gibson Assembly

Multiple overlapping fragments of amplified DNA were ligated into a single segment of DNA suitable for transformation of plasmid construction using the Gibson Assembly method (Gibson Assembly® Cloning Kit from NEB). This method is a single reaction at 50°C with 3 components: an exonuclease to resect fragment ends to expose ssDNA, a polymerase to fill in gaps after fragments anneal, and a ligase to seal nicks in the assembled DNA. The assembly was carried out according to the vendors instructions.

2.2.4 Ethanol Precipitation of DNA

DNA from cell preparations, restriction digest or PCR was cleaned to remove reaction components or other contaminants. A 1:10 volume of 3M sodium acetate (Fisher) was added to the DNA and mixed by gentle vortexing. A 2:1 volume of ice-cold 100% ethanol (Fisher chemical) was then added to the DNA + Na-acetate, mixed by inversion, and the tubes then incubated at -20°C for 1 hour to allow the

DNA to precipitate. The samples were next centrifuged at 14,000rpm for 30 minutes at 4°C to isolate the precipitated DNA, and the pellet washed in a volume of 70% ethanol twice that used to precipitate the DNA. Following washing the DNA pellet was air-dried to remove all traces of ethanol, and resuspended in 30-50µl sterile milliQH₂O.

2.2.5 Gel Purification of DNA

DNA from cell preparations, restriction digest or PCR in need of isolation from contaminating DNA was separated by agarose gel electrophoresis in 1% agarose with 1 x TAE and ethidium bromide. The DNA to be isolated was determined by comparison with a standard size ladder, GeneRuler™ 1kb (Thermo Fisher Scientific), and cut from the gel using a razor blade on a UV visualiser, keeping UV exposure to a minimum to avoid DNA damage. DNA was then purified from the agarose using the QIAquick™ Gel Extraction Kit (Qiagen) or the Monarch™ DNA Gel Extraction Kit (NEB) according to the manufacturer's instructions.

2.2.6 Polymerase chain reaction (PCR)

Routine PCR

For PCR of templates for diagnostic use, amplification of probe DNA, or uses other than amplification of DNA to be used in cloning and expression, a non-proofreading enzyme was used, MangoTaq™ from Bionline. The error rate of MangoTaq™ is between 0.8 – 2.7x10⁻⁴/bp. For a standard 50µl reaction:

- 10µl 5x MangoTaq™ reaction buffer
- 2mM MgCl₂ (2µl 50mM stock)
- 2mM dNTP (1µl 100mM stock)
- Template DNA (100-1000ng gDNA, 0.1-10ng plasmid or 1-100ng PCR)
- 0.5µM each Primer (1µl 25µM stock)
- 0.02U/µl MangoTaq™ enzyme (1µl of 1U/µl as sold)

Typical thermo-cycling steps were 94°C initial denaturation for 2 minutes, followed by 25-35 cycles of: 94°C 30 seconds denaturation, x°C for 30 seconds annealing and 72°C for y seconds extension, where x = the lower of the two

recommended primer annealing temperatures and $y = 30$ seconds per kb of template DNA; e.g. an expected product of 3.8kb would require 120 seconds extension. Reactions were terminated with a final extension of 5 minutes at 72°C and then held at 10°C until subsequent use, or stored at -20°C.

Proofreading PCR

For high fidelity PCR of templates to be used in cloning and transformation, an enzyme with proofreading activity was used, Q5™ DNA Polymerase from NEB. The error rate of Q5™ is between 0.6 – 1.4x10⁻⁶/bp. For a standard 50µl reaction:

- 10µl 5x Q5 reaction buffer
- 10µl 5x Q5 High GC enhancer (optional)
- 200µM dNTP (1µl 10mM stock)
- Template DNA (100-1000ng gDNA, 0.1-10ng plasmid or 1-100ng PCR)
- 0.5µM each Primer (1µl 25µM stock)
- 0.02U/µl Q5™ enzyme (0.5µl of 2U/µl as sold)

Typical thermo-cycling steps were 98°C initial denaturation for 2 minutes, followed by 25-35 cycles of: 98°C 30 seconds denaturation, x °C for 30 seconds annealing and 72°C for y seconds extension, where x = the lower of the two recommended primer annealing temperatures plus ~3°C (used NEB T_m Calculator for optimum) and $y = 20$ seconds per kb of template DNA; e.g. an expected product of 3.8kb would require 80 seconds extension. For targets longer than 6kb an extension time of 45kn/second was used. Reactions were terminated with a final extension of 5 minutes at 72°C and then held at 10°C until subsequent use, or stored at -20°C.

2.2.7 PCR clean-up

DNA from PCR reactions or restriction digests was purified to remove enzymes, primers, detergents and any other reactants, using the Monarch™ PCR & DNA Clean-up kit (NEB). DNA was purified according to the manufacturer's instructions, and finally eluted in 30-50µl sterile mqH₂O. To concentrate products, up to 4 identical PCR reactions were combined and purified on one column, and

finally eluted into 50µl sterile mqH₂O. Obtaining more concentrated products permitted smaller volume reactions for downstream cloning steps.

2.2.8 Colony PCR

Yeast Colony PCR

For quick screening of large numbers of yeast colonies, diagnostic PCR was carried out on crudely extracted template DNA of fresh colonies. A single colony was picked from the plate using a 1µl sterile loop and resuspended in 10µl of zymolyase solution (500U/ml in SCE; 5mg/ml 100T zymolyase MP Biomedicals). This was incubated at 37°C for 15 minutes to spheroplast the cells. 1µl of this reaction was added to a 50µl routine PCR reaction (section 2.2.6) as template DNA.

E. coli Colony PCR

For quick screening of large numbers of *E. coli*, diagnostic PCR was carried out on crudely extracted template DNA of fresh bacterial colonies. A sterile p10 pipette tip was touched to the middle of a colony, and the recovered cells resuspended in 10µl sterile mqH₂O. The cells were boiled for 10 minutes at 95°C to destroy the cells and then immediately transferred to ice for 5 minutes. The tubes were then centrifuged at 14,000rpm for 1 minute to pellet cell debris, leaving any DNA in the supernatant. 4µl of this supernatant was added to a 25µl routine PCR reaction (section 2.2.6) as template DNA.

2.2.9 Simple extraction of yeast DNA

Standard extraction of yeast genomic DNA was carried out on either 1.5ml of a standard overnight culture (section 2.5.5) or single colonies (section 2.5.2) using the MasterPure™ Yeast DNA Purification kit (Epicentre) according to the manufacturer's instructions. DNA pellets were air-dried and resuspended in 30-50µl of sterile mqH₂O.

2.2.10 CTAB extraction of yeast DNA

RNase 10mg/ml RNase A in 10mM Tris-HCl pH7.5 and 22.5mM NaCl (heated to 100°C for 15 minutes, slowly cooled to room temp, aliquoted and stored at -20°C).

Proteinase K 20mg/ml proteinase K in 10mM Tris-HCl, 2mM CaCl₂ and 50% glycerol (filter sterilised before addition of proteinase K, aliquoted and stored at -20°C).

Spheroplasting solution 1M sorbitol, 50mM KPO₄ pH7.5, 10mM EDTA pH7.5 (filter sterilised and stored at 4°C).

CTAB Extraction solution 3% CTAB (hexadecyltrimethylammonium bromide (Sigma Aldrich)), 100mM Tris-HCl pH7.5, 25mM EDTA pH8.0, 2M NaCl, 2% PVP₄₀ (Fisher). CTAB and PVP₄₀ were dissolved separately prior to filtration and microwaved to dissolve. The solutions were filter sterilised to combine, with PVP₄₀ and CTAB filtered after the Tris, salt and EDTA so as to avoid problems caused by viscosity. Once filtered and mixed solution was stored at 37°C.

CTAB Dilution solution 1% CTAB, 50mM Tris-HCl pH7.5, 10mM EDTA pH8.0 (filter sterilised and stored at room temperature).

This DNA extraction method is modified from that of (Allers & Lichten 2000) and is more complex and gentle than a simple kit extraction. This is to minimise damage caused to the DNA during the extraction process, maintaining the integrity of the DNA for subsequent Southern analysis. The increased complexity renders it more time-consuming as only a limited number of samples can be processed simultaneously. Frozen cell pellets harvested from meiotic time courses (section 2.5.12) were thawed on ice and washed in 1ml of ice-cold Spheroplasting solution. Cells were centrifuged at 4000rpm for 1 minute and resuspended in 100µl Spheroplasting solution with 50U/ml 100T zymolyase (0.5mg/ml) and 1% B-mercaptoethanol (Sigma Aldrich). Cells were then incubated at 37°C for 10 minutes on a Thermomixer at 500rpm. Next 200µl of CTAB extraction solution

was added along with RNase A to 0.5mg/ml final (10µl was sufficient), mixed thoroughly by pipetting, and left at room temperature for 10 minutes with occasional inversion. Following RNase treatment, proteinase K was added to 0.5ml/ml final (10µl was sufficient) and mixed by gentle pipetting and inversion. Samples were then incubated at 37°C for 15 minutes on a Thermomixer at 500rpm. During this time CTAB-DNA complexes form, and are then extracted by the addition of 100µl chloroform : isoamylalcohol (24:1, both Sigma Aldrich). The tubes were then vortexed hard for 20 seconds, rested for 2 minutes and then vortexed for a further 20 seconds. The samples were then centrifuged at 14,000rpm for 5 minutes at 18°C. The aqueous upper phase, usually ~300µl and containing CTAB-DNA complexes, was transferred to a fresh tube. Extreme care must be taken at this stage not to disturb the interphase or co-extract any of the solvent beneath. Three volumes (usually 900µl) of CTAB dilution solution were layered on top by gentle pipetting down one side of the tube, and the phases mixed by gentle inversion 10-15 times. At this stage cotton wool-like strands should have appeared. The tubes were left at 4°C for between 30 minutes and 10 hours to allow CTAB-DNA complexes to fully precipitate. These complexes were then pelleted by centrifugation at 14,000 rpm for 1 minute and the pellet washed twice in 1ml ice-cold 0.4M NaCl, 10mM Tris-HCl pH7.5, 1mM EDTA pH8.0. DNA at this stage was very “sticky” and care was taken to avoid the pellet becoming stuck to the side of a pipette tip. After washing the pellet was dried briefly before resuspension in 300µl ice-cold 1.42M NaCl, 10mM Tris-HCl pH7.5, 1mM EDTA pH8.0. DNA was then precipitated by the addition of 600µl 100% ethanol. Precipitated DNA was washed twice in 600µl of 70% ethanol and left to air dry. Centrifugation may be required between each wash if the pellet is particularly small or fragmented. At this stage the pellet would become translucent. Dry DNA pellets were resuspended in 30-80µl sterile mqH₂O depending on the pellet size. DNA was left overnight at 4°C and then the tubes were flicked to ensure the pellet was fully dissolved before quantification. Once DNA was fully dissolved the solution would become more viscous and splash less upon flicking.

2.2.11 Measurement of DNA concentration in solution

DNA concentration was measured by two methods; by densitometry of DNA visualised by gel electrophoresis or by using the NanoDrop™ Lite spectrophotometer (Thermo Scientific).

Densitometry

DNA was separated by agarose gel electrophoresis in 1% agarose with 1 x TAE and visualised with ethidium bromide (Sigma Aldrich) under UV light. The DNA to be quantified was compared with a band of similar mass in the standard size ladder, GeneRuler™ 1kb (Thermo Fisher Scientific). A digital image of the gel was taken using a ChemiDoc MP imager (BioRad) and analysed using Quantity-One 1-D analysis software (BioRad). The signal intensity for a band of similar mass to the sample and known concentration was noted from the ladder, and used as a standard to determine the sample concentrations by relative intensity per unit loaded (in μl). This method was useful for quantifying DNA for Southern blot; it gave an indication of the intensity of the samples on a gel relative to one another, as even loading of lanes relative to each other is important for Southern blot analysis.

NanoDrop™ Lite

The sample pedestal and light source were cleaned by pipetting several microliters of sterile mqH_2O directly on, closing the lid and then drying with a Whatman lens tissue (Fisher scientific). The instrument was blanked twice using $1\mu\text{l}$ of sterile mqH_2O , and then sample measurements taken twice for $1\mu\text{l}$ of sample. If there was >1% variation between, a third sample was taken and the mean calculated.

2.2.12 Native DNA gel electrophoresis

DNA fragments were separated by size using agarose gel electrophoresis. Agarose gels were prepared to the desired percentage (w/v), 1% for standard analysis, in 1 x TAE, and samples prepared by addition of 6 x purple loading dye

(NEB). For quantitative Southern blot analysis, digested yeast genomic DNA (section 2.2.1) was separated in 250ml 25cm x 15cm 0.75% agarose gels in 1% TAE at 75 volts for 17.5 hours. 200µg/litre ethidium bromide was added to the running buffer before running for all native agarose gels. For separation of yeast genomic DNA for Southern blot the standard size marker used was *BstEII*-digested Lambda DNA (NEB) and for standard analysis the size marker used was GeneRuler™ 1kb ladder. Gels were visualised on a ChemiDoc MP imager.

2.2.13 Pulsed-field gel electrophoresis

Unlike standard native gel electrophoresis, which mobilises DNA within a linear electric field, pulsed field electrophoresis (PFGE) exposes DNA to a field which periodically changes direction. The field switches between the *y* axis and axes 60° either side for equal pulse times, resulting in a net forward movement. By varying the switching times this method permits resolution of very large molecules, such as entire chromosomes, or chromosomes fragmented during meiosis. Volumes of cells were taken from meiotic time courses (30ml from hours 0-4 and 15ml from hours 5-8) and centrifuged at 3500rpm for 5 minutes. The cell pellets were washed twice with 5ml 50mM EDTA pH7.5 and then resuspended in 100µl 50mM EDTA pH7.5. Cells were stored on ice while a solution of 1% low melting-point agarose (Fisher) (1% LMP agarose, 0.125M EDTA pH7.5 kept at 60°C until use) and Solution I (5% β-mercaptoethanol, 25U/ml 100T zymolyase (0.25mg/ml) in 1 x SCE kept on ice until use) were prepared. 200µl of Solution I : 1% LMP agarose (1:5) was added to briefly warmed cell pellets and then the resuspended cells cast into moulds (BioRad), around 90µl per plug, to create a set of plugs. These were set for 10 minutes at 4°C. During setting time Solution II was prepared (10mM Tris-HCl pH7.5, 7.5% β-mercaptoethanol, 1mg/ml RNase made in 0.5M EDTA pH7.5, not water). After setting the plugs were incubated in 3ml of Solution II at 37°C for 1 hour, during which Solution III was prepared (0.25M EDTA pH7.5, 10mM Tris-HCl pH7.5, 1% sarkosyl (Sigma Aldrich) and 1mg/ml proteinase K stored at 4°C until use). Following incubation, the plugs were transferred to 3ml of pre-warmed Solution III and incubated at 50°C overnight. The next day the plugs were washed in 50mM EDTA pH7.5 and transferred into 0.5 x TBE for cutting to

the appropriate size for PFGE (~4 x 6mm, the width of the gel comb). 150ml 1.3% agarose in 0.5 x TBE was prepared and kept at 50°C. A single cut fragment from each time point was applied to the tooth of a gel comb (BioRad) as well as 1mm depth of PFGE Mid-range PFGE Marker Ladder I (NEB; discontinued) and the plugs sealed with a drop of 1.3% agarose applied using a disposable Pasteur pipette (Sarstedt) and set at 4°C for 10 minutes. The gel was cast with the comb and attached plugs in a pre-chilled tray (BioRad) and set at 4°C for 30 minutes. Following gentle removal of the comb, the wells created were filled in with agarose prior to running. Gels were run using a CHEF-DRII system (BioRad) with run condition as follows: 120° field angle, 6 volts/cm, initial and final switch time 15 seconds, run for 45 hours at 14°C.

2.2.14 Southern blotting

20 x SSPE 3.6M NaCl, 200mM NaH₂PO₄, 20mM EDTA, pH 7.4

Following digestion of genomic DNA (section 2.2.1) or production of genomic DNA plugs (section 2.2.12) and resolution of DNA by DNA gel electrophoresis (section 2.2.11 and 2.2.12), agarose gels were washed in dH₂O with gentle shaking for 10 minutes. Next the gel was soaked in 1L 0.25M HCl for 30 minutes with gentle shaking to depurinate the DNA, followed by a further water wash and then soaking in 1L 0.4M NaOH for 45 minutes with gentle shaking to denature the DNA. In this time the apparatus for vacuum blotting was prepared; this involved the soaking of a support screen, blue mask, Whatman 3MM paper and Hybond N+ nylon membrane (Amersham) (both cut to suitable size for gasket and gel) in dH₂O for 5 minutes before arranging onto the VacugeneXL transfer system (Amersham). The agarose gel was then transferred onto the apparatus, ensuring no bubbles or gaps between the gel, mask and nylon membrane. The DNA was transferred onto the membrane at ~75mbar for 2 hours in 0.4M NaOH. Following transfer the mask corners were marked and the membrane rinsed for 2 minutes in 2 x SSPE to neutralise residual NaOH. The DNA was then cross-linked to the membrane using a UV cross-linker (XL-1500 Spectronics). If being stored before hybridisation, membranes were air dried and wrapped in cling-film to be kept in a

dark, dry cupboard until further use.

2.2.15 Generation of ³²P-labelled probes

DNA probes for Southern blot hybridisation were prepared by PCR of yeast genomic DNA in several reaction volumes. The total volume was then pooled for gel electrophoresis and the probe DNA isolated and purified by gel extraction. For PFGE, the CHA1 probe was used (Table 2.7). For the ARE1 hotspot, the ARE1 probe was used (Table 2.7). ³²P-dCTP (Amersham) labelled DNA probes were synthesised using the dCTP High Prime random priming labelling kit (Roche); the quantity of probe used was between 50-100ng of probe template per reaction and 0.2ng of *Bst*EII-digested Lambda DNA (NEB) for standard gels (not including PFGE). Probe and ladder were boiled for 5 minutes in an 11µl volume followed by 5 minutes on ice. The tube was spun briefly and 4µl d-CTP High Prime added before continuing in the radiation lab. Here, 5µl of ³²P-dCTP was added to the reaction and the tube incubated at 37°C for 30 minutes. Following incubation, the labelled probe was isolated from unincorporated nucleotides using a G30 Biospin column (Bio-Rad) at 4500rpm for 4 minutes.

2.2.16 Hybridisation of Probe to Membrane

Pre-Hybridisation Buffer 2 x SSPE, 1% SDS, 5% w/v skimmed milk powder (Sigma Aldrich), 125µg/ml boiled salmon sperm DNA

Hybridisation Buffer 2x SSPE, 1% SDS, 5% w/v skimmed milk powder, 10% dextran-sulphate (Sigma Aldrich), 125µg/ml salmon sperm DNA

Washing Buffers First wash: 2 x SSPE, 0.1% SDS

Second wash: 0.5 x SSPE, 0.1% SDS

Third wash: 0.2 x SSPE, 0.1% SDS

Membranes were pre-hybridised for 3 hours to overnight at 65°C in 40ml of pre-hybridisation buffer using a rolling oven in tubes washed and pre-warmed. Tubes were washed before use with three steps; firstly in warm water and Decon-90

(Fisher), secondly rinsed with hot water and sprayed with ethanol before air drying, and finally the inner surface was rinsed with SigmaCote™ (Sigma Aldrich) before air drying and pre-warming. Labelled DNA probes (section 2.2.15) were denatured for 5 minutes at 100°C in 250µl pre-boiled salmon sperm DNA (10mg/ml), chilled on ice and then added to 20ml of hybridisation buffer pre-heated to 65°C. The pre-hybridisation buffer was then poured off and the hybridisation buffer with probe added to the membrane. Membranes were incubated at 65°C in a rolling oven over overnight. Subsequently membranes were washed in each washing buffer sequentially for 30 minutes each at room temperature with shaking. The signal of bands versus background was checked using a Geiger counter between the second and third wash to modify the time needed for the final wash if necessary. A well hybridised membrane should have a background <10 counts and band signal of ~50 counts. Membranes were then air-dried and wrapped in cling-film before exposure to a blanked phosphor-screen (K-screen, Kodak).

2.2.17 Scanning densitometry

Phosphor screens were scanned following appropriate exposure using a Personal FX phosphorimager (Bio-Rad). The signal detected was quantified using Quantity One 1-D software (Bio-Rad). Bands to be measured were identified and the signal isolated by lane identification and boxes applied to the band limits. Parameters were added to exclude background signal on a rolling lane-by-lane basis, and then the relative trace signal for each band quantified using the “trace quantity” function, integrating the area under each peak in isolated regions and deducting the background signal. These values were then exported as an Excel (Microsoft Office) spreadsheet for further analysis.

2.2.18 Stripping of Southern Blot for re-Probing

For re-probing, the membrane was washed three times, with shaking, in 500ml boiling 0.1% SDS, each wash lasting until the buffer cooled to ~45°C, usually around 10-15 minutes. The blot was then rinsed in 2 x SSPE and re-hybridised as

described (section 2.2.16).

2.3 Biochemistry techniques

2.3.1 Soluble protein extraction

Lysis Buffer 50mM Tris-HCl pH 8.0, 75mM NaCl, 10% glycerol, 1% NP40 (Sigma Aldrich), 1mM PMSF, 1 complete protease inhibitor tablet EDTA free/20ml (Roche) plus phosphatase inhibitors – *20mM sodium pyrophosphate, 30mM sodium fluoride, 60mM glycerophosphate and 2mM sodium orthovanadate (all Sigma Aldrich)*. Volume was made up with sterile mqH₂O. For lysis buffer without phosphatase inhibitors, sodium molarity was restored by the addition of extra NaCl.

25 O.D.s of cells were harvested from either exponentially growing cells (section 2.5.7) or synchronous meiotic cell cultures (section 2.5.12) and PMSF (Sigma Aldrich) added to a final concentration of 5mM. Cells were incubated on ice for 5 minutes and then centrifuged at 4,500 rpm for 2 minutes. The cells were then washed in 1ml lysis buffer and frozen in liquid nitrogen to be stored at -80°C until ready for the next step. Pellets were thawed on ice and resuspended in 200µl lysis buffer. An equal volume of sterile glass beads (Sigma Aldrich) was added and the cells subjected to bead beating (Biospec Mini-Beadbeater-24) 4 x 20 seconds with 5 minutes on an ice block between. A hole was punctured in the base of the eppendorf using a hot 19G Microlance needle (BD) and the lysate removed by brief centrifugation into a fresh tube. The lysate was cleared by centrifugation at 14,000 rpm, 4°C for 10 minutes. The supernatant was transferred to a fresh eppendorf and total protein concentration determined by Bradford assay (section 2.3.3). 30µg of protein was loaded onto a polyacrylamide gel, made up to 10µl final volume containing 1 x protein loading buffer (PLB).

2.3.2 Total protein extraction

4 O.D.s of cells were harvested from either exponentially growing or synchronous meiotic cell cultures and centrifuged at 5,000rpm for 5 minutes. The cell pellets were transferred in 1ml distilled water to a 1.5ml screw cap tube and

harvested by micro-centrifugation at 13,000rpm for 1 minute, before being frozen in liquid nitrogen; at this stage cells could be kept at -80°C or thawed immediately on ice for use. Cell pellets were re-suspended in 500µl ice-cold 0.2M NaOH + 0.2% β-mercaptoethanol (Sigma-Aldrich), and incubated on ice for 10 minutes. Trichloroacetic acid (TCA) (Fisher chemical) was added to a final concentration of 5% and incubated on ice for 10 minutes. The cells were then harvested by micro-centrifugation at 13,000rpm for 5 minutes at 4°C and the pellet re-suspended in 15µl 1M Tris-base pH 9.4. 135µl 1x protein loading buffer (PLB) was then added. The tubes were boiled at 95°C for 10 minutes and then placed on ice for 2 minutes. Insoluble protein was pelleted by micro-centrifugation at 13,000rpm 4°C for 1 minute, and 10µl supernatant loaded onto a polyacrylamide gel.

2.3.3 Determination of protein concentration

Bradford reagent (BioRad) was diluted 1:4 with m_qH₂O. Bovine serum albumin (BSA) (New England BioLabs) was diluted to 1mg/ml in lysis buffer to use as a standard. 1µl, 2µl, 5µl, 10µl and 15µl of the 1mg/ml BSA was added to 1ml diluted Bradford reagent, and vortexed to mix. The standards were incubated for 2-3 minutes and then the O.D.₅₉₅ measured. 1µl of the sample to be quantified was then added to 1ml diluted Bradford reagent, mixed, and incubated for the same length of time as the standards. O.D.₅₉₅ was then measured for the samples. The values for the standards were plotted onto a scatter graph using Microsoft™ Excel, and a line of best fit assigned to generate the gradient equation. This equation was then used to approximate the total protein concentration of the samples. A desirable concentration is >8µg/µl if subsequent experiments are required.

2.3.4 Immunoprecipitation (IP) of target proteins

50µl of Dynabeads™ Protein A (ThermoFisher Scientific) was washed three times in 200µl lysis buffer using a magnetic rack. The beads were incubated with 5µl anti-V5 (AbD Serotec Ltd) in 100µl lysis buffer on a wheel at room temperature for 40 minutes, followed by washing three times in ice-cold 200µl lysis buffer using the magnetic rack. The beads were then incubated with the volume of lysate required for 1-2mg of protein, made up to 200µl with ice-cold

lysis buffer, on a wheel for 1 hour at 4°C. At this stage samples requiring phosphatase treatment may be processed (section 2.3.5). Next, the beads and bound protein were washed three times in 400µl lysis buffer (if sample was split for phosphatase treatment, the untreated remaining sample was washed in 200µl and the treated samples in 100µl). Finally, the beads were resuspended in 48µl (or a proportion of this if split for phosphatase treatment i.e. 24µl, 12µl and 12µl) 1x PLB diluted with lysis buffer from 4x stock. The samples were boiled for 5 minutes, briefly centrifuged, and put onto a chilled magnetic rack to remove the beads from solution. 12µl of supernatant was loaded onto a polyacrylamide gel.

2.3.5 Phosphatase treatment of immuno-precipitated protein

100µl of the incubating IP reaction was isolated and split across two fresh tubes equally. One half was washed three times with 100µl lysis buffer void of phosphatase inhibitors, while the other half was washed with 100µl normal lysis buffer, both using the magnetic rack. The beads were then resuspended in 40µl lysis buffer (+/- phosphatase inhibitors as appropriate) and PMP buffer, MnCl₂ and 1µl Lambda phosphatase (New England BioLabs) were added. The reaction was shaken at 30°C for 30 minutes at 500rpm using a Thermomixer (Eppendorf). Following treatment, the samples continued to be processed as described (section 2.3.4).

2.3.6 SDS-polyacrylamide gel electrophoresis

Stacking Gel 170mM Tris-HCl pH 6.8, 3.6% acrylamide (National Diagnostics Protogel30), 1% SDS, 1% APS (Fisher chemical), 0.15% TEMED (Sigma Aldrich)

8% Resolving Gel 390mM Tris-HCl pH 8.8, 8% acrylamide, 1% SDS, 1% APS, 0.15% TEMED

Protein samples prepared in 1x PLB and boiled for 5 minutes at 95°C, and 10µl ColorPlus™ Pre-stained Protein Ladder Broad Range (New England BioLabs), were separated on 8% mini SDS-PAGE gels (Mini-PROTEAN™ Tetra vertical electrophoresis cell) in Tris-Glycine SDS running buffer (Invitrogen™ Novex™).

Proteins denatured in the presence of SDS and reducing agents acquire a more linear shape with a uniform charge-to-mass ratio, proportional to their molecular weight, allowing separation based on size. Routinely gels were run at 120 volts for 120 minutes at 30 milliamps, or until the 50kDa marker was nearing the bottom of the gel. Gels were then either stained with Instant *Blue*[™] Ultrafast Protein Stain (Sigma Aldrich) or prepared for Western blot.

2.3.7 Western blotting

Proteins were transferred from SDS gel onto nitrocellulose membrane (Amersham Protran[™] 0.45 NC) for 12 minutes using a large MW program on the Pierce[™] Power Blotter semi-dry transfer system (Thermo Fisher Scientific). The membrane was briefly rinsed with dH₂O and incubated with Ponceau stain (Thermo Fisher Scientific) to visualise transferred protein bands.

2.3.8 Immunodetection of blotted proteins

Membranes were rinsed in TBS-0.1% TWEEN (TBS-T) and then incubated with gentle agitation in blocking buffer at room temperature for at least one hour, to reduce non-specific binding. The membrane was then incubated with primary antibody, diluted appropriately in blocking buffer, at 4°C with gentle agitation, for 90 minutes to overnight. Next the membrane was washed four times with TBS-T for 3 minutes each, and once with TBS, before incubation with the secondary antibody diluted appropriately in blocking buffer for one hour at 4°C. The membrane was washed as previously and the bands detected on a Gene-NOME visualizer using high-sensitivity chemi-luminescent substrate (Millipore).

2.4 *E. coli* techniques

2.4.1 Production of DH5α cells chemically competent for transformation

DH5α cells from -80°C stocks were streaked onto a 2TY plate for single colonies, and incubated at 37°C overnight. 100ml of 2TY was inoculated with a single colony using 1 1µl sterile loop, and incubated with vigorous shaking at 37°C to an O.D.₅₅₀ of 0.5. Cells were harvested by centrifugation at 4°C 6000rpm and resuspended in

25ml TFBI (100mM RbCl, 50mM MnCl₂, 30mM K-acetate, 10mM CaCl₂, 15% glycerol, pH5.8), and incubated on ice for 15 minutes. Cells were harvested as previously, resuspended in 4ml TFBII (10mM MOPS, 10mM RbCl, 75mM CaCl₂, 15% glycerol, pH6.8), and incubated on ice for 15 minutes. 100µl aliquots were snap-frozen in liquid nitrogen and stored at -80°c.

2.4.2 Transformation of chemically competent *E. coli* cells

DNA for transformation (1-50ng of purified plasmid or up to 15µl of a ligation reaction) was incubated with 100µl of chemically competent *E. coli* cells (DH5α or Alpha-Select silver efficiency (BioLine)) in sterile 1.5ml eppendorf tubes on ice for 30 minutes, followed by heat shock at 42°c for 90 seconds. The tubes were then immediately transferred back on to ice for 2 minutes, and 200µl SOC media added. The cells were allowed to grow for 1 hour at 37°c with agitation. Appropriate antibiotic selection LB plates were dried in a sterile hood in this time. Following this growth period, the tubes were centrifuged for 2 minutes at 6000rpm and the cells resuspended in 200µl sterile mqH₂O. Cells were spread onto the pre-dried plates by gently shaking with sterile glass beads 5mm (VWR) until the surface appeared dry. For each reaction two plates were spread, one with 50µl of cells and the second with the remaining 150µl of cells, to allow for variable transformation efficiency. Plates were incubated at 37°c

2.4.3 Small-scale isolation of plasmid DNA (Minipreps)

5ml LB medium with the appropriate antibiotic (section 2.1.1) was inoculated with *E. coli* cells from a single colony following transformation or recovery from a freezer stock. The culture was incubated at 37°c on a wheel overnight and then plasmid extracted using the QIAprep™ Spin Miniprep Kit (Qiagen) or the Monarch™ Plasmid Miniprep Kit (NEB) according to the manufacturer's instructions. Plasmid was eluted in 50µl mqH₂O and quantified using a NanoDrop™ Lite spectrophotometer.

2.5 Growth and culture of *S. cerevisiae*

The majority of strains used in this study were of the SK1 background; this background facilitates synchronous sporulation as it will readily and rapidly sporulate following nitrogen starvation when in the presence of a non-fermentable carbon source, such as potassium acetate. This is thought to be due to the expression of genes involved in the Ume6 regulon, rendering SK1 strains better at respiration and responding to acetate induction when compared to other *S. cerevisiae* strains, such as W303 (Williams et al. 2002).

2.5.1 General methods for production of yeast strains with desired phenotype

Using strains already containing the required mutations, it was possible to produce haploids with combinations of desired mutations. Haploids containing the desired mutations were mated, and the resulting diploids sporulated and subsequently dissected to allow selection of haploid progeny containing the desired genotype after random segregation of alleles.

Correct genotypes were determined by a number of ways. Primarily, as most non-wild type alleles were marked with genes required for amino-acid prototrophy or drug resistance, correct strains could be identified by growth on SC- plates lacking the appropriate supplement or on plates containing the corresponding drug. When the same marker allele was required more than once in the same strain (e.g. two alleles marked by KanMX resistance) positive colonies were only picked from tetrads that segregated 2:2 on the appropriate plates; e.g. 2 Kan⁺: 2 Kan⁻ on G418-containing plates, indicating the presence of both marked alleles in those haploids alone. Where no prototrophic or resistance marker was available for a particular allele, PCR was used with primers specific to the locus of interest. This was the case for the screening of colonies for VDE at the *TFP1* (or *VMA1*) locus; PCR of the locus positive for VDE would yield a larger fragment than that without, a difference observable by gel electrophoresis. For loci containing only a differing sequence, if the mutation introduced or abolished the presence of a restriction site, it was necessary to use restriction digest and subsequent gel

electrophoresis following PCR to identify the mutated allele. Haploid colonies were only selected from four spore viable (on YPAD) tetrads.

In some cases, several rounds of mating and dissection would be required to produce the final experimental diploid or haploid strains. The haploid strain list (Table 2.3) contains only strains from which experimentally relevant diploids originate, not all intermediates necessary prior to strain completion. The diploid list (Table 2.4) contains all strains used in experiments.

For construction of VDE cut site or endonuclease expressing diploids, it was essential to not cross haploids expressing VDE nuclease (*TFP1::VDE*) with those containing the cut site (*arg4-vde*) until production of the final experimental diploid. This prevented unwanted VDE restriction and loss of cut site during mating and dissection.

2.5.2 Production of single yeast colonies

Yeast strains recovered from -80°C stocks were first patched on to YPG plates for 24 hours to select for healthy mitochondria. Cells were then streaked to fresh YPAD plates using a sterile flat-bladed toothpick. Colonies were visible after 24 hours' growth at 30°C and ready to use after 48 hours. Plates were always incubated inverted (lid-side down) and preferably in a loose-lidded box or bag to maintain humidity, protecting the agar from desiccation.

2.5.3 Mating of haploid yeast colonies

Haploids of *a* and α mating type when grown as a mixed population may undergo spontaneous cell fusion to produce a diploid (*a*/ α) cell. Approximately equal quantities of fresh *a*/ α haploid colonies with desired genotype were mixed in a patch on a fresh YPAD plate in an area approximately 1cm², and the plate incubated at 30°C overnight. The following afternoon the patch was streaked to a fresh YPD plate to produce single colonies. After 48 hours growth at 30°C colonies were checked for ploidy by crossing with mating type testers (hAG55 *MATa*/hAG56 *MAT α*) (section 2.5.4). Diploid cells were re-streaked to fresh YPAD

plates and prepared for storage at -80°C (section 2.5.6).

2.5.4 Checking of Colony Mating Type & Ploidy

Single colonies of interest were picked and streaked to a fresh YPAD plate, each in a line parallel to the next like rungs of a ladder. A clean microscope slide edge was used to transfer hAG55 MAT α or hAG56 MAT α cells to the plate, as the ladder struts, intersecting the rungs distally to create an area of mixed tester and strain of interest at each pole. Following overnight incubation at 30°C the plates were replicated onto minimal media and incubated for a further 24-48 hours. Haploids were identified by growth on minimal media and mating type noted by growth when combined with either hAG55 MAT α or hAG56 MAT α cells. In the case of mating type tests for dissection plates, it was not necessary to pick individual colonies. Instead the dissection was replicated onto a fresh YPAD plate, followed by replication of a plate with hAG55 MAT α or hAG56 MAT α cells growing as a lawn. This was then incubated and replicated to minimal media as previously described and growth on minimal media used to deduce mating type.

2.5.5 Standard liquid cultures

A fresh single colony was inoculated into 10ml liquid YPAD in a 50ml Erlenmeyer flask and, following brief vortexing, incubated at 30°C overnight with vigorous shaking. Where cells appeared to clump or flocculate, incubation at 25°C instead of 30°C would sometimes resolve this.

2.5.6 Storage of yeast clones at -80°C

To prevent spontaneous sporulation of diploids, or acquisition of mutations, yeast cell clones were stored at -80°C in 25% glycerol. Cells from overnight liquid YPAD cultures were added to a 2ml glass vial containing 1ml autoclaved 50% glycerol. Duplicate tubes were made and labelled, and the strain genotype catalogued in a communal Microsoft™ Excel folder.

2.5.7 Culture of exponentially growing yeast

10ml liquid YPAD in a sterile 50ml Erlenmeyer flask was inoculated with a single colony at 9am and incubated until the same afternoon at 25°C. The O.D.₆₀₀ was measured and an appropriate volume for inoculation of overnight culture to obtain 10 O.D.s of exponentially growing cells in 15ml YPAD was calculated using the following equation:

$$\left[\frac{\left(\frac{\text{Desired O.D} \times \text{ml YPD}}{2^{\text{hours/doubling time}}} \right)}{\text{O.D}_{600}} \right] = \text{no. ml to inoculate}$$

E.g. $\left[\frac{\left(\frac{0.67 \times 15}{2^{(17/1.45)}} \right)}{1.35} \right] = 2.2 \times 10^{-3} \text{ ml to inoculate (2.2}\mu\text{l) into 15ml}$

2ml of the overnight culture was inoculated into 50ml liquid YPAD and incubated at 30°C for 1 hour on a shaking platform. When the culture optical density₆₀₀ (OD₆₀₀) reached 0.2-0.5, cells were harvested by centrifugation at 2000rpm for 5 minutes.

2.5.8 Lithium-acetate high efficiency transformation

Exponentially growing cells were harvested (section 2.5.7), washed twice in 5ml 100mM lithium acetate (Sigma Aldrich) and pelleted by centrifugation at 2000rpm for 5 minutes. The cell pellets were re-suspended in 200-500μl 100mM lithium acetate – depending on the size of the cell pellet – and 50μl aliquots were incubated at 30°C for 30 minutes. During this time, 10mg/ml salmon sperm DNA (Sigma Aldrich) was denatured at 95°C for 5 minutes, and then chilled on ice. 240μl 50% polyethylene glycol (PEG) (Sigma Aldrich), 36μl 1M lithium acetate, 25μl salmon sperm DNA and 20μl transforming DNA (50-200ng plasmid, 500ng-1μg PCR) were added to each aliquot of cells in this order. The cells were incubated at 30°C for 30 minutes and then heat shocked at 42°C for 15 minutes. Cells were harvested by micro-centrifugation at 6000rpm for 5 minutes, re-suspended in 1ml YPAD and then incubated at 30°C for 90 minutes with shaking.

Cells were harvested by centrifugation at 2000rpm for 5 minutes and re-suspended in 150µl of distilled water, then spread onto appropriate plates. The plates were incubated at 30°C for 48 hours.

2.5.9 Bleomycin-induced DNA damage of cells

Bleomycin is a DNA intercalating agent that can induce both single and double strand breaks. Cells were grown overnight using the calculation in section 2.5.7 to O.D.₆₀₀ 0.8 in YPAD, in a volume sufficient for the desired number of samples for protein extraction. Once cells were O.D.₆₀₀ 0.8, bleomycin (Melfords) was added to a final concentration of 50µg/ml from a 50mg/ml stock. The cultures were incubated with shaking at 25°C for 4 hours. Samples were taken at 0 hours and after 4 hours of treatment for protein extraction and Western blot analysis.

2.5.10 Sporulation of diploid strains (solid media)

For asynchronous sporulation of diploid cells, patches of candidate strains grown on YPAD plates for 24 hours were replicated onto K-acetate plates and allowed to sporulate at 30°C for 48-72 hours. The cells were then checked for tetrads by light microscopy (100x).

2.5.11 Tetrad dissection

Cells sporulated on solid media were collected by scraping a loop full of cells using a disposable 1µl sterile loop (Sarstedt). Cells were then resuspended in 20µl final volume of 1 in 10 diluted stock β-glucuronidase (Roche) and incubated at 30°C for 20 minutes to release spores from the ascus. Following treatment, the cell density was diluted by addition of 200µl sterile mqH₂O. 20µl of this was pipetted onto a briefly dried YPAD plate, and allowed to run along a chord creating a segment approximately 1.5cm deep. The plate was briefly allowed to dry. Tetrads were arranged as arrays of four vertical spores on the YPAD plate in the upper segment using a micromanipulator (Singer MSM system series 200) and then allowed to grow at 30°C for 48 hours. Spores are considered viable if they can germinate and produce a colony when grown on a rich medium. A minimum of 40

tetrads, were dissected to determine the proportion of viable meiotic products.

2.5.12 Synchronous sporulation of *Saccharomyces cerevisiae*

A single colony was used to inoculate 15ml YPAD in a sterile 50ml Erlenmeyer flask and incubated overnight at 25°C with vigorous shaking. The O.D.₆₀₀ a 10-fold diluted sample was checked at about 12-2pm (depending on the strain cells may grow at different rates). Once O.D.₆₀₀ 5-10 was reached, cells were transferred to BYTA, a pre-sporulation medium low in nutrients containing a non-fermentable carbon source to encourage preparation for sporulation. The inoculum required for O.D.₆₀₀ 0.3 in a 200ml BYTA culture was calculated according to the following equation:

$$\frac{\text{Volume to grow (ml)}}{O.D_{600} / \text{Desired } O.D_{600}} = \text{no. ml to inoculate}$$

E.g.

$$\frac{200}{7.29 / 0.3} = 8.23 \text{ ml to inoculate}$$

The appropriate volume of cells was inoculated into BYTA, and incubated at 30°C in a shaking incubator at 270rpm for approximately 20 hours. Following incubation cell growth was assessed by measuring O.D.₆₀₀ of a 10-fold diluted sample. The ideal actual O.D.₆₀₀ should be between 6-10. Cells were checked by light microscopy at this stage; <5% of cells should be budding, and the cells should look fat and round. The volume of cells required for a starting O.D.₆₀₀ of 1.9 was calculated, and the cells rapidly harvested in a Beckman centrifuge at 4500rpm for 2 minutes. The inoculum volume required for well-prepared cells was usually around 70ml (±15ml). Cells were washed in 100ml autoclaved water and resuspended in 250ml SPM media plus any necessary amino acid supplements, and transferred to a 2.8l baffled flask, pre-warmed to 30°C. This was incubated at 30°C, 270rpm in a shaking incubator for the duration of the time course. Time point zero was taken immediately prior to the flask being placed in the shaking incubator.

2.5.13 Harvesting cells for DNA extraction

At hourly intervals, 25ml of synchronously sporulating cells were removed and transferred to a falcon tube containing ice-cold 6ml 50% glycerol + 300µl 10% Nazide (Sigma Aldrich). The cells were centrifuged at 4000rpm for 2 minutes and the pellet washed in 1ml spheroplasting solution + 20% glycerol (section 2.2.9), then transferred to an eppendorf tube. Cells were then centrifuged at 4000rpm for 2 minutes, the supernatant removed and the cell pellet flash frozen in liquid nitrogen for later DNA extraction.

2.5.14 DAPI staining of cells to monitor nuclear divisions

Approximately 750µl of synchronously sporulating cells were removed at hourly intervals and fixed in ice-cold 100% ethanol, and stored at -20°C. 1µl of DAPI 1mg/ml was added and the tube inverted then left at room temperature for one minute. Following this the cells were pelleted at 4000rpm in a micro-centrifuge, and then resuspended thoroughly in 100µl 50% glycerol. Cell nuclei were visualised using a Xuorescence microscope (DMLB Leica) with a standard DAPI filter for monitoring of meiotic progression by scoring of nuclei. 100 cells were scored from each time point for the number of discrete DAPI-stained nuclei present.

2.6 Yeast, plasmids & primers

2.6.1 Nomenclature of diploid strains used in this study

Strains which contain single residue mutations are referred to as the original residue and number followed by the mutated version, e.g. *spo11-Y135F-HA* indicates *spo11-Y135F-HA3-His6::KanMX4* in which there is a substitution of tyrosine 135 to phenylalanine.

Strains containing multiple residue mutations are referred to as the quantity and letter of the original residue followed by the mutated residue, e.g. *exo1-4S::A-PK9* indicates *exo1-4S::A-PK9::KanMX* in which there are 4 individual serine residues substituted to alanine.

Tagged strains are referred to as their allele followed by a tag suffix, e.g. *exo1-4S::A-PK9* indicates *exo1-4S::A* with a PK9 tag.

Deletion of a gene is indicated by Δ , e.g. *exo1 Δ* indicates *exo1 Δ ::KANMX*.

Strains expressing a mutant allele exogenously, such as from a plasmid, are referred to as the endogenous allele followed by that which is being expressed from the plasmid, e.g. dAG1686 (dAG1300 + pAG457) is referred to as *exo1 Δ + 4S::A*.

2.6.2 Yeast strains used in this study

The strains used in this study are of the SK1 background (Kane & Roth 1974). The *exo14S::A* allele was provided in vector pAG451 (pDL1134 David Lydall). The *spo11(Y135F)-HA3His6::KanMX* allele was provided in hAG209 (SKY268 Scott Keeney). The *mek1 Δ ::LEU2* allele was provided in hAG702 (S2683 Nancy Hollingsworth). The *Mre11-58S* allele was provided in hAG678 (S1359 Michael Lichten). The *mre11-H125N* allele was provided in hAG953 (from pAG189/pSM438 Alastair Goldman). The *CLB2-MEC1-HA3-KanMx6* allele was provided in hAG1508 (Alastair Goldman). The *dmc1::KanMX4* allele was provided in hAG319 (from M. J. Neale). The *sae2::KanMX6* allele was provided in hAG288 (S1196 Valerie Borde). The *tel1 Δ ::HphMX* allele was provided in hAG2167. The strains hAG55 and hAG56 were used in crosses to determine the ploidy and mating type of constructed strains.

2.6.3 Plasmids

The *LEU2* coding region of pAG311 was used as template DNA to produce fragments suitable for transformation. The *hph^R* hygromycin resistance coding region of pAG354 was used to produce fragments suitable for cloning and transformation. The *EXO1/exo1-4S::A/exo1-4S::E* coding regions of pAG450/451/452 respectively were used to produce fragments suitable for cloning various constructs such as those tagged with -PK9. The vectors pAG450/451/452 were also used to construct pAG456/457/458 for expression.

2.6.4 Primers

All primers were synthesised by Eurofins MWG Opern with high-purity salt free (HPSF) purification, except for those greater in length than 50bp which were purified by high performance liquid chromatography.

Table 2.3 Haploid *S. cerevisiae* strains

Name	Genotype	Source
hAG1	MAT α lys2 ura3 ho::LYS2 trp1::hisG	M. Lichten (S4)
hAG55	MAT α ura2 (ura2 tester)	M. Lichten (H317)
hAG56	MAT α ura2 (ura2 tester)	M. Lichten (H318)
hAG195	MAT α ura3 lys2 ho::LYS2 leu2-R arg4-nsp,bgl trp1::hisG ade2 his3::TRP1 (K.lact)	Anna
hAG1250	MAT α ho::LYS2 lys2 LEU2::VMA1::URA3 leu2 ura3 trp1 exo1 Δ ::KANMX	Anna
hAG1251	MAT α ho::LYS2 lys2 LEU2::VMA1::URA3 leu2 ura3 trp1 exo1 Δ ::KANMX	This study
hAG1886	MAT α ho::LYS2 TRP1 ura3 (VMA-201?)	This study
hAG1887	MAT α ho::LYS2 TRP1 ura3 (VMA-201?)	This study
hAG1929	MAT α ho::LYS2 TRP1 ura3 (VMA-201?) exo1 Δ ::KANMX	This study
hAG1951	MAT α ho::LYS2 TRP1 ura3 (VMA-201?) EX01-PK9::KanMX	This study
hAG1952	MAT α ho::LYS2 trp1::hisG ura3 (VMA-201?) EX01-PK9::KanMX	This study
hAG1953	MAT α ho::LYS2 TRP1 ura3 (VMA-201?) exo14S::A-PK9::KanMX	This study
hAG1954	MAT α ho::LYS2 TRP1 ura3 (VMA-201?) exo14S::A-PK9::KanMX	This study

Table 2.4 Diploid *S. cerevisiae* strains

Name	Genotype	Source
dAG206 (219 x 251)	MATa ho::LYS2 lys2 ura3::URA3-[arg4-rv::VDE] TFP1 leu2-? nuc1D::LEU2 spo11(Y135F)-HA3HIS6::KanMx arg4-nsp,bgl	Matt Neale
	MATα ho::lys2 lys2 ura3::URA3[arg4-bgl] TFP1:VDE1 leu2-? nuc1D::LEU2 SPO11 arg4-nsp,bgl	
dAG1300	MATa ho::LYS2 leu2 ura3 lys2 TRP1 VMA1-201 exo1Δ::KANMX	Anna
	MATα ho::hisG leu2 ura3 lys2 trp1 LEU2::VMA1::URA3 exo1Δ::KANMX	
dAG1626 (52 x 53)	MATα ura3 lys2 ho::LYS2 leu2-K arg4-bgl smo1-1	Ta- Chung Chou
	MATa ura3 lys2 ho::LYS2 leu2-R arg4-nspsmo1-1	
dAG1680 (1886 x 1887)	MATa ho::LYS2 TRP1 ura3 (VMA-201?)	This study
	MATα ho::LYS2 TRP1 ura3 (VMA-201?)	
dAG1685 (dAG1300 + pAG456)	MATa ho::LYS2 leu2 ura3 lys2 TRP1 VMA1-201 exo1Δ::KANMX	This study
	MATα ho::hisG leu2 ura3 lys2 trp1 LEU2::VMA1::URA3 exo1Δ::KANMX	
dAG1686 (dAG1300 + pAG457)	MATa ho::LYS2 leu2 ura3 lys2 TRP1 VMA1-201 exo1Δ::KANMX	This study
	MATα ho::hisG leu2 ura3 lys2 trp1 LEU2::VMA1::URA3 exo1Δ::KANMX	
dAG1687 (dAG1300 + pAG458)	MATa ho::LYS2 leu2 ura3 lys2 TRP1 VMA1-201 exo1Δ::KANMX	This study
	MATα ho::hisG leu2 ura3 lys2 trp1 LEU2::VMA1::URA3 exo1Δ::KANMX	
dAG1694 (1910 x 1911)	MATa ho::HISG? leu2 ura3 lys2 VMA1-201? exo1Δ::KANMX	This study
	MATα ho::HISG? leu2 ura3 lys2 VMA1-201? exo1Δ::KANMX	
dAG1713 (1951 x	MATα ho::LYS2 TRP1 ura3 (VMA-201?) EXO1::PK9::KanMX	This study

1952)	MATa ho::LYS2 trp1::hisG ura3 (VMA-201?) EX01::PK9::KanMX	
dAG1714 (1953 x 1954)	MAT α ho::LYS2 TRP1 ura3 (VMA-201?) exo14S-A::PK9::KanMX	This study
	MATa ho::LYS2 TRP1 ura3 (VMA-201?) exo14S-A::PK9::KanMX	
dAG1751 (2017x 2018)	MATa ho::LYS2 TRP1 ura3 (VMA-201?) exo1::KANMX	This study
	MAT α ho::LYS2 TRP1 ura3 (VMA-201?) exo1::KANMX	
dAG1822 (2184 x 2185)	MAT α ho::LYS2 lys2 ura3 leu2::hisG his3::hisG trp1::hisG mek1 Δ ::LEU2 EX01::PK9::KanMX	This study
	MATa ho::LYS2 lys2 ura3 leu2::hisG his3::hisG trp1::hisG mek1 Δ ::LEU2 EX01::PK9::KanMX	
dAG1823 (2186 x 2187)	MATa ho::LYS2 lys2 ura3 leu2::hisG his3::hisG trp1::hisG Mre11-58S(seq) EX01::PK9::KanMX	This study
	MAT α ho::LYS2 lys2 ura3 leu2::hisG his3::hisG trp1::hisG Mre11-58S(seq) EX01::PK9::KanMX	
dAG1824 (2188 x 2189)	MATa ho::LYS2 lys2 ura3 leu2::hisG his3::hisG trp1::hisG spo11-Y135F-HA3-His6::KanMX4 EX01::PK9::KanMX	This study
	MAT α ho::LYS2 lys2 ura3 leu2::hisG his3::hisG trp1::hisG spo11-Y135F-HA3-His6::KanMX4 EX01::PK9::KanMX	
dAG1825 (2190 x 2191)	MATa ho::LYS2 lys2 ura3 leu2::hisG his3::hisG trp1::hisG mre11-H125N (seq) EX01::PK9::KanMX	This study
	MAT α ho::LYS2 lys2 ura3 leu2::hisG his3::hisG trp1::hisG mre11-H125N (seq) EX01::PK9::KanMX	
dAG1826 (2192 x 2193)	MATa ho::LYS2 lys2 ura3 leu2::hisG his3::hisG trp1::hisG CLB2-MEC1-HA3-KanMx6 EX01::PK9::KanMX	This study
	MAT α ho::LYS2 lys2 ura3 leu2::hisG his3::hisG trp1::hisG CLB2-MEC1-HA3-KanMx6 EX01::PK9::KanMX	
dAG1827 (2194 x 2195)	MATa ho::LYS2 lys2 ura3 leu2::hisG his3::hisG trp1::hisG dmc1::KanMX4 EX01::PK9::KanMX	This study
	MAT α ho::LYS2 lys2 ura3 leu2::hisG his3::hisG trp1::hisG dmc1::KanMX4 EX01::PK9::KanMX	
dAG1828 (2196 x 2197)	MATa ho::LYS2 lys2 ura3 leu2::hisG his3::hisG trp1::hisG sae2::KanMX6 EX01::PK9::KanMX	This study
	MAT α ho::LYS2 lys2 ura3 leu2::hisG his3::hisG trp1::hisG sae2::KanMX6 EX01::PK9::KanMX	

dAG1829 (2198 x 2199)	MATa ho::LYS2 lys2 ura3 leu2::hisG his3::hisG trp1::hisG tel1Δ::HphMX arg4-nsp/nsp,bgl? EX01::PK9::KanMX	This study
	MATα ho::LYS2 lys2 ura3 leu2::hisG his3::hisG trp1::hisG tel1Δ::HphMX arg4-nsp/nsp,bgl? EX01::PK9::KanMX	
dAG1830 (2165 x 2166)	MATa ho::LYS2 lys2 ura3 leu2::hisG his3::hisG trp1::hisG EX01::PK9::KanMX	This study
	MATα ho::LYS2 lys2 ura3 leu2::hisG his3::hisG trp1::hisG EX01::PK9::KanMX	
dAG1831 (2213x 2214)	MATa ho::LYS2 lys2 ura3 leu2::hisG his3::hisG trp1::hisG tel1Δ::HphMX arg4-nsp/nsp,bgl? EX01::PK9::KanMX CLB2-MEC1-HA3-KanMx6	This study
	MATα ho::LYS2 lys2 ura3 leu2::hisG his3::hisG trp1::hisG tel1Δ::HphMX arg4-nsp/nsp,bgl? EX01::PK9::KanMX CLB2-MEC1-HA3-KanMx6	

Table 2.5 *E. coli* strains

Name	Description	Source
DH5α	supE44 ΔlacU169(φ80 lacZΔM15) hsdR17 recA1 endA1 gyrA96 thi-1 relA1	Lab resource
Alpha-select silver efficiency cells	F- deoR endA1 recA1 relA1 gyrA96 hsdR17(rk-, mk+) supE44 thi-1 phoA Δ(lacZYA-argF)U169 φ80lacZΔM15 λ-	Bioline

Table 2.6 Plasmids

Plasmid	Description	Source
pAG354	Contains Hph gene from <i>Klebsiella pneumoniae</i> encoding hygromycin B phosphotransferase and confers resistance to the antibiotic hygromycin B of transformed yeasts.	pAG32 John McCusker
pAG450	EX01 wild type (PMID 18756267 for info) HIS3/cen, ampicillin marker (made in pRS413). <i>Sequenced</i>	pDL1124 David Lydall Morin et al. 2008
pAG451	Non Phosphorylatable Exo1 exo1-4S::A (PMID 18756267 for info) HIS3/cen, ampicillin marker (made in pRS413). <i>Sequenced</i>	pDL1143 David Lydall Morin et al. 2008
pAG452	Phosphomimetic Exo1 exo1-4S::E (PMID 18756267 for info) HIS3/cen, ampicillin marker (made in pRS413). <i>Sequenced</i>	pDL1146 David Lydall Morin et al. 2008
pAG453	URA3/cen, ampicillin marker.	YCplac33

pAG456	pAG450 + Hygromycin Resistance Cassette amplified from pAG354 inserted at NotI. <i>Sequenced</i>	This study
pAG457	pAG451 + Hygromycin Resistance Cassette amplified from pAG354 inserted at NotI. <i>Sequenced</i>	This study
pAG458	pAG452 + Hygromycin Resistance Cassette amplified from pAG354 inserted at NotI. <i>Sequenced</i>	This study
pAG481	pBH259 - <i>EXO1</i> wild type tagged with PK9 in pBlueScript with KANMX and 1kb downstream homology of <i>EXO1</i> for chromosomal integration.	This study Bin Hu
pAG482	As pAG481 modified by Gibson assembly to include 4S::A	This study
pAG483	As pAG481 modified by Gibson assembly to include 4S::E	This study

Table 2.7 Primers

Primer	Sequence (5' → 3')	Description
Exo1KanMX5'	AATCCATATGATTTTCACCAACCTCTAGCCAACAGAGAGCGTTTAGCTTGCCCTCGTCCCGC	<i>KANMX</i> <i>exo1Δ</i> cassette 1.5kb product
Exo1KanMX3'	GAAAAATATACCTCCGATATGAAACGTGCAGTACTTAACTTTTAAACTGGATGGCGGCGTTAGTATCGAATC	<i>KANMX</i> <i>exo1Δ</i> cassette 1.5kb product
HYG (NotI) 5'	GAACGCGGCCGCCAGCTGAAGCTTCCG	<i>HYG^R</i> cassette 1.7kb product
HYG (NotI) 3'	CCGGCAGATCCGCGGCCGCATAGG	<i>HYG^R</i> cassette 1.7kb product
ARE1 Probe 5'	CCAATGCCTAACGCTTCCC	Downstream of <i>ARE1</i> locus 941bp
ARE1 Probe 3'	TTCTGTGGCGCAAACACCG	Downstream of <i>ARE1</i> locus 941bp
CHA1 5' For 1	GTCTACAATAAAAACACCATTATTACG	CHA1 probe first PCR 1.1kb product
CHA1 5' For 2	GGAAAGGCTTCTGCACAATTTTTC	CHA1 probe second PCR 1kb product
CHA1 3' Rev 1	CAGCGACTTCTATTACAGGAGTG	CHA1 probe first PCR 1.1kb product
CHA1 3' Rev 2	CTTTTTAAATTCACAATATTTTTTCTGG	CHA1 probe second PCR 1kb product
Exo1 mut 5'	GCAAATGTTCATTTTCGACGACG	Putative phospho-mutant region of Exo1 1.1kb product
Exo1 mut 3'	CCTTTATAAACAAATTTGGGAAAGCAAGG	Putative phospho-mutant region of Exo1 1.1kb product
Exo1 PK9 5'	CCTTGCTTTCCAATTTGTTTATAAAGG	pBH259 minus putative phospho-mutant region 6.7kb product
Exo1 PK9 3'	CGTCGTGAAATGAACAATTTGC	pBH259 minus putative phospho-mutant region 6.7kb product

3. Characterisation of exogenously expressed *exo1* mutants

Introduction

Exo1 is a nuclease that functions in DNA repair in both meiosis and mitosis. When Exo1 is absent, mitotically cycling cells are more sensitive to DNA damaging agents camptothecin and bleomycin, as well as telomere uncapping in the temperature sensitive *YKU70* mutant (Morin et al. 2008). This increased sensitivity may be due to a modest but functionally significant reduction in resection at mitotic DSBs. Conversely, increased expression of Exo1 leads to hyper-resection of DNA, and this can suppress sensitivity to DNA damaging agents (Tsubouchi & Ogawa 2000) by exposing distal regions of homology suitable for repair by SSA. It has previously been demonstrated that phosphorylation plays a role in the regulation of Exo1 in *S. cerevisiae* and mammalian models (Morin et al. 2008; Bolderson et al. 2010; Engels et al. 2011; Tomimatsu et al. 2014; see Section 1.7). However, so far no published studies have addressed the potential influence of this post-translational modification on the functions of Exo1 during meiosis.

Morin et al. 2008 demonstrated that phosphorylation is triggered in response to DNA damage, by treatment with bleomycin in cells from the W303 background. They identified four serine residues S372, S567, S587 and S692, that were phosphorylated in *S. cerevisiae* in response to DNA damage induction. From this they produced mutant alleles of EXO1 that were either non-phosphorylatable (*exo1-4S::A*) or mimicked phosphorylation (*exo1-4S::E*) by the substitution of serine with alanine or glutamic acid respectively. Examining sensitivity to DNA damage in these mutants has suggested that phosphorylation inhibits the activity of Exo1. This inhibition may serve to regulate the resection carried out by Exo1, preventing hyper-resection. A constitutively active mutant of Exo1 might therefore be anticipated to have decreased sensitivity to DNA damage due to an ability to hyper-resect. Morin et al. 2008 showed that the non-phosphorylatable

mutant *exo1-4S::A* is less sensitive to DNA damage than its wild type or phosphomimetic counterparts.

The aim of the work described in this chapter was to determine whether the key residues identified by Morin et al. might also influence the response of Exo1 to meiotic DNA damage. The mutants designed by Morin et al. were produced by subcloning an *EXO1-tap* construct into the pRS413 vector, and introducing the mutations into *EXO1* directly through site directed mutagenesis. The resulting vector was centromeric, making it suitable for supplementing expression in deletion mutants. The vectors containing one of the alleles *EXO1*, *exo1-4S::A*, or *exo1-4S::E* were used in an *exo1Δ* strain to investigate whether the residues might also influence the response to meiotic DNA damage. A hygromycin resistance cassette was inserted into the vector to enable selection of positive transformants. Potential effects on meiosis can be observed in various ways, including: the progression of meiosis over time observed by the number of nuclei visible per cell, the viability of meiotic products following dissection of tetrads, and the proportion of DNA existing as intact or broken fragments at given time points through the course of meiosis. By employing a variety of methods it is possible to build a picture of how meiosis progresses, and infer the effect an agent has on meiotic recombination.

Results

3.1 Hygromycin resistance marker integration affects meiotic progression

In order to select for and maintain positive transformants a hygromycin resistance cassette was inserted into the multiple cloning site of plasmid pAG450 (*EXO1*), creating pAG456. This vector was then transformed into the *exo1Δ* strain dAG1300. The hygromycin resistance (HYG^{R}) cassette was cloned into a single NotI restriction site and so could end up in two possible orientations; either expressing in opposition to *EXO1*, annotated as $\text{EXO1}<\text{HYG}$ (figure 3.1 A), or expressing subsequently to *EXO1*, annotated as $\text{EXO1}>>\text{HYG}$ (figure 3.2 B). In order to examine whether the orientation had an impact on the level of *EXO1* activity, dAG1300 cells transformed with either $\text{EXO1}<\text{HYG}$ or $\text{EXO1}>>\text{HYG}$ were synchronised into meiosis and sampled at hourly time points in order to examine

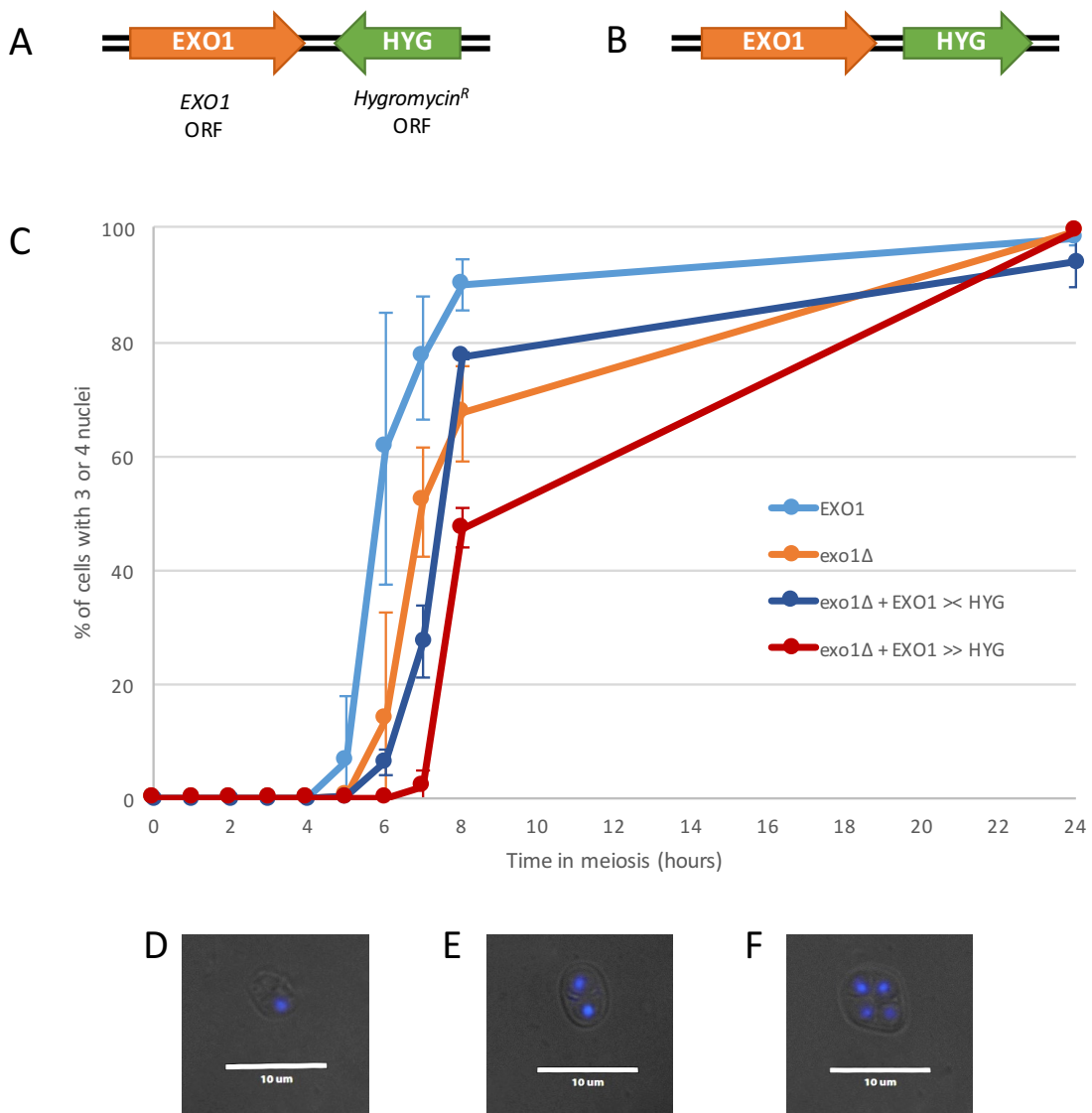


Figure 3.1 Meiotic progression is affected by marker integration

(A) & (B) illustrate the two possible orientations of Hygromycin^R insertion into the vector. The arrows indicate 5'-3' orientation of gene expression. (A) is referred to as *exo1Δ* + EXO1 <>HYG while (B) is *exo1Δ* + EXO1 >>HYG.

(C) In *exo1Δ* there is a one hour delay of appearance of tri/tetranucleate cells when compared to EXO1, as well as fewer tri/tetranucleates by 8 hours. The orientation of the hygromycin cassette insertion appears to significantly affect the progression of meiosis, as when hygromycin is expressed linearly following EXO1 (*exo1Δ* + EXO1 >>HYG) the number of tetranucleates at 8 hours is ~30% less than that when hygromycin is expressed in opposition to EXO1 (*exo1Δ* + EXO1 <>HYG). This oppositional orientation gives progression more similar to EXO1 (light blue) than *exo1Δ* (orange). Error bars calculated from >2 independent repeats.

(D), (E) & (F) show typical examples of mononucleate (B), binucleate (C), and tetranucleate cells as visualised by DAPI staining.

DAPI stained nuclei at each stage (section 2.5.14) (Figure 3.1 D, E & F). Cells were scored for the number of nuclei visible, as an indicator of meiotic progression. Cells displaying 3 or 4 nuclei were scored as having completed the second nuclear division (MII). Wild type cells (*EXO1*) showed 90% progression through MII by 8 hours of meiosis (figure 3.1 C), while *exo1Δ* progression was impaired, with 68% of cells having progressed through MII by 8 h. By the same time, cells transformed with *EXO1*><HYG showed 78% MII nuclei, while *EXO1*>>HYG MII progression was reduced with 48% of cells having 3 or 4 nuclei. As the *EXO1*><HYG integration appeared to show progression more similar to that of wild type cells, this orientation was selected for when inserting HYG^R into pAG451 (*exo1-4S::A*) and pAG452 (*exo14S::E*) to create pAG457 and pAG458.

3.2 Sporulation defect of *exo1Δ* is partially rescued by transformation with *Exo1* plasmids

Timely meiotic progression depends on punctual and successful completion of each stage of meiosis, fulfilling various checkpoints along the way (section 1.6). *Exo1* is implicated in two stages of meiotic recombination; 5' to 3' resection of DSBs and resolution of dHJs (Zakharyevich et al. 2010). Disruption of either of these processes could influence meiotic progression, an effect which is detectable experimentally. To examine whether these mutations in *EXO1* (reported to influence phosphorylation status) influenced meiotic progression, the vectors containing *EXO1*, *exo1-4S::A*, and *exo1-4S::E* were transformed into an *exo1Δ* strain (dAG1300) and maintained under hygromycin selection. It is worth acknowledging here that exogenous expression is not the most straight-forward or physiologically representative way of carrying out this experiment. Prior to using this method, various attempts at integration for exogenous expression of the mutants were tried, unsuccessfully. These attempts included use of transformation cassettes using antifungal resistance genes or amino acid markers, and employed various lengths of homology and methods of transformation to try and integrate the cassettes. In the absence of success, it was decided to examine exogenous expression to determine whether there might be any influence on meiotic expression, instead of continuing to lose time to the endogenous attempts.

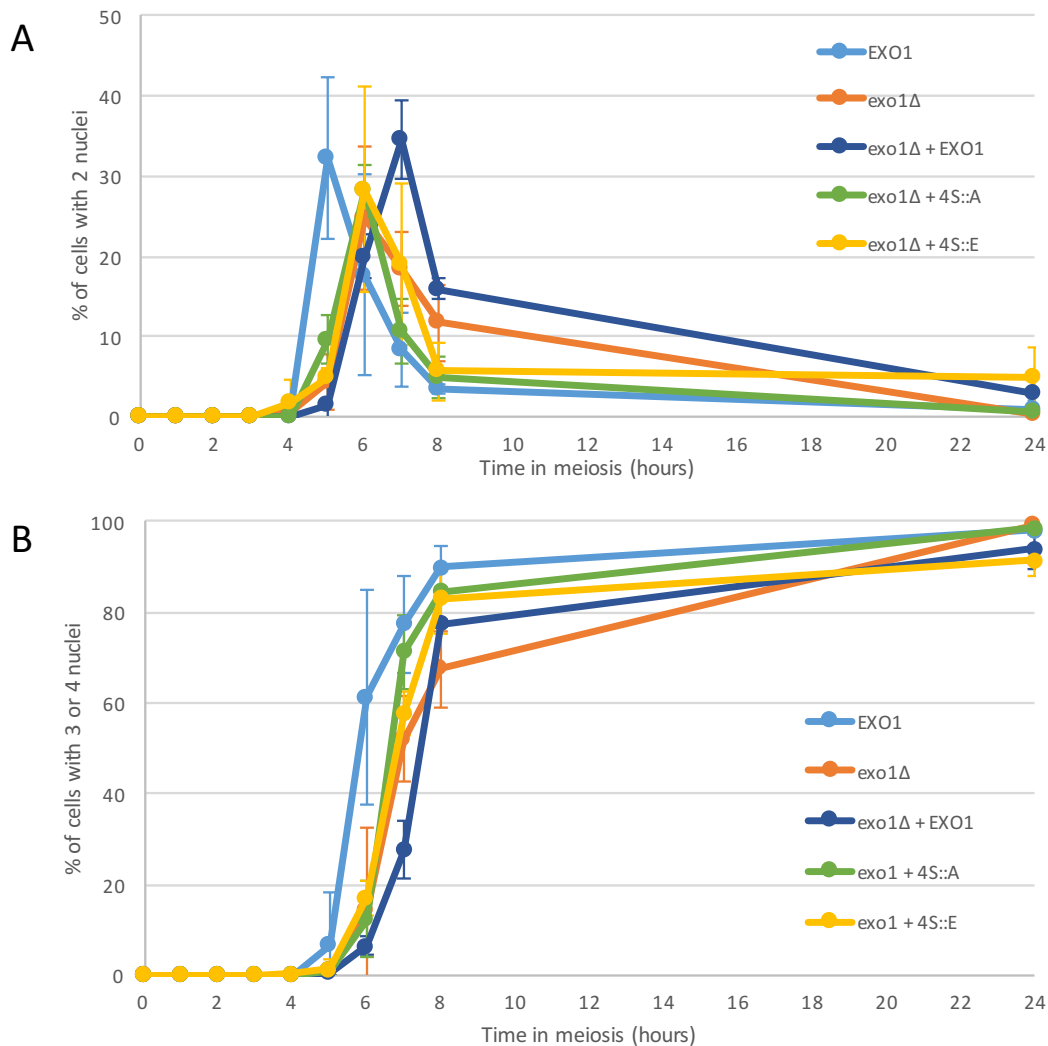


Figure 3.2 Meiotic progression is partially rescued by exogenous expression of *EXO1*, *exo1-4S::A* and *exo1-4S::E*.

(A) In *exo1Δ* there is a one hour delay of appearance of binucleate cells compared to *EXO1*, as well as a higher proportion of binucleates remaining at 8 hours. Expression of the mutant alleles of *Exo1* show a binucleate appearance rate more similar to that of *EXO1*, while exogenously expressed *EXO1* shows a 2 hour delay. Error bars calculated from >2 independent repeats.

(B) In *exo1Δ* there is a one hour delay of appearance of tri/tetranucleate cells when compared to *EXO1*, as well as fewer tri/tetranucleates by 8 hours. Mutant alleles of *Exo1*, while maintaining this delay, attain similar levels of these cells at 8 hours as *EXO1*, and this is also the case for exogenously expressed *EXO1* despite an initial 1 hour delay. Error bars calculated from >2 independent repeats.

At 5 h after induction of meiosis, most wild-type cells had progressed through the resulting strains (dAG1685, dAG1686 & dAG1687) were synchronised into meiosis and cell samples were collected at hourly intervals for DAPI analysis of nuclei (section 2.5.14). Cells were scored for number of nuclei visible. MI, while *exo1Δ*, *+exo1-4S::A*, and *+exo1-4S::E* were delayed by one hour, and *+EXO1* by two hours (Figure 3.2 A). Exogenous expression of *EXO1* does not appear to rescue the delay of MI seen in *exo1Δ*. This delay persists in to MII (Figure 3.2 B). Over half of wild-type cells have completed meiosis by 6 h, while for *exo1Δ*, *+exo1-4S::A*, and *+exo1-4S::E* it took 7h for 50% of cells to complete meiosis, and for *+EXO1* this took 8 h to achieve. By 8 h approximately 80% of wild-type, *+EXO1*, *+exo1-4S::A*, and *+exo1-4S::E* cells showed nuclei that had completed meiosis, as compared to *exo1Δ* cells, for which over 30% still remained in meiosis. While the progression of the exogenously expressed variants of Exo1 were delayed through MI, they all had rates of MII completion more similar to that of WT by 8 hours. As MII completion rates were higher than those of *exo1Δ* it can be concluded that exogenous expression of Exo1 variants partially rescues the decreased sporulation phenotype of *exo1Δ* cells. Whether or not this rescue reflects completion of faithful meiosis depends on the outcome of spore viability assays. This result does however indicate that the presence of Exo1, or its phospho-mutants, is important for punctual completion of meiosis, in agreement with previous findings (Fiorentini et al. 1997). Later in the experiments, attempts were made to investigate the expression levels of Exo1 and its phospho-mutants, as this would help support the hypothesis that the presence of the protein is necessary for timely meiotic progression. The vectors contained TAP-tagged Exo1 and its phospho-mutants, however no protein was detectable by Western blot, making it difficult to conclude whether the protein was present or whether the tag was effective.

3.3 Spore Viability is reduced in *exo1-4S::A*

Wild type cells, *exo1Δ* cells, and *exo1Δ* cells expressing *EXO1*, *exo1-4S::A*, or *exo1-4S::E* exogenously were sporulated, and the resulting tetrads dissected as described (section 2.5.11) in order to determine the viability of meiotic products. The average spore viability of wild type cells was 96% (± 3.75) (Figure 3.3),

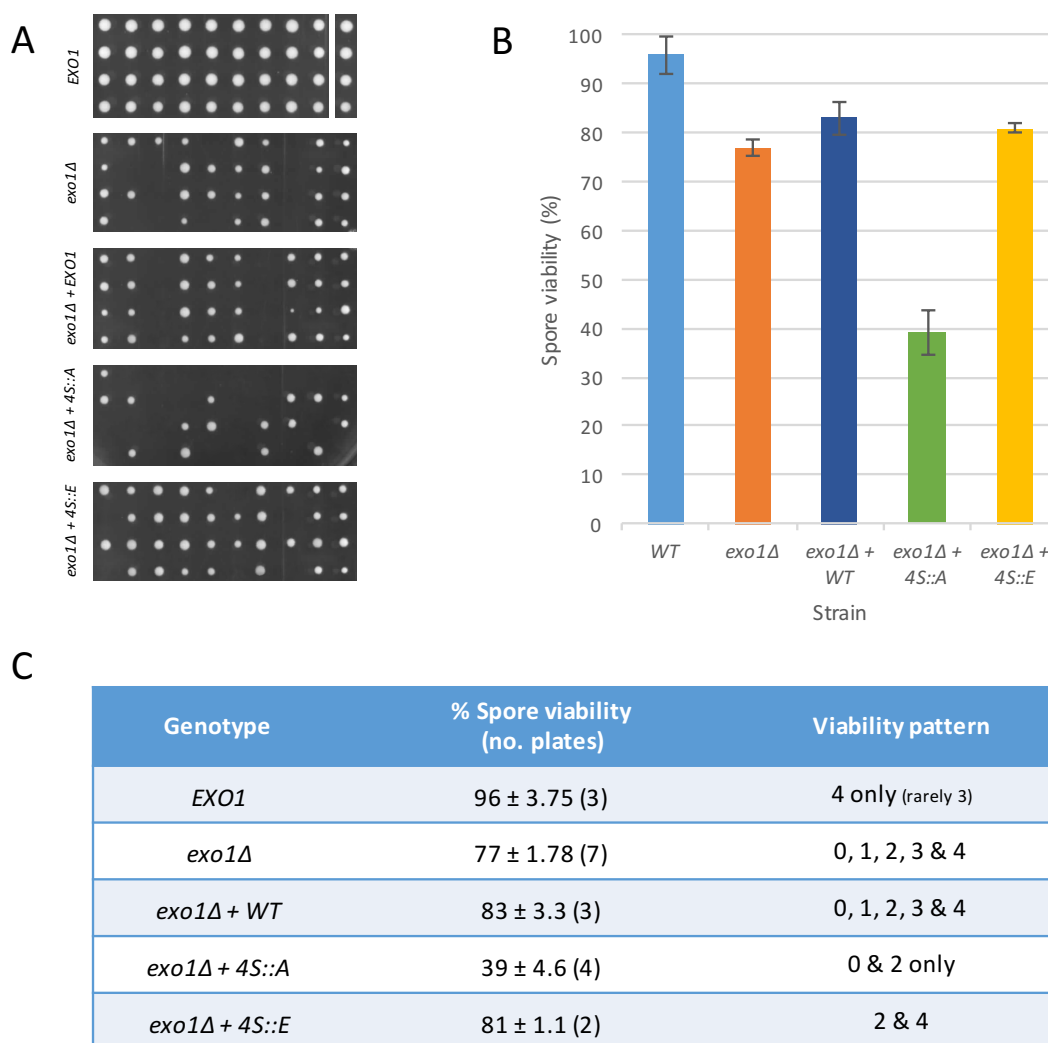


Figure 3.3 Spore viability analysis of *exo1Δ* transformed with plasmids containing *EXO1*, *exo1Δ + 4S::A*, *exo1Δ + 4S::E*

- (A) Illustrative examples of the spore viability patterns observed of tetrads dissected onto YPD agar plates and left to grow at 30°C for 48 hours. Each plate contained 80 spores.
- (B) Graph illustrating the spore viability of each strain. Error bars calculated from >2 independent repeats.
- (C) Table summarising the mean spore viabilities of each strain and their standard deviation from the mean, calculated from the individual viabilities of each independent repeat. The spore viability pattern can be used as an indication as whether a non-disjunction has occurred during MI (2 spore viable) or MII (combinations of 1, 2 and 3 spores viable).

representing the viability achieved by cells progressing through a normal meiosis. In *exo1Δ* cells the viability was reduced to 77% (± 1.78), indicating an increase in lethal aneuploidies, and in line with previous findings (Fiorentini et al. 1997).

The spore viability pattern of *exo1Δ* varied, showing a range of 0, 1, 2, 3 or 4 spores viable in any given tetrad, suggesting either a mix of both MI and MII non-disjunctions or several MII non-disjunctions. Exogenous *EXO1* expression from pAG456 partially rescued this, improving spore viability to 83%, showing a similar pattern, with only 39% of spores viable, indicative of an MI defect (figure 1.3). *EXO1* has two distinct roles, one during leptotene in resection and the other later during cross-over resolution (Keelagher et al. 2010; Zakharyevich et al. 2010). Both of these roles are prior to MI, suggesting that the *exo1-4S::A* mutant is deficient in proper homologue segregation due to a defect in one of these roles. This phenotype is more severe than that of *exo1Δ*, which can perhaps be explained by the proposed role of phosphorylation in the control of Exo1 function. It has been hypothesised that Exo1 phosphorylation negatively regulates its nuclease activity (Morin et al. 2008), and so perhaps a constitutively-active protein is toxic to meiosis. pAG458 expressing *exo1-4S::E* shows a viability of 81%, similar to that of pAG456 expressing *EXO1*. However, the pattern of spore viability is different, showing only 0, 2 & 4 spore viability. This could be indicative of an MI non-disjunction. While these results suggest *exo1-4S::E* may behave differently to *EXO1* in meiosis, they do not indicate whether this is an early effect upon resection or a later effect on cross-over resolution.

3.4 DSB turnover at the *ARE1* locus is not influenced by the Exo1 alleles tested

3.4.1 Redefining the base level of DSB turnover

Although various wild type controls already existed in the lab, these contained background mutations each relevant to particular models for the study of meiotic recombination (e.g. the VDE system). Therefore, a new “clean” wild type strain was made to remove these background mutations. It was necessary to determine the level of DSB activity in this new strain to provide a baseline control for

prospective experiments. Specific loci may be identified and exploited for physical assaying of DSB turnover. Genomic DNA can be digested by restriction endonucleases with specific recognition sequences flanking a DSB site, and using gel electrophoresis it is possible to then isolate the region of DNA likely to become a DSB. The fragment of DNA containing the potential DSB site may be visualised as a discrete band known as the *parental* band, and in the event of a DSB an additional lower weight band will become transiently present prior to its repair (Figure 3.4 A). DSB formation and repair rate can be extrapolated from the proportion of DSB fragment to parental at given time points through meiosis. This can demonstrate the rate and timing of DSB turnover. This assay was carried out at hotspot 3-6 on chromosome III identified as having one of the highest levels of recombination in the *S. cerevisiae* genome (Gerton et al. 2000). This characteristic is useful for obtaining levels of DSBs that are observable by Southern blot. The probe used was homologous to a region of DNA distal to the break within a 20kb restriction fragment produced by SpeI digestion. This region of probe homology lies near to the *ARE1* ORF, and so this assay is referred to as being carried out at the *ARE1* hotspot. If a DSB is present the restriction fragment is reduced to ~8kb, and so distinguishable from the 20kb parental band (Figure 3.4 A). For wild-type cells (dAG1680) the level of Spo11-DSBs peaks at 3 h with approximately 5% of the total DNA appearing the DSB band. This profile is similar to other published timings (Gray et al. 2013), providing the baseline control for prospective experiments.

3.4.2 DSB turnover in *Exo1* and phospho-mutants

In order to elucidate which role of Exo1 is being influenced by the mutations, DSB formation and repair was examined at a single hot spot locus, *ARE1*, as described in section 3.1. The early role of Exo1 is to carry out resection of DNA at DSBs in a 5' to 3' direction, exposing a length of 3' ssDNA (Lieber 1997; Zakharyevich et al. 2010). Other nucleases also partake in this; the MRX complex is believed to perform short resection in the initial processing, followed by longer resection more distal to the break by Exo1 (Neale et al. 2005; Hodgson et al. 2011; Garcia et al. 2011). The proportion of DNA seen in a DSB band is a function of the

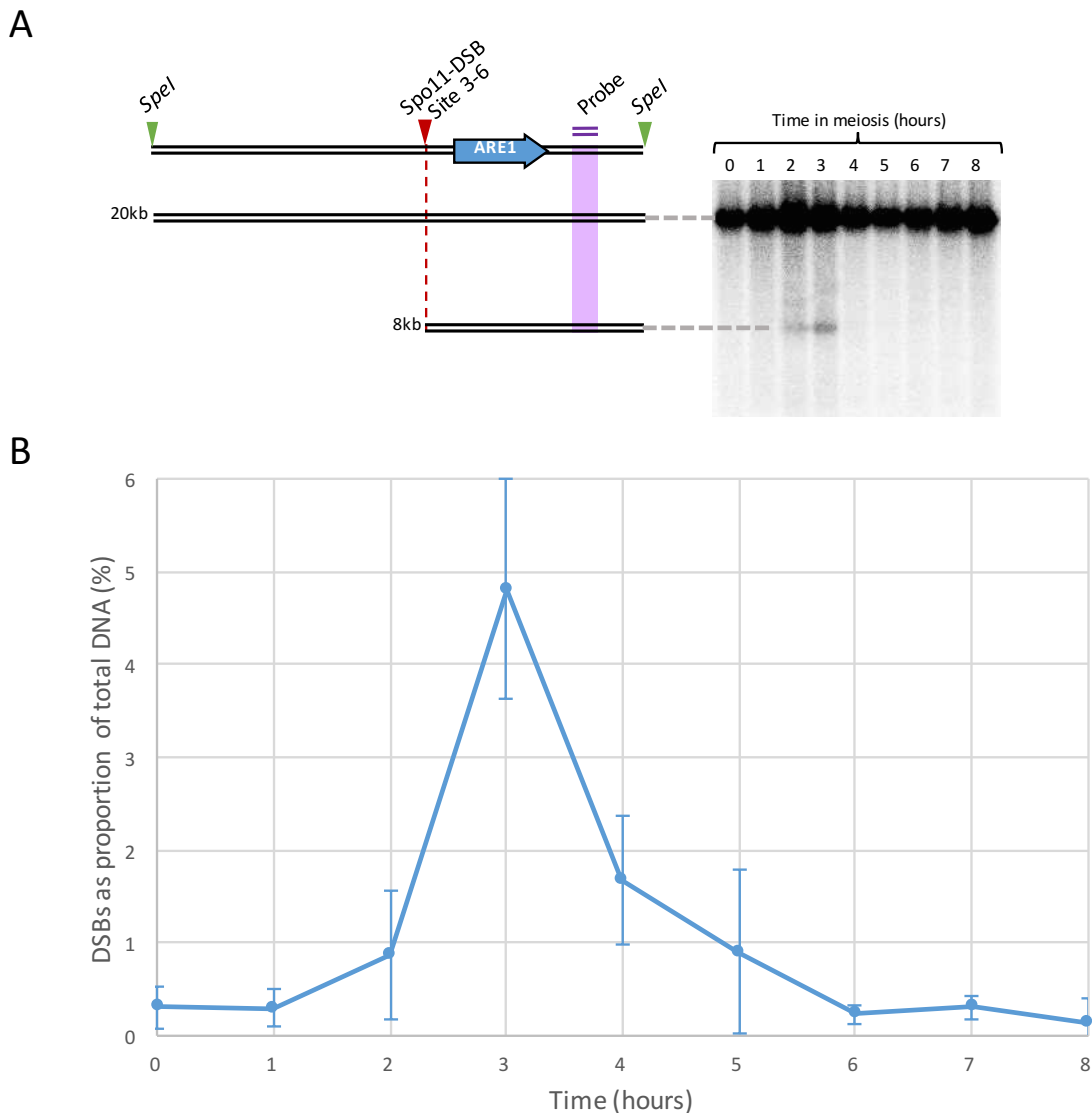


Figure 3.4 - Analysis of the Spo11-DSB turnover at the ARE1 hotspot

(A) WT cells progressing through a synchronous meiosis were sampled at hourly intervals. CTAB extracted DNA was digested with *SpeI* and fractionated on a 0.75% 1xTAE agarose gel, blotted onto a nylon membrane via vacuum transfer and hybridised with a probe specific to a region downstream of the *ARE1* ORF and hotspot 3-6 on Chr. III. *SpeI* Digestion yields a parental fragment of 20kb and DSB fragment of 8kb. *ARE1* transcription direction is indicated as an arrow.

(B) Quantification of the Spo11-DSB band as a proportion of the total lane DNA shows maximum Spo11-DSB signal peaks at 3 hours (T=3) in meiosis. This indicates that at this stage more breaks are being formed than repaired. Error bars indicate a single standard deviation from the mean of three data sets produced from independent repeats.

proportion of chromatids receiving a DSB and the proportion of DSBs repaired following resection, strand invasion Resection is the key function of Exo1 and so changes in DSB turnover observed in the *exo1* mutant cells can most likely be attributed to an impact on the resection activity.

In WT and *exo1Δ* cells, DSBs peaked at 3 h (4-4.5% of total DNA) reducing to background levels by 6 h (Figure 3.5 A). In *exo1Δ* cells there was a delay in repair by approximately one hour, indicated by a shallower gradient between 3 h and 4 h (figure 3.5 B). This delay may be due to a lack of long resection at the DSBs, necessary for normal progression (Mimitou & Symington 2008; Zakharyevich et al. 2010; Hodgson et al. 2011), and is in keeping with the one-hour delay observed in meiotic progression of *exo1Δ* discussed in section 3.2.

Cells exogenously expressing *EXO1* had a DSB peak at 4 h, representing approximately 3.5% of total DNA, reducing to background levels by 8 h, decreasing at a shallow gradient between 3 h and 4 h post-induction (Figure 3.6 A & B). This finding is also consistent with the delay in sporulation discussed in section 3.3. This delay in turnover is more significant than that of *exo1Δ*, which was an unexpected result. This could perhaps be due to variance in several factors, such as expression levels or timing of expression. Cells expressing *EXO1* from pAG456 can be used as a control for those expressing the mutant alleles of Exo1, to account for these unknown variations.

Cells expressing *exo1-4S::A*, or *exo1-4S::E* exogenously, reveal a DSB peak at 2.5-3% of total DNA at 4 h, and decline at a shallow gradient similar to that of cells expressing *EXO1*, returning to background levels by 8 h. The levels and timing of DSBs are consistent with the delay in sporulation of cells expressing *exo1-4S::A*, or *exo1-4S::E* exogenously, as discussed in section 3.3. While there is some variation, the levels of DSBs overall were not significantly different to those of the cells exogenously expressing *EXO1*. This could suggest that phosphorylation of Exo1 at these 4 residues does not significantly impact resection by Exo1 at this locus.

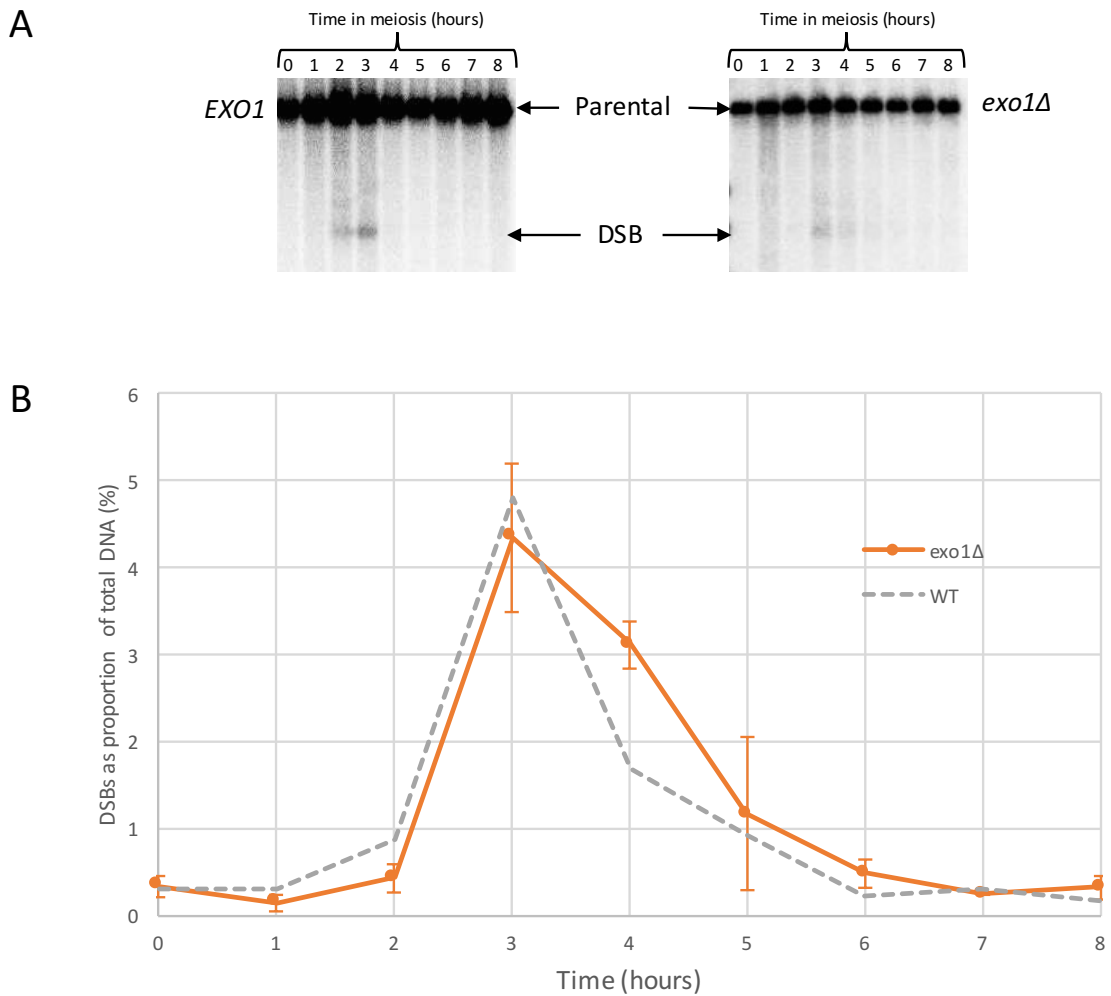


Figure 3.5 - Analysis of the Spo11-DSB turnover in *exo1Δ* at the ARE1 hotspot
 (A) Synchronous meiotic cultures of *exo1Δ* cells (dAG1300) were sampled at hourly intervals. CTAB extracted DNA was digested and treated as shown in figure 3.4.
 (B) Quantification of the Spo11-DSB band as a proportion of the total lane DNA shows maximum Spo11-DSB signal peaks at 3 hours (T=3) in meiosis in *exo1Δ* (orange), as seen in *EXO1* (dashed). The DSBs persist at significantly higher levels, almost twice the amount, for 1 hour longer in *exo1Δ* when compared to *EXO1*, however from 5 hours (T=5) the DSB levels become consistent with those seen in *EXO1* again. Error bars indicate a single standard deviation from the mean of three data sets produced from independent repeats.

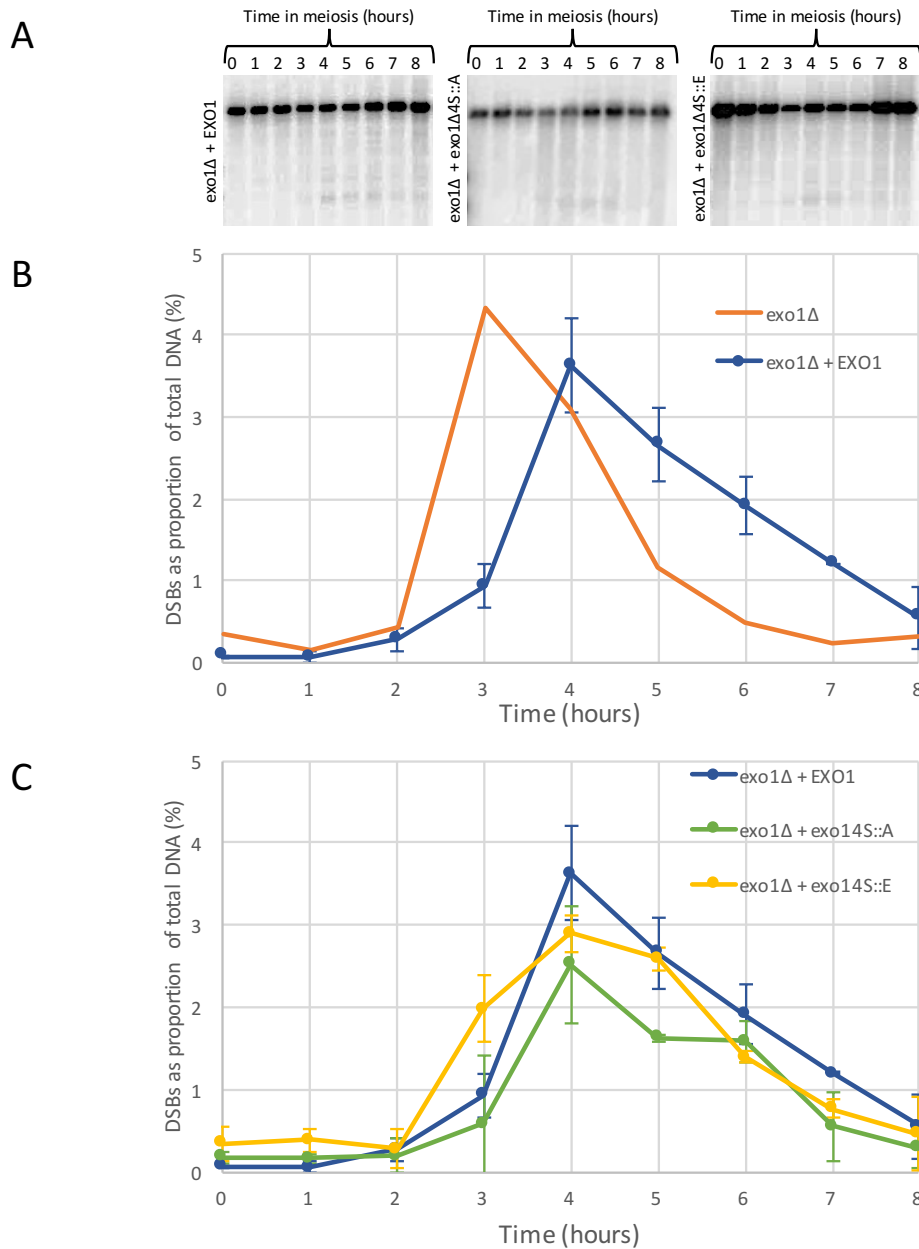


Figure 3.6 - Analysis of the Spo11-DSB turnover in *exo1Δ* at the ARE1 hotspot

- (A) Synchronous meiotic cultures of *exo1Δ* cells exogenously expressing *EXO1*, *exo14S::A* or *exo14S::E* were sampled at hourly intervals. CTAB extracted DNA was digested and treated as described in figure 3.4 A. The amount of probe hybridised to each band was determined by scanning densitometry.
- (B) Quantification of the Spo11-DSB band as a proportion of the total lane DNA shows maximum Spo11-DSB signal peaks at 4 hours (T=4) in *exo1Δ* cells exogenously expressing Exo1, a delay of one hour when compared to *exo1Δ* and *EXO1* (figure 3.5 B). Error bars indicate a single standard deviation from the mean of two data sets produced from independent repeats.
- (C) Quantification of the Spo11-DSB band as a proportion of the total lane DNA shows no significant difference between the rate of DSB turnover in cells exogenously expressing *EXO1*, *exo14S::A* or *exo14S::E*. Error bars indicate a single standard deviation from the mean of two data sets produced from independent repeats.

3.5 Chromosome-wide DSB turnover may be Influenced by Exo1 phosphorylation

DSBs are distributed in a non-random fashion at recombination hotspots. There are between 6 and 20 hotspots be dispersed along a chromosome (Gerton et al. 2000), depending on its size, though not all will be subject to recombination at any given time. Specific hot spots may be exploited for physical assay of DSB turnover. A wider look at hotspots over a chromosome collectively may also be used to give a more general view of DSB turnover. This can be useful in establishing the broader influence of a variable on DSB turnover, as subsets of breaks may behave differently, affecting the observations at individual hotspots. In order to examine a chromosome wide DSB turnover pulsed-field gel electrophoresis was used for analysis of chromosome III.

3.5.1 Analysis of DSB turnover for chromosome III in WT cells as a baseline

Wild type dAG1680 cells were triggered into synchronous meiosis and sampled at hourly time points from 0 h to 8 h (section 2.5.12). Agarose plugs containing treated cells were used for PFGE of the chromosomal DNA (section 2.5.13), and the resulting gel was subjected to Southern analysis using a probe specific to the distal end of the short-arm of chromosome III (section 2.2.14) (Figure 3.7 A). The signal at discrete points along the relative front (a value between 0 and 1 representing the distance along the gel relative to the starting point) was converted into a percentage of the total lane signal, and the proportions were plotted to give a profile of the DNA fragments (Figure 3.7 B). DSBs were first detectable at 2 h of meiosis and persisted at detectable levels until at least 4 h, particularly at hotspots 3-2, 3-3, 3-6, 3-7 and 3-8. Hotspots 3-3 and 3-6 have been shown to be amongst the hottest 10 ORFs in the genome (Gerton et al. 2000), and so this pattern of break intensity is as expected. From 6 h the DSB levels returned back to 0 h levels (data not shown), as shown by the 8 h profile. This profile provides the control baseline for prospective experiments.

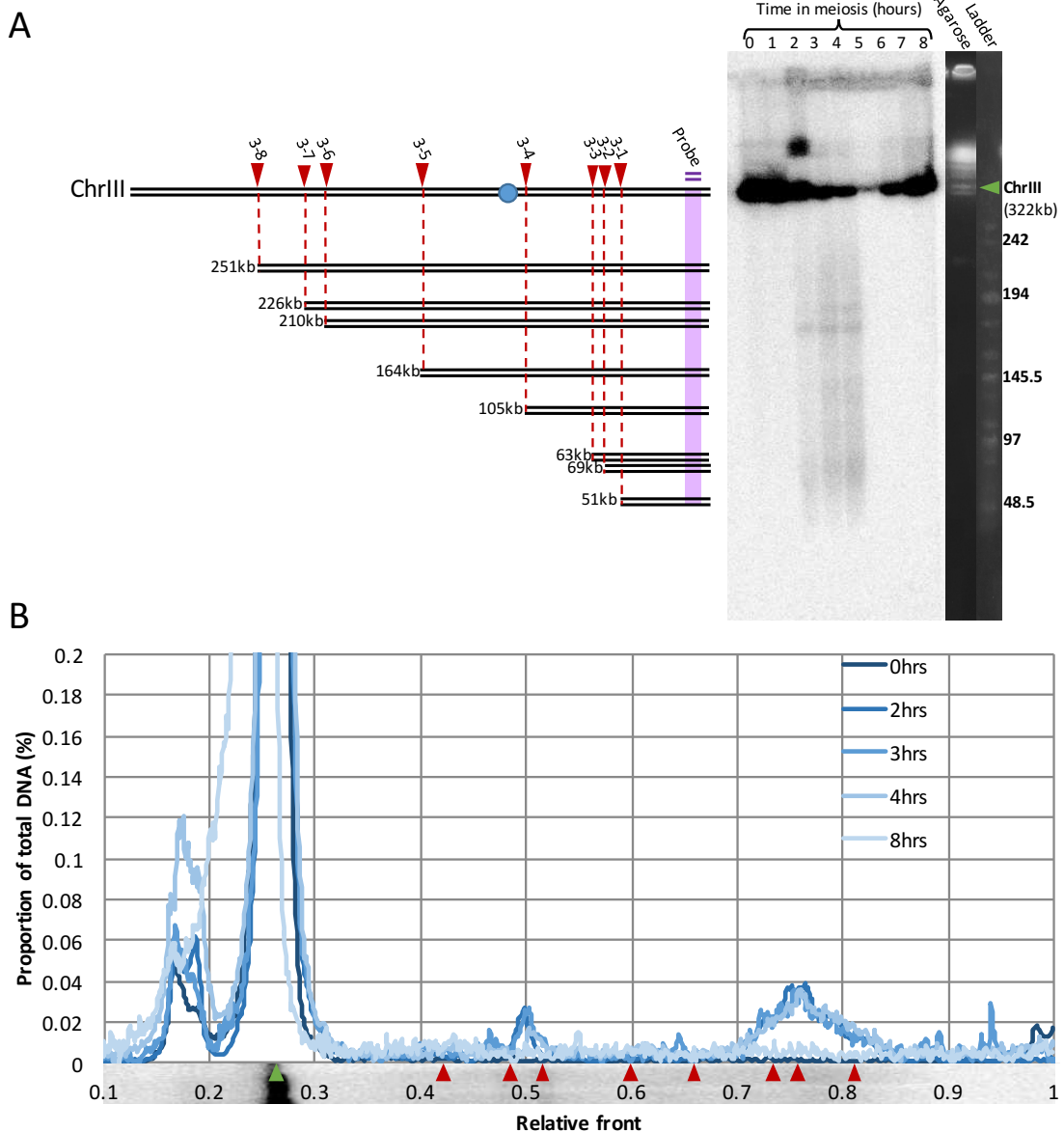


Figure 3.7 - Global analysis of turnover of Spo11-DSBs in wild type

(A) WT cells progressing through a synchronous meiosis were sampled at hourly intervals. Cells were treated in agarose plugs to isolate chromosomes and these were then fractionated on a 1.3% 0.5xTBE agarose gel, blotted onto a nylon membrane via vacuum transfer and hybridised with a probe specific to the *CHA1* ORF at the distal end of the p-arm of Chr. III. Spo11 hotspots are indicated with red arrows, and the fragment sizes detected illustrated beneath. A Southern blot is aligned next to a representative lane from an agarose gel prior to blotting to illustrate chromosome separation and the ladder used to extrapolate fragment size.

(B) Lane densitometry profile values were used to calculate the quantity of DNA present at each point as a percentage of the total lane signal. The complete ChrIII band, around relative front 0.26, is cropped to allow visualisation of DSB site signal, and usually constitutes ~3% of the total lane signal at each time point. The x axis begins as 0.1 to remove signal originating in the wells. Comparison of profiles at 0, 2, 3, 4 and 8 hours show the turnover of Spo11 DSB's along the chromosome. The signal increases in the region of known hotspot locations, indicated by the red arrows along the x axis of (B).

3.5.2 Analysis of DSB turnover for chromosome III in *exo1* mutant cells

For *exo1Δ* cells DSBs were first detectable at 2 h (Figure 3.8 A & B), however the peaks appear at slightly different distances from the beginning of the lane (termed relative front). There are more prominent peaks around hotspots 3-1, 3-2, and 3-3 (around relative front 0.4-0.5), indicating breaks are either more frequently made here or more slowly repaired. The peaks near hotspots 3-6, 3-7 and 3-8 (around relative front 0.7-0.8) are not as high signal as those in wild type, indicating that the break level here is decreased compared to wild type; either breaks are less frequently formed or are more quickly repaired. At 3 h in to meiosis, visible breaks at sites 3-1, 3-2 and 3-3 increase, while the signal at 3-6, 3-7 and 3-8 remains similar to that seen at 2 h. From 4 h the signal intensity is decreasing towards background levels (Figure 3.8 D & E).

exo1Δ cells expressing *exo1-4S::A* show background levels of signal in the first three hours of meiosis (Figure 3.8 A, B & C). At 4 h the signal around hotspots 3-2 and 3-3 reach a level similar to that of wildtype at 3 hours, and reduced signal is observed around hotspots 3-6, 3-7 and 3-8 (Figure 3.8 D), either as breaks are less frequently formed or are more quickly repaired here. At 5 hours low levels of DSBs appear to persist, after which the profile returns to that of background levels (Figure 3.8 E). A persistent problem in getting sufficient signal at 5 hours despite independent repeats of each strain (Figure 3.7 A) made it impossible to compare decline in DSB signal. However, it is evident from the earlier time points that the DSBs signal in *exo1Δ* cells expressing *exo1-4S::A* is both delayed in its appearance and altered in its distribution when compared to *exo1Δ* and wild type. The experiments were run several times, however due to the technical complexity it was difficult to obtain images of consistent quality. The gels shown here are each a single experiment with no independent repeats. It was intended that repeats would be carried out, however later results from other experiments showed the method of exogenous expression of Exo1 and the phospho-mutants to be unreliable (Chapter 3 Discussion).

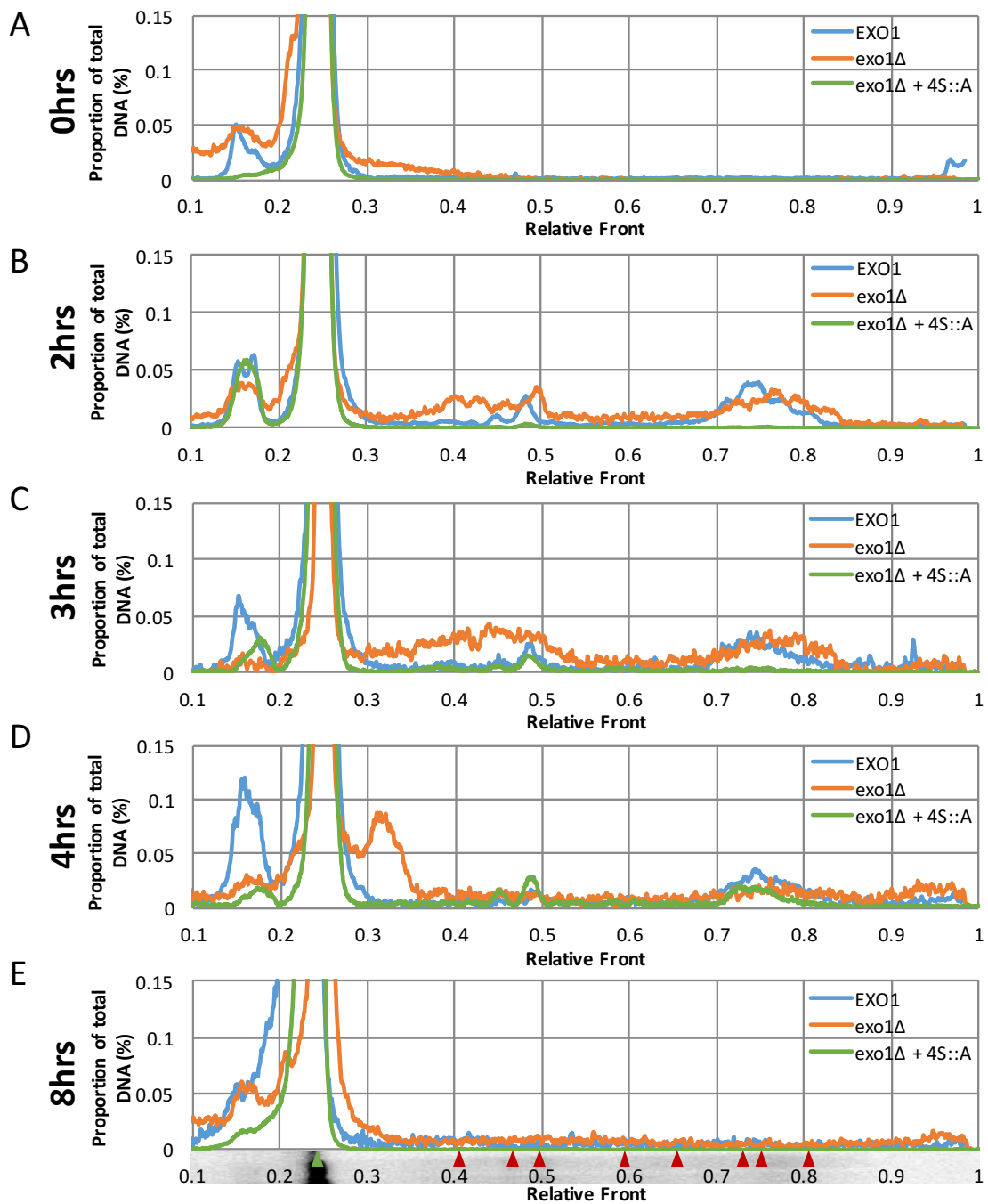


Figure 3.8 - Global analysis of turnover of Spo11-DSBs

(A), (B), (C), (D) & (E) show the quantity of DNA present at each point along the lane as a percentage of the total lane signal for 0, 2, 3, 4 & 8 hours through meiosis respectively. The signal increases in the region of known hotspot locations, indicated by the red arrows along the x axis of (E). *EXO1* and *exo1Δ* begin to show increased DSB turnover at 2 hours while *exo1Δ + 4S::A* is delayed by 1 - 2 hours, depending on the hotspot being examined. By 5 hours all DSB signals have returned to background levels in *EXO1* & *exo1Δ*, however breaks still persist in *exo1Δ + 4S::A* until 6 hours, when the signal returns to background levels (data not shown).

Discussion

The exonuclease Exo1 has been shown to be phosphorylated in response to DNA damage during mitosis (Morin et al. 2008; Bolderson et al. 2010; Engels et al. 2011; Tomimatsu et al. 2014). In order to begin investigating a potential role for phosphorylation during meiosis, mutants of Exo1 that were either non-phosphorylatable (*exo1-4S::A*) or mimicked phosphorylation (*exo1-4S::E*) were obtained. These mutant alleles were then expressed exogenously from a single copy centromeric plasmid under their genomic promoter in an *exo1Δ* background in order to reconstitute Exo1 expression in the cell. Expression of wild type *EXO1* in the same system was used as a control. While the experiments carried out examine Exo1 activity indirectly, no experiments here show whether exogenous Exo1 expression was achieved physiological levels. Unsuccessful attempts were made at examining expression levels using this plasmid system, however endogenous expression was ultimately characterised using Western blots, and is discussed in Chapters 5 and 6.

In constructing the plasmids for expression of Exo1 and its mutants, it was important to consider the orientation of the hygromycin marker. There was a substantial difference in the ability of cells to complete meiosis in a timely manner between *EXO1*<HYG or *EXO1*>>HYG (section 3.1). It was discovered that *EXO1*<HYG oriented constructs progressed through meiosis with a delay of a single hour, while *EXO1*>>HYG was delayed by several hours. This may be as a consequence of spatial overcrowding when both transcription initiation and termination are trying to coordinate in the same region. Overcrowding may result in reduced Exo1 or phospho-mutant protein expression, causing lower levels of protein to be present than might be available during endogenous expression. Orientation is therefore an important consideration in the construction of vectors expressing ORFs in close proximities.

The timing of meiotic progression was analysed in *exo1Δ* cells and compared to cells exogenously expressing *EXO1* and its phospho-mutants (section 3.3). Both phospho-mutants exhibited a profile most similar to that of cells expressing *EXO1*, compared to *exo1Δ* cells of which 30% failed to complete meiosis within 8 hours of

initiation. This indicates that regardless of phosphorylation status, the presence of Exo1 itself contributes to the punctual progression of meiosis. Spore viability was then investigated to see whether the products of these meioses were viable (section 3.4). The viability of *exo1-4S::A* was drastically reduced to 39%, and in a pattern indicative of a MI failure, the time when Exo1 is active. In previous studies it has been hypothesized that phosphorylation negatively regulates the activity of Exo1, inhibiting its nuclease activity (Morin et al. 2008). If this is also the case in meiosis, then it would help to explain the severe defect of *exo1-4S::A*. This non-phosphorylatable allele would be disinhibited during resection, potentially leading to hyper-resection of the 5' strand. Hyper-resection can lead to genomic instability, proposed to be due to a depletion of RPA leaving tracts of exposed ssDNA (Mimitou & Symington 2008; Toledo et al. 2013; Xiaoqing Chen et al. 2015). This mechanism may account for the severe spore viability defect of cells expressing *exo1-4S::A*.

Conversely, the phospho-mimicking mutant *exo1-4S::E* had a less prominent defect in spore viability of 81%, similar to that of *exo1Δ* cells expressing *EXO1*. If phosphorylation is indeed inhibiting the nuclease activity of Exo1, we would expect the phenotype of *exo1-4S::E* to resemble that of a nuclease dead *exo1* mutant. Studies of such mutants have shown that spore viability is reduced to around 88%, with a random pattern of spore death (Zakharyevich et al. 2010). These findings cannot confirm the hypothesis that phosphorylation negatively regulates the nuclease activity of Exo1, and so prompted further investigation into the effects of the Exo1 mutants during meiosis.

The turnover of DSBs was examined, both at a single locus and across a whole chromosome. The aim of this analysis was to investigate whether the phosphorylation status of Exo1 influenced the rate at which breaks were formed and repaired. No notable difference was observed at the ARE1 locus (section 3.5), however there was a difference in the levels of DSBs at various loci across chromosome III (section 3.6.2). These results suggest that perhaps *exo1-4S::A* influenced DSB site choice or the rate at which DSBs were made and repaired.

The lack of an obvious impact on DSB turnover at ARE1 appeared somewhat

paradoxical. A delay is observed at this locus in *exo1Δ*, and for such a severe spore viability defect it was expected that there might be an observable effect here. The effect on the levels of DSBs across chromosome III was also an unexpected one, as Exo1 is not thought to have a role in break site selection. This confusion coincided with some new results following successful integration of the mutant alleles at the *EXO1* locus. Spore viability of these newly integrated mutants revealed no significant difference between *EXO1* and *exo1-4S::A*, contradicting the findings outlined in section 3.3. In response to this discovery, the spore viability was revisited. In order to determine whether an unknown mutation was confounding the result, *exo1Δ* cells expressing *EXO1* and *exo1-4S::A* were sporulated and dissected. The viable products were then replicated on to plates containing hygromycin to select for those strains still containing vector after segregation. Haploids containing the vector were then mated, to reconstitute the *exo1Δ* diploids expressing either *EXO1* or *exo1-4S::A*. The aim of this process was to select viable spores so that any mutation that may be lethal in haploids, therefore causing reduced viability after sporulation, would be eliminated from the new diploids. Following this process the new diploids were dissected, and the viability of the new cells containing *exo1-4S::A* showed no significant difference to that of wild type.

While this was an extremely disappointing outcome, the initial ‘discovery’ of a phenotype had fuelled the creation of integrated tagged mutants, suitable for more reliable and informative experiments. These strains had proven to be promising in the investigation of a role for phosphorylation in meiosis, and will be discussed in the remainder of this thesis.

4. Characterisation of EXO1 phosphorylation during mitosis

Introduction

The nuclease Exo1 is active during both meiosis and mitosis (Mimitou & Symington 2009). In the absence of Exo1, there is reduced resection at mitotic DSBs. Previous studies have investigated the response of Exo1 to DNA damage and telomere uncapping. Bleomycin is an antibiotic with anti-tumour activity commonly used in the treatment of cancer as a chemotherapy agent. The mechanism of DNA damage by bleomycin is still not well understood, but it has been shown to cause DSBs by scission of hairpin DNA (Roy & Hecht 2014). This type of damage to DNA triggers initiation of repair by two key mechanisms, either by non-homologous end-joining (NHEJ pathways) or by homologous recombination (HR pathway) (Hustedt & Durocher 2017). Exo1 is active during homologous recombination in the resection of DNA prior to strand invasion. Unlike during meiosis, where it is required for dHJ resolution, Exo1 is not known to have a role in dissolution of dHJs in mitosis (Zakharyevich et al. 2012).

Chapter 3 described investigations carried out using exogenously expressed mutants of *EXO1*, that are reported either to mimic a constitutively phosphorylated state or to be non-phosphorylatable at the four serine residues S372, S567, S587 and S692 (Morin et al. 2008). Exogenous expression presented problems as the exogenously expressed *EXO1* allele did not fully rescue *exo1Δ*. While it was possible to check the plasmid was retained using selective markers, this did not indicate whether or not the Exo1 protein was being expressed at normal physiological levels. The plasmid contained a Tap tag fusion to the *EXO1* alleles, but the protein was not detectable by Western blot (data not shown), prohibiting direct expression studies.

The aim of the work presented in this chapter was to create a detectable tagged version of Exo1 and the putative phospho-mutants designed by Morin et al. to

overcome the issues faced by exogenous expression (Morin et al. 2008). Tagged Exo1 proteins would be used to study expression and confirm whether Exo1 was phosphorylated in response to DNA damage in the SK1 background. Tagging was carried out by designing and integrating a chromosomal cassette of Exo1, facilitating Western blot analysis of protein purified from mitotic cells. This was necessary in order to ensure that background variations between W303 (used by Morin et al.) and SK1 did not cause a different response to the Exo1 phosphorylation seen in mitosis.

Results

4.1 Tagging of Exo1 for Western blot analysis & integration of tagged Exo1 phosphomutants

To tag Exo1, a chromosomal tagging cassette was designed, incorporating a PK9 tagged *EXO1* ORF, the *KANMX* ORF, and 1kb of sequence downstream of *EXO1* (Figure 4.1 A & B). This cassette was assembled using Gibson assembly, and sub-cloned into pBlueScript between Spe1/Kpn1 restriction sites. The PK9 tag is derived from a short amino-acid epitope taken from simian virus 5 (SV5), selected for its ability to react with a monoclonal antibody (Southern et al. 1991). The PK sequence, GKPIPPLLGLDST, is utilized as a tag by insertion of tandem repeats, and it has been demonstrated that higher numbers of repeats allow more sensitive detection of the target proteins by Western blot (Gadaleta et al. 2013). The PK9 tag consists of 9 tandem repeats, and is tethered to the C-terminus of Exo1 via a short linker sequence. Commercial antibodies against PK with good specificity are readily available. It is worth acknowledging that there are indeed more conventional ways of incorporating tags and mutant cassettes into *S. cerevisiae*. Anecdotally, and within our lab, it has been found that the SK1 strain is less amenable to transformation than others, such as W303, and the *EXO1* locus in particular seems to be resistant to stable transformation. Other tags (FLAG and TAP) were attempted, and other methods such as knock in-knock out (whereby the locus of interest is first interrupted with a marker such as LEU2 and then reconstituted with the mutated version of the original region). As these methods

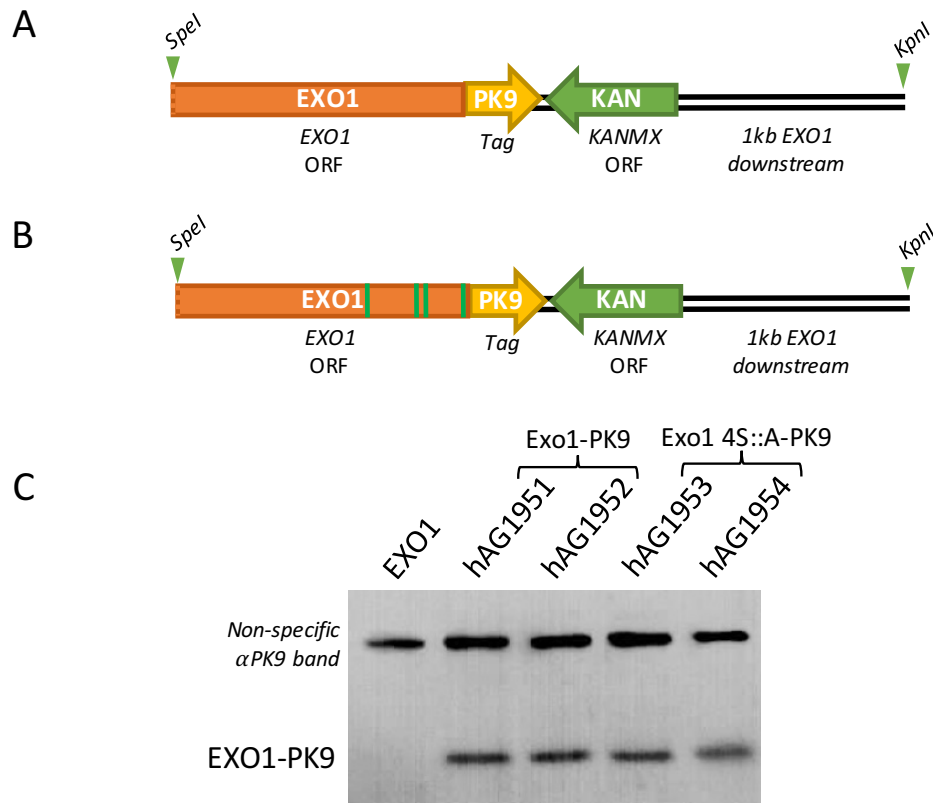


Figure 4.1 Tagging of EXO1/exo1-4S::A with PK9 tag

- (A) Schematic illustration of the construct restricted from pAG481 for transformation into hAG1886 and hAG1887 to yield hAG1952 and 1951, expressing C-terminally tagged Exo1-PK9. The ORF of EXO1 had the start codon missing, indicated by the dashed line, so that only transformants integrated into the correct frame would express. G418 resistance was conferred via the *KANMX* ORF to allow selection of positive transformants. 1000bp of genomic sequence downstream of EXO1 was integrated following *KANMX* to facilitate homologous recombination at integration.
- (B) Schematic illustration of the construct restricted from pAG482 for transformation into hAG1886 and hAG1887 to yield hAG1954 and 1953, expressing C-terminally tagged exo1-4S::A-PK9. Graph illustrating the change in expression of Exo1-PK9 through mitosis.
- (C) Western blot of a 7.5% SDS-PAGE gel illustrating visualisation of Exo1-PK9 using α -PK9 antibody. hAG1951 and 1952 show Exo1-PK9, while hAG1953 and 1954 show exo1-4S::A-PK9. hAG1886 is used as a negative control to show the absence of the Exo1-PK9 band in strains WT for EXO1 but lacking the PK9 tag. Exo1 itself has a molecular weight of approximately 81kDa, however the extra 132 amino acids within the PK9 tag and linker contribute an additional 14kDa, accounting for the discrepancy.

proved unsuccessful the method described here was used instead.

To create tagging cassettes incorporating the Exo1 putative phospho-mutants, *exo1-4S::A* and *exo1-4S::E*, the distal portion of the ORF was amplified from pAG451 or pAG452 by PCR. Flanking homology to pBH259 at the PK9 tag was incorporated to create a fragment with overlapping ends capable of undergoing Gibson assembly with digested pBH259. Assembly yielded vectors with tagged mutant cassettes suitable for chromosomal integration. Tagged cassettes were isolated from the vector by digestion using *SpeI/KpnI* enzymes that recognised specific restriction sites flanking the cassette. The cassette was then integrated by transformation into chemically competent haploids, exploiting yeast's propensity to incorporate new fragments via homologous recombination at the target locus. Positive transformants were selected via growth on media containing G418, and colonies checked for expression of the tagged protein by Western blot analysis. The cassette was designed to lack the start codon of the *EXO1* ORF, and so only those incorporated at the correct locus would express Exo1-PK9. Transformants expressing tagged Exo1 were selected for sequencing to confirm the correct sequences of *EXO1*, *exo1-4S::A* and *exo1-4S::E*. Haploids positive for correct incorporation of both *EXO1* and *exo1-4S::A* were obtained from the first round of transformation. However, several rounds of transformation and sequencing of dozens of PK-9 tagged *exo1-4S::E* transformants did not yield a single haploid in which all four mutated sites were correct for the glutamic acid codon. As a result, only investigations into the *EXO1-PK9* and *exo1-4S::A-PK9* strains are discussed here.

Protein extracts from mitotically cycling transformants positive for *EXO1-PK9* and *exo1-4S::A-PK9* were tested by Western blotting for expression of Exo1-PK9. A non-specific band, approximately 140kDa, was seen in negative control strain (hAG1886) as well as in *EXO1-PK9* strains (hAG1951; hAG1952), and *exo1-4S::A-PK9* strains (hAG1953; hAG1954 (Figure 4.1 C). At approximately 95kDa is the Exo1-PK9/ Exo1-4S::A-PK9. These results demonstrate the successful tagging and chromosomal integration of *EXO1* and the non-phosphorylatable mutant *exo1-4S::A-PK9*, enabling phenotype studies to be carried out.

4.2 Exo1 and Exo1-4S::A-PK9 expression in mitosis changes during the response to bleomycin-induced DNA damage

The signal of the Exo1 band was low and difficult to express, requiring a prolonged exposure of the membrane and use of high-sensitivity reagents in the detection process. This may have been a reflection of a low expression level of Exo1-PK9 during exponential growth. To establish whether DNA damage might increase the level of Exo1-PK9, DSBs were induced in exponentially growing cells through exposure to bleomycin. Cells were sampled at 0 h (before induction of damage), 2 h or 6 h post induction of damage, and total protein was extracted using the TCA method. 10µl of protein was resolved by 12% SDS-PAGE gel, and analysed by Western blot (Figure 4.2 A). Protein levels were calculated using scanning densitometry. The band area was assigned and the total signal computed, giving a value proportional to the quantity of protein present. The P-STAIR antibody recognises cyclin dependent kinase Cdc28 and is used as a loading control. The proportion of Exo1 to Cdc28 was used to account for uneven loading when determining the quantity of Exo1. The fold change in this proportion with respect to the 0 h (pre-damage induction) sample was used to appreciate the relative fluctuations of Exo1 expression.

The fold change in Exo1-PK9 expression between 0 h (before bleomycin exposure) and 2 h (the early stages following initial exposure) was approximately 20% after 2 h for haploid cells, while levels remained unchanged in diploid cells (Figure 4.2 B & C). The similar amounts before and shortly after induction of damage suggest both exponential growth and the response to DNA damage require a similar level of Exo1-PK9 expression. 6 h after exposure to bleomycin the level of Exo1 decreases, falling 70% in haploid cells and 95% in diploid cells. Overall, these results show Exo1-PK9 expression is not increased in response to bleomycin-induced DNA damage, and that Exo1-PK9 is likely to be constitutively expressed at low levels.

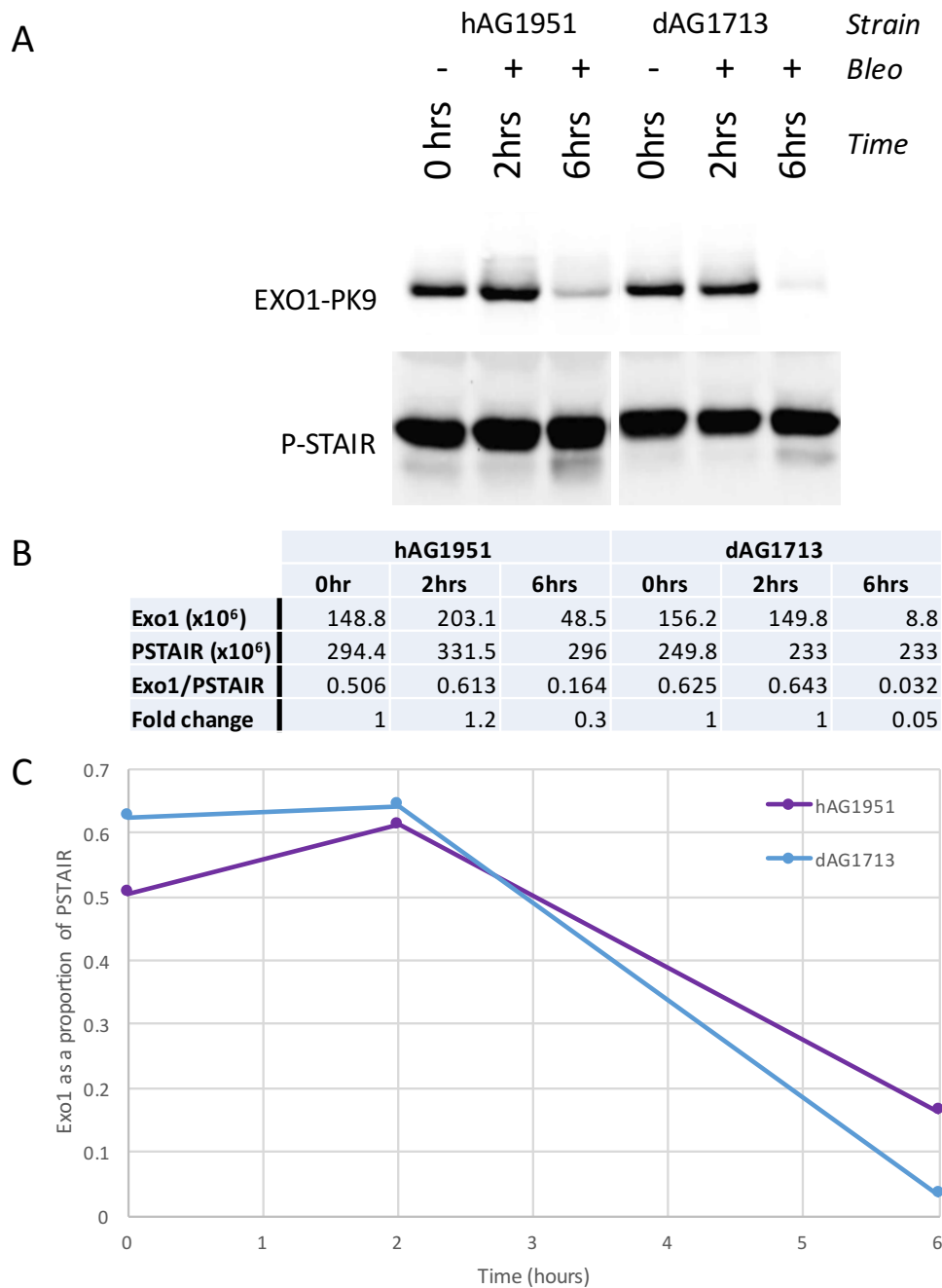


Figure 4.2 EXO1 expression reduces after 2 hours following bleomycin treatment

- (A) Western blot of a 12% SDS-PAGE gel using α PK9 to detect Exo1-PK9 isolated at 0, 2, and 6 hours during mitosis in exponentially growing haploid (hAG1951) and diploid (dAG1713) cells following the addition of bleomycin after sampling of cells at 0hrs. α PSTAIR is used to identify cyclin dependent kinases used as a loading control.
- (B) Densitometry values of each band in Exo1-PK9 and PSTAIR are shown as millions, and the proportion of Exo1-PK9 is calculated relative to the PSTAIR loading control. Fold increase is the change in proportion relative to 0hr.
- (C) Graph illustrating the change in expression of Exo1-PK9 through mitosis. The blot, data and graph are from a single representative blot selected from dozens of independent repeats that all show the same pattern.

4.3 Confirming Exo1 is phosphorylated in response to bleomycin induced-DNA damage

To confirm that DNA damage induces phosphorylation of Exo1, cells were cultured and treated with bleomycin as described in section 4.2. Cells were sampled from cultures treated with bleomycin or no treatment 4 h post-induction, and total protein extracted using the TCA method, resolved by 7.5% SDS-PAGE gel and analysed by Western blot (Figure 4.3 A).

Untagged *EXO1* is shown as a negative control. Exo1-PK9 appears to show a species with reduced motility after damage induction when compared to the untreated sample. This is seen as a smear above the band. Reduced motility of a protein can be due to the protein being more negatively charged, as is the case when a protein is phosphorylated. The smear is not visible in damage-induced dAG1714 cells expressing Exo1-4S::A-PK9, indicating an absence of any slower moving species of the protein. The Western analysis suggests that Exo-PK9 is phosphorylated in response to DNA damage while the non-phosphorylatable mutant Exo1-4S::A-PK9 is not.

Visual analysis of a Western blot is subjective, and a band shift may not be clear when analysed by eye. One way of further examining the Western is to look at the profile of the signal along the lane. Subtle variances or similarities may become more apparent. The lane profiles of dAG1713 and dAG1714 before and after DNA damage induction have been plotted (figure 4.3 B). The first peak (Peak 1) is seen at relative front (RF) 0.2, and corresponds to the non-specific band. This peak was used to align the profiles. Peak 2 represents the signal profile of Exo1 in each strain. Peak 2 of dAG1713 shows a clear shoulder from RF 0.65 that remains 0.05 units ahead of Peak 2 in dAG1714 or dAG1713 prior to induction. The peaks decline together from RF 0.8. The shoulder present in dAG1713 following induction further supports the presence of a species of Exo1 with reduced motility when compared to pre-induced Exo1, suggestive of DNA-damage induced phosphorylation of Exo1.

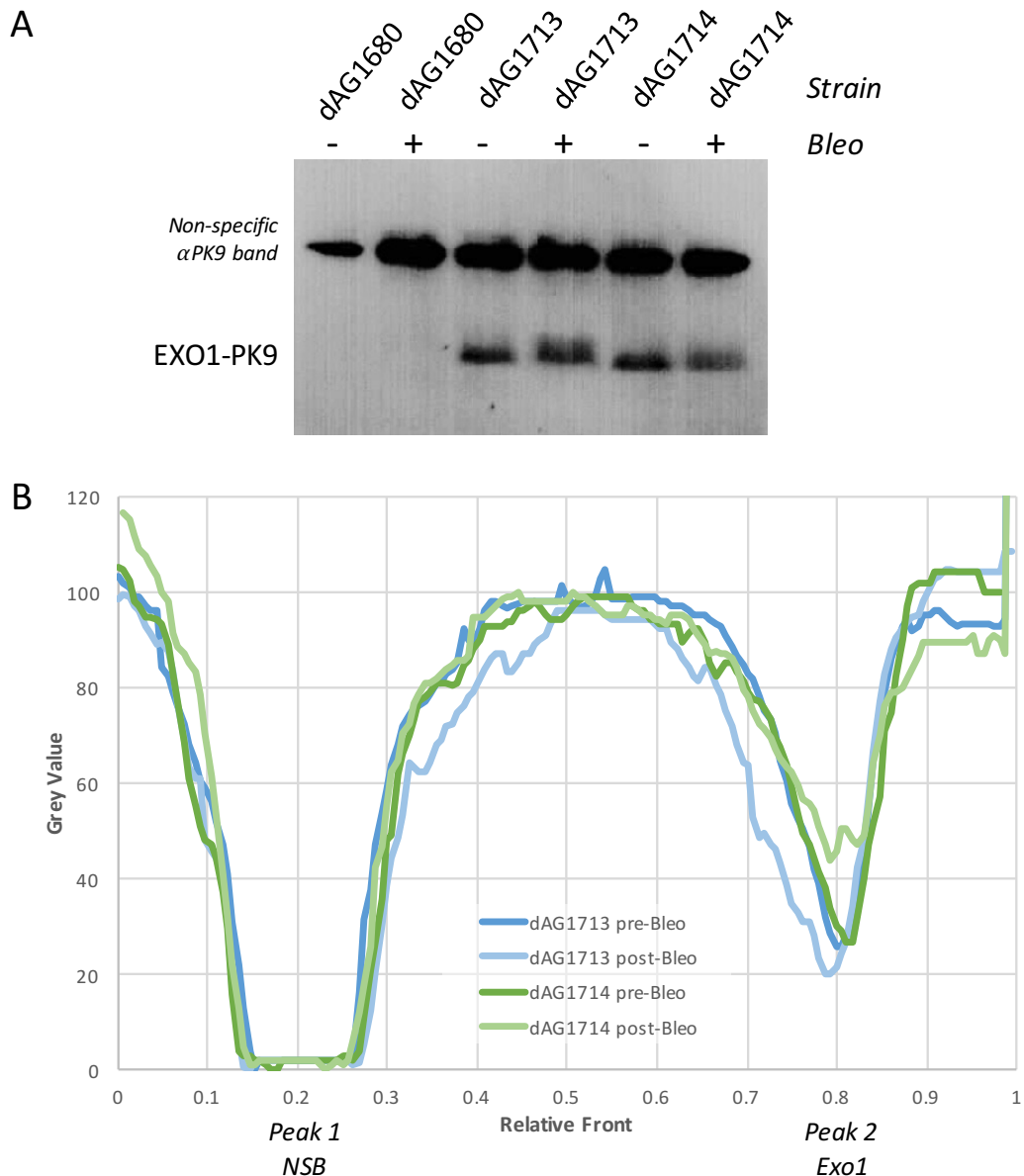


Figure 4.3 EXO1 is phosphorylated in response to DNA damage

- (A) Western blot of a 7.5% SDS-PAGE gel using α PK9 to detect Exo1-PK9 in TCA protein extractions before and after addition of bleomycin to induce DNA damage. dAG1680 is a negative control. dAG1713 shows reduced Exo1-PK9 motility in response to DNA damage, suggestive of phosphorylation. dAG1714 shows exo1-4S::A-PK9 motility is not affected by DNA damage induction as the residues believed to be phosphorylated (as determined by Morin et al. 2008) are absent.
- (B) Graph displaying the grey value lane profile of dAG1713 and dAG1714. The profiles are aligned using peak 1, corresponding to the non-specific band (NSB). Peak 2 of dAG1713 post-bleomycin shows a decrease in grey value significantly earlier than that of dAG1713 pre-bleomycin, again suggesting reduced motility of Exo1-PK9. In contrast, peak 2 of both dAG1714 pre- and post-bleomycin align, suggesting no difference in motility.

Discussion

Previously Morin et al. 2008 demonstrated that Exo1 is phosphorylated in response to DNA damage. They produced the non-phosphorylatable mutant Exo1-4S::A, which was integrated into the meiosis-proficient strain SK1 at the Exo1 locus. Chromosomal integration of tagged Exo1-PK9 or Exo1-4S::A-PK9 allowed analysis of the proteins expressed under their wild-type promoter. Subsequent conclusions could then be drawn with the assumption that the observed results were representative of wild-type protein expression levels and timing. The results presented here support the hypothesis that Exo1 is phosphorylated in response to DNA damage, and show that the findings of Morin et al. 2008 are transferable to diploid yeast of the SK1 background.

Exo1 phosphorylation has also been described in mammalian systems (Bolderson et al. 2010; Manfrini et al. 2010; Engels et al. 2011; Tomimatsu et al. 2014). While phosphorylation of Exo1 is proposed to inhibit its nuclease activity in *S. cerevisiae*, experiments in mammalian systems have suggested an excitatory role for this modification. These conflicting conclusions may be due to more complex regulatory pathways of Exo1 in the mammalian DNA repair processes. Mammalian Exo1 is known to interact with various regulators of repair such as CtIP (Sae2 homolog) (Eid et al. 2010), BLM (Sgs1 homolog) (Nimonkar et al. 2011), and BRCA1 (Tomimatsu et al. 2014). These physical interactions are not observed between *S. cerevisiae* Exo1 and the corresponding homologs, and BRCA1 has no homolog in yeast. These differing interactions may account for the contrary roles of phosphorylation in mammalian systems and *S. cerevisiae*.

Regardless of the role of phosphorylation, thus far its existence has not been investigated during meiosis. The data discussed in this chapter show that Exo1-PK9 and Exo1-4S::A-PK9 are expressed in the meiosis-proficient strain SK1, and that the proteins are detectable by Western blot. Using bleomycin as a DNA damaging agent enabled replication of a band-shift on Western blots, seen by Morin et al. in phosphorylated Exo1. This system in the SK1 background presents an opportunity for the study of Exo1 phosphorylation during meiosis following the findings of Morin et al. 2008 in mitotically cycling cells.

5. Characterisation of EXO1 phosphorylation during meiosis

Introduction

As previously described, the nuclease Exo1 is active during both meiosis and mitosis (Mimitou & Symington 2009). During mitosis Exo1 functions primarily as a nuclease, and in the absence of Exo1 cells are more sensitive to DNA damaging agents such as camptothecin (Morin et al. 2008). This increased sensitivity may be due to a modest but functionally significant reduction in resection at mitotic DSBs. Conversely, increased expression and therefore activity of Exo1 leads to hyper-resection of DNA, and this can suppress sensitivity to DNA damaging agents (Tsubouchi & Ogawa 2000). Morin et al have shown that during mitosis Exo1 is phosphorylated in response to DNA damage and telomere uncapping, a modification thought to inhibit its nuclease activity. This inhibition may serve to regulate the resection carried out by Exo1, preventing hyper-resection. A constitutively active mutant of Exo1 might therefore be anticipated to have decreased sensitivity to DNA damage due to an ability to hyper-resect. Indeed, Morin et al. showed that the non-phosphorylatable mutant *exo1-4S::A* is less sensitive to DNA damage than its wild type or phospho-mimetic counterparts.

During meiosis Exo1 has functions both as a nuclease and in crossover resolution, in temporally distinct roles (Zakharyevich et al. 2010). Lack of Exo1 causes a hypo-resective phenotype in meiosis, and the crossovers formed are both reduced and delayed (Keelagher et al. 2010; Zakharyevich et al. 2010). If phosphorylation during mitosis influences the resection activity of Exo1, it is reasonable to imagine that a similar mechanism may be employed to control resection in meiosis. Exo1 must strike a balance between resection extensive enough for efficient strand invasion, but not too much as this may destabilise the interactions needed to form a dHJ.

The aim of the work presented in this chapter was to establish whether Exo1 was phosphorylated in *S. cerevisiae* during meiosis, in response to the formation of Spo11 DSBs. In addition, the effects of the non-phosphorylatable Exo1 mutant, Exo1-4S::A-PK9, on meiosis were examined.

Results

5.1 EXO1 expression varies through meiosis

In order to examine Exo1-PK9 expression during meiosis cells (dAG1713) were triggered into a synchronous meiosis and sampled at 0, 4 6 and 8 hours of meiosis (section 2.5.12), and total protein was extracted using the TCA method. 10µl of protein was resolved by 12% SDS-PAGE gel, and analysed by Western blot (Figure 5.1 A). Protein levels were calculated using scanning densitometry, and the relative quantity of Exo1-PK9 calculated as described in section 4.2 (Figure 5.1 B). As previously, the fold change in the proportion of Exo1 to PSTAIR with respect to the 0hr sample was used to appreciate the relative fluctuations of Exo1 expression (Figure 5.1 C). Initially at 0 hours, low levels of Exo1-PK9 are expressed, followed by a significant increase at 4 and 6 hours, where Exo1-PK9 levels are almost 5 times higher. By 8 hr levels have returned to a similar level as seen at 0 hrs.

5.2 EXO1 is phosphorylated in meiosis

5.2.1 Analysis of Exo1-PK9 extracted under denaturing conditions

The increase in Exo1-PK9 expression that coincides with DSB formation and repair suggests temporal regulation of Exo1 relative to its meiotic functions. As well as regulating the timing of expression, cells may regulate Exo1 activity during meiosis by post-translational modifications, such as the phosphorylation seen in mitosis. Cells were cultured and synchronised into meiosis. Cells were sampled at 0, 2, 4, 6, and 8 hr post-induction, and total protein extracted using the TCA method. To distinguish between putatively phosphorylated and non-phosphorylated Exo1-PK9 protein a 7.5% gel was used. 15µl of protein was resolved by SDS-PAGE gel, and analysed by Western blot (Figure 5.2 A).

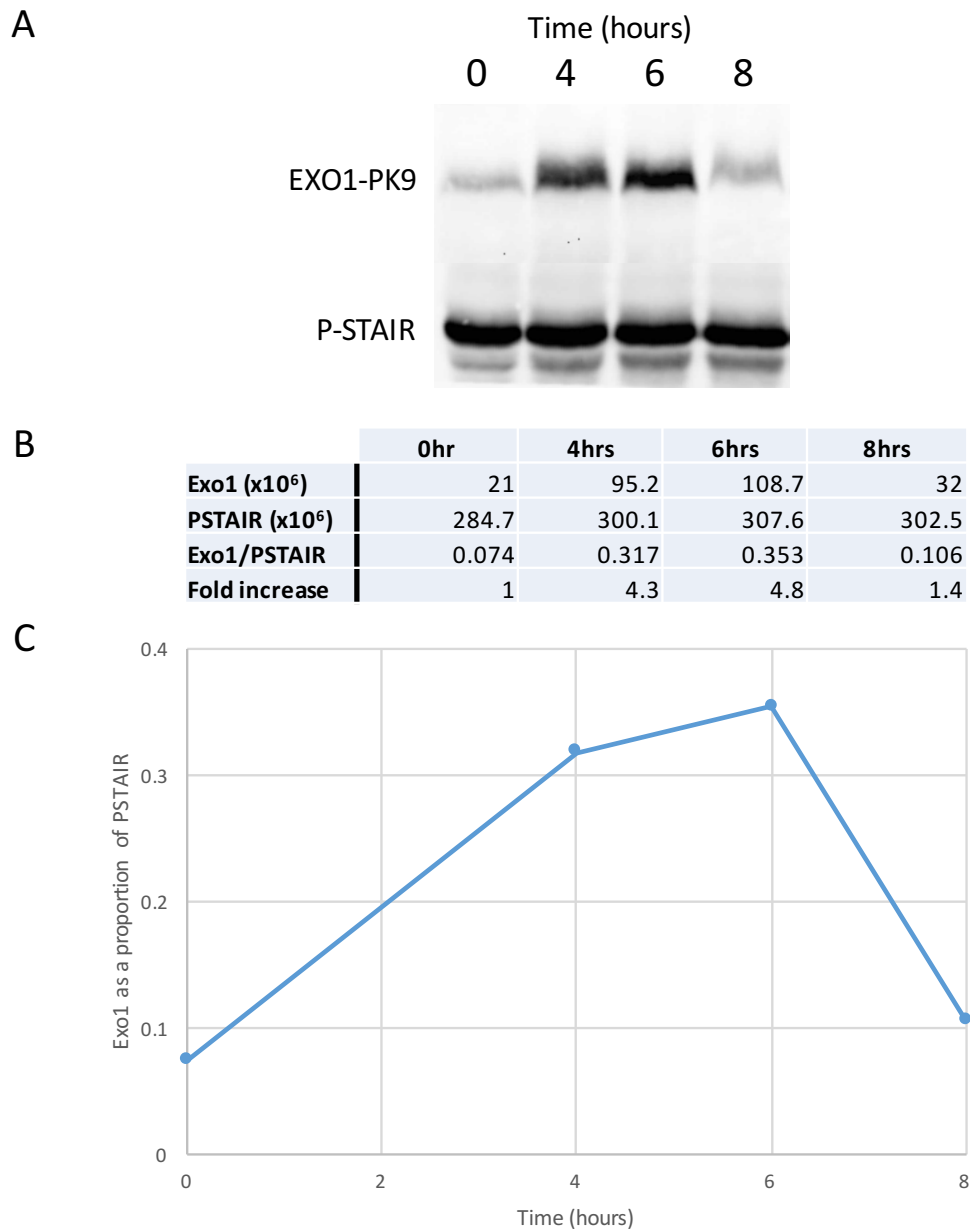


Figure 5.1 EXO1 expression varies over time during meiosis

- (A) Western blot of a 12% SDS-PAGE gel using α PK9 to identify Exo1-PK9 isolated at 0, 4, 6 and 8 hours during meiosis. α PSTAIR is used to identify cyclin dependent kinases used as a loading control. The band intensity of Exo1-PK9 increases from 0-6 hours (hour two similar to 0hrs, not shown) and then returns to a low level at 8hrs.
- (B) Densitometry values of each band in Exo1-PK9 and PSTAIR are shown as millions, and the proportion of Exo1-PK9 is calculated relative to the PSTAIR loading control. Fold increase is the change in proportion relative to 0hr.
- (C) Graph illustrating the change in expression of Exo1-PK9 through meiosis. The blot, data and graph are from a single representative blot selected from dozens of independent repeats that all show the same pattern.

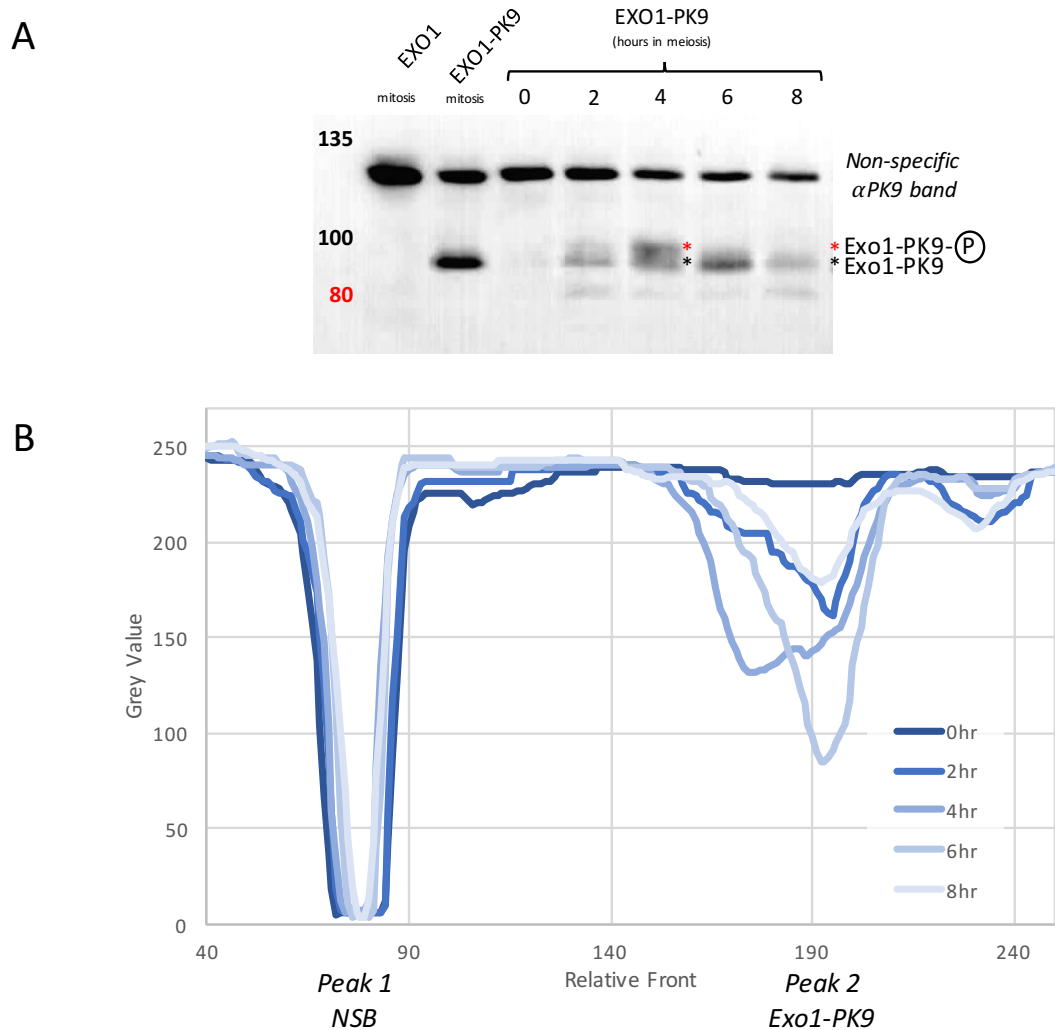


Figure 5.2 Exo1-PK9 has two species of different motility during meiosis

- (A) Western blot of 7.5% SDS-PAGE gel using α PK9 to identify Exo1-PK9 isolated by TCA extraction at 0, 2, 4, 6 and 8 hours during meiosis with mitotic samples of dAG1680 (positive control) and dAG1713 (negative control). Two bands are distinguishable at 4 hours. The higher molecular weight band is suggestive of a post-translationally modified population of Exo1-PK9 (labelled as P).
- (B) Graph displaying the grey value lane profiles of Exo1-PK9 at 0, 2, 4, 6 and 8 hours during meiosis. The profiles are aligned using peak 1, corresponding to the non-specific band (NSB). Peak 2 shows a decrease in grey value prior to the Exo1-PK9 band at RF 190. This difference, appearing as a shoulder on the troughs at 2 and 6 hours, and most prominently at 4 hours as a dual-trough, suggests a lower motility species of Exo1-PK9, consistent with post-translational modification.

Mitotically cycling dAG1680 and dAG1713 in the exponential growth phase were used as negative and positive controls. The non-specific anti-PK9 band is present in both, however Exo1-PK9 is only detected in dAG1713. At 0 hr before meiosis is initiated Exo1-PK9 is undetectable. The protein first becomes visible at 2 hr, with a faint band corresponding to Exo1-PK9 preceded by a fainter smear above it of reduced motility. By 4 hr two bands can be distinguished, separated by a subtle line of reduced signal. At 6 hr the Exo1-PK9 band is at its strongest, and the lower motility species has reduced in intensity. By 8 hr a single faint band at the molecular weight of Exo1-PK9 is visible. As described in section 4.3, a reduction in protein motility can be due to that protein being more negatively charged, such as when a protein is phosphorylated. Figure 5.2 A appears to show a reduced motility species, most significantly present at 4 hr of meiosis. This result is suggestive of meiotic phosphorylation of Exo1-PK9.

In order to eliminate some subjectivity of analysing by eye, the lane signal intensities were plotted using computer software (Fiji) to detect the greyscale intensity. The lane profiles of dAG1713 throughout meiosis was plotted (Figure 5.2 B). The first peak (Peak 1) seen at relative front (RF) 80 corresponds to the non-specific band (NSB). This peak was used to align the profiles. Peak 2 represents the signal profile of Exo1-PK9. At 0 hr, as observed in figure 5.2A, Exo1-PK9 is undetectable. At 2 hr the peak corresponding to Exo1-PK9 at RF 190 is present and has a small shoulder beginning at RF 155. This shoulder represents the reduced motility band seen in figure 5.2 A. At 4 hours there appears to be a broad peak, from RF 150 to 210 that dips in the middle, suggestive of two distinct species of Exo1-PK9. By 6 hr the majority of the signal is at RF 190, and a small shoulder at 155 is still present. Finally, at 8 hr, there is no longer a shoulder accompanying the Exo1-PK9 peak. This quantitative analysis concurs with the observation that Exo1-PK9 appears to be post-translationally modified through meiosis. This modification comprises the largest proportion of protein at 4 hr, when the lower motility band has a signal intensity higher than that of the Exo1-PK9 band. The timing of this band corresponds to that at which DSB turnover is highest, around 3-4 hr (Figure 3.4), during MI. By 8 hr meiosis is complete in most cells, reflected in a decrease of Exo1-PK9 expression and the absence of any lower

motility band.

5.2.2 Analysis of Exo1-PK9 isolated under native conditions

Treatment of protein with phosphatase was carried out to confirm whether the shift in mobility was due to phosphorylation of Exo1-PK9. This was a very complex and time consuming process, and so only the 4 hr sample was used as this had the highest level of signal for the lower-mobility species. Cells were synchronised into meiosis and a 0 hr sample taken as a control. At 4 hours the cells were harvested, and an aliquot was removed for TCA extraction alongside the 0 hr sample. These samples were used as controls for expression levels and the normal pattern of the shift (right-most two lanes of Figure 5.3 A). The remainder of the cells were treated for protein extraction using a gentle protocol under native conditions. This gentle approach was important for maintaining physiological pH and salt concentrations, facilitating immunoprecipitation of Exo1-PK9 and treatment with lambda phosphatase enzyme. Extracted protein was incubated with beads pre-bound to anti-PK9. During immunoprecipitation the extracts were also treated with various combinations of phosphatase and phosphatase inhibitors. Finally, the unbound protein was removed and the bound Exo1-PK9 eluted for resolving on a 7.5% SDS-PAGE gel and Western blot analysis.

Lane 1 of Figure 5.3 A shows the total unbound protein after IP, while lane 2 contains total protein prior to IP. Comparison of these two lanes shows the relative amounts of Exo1-PK9 present after and before IP. The high MW non-specific band remains present in these samples. Lane 3, 4 and 5 show eluted IP samples, with various treatments. All lanes show a band corresponding to the control band for Exo-PK9, indicating successful IP of Exo1-PK9. The non-specific band is no longer present. Lane 3 is IP that contained phosphatase inhibitors without the addition of phosphatase. Lane 4 is IP treated with phosphatase in the absence of inhibitors. Lane 5 is IP treated with phosphatase in the presence of inhibitors. Lanes 3 and 5 both show a lower mobility band, represented as a smear above Exo1-PK9. This smear is absent in lane 4, suggesting that the presence of this species depends upon treatment with phosphatase.

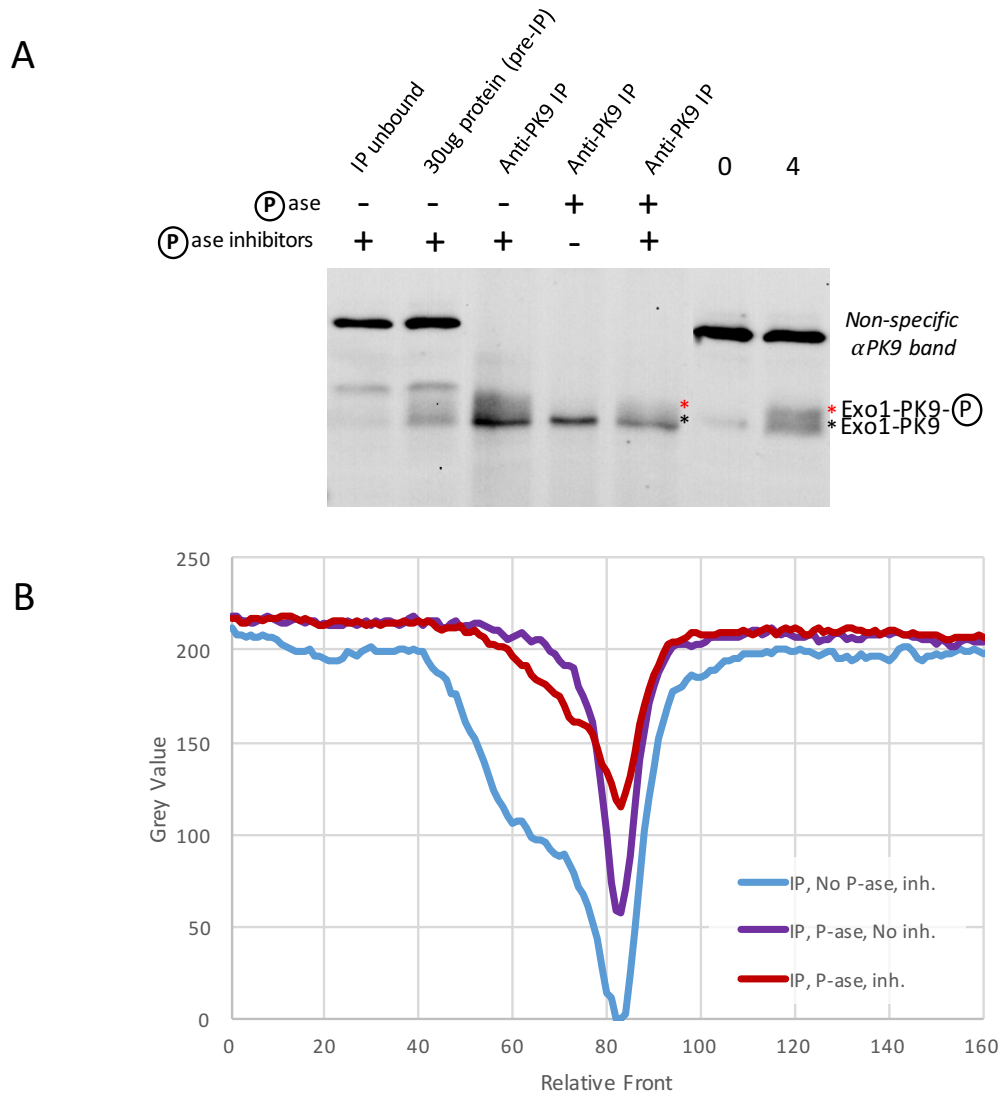


Figure 5.3 Exo1-PK9 is phosphorylated during meiosis

- (A) Western blot of 7.5% SDS-PAGE gel using α PK9 to identify Exo1-PK9 isolated from dAG1713. The five IP (immuno-precipitated) samples were cells at 4 hours of meiosis isolated by native extraction, while the final two lanes were cells at 0 and 4 hours of meiosis isolated by TCA extraction. IP samples have been treated with various combinations of phosphatase and phosphatase inhibitors indicated by + or -. Lanes 3 and 5 show a smear superiorly to the Exo1-PK9, suggestive of the phosphorylated population of Exo1-PK9. This smear is absent in lane 4, in which the sample has been treated with phosphatase in the absence of inhibitors, suggestive of a removal of phosphorylation. This confirms the higher molecular weight band to be phosphorylated Exo1-PK9. TCA extracted samples of Exo1-PK9 in lanes 6 and 7 are provided for comparison of phosphorylated and non-phosphorylated species.
- (B) Graph displaying the grey value lane profiles of lanes 3, 4 and 5. Lanes 3 and 5, corresponding to either IP treated or untreated with phosphatase in the presence of inhibitors, shows a decrease in grey value prior to the Exo1-PK9 band around RF 80. This difference, appearing as a shoulder on the troughs, suggests a lower motility species of Exo1-PK9, consistent with phosphorylation. This shoulder is absent in lane 4, showing IP treated with phosphatase in the absence of inhibitors.

To support the conclusion made from Figure 5.3 A, the Western image was subjected to quantification analysis, and the lane profiles plotted along an axis (Figure 5.3 B). The peaks were aligned at their lowest value, denoting Exo-PK9 at approximately RF 85. Lane 3 (blue line) shows a significant shoulder from RF 40 prior to the Exo1-PK9 signal. Lane 5 has a lower signal for Exo1-PK9, approximately half that of lane 3. Lane 5 also displays a proportionally smaller shoulder, detectable from RF 60. Lane 4 has no such shoulder despite having a stronger signal for Exo1-PK9 than in lane 5, supporting the conclusion that this species is dependent on phosphatase treatment.

It can be concluded that the presence of a lower mobility species of Exo-PK9 seen as a phospho-shift band on Western blot is a phosphorylated species of Exo1-PK9. This phosphorylation of Exo1-PK9 is not initially present, but appears from 2 hours and is most evident at 4 hours of meiosis, corresponding to the time point at which DSB turnover is highest.

5.3 EXO1 is phosphorylated differently in meiosis than in mitosis

5.3.1 Analysis of Exo1-4S::A-PK9 extracted under denaturing conditions

To further investigate the phosphorylation of Exo1-PK9 during meiosis, cells expressing Exo1-4S::A-PK9 (dAG1714) were used. This strain expresses a non-phosphorylatable allele of Exo1, described by Morin et al. The mutated residues were determined to be strongly phosphorylated during mitosis. Investigation of the protein during meiosis by Western blot analysis could show whether this protein is still phosphorylated, or if the phosphorylation seen in section 5.2 was dependent on those same key residues identified in mitosis. Cells were sampled at 0, 2, 4, 6, and 8 hr post-induction, and total protein extracted using the TCA method. The samples were resolved and analysed as described in section 5.3.1 (Figure 5.4 A).

Mitotically cycling dAG1680 and dAG1714 in the exponential growth phase were used as negative and positive controls in the first two lanes. At 0 hours before meiosis is initiated Exo1-4S::A-PK9 is undetectable. The protein first

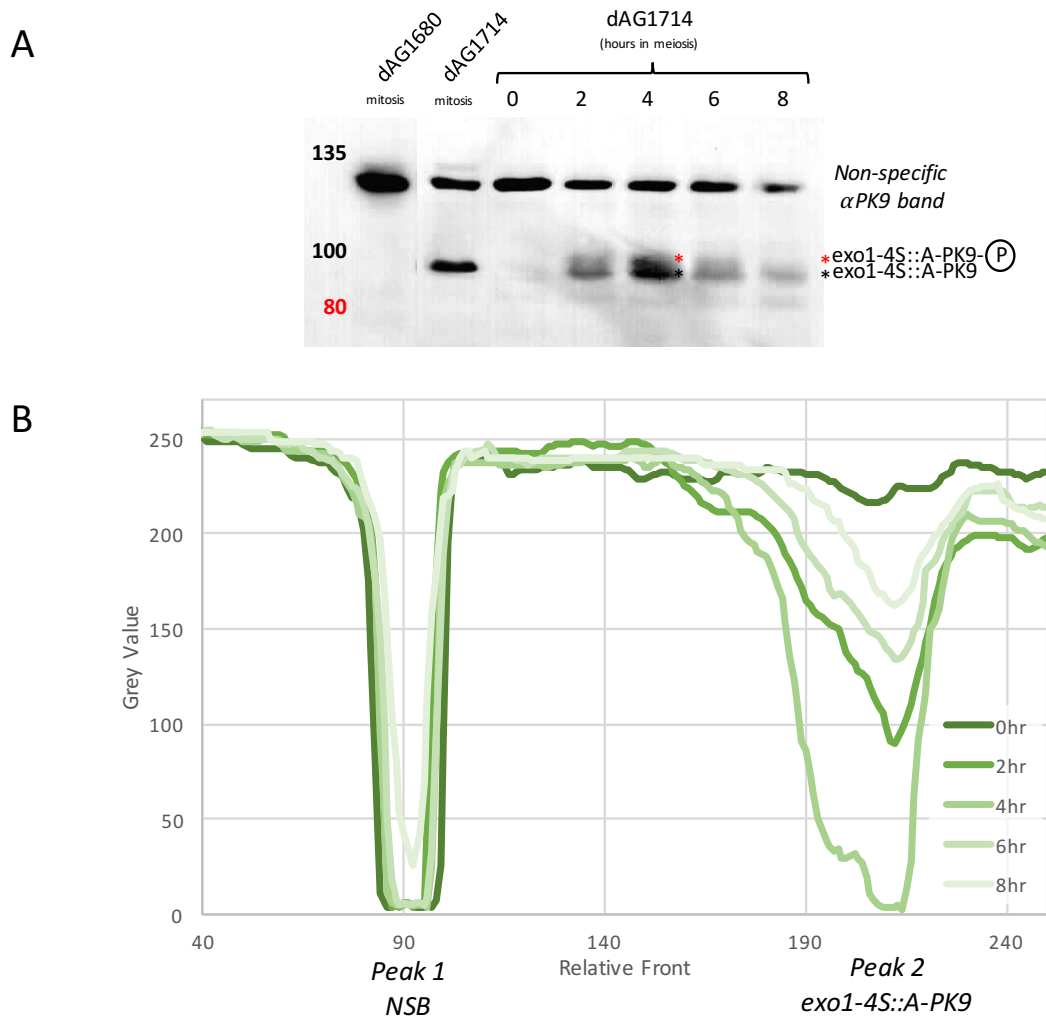


Figure 5.4 exo1-4S::A-PK9 has two species of different motility during meiosis

- (A) Western blot of 7.5% SDS-PAGE gel using α PK9 to identify exo1-4S::A-PK9 isolated by TCA extraction at 0, 2, 4, 6 and 8 hours during meiosis with mitotic samples of dAG1680 (-ve control) and dAG1714 (+ve control). Two bands are distinguishable at 2, 4 & 6 hours. The higher molecular weight band is suggestive of a phosphorylated population of exo1-4S::A-PK9.
- (B) Graph displaying the grey value lane profiles of exo1-4S::A-PK9 at 0, 2, 4, 6 and 8 hours during meiosis. The profiles are aligned using peak 1, corresponding to the non-specific band (NSB). Peak 2 shows a decrease in grey value prior to the Exo1-PK9 band at RF 210. This difference, appearing as a shoulder on the troughs at 2 and 6 hours, and most prominently almost bifurcating at 4 hours, suggests a lower motility species of exo1-4S::A-PK9, consistent with phosphorylation, as seen in Exo1-PK9 (figure 5.3 B)

becomes visible at 2 hr, as seen in Exo1-PK9. Similarly, this band is preceded by a slower motility band, which persist until 6 hours of meiosis, and is no longer detectable by 8 hours. As discussed in section 5.2.1, this type of shift is suggestive of meiotic phosphorylation of Exo1-4S::A-PK9. Quantification of the lane signal by computational analysis supports this conclusion (Figure 5.4 B). Profiles were aligned using the NSB (Peak 1) at RF 90. Exo1-4S::A-PK9 is represented by Peak 2 at RF 210. A similar shoulder to that seen in section 5.2.1 is observed on Peak 2 of samples 2, 4 and 6 hours, representing the signal from the slower motility band preceding Exo1-4S::A-PK9. This is again particularly prominent at 4 hours of meiosis, and is present from approximately RF 160.

5.3.2 Analysis of Exo1-4S::A-PK9 isolated under native conditions

Meiotic samples of Exo1-4S::A-PK9 were treated with phosphatase to confirm whether the shift in mobility was due to phosphorylation. Cells were harvested and treated as described in section 5.2.2. Lane 1 in Figure 5.5 A shows the total unbound protein after IP, while lane 2 contains total protein prior to IP, demonstrating the relative amounts of Exo1-4S::A-PK9 present. The lanes are loaded with samples of Exo1-4S::A-PK9 treated as described for Exo1-PK9 in section 5.2.2. As was seen in Figure 5.3 A, lanes 3 and 5 both show a lower mobility band, represented as a smear above Exo1-4S::A-PK9. This smear is absent in lane 4, suggesting that the presence of this species depends upon treatment with phosphatase. This conclusion is supported by quantification of the lane signals intensity (Figure 5.5 B). The shoulder on peak 2 representative the slower mobility protein is present in both the samples treated with phosphatase inhibitors in the presence or absence of phosphatase. This shoulder is absent in the sample treated with phosphatase in the absence of inhibitors.

It can be concluded that Exo1-4S::A-PK9 is phosphorylated in meiosis, and that this phosphorylation is not dependent upon key serine residues S372, S567, S587 and S692 identified in mitotic experiments by Morin et al. Phosphorylation in meiosis can be distinguished as different from that observed in mitotically cycling cells.

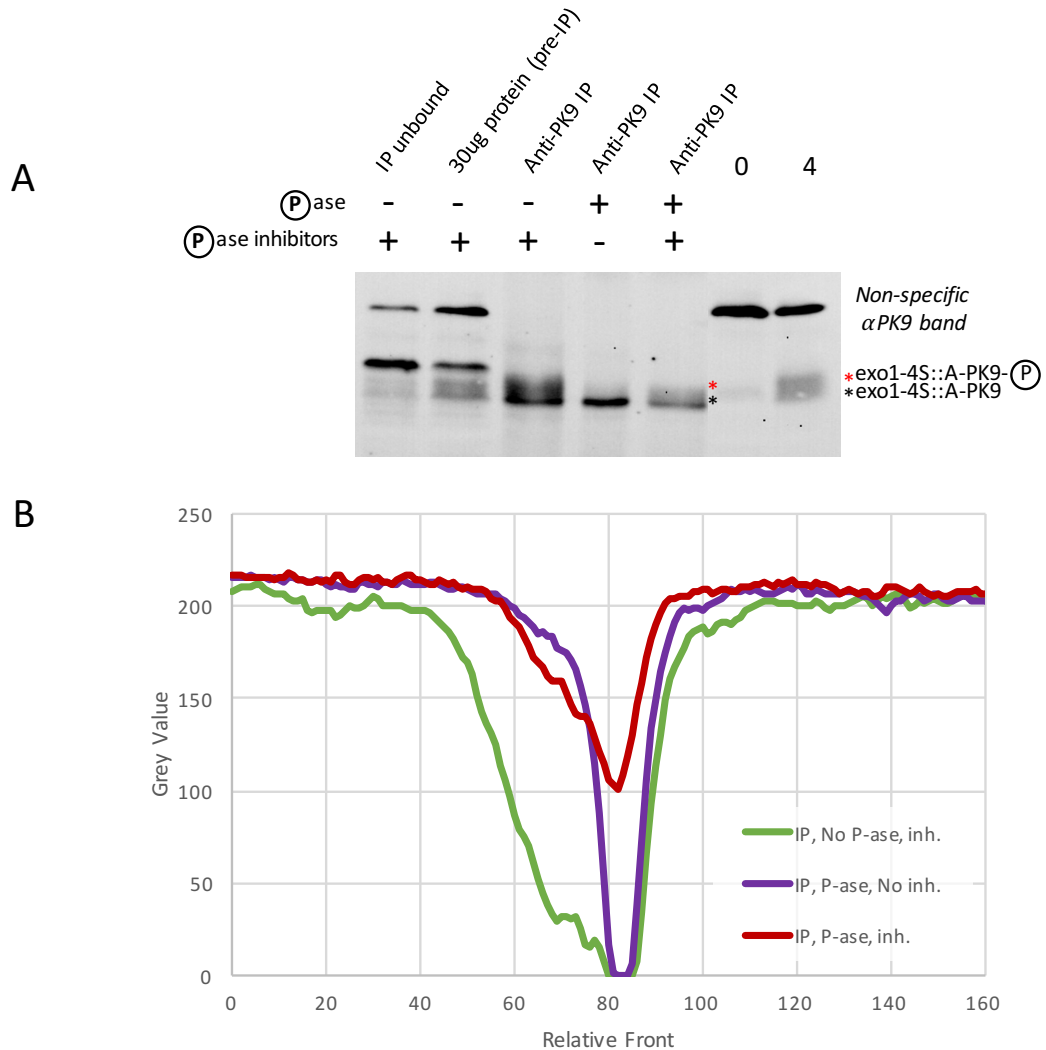


Figure 5.5 *exo1-4S::A-PK9* is phosphorylated during meiosis

(A) Western blot of 7.5% SDS-PAGE gel using α PK9 to identify *exo1-4S::A-PK9* isolated from DAG1713. The five IP (immuno-precipitated) samples were cells at 4 hours of meiosis isolated by native extraction, while the final two lanes were cells at 0 and 4 hours of meiosis isolated by TCA extraction. IP samples have been treated with various combinations of phosphatase and phosphatase inhibitors indicated by + or -. Lanes 3 and 5 show a smear superiorly to the *exo1-4S::A-PK9*, suggestive of the phosphorylated population of *exo1-4S::A-PK9*. This smear is absent in lane 4, in which the sample has been treated with phosphatase in the absence of inhibitors. Absence of this smear following treatment is suggestive of a removal of phosphorylation, confirming the higher molecular weight band was phosphorylated *exo1-4S::A-PK9*. TCA extracted samples of *exo1-4S::A-PK9* in lanes 6 and 7 are provided for comparison of phosphorylated and non-phosphorylated species.

(B) Graph displaying the grey value lane profiles of lanes 3, 4 and 5. Lanes 3 and 5, corresponding to either IP treated or untreated with phosphatase in the presence of inhibitors, shows a decrease in grey value prior to the *exo1-PK9* band around RF 80. This difference, appearing as a shoulder on the troughs, suggests a lower motility species of *Exo1-PK9*, consistent with phosphorylation. This shoulder is absent in lane 4, showing IP treated with phosphatase in the absence of inhibitors.

5.4 Exo1 phosphorylation is dependent upon Spo11 nuclease activity

A strain deficient in Spo11 nuclease activity expressing Exo1-PK9 was designed to investigate whether phosphorylation of Exo1-PK9 was dependent on the formation of meiotic DSBs. These investigations were carried out as part of this project by masters' student Stephen T. Higgins. Spo11 is the catalytic subunit of the DSB forming complex (Keeney et al. 1997). The *spo11-Y135F* allele encodes a nuclease dead Spo11 mutant, incapable of catalysing the formation of DSBs (Bergerat et al. 1997). This mutant does not affect other functions of Spo11 or the progression of meiosis and sporulation (Cha et al. 2000), however no DSBs, dHJs or recombinants are detected (Hunter & Kleckner 2001), and homologue pairing and synapsis are abolished (Neale et al. 2002).

In order to examine Exo1-PK9 phosphorylation in the absence of meiotic DSBs, *spo11-Y135F* cells expressing Exo1-PK9 (dAG1824) were triggered into a synchronous meiosis and sampled at 0, 2, 3, 4 and 5 hours of meiosis (section 2.2.15). *SPO11* cells expressing Exo1-PK9 (dAG1830) were also sampled as a control. Total protein was extracted using the TCA method. 20µl of protein was resolved by 7% SDS-PAGE gel, and analysed by Western blot. In *SPO11* cells, the Exo1-PK9 band is preceded by a fainter, lower-motility band (Figure 5.6 A), suggestive of phosphorylation, as seen previously at 3 and 4 hr (section 5.2). In *spo11-Y135F* cells Exo1-PK9 is also detectable, however no lower motility band is observed at 3, 4 or 5 hr (Figure 5.6 B). This result is reproducible and is suggestive of an absence of phosphorylation, indicating that phosphorylation of Exo1-PK9 is dependent upon formation of meiotic DSBs.

5.5 Exo1 is phosphorylated prior to strand invasion

To investigate whether phosphorylation of Exo1 was dependent on strand invasion a strain deficient in Dmc1 recombinase activity expressing Exo1-PK9 was designed. These investigations were carried out as part of this project by masters' student Stephen T. Higgins. Dmc1 is a recombinase exclusive to meiosis, and is necessary for strand invasion of the homologue (Bishop et al. 1992). *dmc1Δ* cells accumulate hyper resected DSBs in the absence of subsequent repair

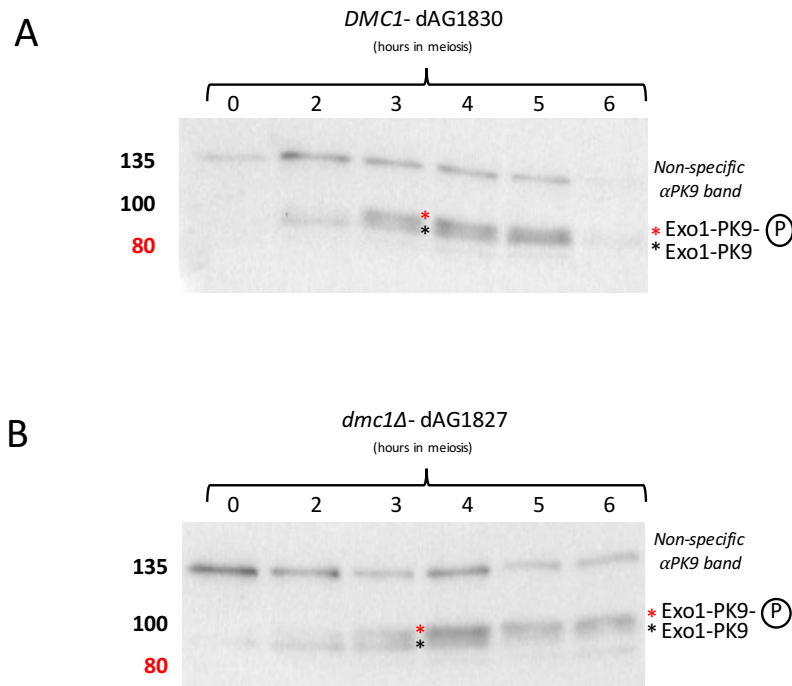


Figure 5.7 - Exo1 is phosphorylated prior to strand invasion

- (A) Western blot of 7% SDS-PAGE gel using α PK9 to identify Exo1-PK9 isolated by TCA extraction at 0, 2, 3, 4, 5 and 6 hr of meiosis in *DMC1* cells. Two distinct bands are distinguishable at 3, 4, and 5 hr. The lower molecular weight band is Exo1-PK9. The higher molecular weight band is suggestive of a phosphorylated species of Exo1-PK9. This band is no longer visible at 6 hr of meiosis.
- (B) Western blot of 7% SDS-PAGE gel using α PK9 to identify Exo1-PK9 isolated by TCA extraction at 0, 2, 3, 4 and 6 hr of meiosis in *dmc1 Δ* cells. Two distinct bands are distinguishable at 3, 4, 5 and 6 hr. The lower molecular weight is Exo1-PK9. The higher molecular weight band is suggestive of a phosphorylated species of Exo1-PK9. This band persists, suggestive of sustained phosphorylation of Exo1-PK9. The majority of Exo1 appears to be in the higher molecular weight band by 6 hours, suggesting that sustained presence of Exo1 leads to hyperphosphorylation.

(Hunter & Kleckner 2001). No single-end invasion intermediates or dHJs are formed, and 85% of cells arrest before MI (Schwacha & Kleckner 1997; Hunter & Kleckner 2001).

In order to examine Exo1-PK9 phosphorylation in the absence of strand invasion, *dmc1Δ* cells expressing Exo1-PK9 (dAG1827) were triggered into a synchronous meiosis and sampled at 0, 2, 3, 4, 5 and 6 hours of meiosis (section 2.2.15). *DMC1* cells expressing Exo1-PK9 (dAG1830) were also sampled as a control. In Western blot analysis of *DMC1* cells, at 3 and 4 hr the Exo1-PK9 band is preceded by a fainter, lower-motility band (Figure 5.7 A), suggestive of phosphorylation, as seen previously (section 5.2). This band disappears by 6hr. In *dmc1Δ* cells Exo1-PK9 is also detectable, and is similarly preceded by the phosphorylated species of Exo1-PK9 from 3 hr (Figure 5.7 B). Unlike in the *DMC1* cells, the whole population of Exo1-PK9 appears as a higher molecular weight band, suggesting that Exo1-PK9 not only persists at 6 hours, but that it also becomes hyperphosphorylated. This result suggests that Exo1-PK9 is phosphorylated prior to strand invasion, and the de-phosphorylation of Exo1-PK9 depends upon strand invasion, or events following strand invasion. In the absence of strand invasion Exo1 continues to become phosphorylated.

5.6 Meiosis is not affected by an inability to phosphorylate mitotically significant residues

It was possible while the residues identified in mitosis were not responsible for the phospho-shift seen in meiotic Exo1-PK9, that the residues still be phosphorylated in response to meiotic damage. Phosphorylation of these residues may be functionally significant but not influence motility due to brevity or a minor overall impact on protein charge. To assess whether these residues may influence meiotic activity of Exo1, meiotic function was analysed by studying spore viability, meiotic progression and DSB turnover at the ARE1 hotspot. The experiments described here are yet to be repeated.

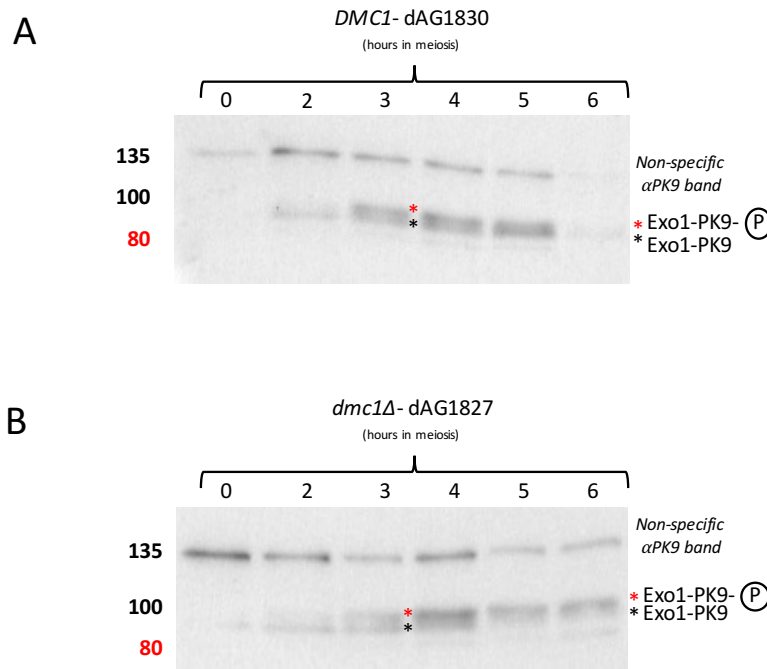


Figure 5.7 - Exo1 is phosphorylated prior to strand invasion

- (A) Western blot of 7% SDS-PAGE gel using α PK9 to identify Exo1-PK9 isolated by TCA extraction at 0, 2, 3, 4, 5 and 6 hr of meiosis in *DMC1* cells. Two distinct bands are distinguishable at 3, 4, and 5 hr. The lower molecular weight band is Exo1-PK9. The higher molecular weight band is suggestive of a phosphorylated species of Exo1-PK9. This band is no longer visible at 6 hr of meiosis.
- (B) Western blot of 7% SDS-PAGE gel using α PK9 to identify Exo1-PK9 isolated by TCA extraction at 0, 2, 3, 4 and 6 hr of meiosis in *dmc1* Δ cells. Two distinct bands are distinguishable at 3, 4, 5 and 6 hr. The lower molecular weight is Exo1-PK9. The higher molecular weight band is suggestive of a phosphorylated species of Exo1-PK9. This band persists, suggestive of sustained phosphorylation of Exo1-PK9. The majority of Exo1 appears to be in the higher molecular weight band by 6 hours, suggesting that sustained presence of Exo1 leads to hyperphosphorylation.

5.6.1 Spore viability is not altered by the inability of Exo1 to be phosphorylated in a mitotic pattern

It has been hypothesised that phosphorylation of Exo1 inhibits the nuclease activity of Exo1 (Morin et al. 2008). Null mutants of Exo1 show a decreased spore viability (Figure 3.3), and so it was predicted that perhaps phospho-mutants would also have a reduced spore viability if the *exo1Δ* phenotype were due to loss of nuclease function. Cells expressing Exo1-PK9 or Exo1-4S::S-PK9 were sporulated, and the resulting tetrads dissected as described (section 2.5.10 and 2.5.11) in order to determine the viability of meiotic products. The spore viability of cells expressing Exo1-PK9 was not significantly different to that of wild type cells (Figure 5.8 A, B & C). If the tag influenced the activity of Exo1 it could be expected that the spore viability would be reduced. However, this result indicates that the tag had no impact upon the faithful segregation of chromosomes. The spore viability of cells expressing Exo1-4S::A-PK9 was also not significantly different to that of either wild type cells or cells expressing Exo1-PK9. It can be concluded that the non-phosphorylatable status of mitotically significant residues in Exo1 does not impact faithful segregation of chromosomes in meiosis.

5.6.2 Meiotic progression is not affected by the inability of Exo1 to be phosphorylated in a mitotic pattern

Cells expressing Exo1-PK9 or Exo1-4S::S-PK9 were synchronized into meiosis and samples collected at bi-hourly intervals for DAPI analysis of nuclei (section 2.5.14). Cells were scored for number of nuclei visible. Cells displaying two nuclei were assumed to have completed MI, and cells displaying three or four nuclei were assumed to have completed MII, so indicating a successful completion of meiosis.

Exo1-PK9 and Exo1-4S::A-PK9 expressing cells show similar proportions of binucleate cells at each stage of meiosis when compared to wild type, and peak at similar levels of ~20% around 6 hours (Figure 5.9 A). Exo1-PK9 does not behave significantly differently to wild type, and so the PK9 tag did not impact upon MI progression. Exo1-4S::A-PK9 demonstrates a higher number of binucleates at 6

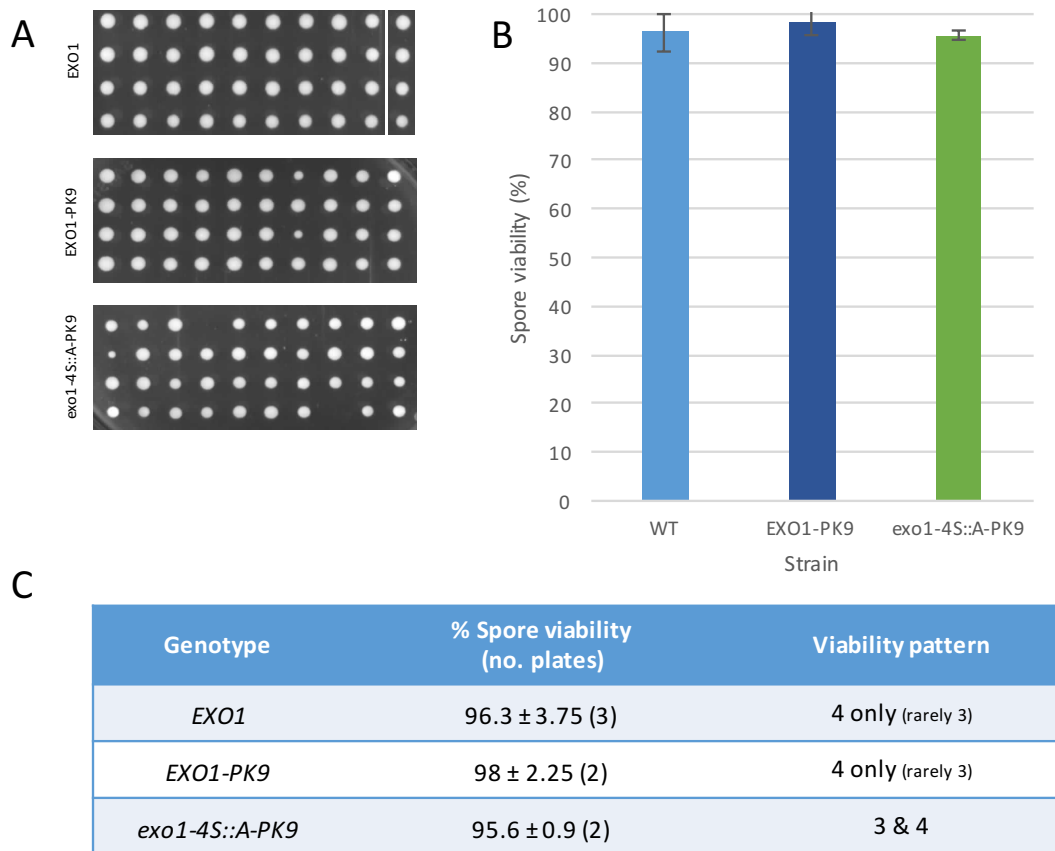


Figure 5.8 Spore viability analysis of tagged Exo1 and exo1-4S::A

(A) Illustrative examples of the spore viability patterns observed of tetrads dissected onto YPD agar plates and left to grow at 30°C for 48 hours.

(B) Graph illustrating the spore viability of each strain.

(C) Table summarising the mean spore viabilities of each strain and their standard deviation from the mean, calculated from the individual viabilities of each repeat. The spore viability pattern can be used as an indication as whether a non-disjunction has occurred during MI (2 spore viable) or MII (combinations of 1, 2 and 3 spores viable).

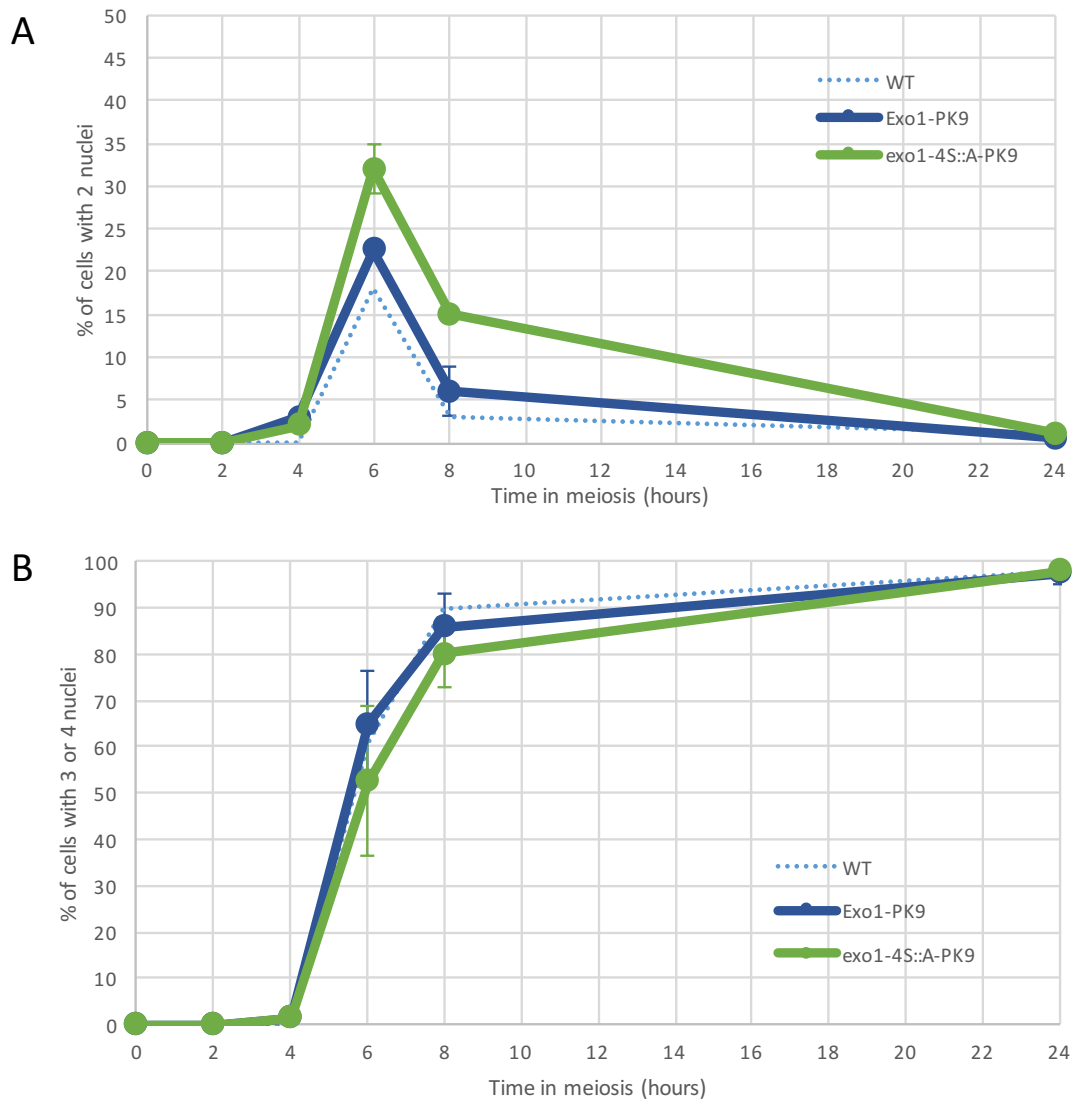


Figure 5.9 Meiotic progression of tagged Exo1 mutants is unchanged from wild type. (A) Exo1-PK9 and exo1-4S::A-PK9 cells show similar proportions of binucleate cells at each stage of meiosis when compared to wild type. Binucleate cells peak at similar levels around 6 hours. exo1-4S::A-PK9 demonstrates a higher number of binucleates at 6 hours, perhaps due to a delay in MI initiation or MII progression. Error bars represent calculations using data from 2 independent repeats. (B) Exo1-PK9 and exo1-4S::A-PK9 cells show similar proportions of tri- or tetranucleate cells at each stage of meiosis compared to wild type. MII cells begin to appear at 6 hours of meiosis and continue to increase at similar rates until 95%+ of cells are tri- or tetranucleate. This indicates that the meiotic progression of Exo1-PK9 and exo1-4S::A-PK9 significantly differ neither from one another or from wild type. Error bars represent calculations using data from 2 independent repeats.

hours, around 30-35%. This could be due to a delay in MI initiation causing binucleates to accumulate at higher levels later, or due to a delay in MII progression causing a build-up of binucleates before entry in to MII. The inability to phosphorylate the mutated residues may modestly impact upon MI progression or MII initiation.

Exo1-PK9 and Exo1-4S::A-PK9 cells show similar proportions of MII stage cells at each stage of meiosis compared to wild type (Figure 5.9 B). Cells in MII begin to appear at 6 hours of meiosis and continue to increase at similar rates until 95%+ of cells are tri- or tetranucleate. This indicates that the meiotic progression of Exo1-PK9 and Exo1-4S::A-PK9 significantly differ neither from one another or from wild type. Over all, despite a small delay on MI progression, the non-phosphorylatable mutant of Exo1 does not appear to have a major impact upon the temporal progression of meiosis.

Exo1-PK9 and Exo1-4S::A-PK9 significantly differ neither from one another or from wild type. Over all, despite a small delay on MI progression, the non-phosphorylatable mutant of Exo1 does not appear to impact upon the temporal progression of meiosis.

5.6.3 DSB turnover at ARE1 is not significantly impacted by the inability of Exo1 to be phosphorylated in a mitotic pattern

Cells expressing Exo1-PK9 or Exo1-4S::S-PK9 were synchronized into meiosis and samples collected at hourly intervals from 0 to 8 hr. The cells were then treated to extract the DNA and the DNA obtained digested and resolved on an agarose gel for analysis by Southern blot. The amount of probe hybridised to each band was determined by scanning densitometry (Figure 5.10 A).

Quantification of the Spo11-DSB band as a proportion of the total lane DNA shows maximum Spo11-DSB signal peaked at 3 hr in both Exo1-PK9 and Exo1-4S::A-PK9 cells, in line with the pattern seen in wild type (Figure 5.10 B). The peak of Exo1-PK9 is reduced, representing approximately 60% of the signal at the same time point in wild type and Exo1-4S::A-PK9. However due to the variance in Exo1-4S::A-PK9 this cannot be distinguished as being significantly different from the

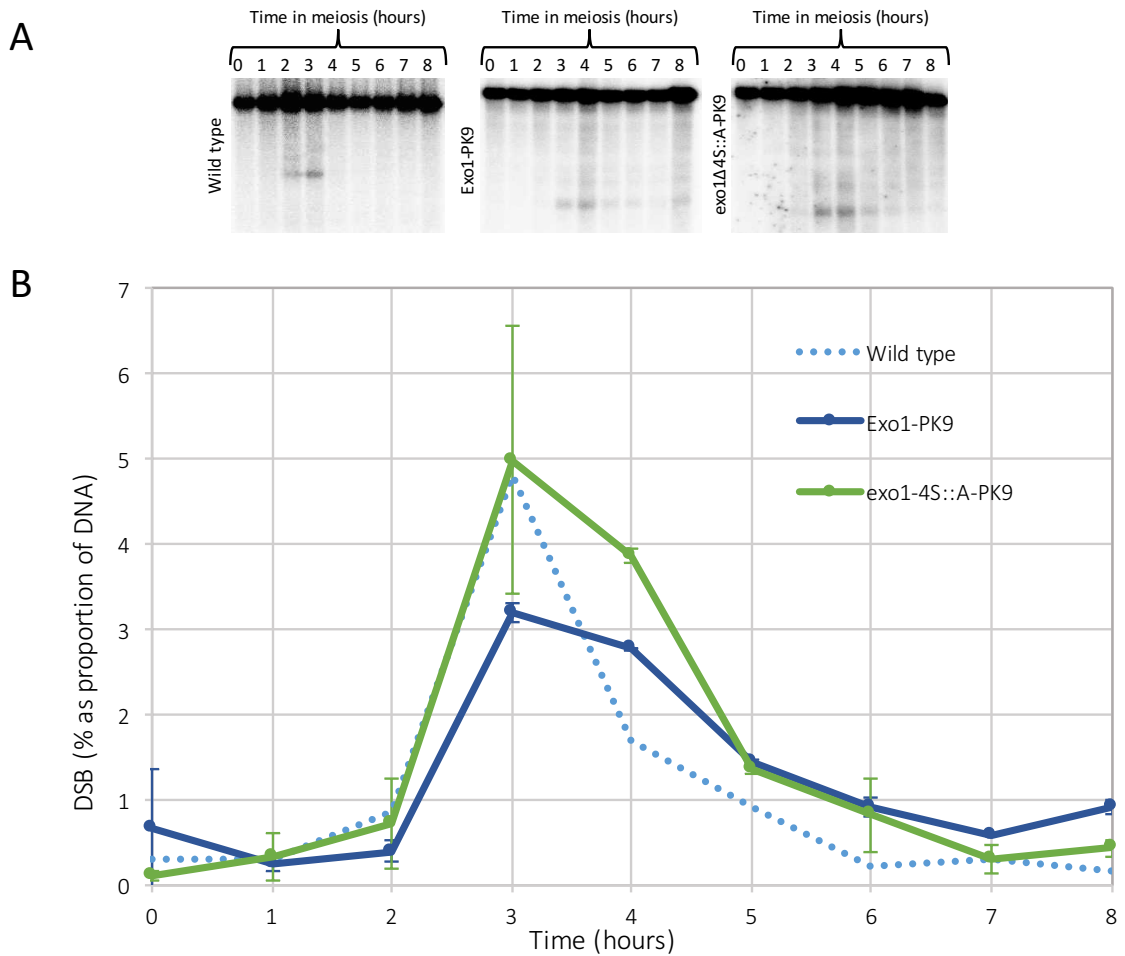


Figure 5.10 - Analysis of the Spo11-DSB turnover in tagged Exo1 mutants at the ARE1 hotspot

(A) Synchronous meiotic cultures of cells expressing Exo1-PK9 or exo1-4S::A-PK9 were sampled at hourly intervals. CTAB extracted DNA was digested and treated as described in section 3.4. The amount of probe hybridised to each band was determined by scanning densitometry.

(B) Quantification of the Spo11-DSB band as a proportion of the total lane DNA shows maximum Spo11-DSB signal peaks at 3 hours (T=3) in both Exo1-PK9 and exo1-4S::A-PK9 cells, in line with wild type. The peak of Exo1-PK9 is reduced, however due to the variance in exo1-4S::A-PK9 this cannot be distinguished as significantly different. Breaks persist at higher levels at 4 hours before returning to wild type level from 5 hours onwards. DSB turnover is not significantly affected by the non-phosphorylatable mutant exo1-4S::A-PK9.

mutant. Breaks persist at higher levels at 4 hr in Exo1-PK9 compared to the reduction seen in wild type and Exo1-4S::A-PK9, before returning to wild type level from 5 hr onwards. This persistence may be a consequence of the lower level seen at the previous 3 hr time point. DSB turnover is likely not significantly affected by the non-phosphorylatable mutant Exo1-4S::A-PK9, as the profile of Exo1-4S::A-PK9 does not significantly differ to that of wild type.

Pulsed-field gel experiments were not carried out on these strains due to the complex nature of the experiments, and time constraints. It is worth acknowledging that carrying out PFGE analysis in the future would be important to ascertain whether this lack of effect is maintained across all DSB sites.

Discussion

Phosphorylation of Exo1 during mitosis in response to DNA damage has only been relatively recently described (Morin et al. 2008; Bolderson et al. 2010; Engels et al. 2011; Tomimatsu et al. 2014). In *S. cerevisiae* four key residues (S372, S567, S587 and S692) have been identified and studied in mitosis (Morin et al. 2008), however at the time of writing no such experiments had been published during meiosis. Exo1 plays an important role in two stages of meiosis: ssDNA resection and dHJ resolution. Control of these processes by modifications such as phosphorylation may therefore be important for successful recombination, as in the absence of Exo1 cells display 50% less crossing over (Zakharyevich et al. 2010). It was therefore of interest to investigate whether Exo1 was phosphorylated in meiosis.

All together the data in this chapter examine the expression of Exo1-PK9, and demonstrate that Exo1-PK9 is phosphorylated during meiosis. Furthermore, this phosphorylation is different to that observed by Morin et al. in mitosis, and is dependent upon the formation of Spo11 DSBs. Finally, this phosphorylation persists until at least strand invasion. Exo1-PK9 also appears to undergo changes in expression through meiosis.

Visualising Exo1 by Western proved challenging even once the earlier problems with tagging were overcome. Exo1 expression is very low during meiosis,

requiring long exposures and avoidance of excessive background noise. In the early phases of meiosis, the level of Exo1-PK9 was almost undetectable. At the beginning of meiosis (0 hr), cells are no longer undergoing replication due to the near-starvation conditions imposed to synchronise entry in to meiosis. This arrest in division may account for the low level of Exo1-PK9 expression; this stationary phase doesn't generate substrate for Exo1 as DNA is not replicating or being as heavily transcribed. As the cells are triggered in to meiosis, many breaks are formed, requiring Exo1 activity for their repair. DSB levels are highest around 3-4 hours (section 3.4.1), and their subsequent need for repair and crossover resolution correlates with the highest levels of Exo1-PK9. By 8 hr meiosis is complete in most cells. The vast majority of breaks have been repaired, and COs resolved, leading to a decrease in Exo1-PK9 expression as it's activity is no longer necessary, and cells are entering another stationary phase as spores.

The band shift indicative of phosphorylated Exo1-PK9 was first observed using denaturing TCA extraction. Subsequently determining a native extraction method suitable for IP experiments and phosphatase treatments was time consuming. The data presented in sections 5.2 and 5.3 suggest that Exo1-PK9 is transiently phosphorylated during meiosis, peaking at 4hr, as the band shift is sensitive to phosphatase treatment. This timing coincides with both the increased expression of Exo1-PK9 and the increased levels of DSBs, suggesting Exo1-PK9 activity and availability is moderated when breaks are most abundant. Parallel experiments using the mitotically non-phosphorylatable allele *exo1-4S::A-PK9* showed that Exo1-4S::A-PK9 was still phosphorylated during meiosis. This result shows that meiotic phosphorylation of Exo1-PK9 is distinguishable from that observed during mitosis, and is suggestive of distinct mechanisms for the moderation of Exo1-PK9 activity in response to different types of DNA damage induction.

The temporally distinct roles of Exo1 in resection and CO resolution (Zakharyevich et al. 2010) raised the possibility that this phosphorylation may coincide with a particular Exo1 activity. Various mutant backgrounds were considered to try and investigate this possibility further. The full catalogue of useful mutants is yet to be completed (*Mec1*, *Tel1*, *Mek1*, and *Trm2*), however two

were investigated and are discussed here: *spo11-Y135F* and *dmc1Δ*. While Exo1-PK9 was expressed, phosphorylation was abolished in the *spo11-Y135F* background, indicating a dependency of phosphorylation on DSB formation. Furthermore, in the *dmc1Δ* background in which cells arrest prior to strand invasion, Exo1-PK9 persisted from 3 hours throughout meiosis, instead of appearing transiently, and became hyperphosphorylated. Prior to strand invasion Exo1 is active as a 5' to 3' nuclease, while its role as a resolvase follows strand invasion and dHJ formation. Persistent expression and phosphorylation of Exo1-PK9 in the absence of strand invasion is an interesting finding; however without knowing what type of influence phosphorylation has upon Exo1 it is difficult to determine the significance. If strand invasion fails, then the cell will be unable to carry out homologous recombination. There are other types of repair mechanisms the cell can employ to try and rescue the division (section 1.5.2). As Exo1 has already initiated resection, it may be that this resection continues in order to try to expose regions of homology suitable for SSA. The resection necessary for SSA can proceed over many kilobases, while HR only requires around 800 bases. Therefore, one explanation could be that if phosphorylation of Exo1 stimulates its activity, the hyperphosphorylation observed here would be as a result of increased activity of Exo1, necessary for sufficient resection for SSA. The length of resection could be tested using a VDE system experiment developed within our lab.

A final point of interest was whether the putative phospho-mutant *exo1-4S::A* exerted any effect upon meiosis. During mitosis, this mutant displayed decreased sensitivity to DNA damage, perhaps due to increased Exo1 activity (Morin et al. 2008). Exo1-4S::A-PK9 expression does not appear to impact upon spore formation, spore viability, or DSB levels. When considering the mitotic phenotype, the lack of meiotic phenotype in *exo1-4S::A* cells may be expected, as an increased resistance to DNA damage may not generate a change in meiosis where repair is already proficient. The mitotically significant residues S372, S567, S587 and S692, would therefore appear to have no significant role in meiotic function of Exo1 when assessed by these methods. It may be worth investigating the repair efficiency in double mutants, containing Exo1 phospho-mutants with a second

mutation known to cause reduced repair phenotypes. If the Exo1 phospho-mutants are having a masked effect, weakening the redundant pathways might reveal this.

6. General discussion & future directions

General Discussion

Meiosis is a tightly controlled reductive cell division specialized for the formation of haploid gametes. During meiosis homologous chromosomes are transiently paired by the formation of crossovers at recombination hotspots. These interactions arise from the processing of double strand breaks in the DNA formed early in meiosis, and are important for ensuring faithful segregation of chromosomes, and ultimately formation of balanced gametes. Exo1, a conserved 5' to 3' exonuclease and flap endonuclease, is implicated in both the processing of meiotic DSBs and the resolution of crossovers (Tishkoff et al. 1997a; Kirkpatrick et al. 2000; Zakharyevich et al. 2010; Tishkoff et al. 1998; Tran et al. 2004). This protein is also important in the repair of damaged DNA during mitosis, during which its activity is regulated by phosphorylation (Morin et al. 2008; Bolderson et al. 2010; Engels et al. 2011; Tomimatsu et al. 2014). Phosphorylation of S372, S567, S587 and S692 in *S.cerevisiae* is believed to negatively regulate the resection activity of Exo1 (Morin et al. 2008), and phosphorylation of S714 in hExo1 is both a negative regulator of resection and appears to be required for recruitment of DNA repair proteins such as Rad51 (Bolderson et al. 2010). Tomimatsu et al. 2014 identified four further sites of hExo1 phosphorylation, S639, T732, S815, and T824, and demonstrated that phosphorylation at these sites promotes resection, rather than inhibiting it, suggesting that differential phosphorylation can have varying effects. These different finding may be due to more complex regulatory pathways of Exo1 in the mammalian DNA repair processes. Mammalian Exo1 is known to interact with various regulators of repair such as CtIP (Sae2 homolog) (Eid et al. 2010), BLM (Sgs1 homolog) (Nimonkar et al. 2011), and BRCA1 (Tomimatsu et al. 2014). These physical interactions have not been observed between *S. cerevisiae* Exo1 and the corresponding homologs, and BRCA1 has no homolog in yeast. These differing interactions may account for the contrary roles of phosphorylation in mammalian systems and *S. cerevisiae*.

Earlier studies in *S. cerevisiae* by Morin et al. identified four serine residues, S372, S567, S587 and S692, that were phosphorylated in response to DNA damage induction. They produced mutant alleles of *EXO1* that were either non-phosphorylatable (*exo1-4S::A*) or mimicked phosphorylation (*exo1-4S::E*) in order to characterize this modification. However, so far no published studies have addressed the potential influence of this post-translational modification on the functions of Exo1 during meiosis. One of the aims of this study was to investigate whether these putative phosphomutants of Exo1 had an impact on meiosis by examining sporulation, spore viability, and DSB turnover at an individual hotspot as well as across an entire chromosome. This study also aimed to investigate if Exo1 was phosphorylated during meiosis, and if so attempt to further characterise the modification in terms of its purpose, timing, and regulation.

6.1 Exogenous expression of Exo1 and putative phosphomutants was not successful for the investigation of meiotic effects

The exonuclease Exo1 has been shown to be phosphorylated in response to DNA damage during mitosis (Morin et al. 2008; Bolderson et al. 2010; Engels et al. 2011; Tomimatsu et al. 2014). In order to begin investigating a potential role for phosphorylation during meiosis, *EXO1* and mutants of Exo1 that were either non-phosphorylatable (*exo1-4S::A*) or mimicked phosphorylation (*exo1-4S::E*) were expressed exogenously in an *exo1Δ* background to reconstitute Exo1 expression in the cell.

Plasmids expressing Exo1 and the putative phosphomutants were constructed, with particular consideration given to how the orientation of ORFs influenced meiosis (section 3.1). Meiotic progression was adversely affected when the ORFs were oriented *EXO1>>HYG*, perhaps as a consequence of spatial overcrowding when both transcription initiation and termination are trying to coordinate in the same region. This incidental finding could offer important implications in vector design. An initial search of the literature did not reveal any reports of such considerations, however pursuing this finding was not within the scope of this project. A short future project might further investigate this by directly comparing

levels of expressed proteins, by Western blot for example.

Meiotic progression, spore viability, and turnover of DSBs at both a single locus and across a chromosome were examined in *exo1Δ* cells transformed with the plasmids. Progression of the putative mutants through MI and MII was similar to cells exogenously expressing *EXO1*, suggesting no influence on spore formation. Of more interest was the finding that the viability of *exo1-4S::A* was reduced to 39%, and in a pattern indicative of a MI failure, when Exo1 is active. Previous studies hypothesized that phosphorylation negatively regulates the activity of *S. cerevisiae* Exo1, inhibiting its nuclease activity during mitosis (Morin et al. 2008). Failure to inhibit resection by *exo1-4S::A-PK9* in meiosis would potentially lead to hyper-resection of the 5' strands. Hyper-resection can cause genomic instability, proposed to be due to a depletion of RPA leaving tracts of exposed ssDNA (Mimitou & Symington 2008; Toledo et al. 2013; Xiaoqing Chen et al. 2015). This mechanism may account for the severe spore viability defect of cells expressing *exo1-4S::A*.

As phosphorylation is proposed to attenuate the nuclease activity of Exo1, the phospho-mimic was expected to perhaps behave like a nuclease dead allele of Exo1, which has a spore viability of 88% (Zakharyevich et al. 2010). However the putative phospho-mimicking mutant *exo1-4S::E* had a more prominent defect in spore viability of 81%, more similar to that of *exo1Δ* cells expressing *EXO1*. Why the putative phospho-mimic mutant would have a more severe defect than a nuclease dead allele prompted further investigation in to break levels of the mutants at both a single locus and across chromosome III. No notable difference was observed at the *ARE1* locus (section 3.5), however there was a difference in the levels of DSBs at various loci across chromosome III (section 3.6.2). These results suggest that perhaps *exo1-4S::A* influenced DSB site choice or the rate at which DSBs were made and repaired at different sites.

A severe spore viability defect would normally suggest some impairment of meiosis causing a large number of non-disjunction events. A cause for such events could not be explained using these preliminary experiments, so once the putative phospho-mutants were integrated at the *EXO1* locus, spore viability was re-

examined. Spore viability of these newly integrated mutants revealed no difference between *EXO1* and *exo1-4S::A*, contradicting the findings outlined in section 3.3, and prompting a repeat of the original dissections in *exo1Δ* cells expressing the mutants. The repeat confirmed that there was no difference in the spore viabilities, and that the original strain must have harboured some other mutation causing the spore viability phenotype. The phenotype itself was still an interesting result, however there was not time within this project to further investigate the potential cause. While this result was extremely frustrating, the initial findings had prompted the design of the more useful integrated mutants, and the experience and practical skills gained during the investigation were useful.

6.2 Exo1 is phosphorylated during mitosis in the SK1 background in response to bleomycin-induced DSB formation

Morin et al. have shown that Exo1 is phosphorylated in response to various types of DNA damage, including telomere uncapping, camptothecin treatment and bleomycin treatment (Morin et al. 2008). They observed this modification through Western blot analysis of Exo1, which demonstrated a slower migrating band indicative of phosphorylation. In order to build on these findings in meiosis, this project first aimed to replicate these findings in the SK1 background using bleomycin. Bleomycin is an antibiotic with anti-tumour activity commonly used in the treatment of cancer as a chemotherapy agent. It has been shown to cause double strand breaks by scission of hairpin DNA (Roy & Hecht 2014). A slower mobility species of Exo1-PK9 was seen on Western blot, while no such band was seen in the putative phospho-mutant Exo1-4S::A-PK9. These results support the hypothesis that Exo1 is phosphorylated in response to DNA damage, and show that the findings of Morin et al. are transferable to diploid yeast of the SK1 background. This system in the SK1 background presented an opportunity for the study of Exo1 phosphorylation during meiosis.

6.3 Exo1 is phosphorylated during meiosis in response to DSB formation

While phosphorylation of Exo1 during mitosis in response to DNA damage has been described by several groups in both yeast and humans, prior to this project

the phosphorylation status during meiosis had not been investigated (Morin et al. 2008; Bolderson et al. 2010; Engels et al. 2011; Tomimatsu et al. 2014). Exo1 plays an important role in two stages of meiosis: ssDNA resection and dHJ resolution. Control of these processes by modifications such as phosphorylation may therefore be important for successful recombination, as in the absence of Exo1 cells display 50% less crossing over (Zakharyevich et al. 2010). It was therefore of interest to investigate whether Exo1 was phosphorylated in meiosis.

Exo1-PK9 is phosphorylated during meiosis, and this phosphorylation is presumed to be different to that observed in mitosis, as the putative non-phosphorylatable Exo1-4S::A-PK9 is also phosphorylated in meiosis. This may be due to there being ten Mec1/Tel1 consensus sequences and four Mek1 consensus sequences throughout Exo1, none of which were implicated as potential mitotic sites by Morin et al. 2008 (figure 1.8). Indeed, Mek1 is a meiosis specific kinase, and so it is expected that these sites would not be identified. Site directed mutagenesis of these sequences, or mass spectrometry of Exo1, might reveal whether these sites are indeed phosphorylated during meiosis.

It was expected that levels of Exo1 would vary in response to DNA damage. The protein level was seen to increase in line with break levels. In the initial phase of meiosis, the level of Exo1-PK9 was almost undetectable, and this was believed to be because at 0 hr of meiosis cells are no longer cycling in mitosis as they reach near-starvation. Later as the cells progress through meiosis, many breaks are formed, requiring Exo1 activity for their repair. DSB levels are highest around 3-4 hours (section 3.4.1), and their subsequent need for repair and crossover resolution correlates with the highest levels of Exo1-PK9. The level of Exo1-PK9 increases at around 3 to 4 hr of meiosis, coinciding with the presence of the phosphorylated species. Exo1-PK9 phosphorylation is dependent upon the formation of Spo11 DSBs, and persists until at least strand invasion. By 8 hr meiosis is complete in most cells, and Exo1-PK9 begins to reduce back toward pre-meiotic levels.

As well as varying in expression levels, Exo1-PK9 is transiently phosphorylated during meiosis, most notably at 4hr. This timing coincides with the higher

expression of Exo1-PK9 and increased levels of DSBs, suggesting Exo1-PK9 activity and availability is moderated when breaks are most abundant. Parallel experiments using the mitotically non-phosphorylatable allele *exo1-4S::A-PK9* showed that Exo1-4S::A-PK9 was still phosphorylated during meiosis. This result shows that meiotic phosphorylation of Exo1-PK9 is distinguishable from that observed during mitosis, and is suggestive of distinct mechanisms for the moderation of Exo1-PK9 activity in response to different types of DNA damage induction.

It was hypothesised that change in expression and phosphorylation of Exo1-PK9 was related to the formation of double strand breaks. To investigate this Exo1-PK9 was analysed in the absence of DSB formation (*spo11-Y135F*) and in the absence of strand invasion (*dmc1Δ*). In *spo11-Y135F* an increase in Exo1-PK9 was seen, however phosphorylation was abolished, suggesting that phosphorylation but not Exo1-PK9 itself is dependent upon the formation of meiotic DSBs. In *dmc1Δ* Exo1-PK9 persisted throughout meiosis from 3 hr and became hyperphosphorylated, instead of appearing transiently and a sub-population being phosphorylated. Prior to strand invasion Exo1 is active as a 5' to 3' nuclease, while its role as a resolvase follows strand invasion and dHJ formation (Zakharyevich et al. 2010). Phosphorylation of Exo1-PK9 may therefore serve to discern between these two functions, and if cells fail to strand invade this switch in moderation is not initiated.

A final point of interest was whether the putative phospho-mutant *exo1-4S::A* exerted any effect upon meiosis. During *S. cerevisiae* mitosis, this mutant displayed decreased sensitivity to DNA damage, perhaps due to increased Exo1 activity (Morin et al. 2008). Exo1-4S::A-PK9 expression does not appear to impact upon spore formation, spore viability, or DSB levels. When considering the mitotic phenotype, the lack of meiotic phenotype in *exo1-4S::A* cells may be as expected, as an increased resistance to DNA damage may not generate a change in meiosis where repair is already proficient. Bolderson et al. 2010 demonstrated that resection remained unaffected in the non-phosphorylatable hExo1 mutant S714A, and that a phenotype was only observable in the phospho-mimetic mutant. The

inability to phosphorylate mitotically significant residues S372, S567, S587 and S692, would therefore appear to have no significant role in meiotic function of Exo1 when assessed by these methods. However, as the phospho-mimetic mutants of *S. cerevisiae* are yet to be investigated, it cannot be concluded that phosphorylation at these sites does not influence meiosis.

Future directions

In terms of future directions, this study has considered the various roles for phosphorylation of Exo1 during meiosis, and postulated which proteins may be responsible for this. There are several ways in which these hypotheses could be further examined, including:

- Mapping of the residues phosphorylated in meiosis using mass spectrometry, and subsequent generation of phospho-mutants. This would enable the study of non-phosphorylatable and phospho-mimetic Exo1 mutants that were meiosis specific. Phospho-mutants could be used to examine the role of meiotic phosphorylation of Exo1.
- Identification of the kinase responsible for Exo1 phosphorylation, and the timing of this activity. Further studies could look for changes in the phospho-shift on Western blot in backgrounds containing mutants of candidate kinases, or mutants causing arrest at specific checkpoints of meiosis.
- Study of phosphomutants designed in nuclease mutants of Exo1 could distinguish between the dual roles of Exo1 and whether phosphorylation plays a part in this splitting of activities.
- Exo1 in its entirety has been difficult to characterize structurally (both in published work on human Exo1 and in *S. cerevisiae* based crystallography experiments attempted in the process of this project) (Orans et al. 2011). Only the N-terminal region structure of Exo1 has been solved. Perhaps some of the challenges faced in studying the structure could be overcome using phospho-mutants, as changes in charge can stabilize proteins in conformations more compliant for expression and purification.

Concluding remarks

This study has provided evidence that the nuclease Exo1 is phosphorylated in response to meiotic DSBs. This phosphorylation is regulated over time, appearing at its strongest levels around 4 hours of meiosis alongside the highest levels of DSBs, then disappearing following strand invasion. The phosphorylation demonstrated during meiosis differs to that seen in mitosis (Morin et al. 2008). So far a potential role for this meiotic post-translational modification is yet to be determined. Resection of DNA must be tightly regulated to ensure neither too much nor too little DNA is removed for successful homologous recombination. The role of Exo1 in resection is conserved between meiosis and mitosis. Exo1 is also required for normal levels of crossovers to be formed during meiosis. It is likely that phosphorylation of Exo1 could play an important part in regulating these key activities of Exo1. Future study will hopefully shed more light upon the factors involved and role of Exo1 phosphorylation.

7. References

- Acosta, I., Ontoso, D. & San-Segundo, P.A., 2011. The budding yeast polo-like kinase Cdc5 regulates the Ndt80 branch of the meiotic recombination checkpoint pathway. *Molecular biology of the cell*, 22(18), pp.3478–3490.
- Acquaviva, L., Drogat, J., et al., 2013. Spp1 at the crossroads of H3K4me3 regulation and meiotic recombination. *Epigenetics : official journal of the DNA Methylation Society*, 8(4), pp.355–360.
- Acquaviva, L., Székvölgyi, L., et al., 2013. The COMPASS subunit Spp1 links histone methylation to initiation of meiotic recombination. *Science (New York, N.Y.)*, 339(6116), pp.215–8.
- Agarwal, S. & Roeder, G.S., 2000. Zip3 provides a link between recombination enzymes and synaptonemal complex proteins. *Cell*, 102(2), pp.245–255.
- Allers, T. & Lichten, M., 2000. A method for preparing genomic DNA that restrains branch migration of Holliday junctions. *Nucleic acids research*, 28(2), p.e6.
- Allers, T. & Lichten, M., 2001. Differential timing and control of noncrossover and crossover recombination during meiosis. *Cell*, 106(1), pp.47–57.
- Altmannová, V., Kolesár, P. & Krejčí, L., 2012. SUMO Wrestles with Recombination. *Biomolecules*, 2(3), pp.350–75.
- Anderson, S.L. & Sekelsky, J., 2010. Meiotic versus Mitotic Recombination: Two Different Routes for Double-Strand Break Repair. *Bioessays*, 32(12), pp.1058–1066.
- Arora, C. et al., 2004. Antiviral Protein Ski8 Is a Direct Partner of Spo11 in Meiotic DNA Break Formation, Independent of Its Cytoplasmic Role in RNA Metabolism. *Molecular Cell*, 13, pp.549–559.
- Asefa, B., Kauler, P. & Cournoyer, D., 1998. Genetic analysis of the yeast NUD1 endo-exonuclease: a role in the repair of DNA double-strand breaks. , pp.360–367.
- Bailis, J.M., Smith, A. V. & Roeder, G.S., 2000. Bypass of a meiotic checkpoint by overproduction of meiotic chromosomal proteins. *Mol Cell Biol*, 20(13), pp.4838–48.
- Bardhan, A., Chuong, H. & Dawson, D.S., 2010. Meiotic Cohesin Promotes Pairing of Nonhomologous Centromeres in Early Meiotic Prophase. *Molecular biology of the cell*, 21(22), pp.1799–1809.
- Baroni, E. et al., 2004. The functions of budding yeast Sae2 in the DNA damage response require Mec1- and Tel1-dependent phosphorylation. *Molecular and*

- Cellular Biology*, 24(10), pp.4151–4165.
- Baudat, F. et al., 2000. Chromosome synapsis defects and sexually dimorphic meiotic progression in mice lacking Spo11. *Mol Cell*, 6(5), pp.989–998.
- Baudat, F. & Nicolas, A., 1997. Clustering of meiotic double-strand breaks on yeast chromosome III. *Proceedings of the National Academy of Sciences of the United States of America*, 94(10), pp.5213–8.
- Ben-Ari, G. et al., 2006. Four linked genes participate in controlling sporulation efficiency in budding yeast. *PLoS Genetics*, 2(11), pp.1815–1823.
- Berchowitz, L.E. & Copenhaver, G.P., 2010. Genetic interference: don't stand so close to me. *Current genomics*, 11(2), pp.91–102.
- Berg, I.L. et al., 2010. PRDM9 variation strongly influences recombination hot-spot activity and meiotic instability in humans. *Nature genetics*, 42(10), pp.859–863.
- Bergerat, A. et al., 1997. An atypical topoisomerase II from Archaea with implications for meiotic recombination. *Nature*, 386(6623), pp.414–417.
- Bertuch, A.A. & Lundblad, V., 2004. EXO1 Contributes to Telomere Maintenance in Both Telomerase-Proficient and Telomerase-Deficient *Saccharomyces cerevisiae*. *Genetics*, 166(4), pp.1651–1659.
- Bianchi, A. & Shore, D., 2007. Increased association of telomerase with short telomeres in yeast. *Genes and Development*, 21(14), pp.1726–1730.
- Bishop, D.K. et al., 1992. DMC1: a meiosis-specific yeast homolog of *E. coli* recA required for recombination, synaptonemal complex formation, and cell cycle progression. *Cell*, 69(3), pp.439–56.
- Bisig, C.G. et al., 2012. Synaptonemal complex components persist at centromeres and are required for homologous centromere pairing in mouse spermatocytes. *PLoS Genetics*, 8(6).
- Blitzblau, H.G. & Hochwagen, A., 2013. ATR/Mec1 prevents lethal meiotic recombination initiation on partially replicated chromosomes in budding yeast. *eLife*, 2013(2), p.e00844.
- Boddy, M.N. et al., 2001. Mus81-Eme1 are essential components of a Holliday junction resolvase. *Cell*, 107(4), pp.537–548.
- Bolderson, E. et al., 2010. Phosphorylation of Exo1 modulates homologous recombination repair of DNA double-strand breaks. *Nucleic acids research*, 38(6), pp.1821–31.
- Borde, V. et al., 2004. Association of Mre11p with double-strand break sites during yeast meiosis. *Molecular cell*, 13(3), pp.389–401.

- Borde, V., 2007. The multiple roles of the Mre11 complex for meiotic recombination. *Chromosome research: an international journal on the molecular, supramolecular and evolutionary aspects of chromosome biology*, 15(5), pp.551–63.
- Borde, V., Goldman, A.S. & Lichten, M., 2000. Direct coupling between meiotic DNA replication and recombination initiation. *Science (New York, N.Y.)*, 290(5492), pp.806–9.
- Bowring, F.J. et al., 2006. Chromosome pairing and meiotic recombination in *Neurospora crassa* spo11 mutants. *Current Genetics*, 50(2), pp.115–123.
- Brar, G. a et al., 2006. Rec8 phosphorylation and recombination promote the step-wise loss of cohesins in meiosis. *Nature*, 441(7092), pp.532–536.
- Bressan, D. a, Baxter, B.K. & Petrini, J.H., 1999. The Mre11-Rad50-Xrs2 protein complex facilitates homologous recombination-based double-strand break repair in *Saccharomyces cerevisiae*. *Molecular and cellular biology*, 19(11), pp.7681–7.
- Brito, I.L., Yu, H.G. & Amon, A., 2010. Condensins promote coorientation of sister chromatids during meiosis I in budding yeast. *Genetics*, 185(1), pp.55–64.
- Brown, M.S. et al., 2015. Small Rad51 and Dmc1 Complexes Often Co-occupy Both Ends of a Meiotic DNA Double Strand Break. *PLoS Genetics*, 11(12), pp.1–22.
- Buhler, C., Borde, V. & Lichten, M., 2007. Mapping meiotic single-strand DNA reveals a new landscape of DNA double-strand breaks in *Saccharomyces cerevisiae*. *PLoS biology*, 5(12), p.e324.
- Buonomo, S.B. et al., 2000. Disjunction of homologous chromosomes in meiosis I depends on proteolytic cleavage of the meiotic cohesin Rec8 by separin. *Cell*, 103(3), pp.387–398.
- Burgess, S.M., Kleckner, N. & Weiner, B.M., 1999. Somatic pairing of homologs in budding yeast: Existence and modulation. *Genes and Development*, 13(12), pp.1627–1641.
- Busygina, V. et al., 2008. Hed1 regulates Rad51-mediated recombination via a novel mechanism. , pp.786–795.
- Busygina, V. et al., 2012. Novel attributes of Hed1 affect dynamics and activity of the Rad51 presynaptic filament during meiotic recombination. *The Journal of biological chemistry*, 287(2), pp.1566–75.
- Bystricky, K. et al., 2005. Chromosome looping in yeast: Telomere pairing and coordinated movement reflect anchoring efficiency and territorial organization. *Journal of Cell Biology*, 168(3), pp.375–387.
- Cao, L., Alani, E. & Kleckner, N., 1990. A pathway for generation and processing of double-strand breaks during meiotic recombination in *S. cerevisiae*. *Cell*,

- 61(6), pp.1089–101.
- Carballo, J.A. et al., 2013. Budding Yeast ATM/ATR Control Meiotic Double-Strand Break (DSB) Levels by Down-Regulating Rec114, an Essential Component of the DSB-machinery M. Lichten, ed. *PLoS Genetics*, 9(6), p.e1003545.
- Carballo, J. a et al., 2008. Phosphorylation of the axial element protein Hop1 by Mec1/Tel1 ensures meiotic interhomolog recombination. *Cell*, 132(5), pp.758–70.
- Carle, G.F. & Olson, M. V, 1985. An electrophoretic karyotype for yeast. *Proceedings of the National Academy of Sciences of the United States of America*, 82(11), pp.3756–3760.
- Carpenter, a T., 1975. Electron microscopy of meiosis in *Drosophila melanogaster* females: II. The recombination nodule--a recombination-associated structure at pachytene? *Proceedings of the National Academy of Sciences of the United States of America*, 72(8), pp.3186–3189.
- Cartagena-Lirola, H. et al., 2008. Role of the *Saccharomyces cerevisiae* Rad53 checkpoint kinase in signaling double-strand breaks during the meiotic cell cycle. *Molecular and cellular biology*, 28(14), pp.4480–93.
- Cassani, C. et al., 2016. Tel1 and Rif2 Regulate MRX Functions in End-Tethering and Repair of DNA Double-Strand Breaks. *PLoS biology*, 14(2), p.e1002387.
- Cavero, S. et al., 2016. REVISION MIC0176E172 Impact of histone H4K16 acetylation on the meiotic recombination checkpoint in *Saccharomyces cerevisiae*. , 3(12).
- Celerin, M. et al., 2000. Multiple roles of Spo11 in meiotic chromosome behavior. *The EMBO journal*, 19(11), pp.2739–50.
- Cha, R.S. et al., 2000. Progression of meiotic DNA replication is modulated by interchromosomal interaction proteins, negatively by Spo11p and positively by Rec8p. *Genes and Development*, 14(4), pp.493–503.
- Chamankhah, M., Fontanie, T. & Xiao, W., 2000. The *Saccharomyces cerevisiae* mre11 (ts) allele confers a separation of DNA repair and telomere maintenance functions. *Genetics*, 155(2), pp.569–576.
- Charron, M.J., Dubin, R. a & Michels, C. a, 1986. Structural and functional analysis of the MAL1 locus of *Saccharomyces cerevisiae*. *Molecular and cellular biology*, 6(11), pp.3891–3899.
- Chen, J.M. et al., 2007. Gene conversion: mechanisms, evolution and human disease. *Nature Reviews Genetics*, 8(10), pp.762–775.
- Chen, X. et al., 2015. 14-3-3 proteins restrain the Exo1 nuclease to prevent overresection. *The Journal of biological chemistry*, 290(19), pp.12300–12.

- Chen, X. et al., 2011. Cell cycle regulation of DNA double-strand break end resection by Cdk1-dependent Dna2 phosphorylation. *Nature structural & molecular biology*, 18(9), pp.1015–1019.
- Chen, X. et al., 2015. Phosphorylation of the Synaptonemal Complex Protein Zip1 Regulates the Crossover/Noncrossover Decision during Yeast Meiosis. *PLoS Biology*, 13(12), pp.1–35.
- Choudhury, S. a, Asefa, B., Webb, A., et al., 2007. Functional and genetic analysis of the *Saccharomyces cerevisiae* RNC1/TRM2: evidences for its involvement in DNA double-strand break repair. *Molecular and cellular biochemistry*, 300(1–2), pp.215–226.
- Choudhury, S. a, Asefa, B., Kauler, P., et al., 2007. Synergistic effect of TRM2/RNC1 and EXO1 in DNA double-strand break repair in *Saccharomyces cerevisiae*. *Molecular and cellular biochemistry*, 304(1–2), pp.127–134.
- Chua, P.R. et al., 1998. Zip2, a meiosis-specific protein required for the initiation of chromosome synapsis. *Cell*, 93(3), pp.349–59.
- Cloud, V. et al., 2012. Rad51 Is an Accessory Factor for Dmc1-Mediated Joint Molecule Formation During Meiosis. *Science*, 337(6099), pp.1222–1225.
- Cohen-Fix, O. et al., 1996. Anaphase initiation in *Saccharomyces cerevisiae* is controlled by the APC-dependent degradation of the anaphase inhibitor Psd1p. *Genes & Dev*, 10, pp.3081–3093.
- Conrad, M.N. et al., 2007. MPS3 mediates meiotic bouquet formation in *Saccharomyces cerevisiae*. *Proceedings of the National Academy of Sciences USA*, 104(21), pp.8863–8.
- Conrad, M.N. et al., 2008. Rapid Telomere Movement in Meiotic Prophase Is Promoted By NDJ1, MPS3, and CSM4 and Is Modulated by Recombination. *Cell*, 133(7), pp.1175–1187.
- Conrad, M.N., Dominguez, A.M. & Dresser, M.E., 1997. Ndj1p, a meiotic telomere protein required for normal chromosome synapsis and segregation in yeast. *Science (New York, N.Y.)*, 276(5316), pp.1252–5.
- Consortium, T.C. *elegans* S., 1998. Genome Sequence of the Nematode *C. elegans*: A Platform for Investigating Biology. *Science (New York, N.Y.)*, 282(5396), pp.2012–2018.
- Cooper, T.J., Garcia, V. & Neale, M.J., 2016. Meiotic DSB patterning: A multifaceted process. *Cell Cycle*, 15(1), pp.13–21.
- Covitz, P.A., Herskowitz, I. & Mitchell, A.P., 1991. The yeast RME1 gene encodes a putative zinc finger protein that is directly repressed by a1-??2. *Genes and Development*, 5(11), pp.1982–1989.
- Cowan, C.R., Carlton, P.M. & Cande, W.Z., 2001. The polar arrangement of

- telomeres in interphase and meiosis. Rab1 organization and the bouquet. *Plant physiology*, 125(2), pp.532–538.
- Cremer, T. & Cremer, C., 2001. Chromosome Territories, Nuclear Architecture and Gene Regulation in Mammalian Cells. *Nature Reviews Genetics*, 2(4), pp.292–301.
- Cromie, G.A. et al., 2006. Single Holliday Junctions Are Intermediates of Meiotic Recombination. *Cell*, 127(6), pp.1167–1178.
- Danilowicz, C. et al., 2009. Single molecule detection of direct, homologous, DNA/DNA pairing. *Proceedings of the National Academy of Sciences of the United States of America*, 106(47), pp.19824–9.
- Dehé, P.-M. & Géli, V., 2006. The multiple faces of Set1. *Biochemistry and cell biology = Biochimie et biologie cellulaire*, 84(4), pp.536–548.
- Dernburg, A.F. et al., 1995. 11 Cytology of Telomeres. *Cold Spring Harbor Monograph Archive*, 29(0), pp.295–338.
- Dernburg, A.F. et al., 1998. Meiotic recombination in *C. elegans* initiates by a conserved mechanism and is dispensable for homologous chromosome synapsis. *Cell*, 94(3), pp.387–398.
- Deutschbauer, A.M. & Davis, R.W., 2005. Quantitative trait loci mapped to single-nucleotide resolution in yeast. *Nature genetics*, 37(12), pp.1333–1340.
- Diaz, R.L. et al., 2002. Identification of residues in yeast Spo11p critical for meiotic DNA double-strand break formation. *Molecular and cellular biology*, 22(4), pp.1106–15.
- Digilio, F.A. et al., 1996. Tosca: a *Drosophila* gene encoding a nuclease specifically expressed in the female germline. *Dev Biol*, 178(1), pp.90–100.
- Dupaigne, P. et al., 2008. The Srs2 helicase activity is stimulated by Rad51 filaments on dsDNA: implications for crossover incidence during mitotic recombination. *Molecular cell*, 29(2), pp.243–54.
- Eichinger, C.S. & Jentsch, S., 2010. Synaptonemal complex formation and meiotic checkpoint signaling are linked to the lateral element protein Red1. *Proceedings of the National Academy of Sciences of the United States of America*, 107(25), pp.11370–5.
- Eid, W. et al., 2010. DNA end resection by CtIP and exonuclease 1 prevents genomic instability. *EMBO reports*, 11(12), pp.962–8.
- Engels, K. et al., 2011. 14-3-3 Proteins regulate exonuclease 1-dependent processing of stalled replication forks. *PLoS genetics*, 7(4), p.e1001367.
- Falk, J.E. et al., 2010. A Mec1- and PP4-Dependent checkpoint couples centromere

- pairing to meiotic recombination. *Developmental Cell*, 19(4), pp.599–611.
- Fan, Q.Q. & Petes, T.D., 1996. Relationship between nuclease-hypersensitive sites and meiotic recombination hot spot activity at the HIS4 locus of *Saccharomyces cerevisiae*. *Molecular and cellular biology*, 16(5), pp.2037–43.
- Farcas, A.M. et al., 2011. Cohesin's Concatenation of Sister DNAs Maintains Their Intertwining. *Molecular Cell*, 44(1), pp.97–107.
- Farmer, S. et al., 2012. Budding yeast Pch2, a widely conserved meiotic protein, is involved in the initiation of meiotic recombination. *PLoS ONE*, 7(6), p.e39724.
- Faseena, M. & Thoppil, J.E., 2007. A High Polyploid Chromosome Complement of *Ophioglossum nudicaule* L. f. *Cytologia*, 72(2), pp.161–164.
- Fawcett, D.W., 1956. The fine structure of chromosomes in the meiotic prophase of vertebrate spermatocytes. *The Journal of biophysical and biochemical cytology*, 2(4), pp.403–406.
- Fekairi, S. et al., 2009. Human SLX4 Is a Holliday Junction Resolvase Subunit that Binds Multiple DNA Repair/Recombination Endonucleases. *Cell*, 138(1), pp.78–89.
- Fikus, M.U. et al., 2000. The product of the DNA damage-inducible gene of *Saccharomyces cerevisiae*, DIN7, specifically functions in mitochondria. *Genetics*, 154(1), pp.73–81.
- Fiorentini, P. et al., 1997. Exonuclease I of *Saccharomyces cerevisiae* functions in mitotic recombination in vivo and in vitro. *Molecular and cellular biology*, 17(5), pp.2764–73.
- Foss, E.J. & Stahl, F.W., 1995. A test of a counting model for chiasma interference. *Genetics*, 139(3), pp.1201–1209.
- Freeman, L., Aragon-Alcaide, L. & Strunnikov, A., 2000. The condensin complex governs chromosome condensation and mitotic transmission of rDNA. *Journal of Cell Biology*, 149(4), pp.811–824.
- Fu, Q. et al., 2014. Phosphorylation-regulated transitions in an oligomeric state control the activity of the Sae2 DNA repair enzyme. *Molecular and cellular biology*, 34(5), pp.778–93.
- Gadaleta, M.C. et al., 2013. New vectors for epitope tagging and gene disruption in *Schizosaccharomyces pombe*. *BioTechniques*, 55(5), pp.257–263.
- Galbraith, A.M. & Malone, R.E., 1992. Characterization of REC104, a gene required for early meiotic recombination in the yeast *Saccharomyces cerevisiae*. *Developmental Genetics*, 13(6), pp.392–402.
- Garcia, V. et al., 2011. Bidirectional resection of DNA double-strand breaks by

- Mre11 and Exo1. *Nature*, 479(7372), pp.241–244.
- Garcia, V. et al., 2015. Tel1(ATM)-mediated interference suppresses clustered meiotic double-strand-break formation. *Nature*, 520, pp.114–118.
- Gasior, S.L. et al., 1998. Rad52 associates with RPA and functions with Rad55 and Rad57 to assemble meiotic recombination complexes. *Genes and Development*, 12(14), pp.2208–2221.
- Gerton, J.L. et al., 2000. Global mapping of meiotic recombination hotspots and coldspots in the yeast *Saccharomyces cerevisiae*. *Proceedings of the National Academy of Sciences of the United States of America*, 97(21), pp.11383–90.
- Gilbertson, L.A., 1996. A test of the double-strand break repair model for meiotic recombination in *Saccharomyces cerevisiae*. *Genetics*, 144(1), pp.27–41.
- Gilmour, D.S. & Lis, J.T., 1984. Detecting protein-DNA interactions in vivo: distribution of RNA polymerase on specific bacterial genes. *Proceedings of the National Academy of Sciences of the United States of America*, 81(14), pp.4275–4279.
- Glynn, E.F. et al., 2004. Genome-wide mapping of the cohesin complex in the yeast *Saccharomyces cerevisiae*. *PLoS biology*, 2(9), p.E259.
- Gobbini, E. et al., 2016. Functions and regulation of the MRX complex at DNA double-strand breaks. *Microbial Cell*, 3(8), pp.329–337.
- Goffeau, A. et al., 1996. Life with 6000 Genes. *Science*, 274(October), pp.546–567.
- Goldfarb, T. & Lichten, M., 2010. Frequent and efficient use of the sister chromatid for DNA double-strand break repair during budding yeast meiosis. *PLoS Biology*, 8(10), pp.10–12.
- Goldman, A.S. & Lichten, M., 2000. Restriction of ectopic recombination by interhomolog interactions during *Saccharomyces cerevisiae* meiosis. *Proc Natl Acad Sci U S A*, 97(17), pp.9537–9542.
- Goloborodko, A. et al., 2016. Compaction and segregation of sister chromatids via active loop extrusion. *eLife*, 5(MAY2016), pp.1–16.
- Gray, S. et al., 2013. Positive regulation of meiotic DNA double-strand break formation by activation of the DNA damage checkpoint kinase Mec1(ATR). *Open biology*, 3(7), p.130019.
- Gray, S. & Cohen, P.E., 2016. Control of Meiotic Crossovers: From Double-Strand Break Formation to Designation. *Annual Review of Genetics*, 50(1), p.annurev-genet-120215-035111.
- Grey, C. et al., 2011. Mouse Prdm9 DNA-binding specificity determines sites of histone H3 lysine 4 trimethylation for initiation of meiotic recombination.

- PLoS Biology*, 9(10).
- Guacci, V. & Kaback, D.B., 1991. Distributive disjunction of authentic chromosomes in *Saccharomyces cerevisiae*. *Genetics*, 127(3), pp.475–488.
- Haering, C.H. et al., 2002. Molecular architecture of SMC proteins and the yeast cohesin complex. *Molecular Cell*, 9(4), pp.773–788.
- Hartsuiker, E., Mizuno, K., et al., 2009. Ctp1CtIP and Rad32Mre11 nuclease activity are required for Rec12Spo11 removal, but Rec12Spo11 removal is dispensable for other MRN-dependent meiotic functions. *Molecular and cellular biology*, 29(7), pp.1671–81.
- Hartsuiker, E., Neale, M.J. & Carr, A.M., 2009. Distinct Requirements for the Rad32Mre11 Nuclease and Ctp1CtIP in the Removal of Covalently Bound Topoisomerase I and II from DNA. *Molecular Cell*, 33(1), pp.117–123.
- Hartung, F. & Puchta, H., 2000. Molecular characterisation of two paralogous SPO11 homologues in *Arabidopsis thaliana*. *Nucleic acids research*, 28(7), pp.1548–1554.
- Hayashi, M., Mlynarczyk-Evans, S. & Villeneuve, A.M., 2010. The Synaptonemal Complex Shapes the Crossover Landscape Through Cooperative Assembly, Crossover Promotion and Crossover Inhibition During *Caenorhabditis elegans* Meiosis. *Genetics*, 186(1).
- Hector, R.E. et al., 2012. Mec1p associates with functionally compromised telomeres. *Chromosoma*, 121(3), pp.277–290.
- Henderson, K. a et al., 2006. Cyclin-Dependent Kinase Directly Regulates Initiation of Meiotic Recombination. *Cell*, 125(7), pp.1321–1332.
- Henry, J.M. et al., 2006. Mnd1 / Hop2 Facilitates Dmc1-Dependent Interhomolog Crossover Formation in Meiosis of Budding Yeast Mnd1 / Hop2 Facilitates Dmc1-Dependent Interhomolog Crossover Formation in Meiosis of Budding Yeast †. , 26(8), pp.2913–2923.
- Hochwagen, A. & Amon, A., 2006. Checking your breaks: surveillance mechanisms of meiotic recombination. *Current biology : CB*, 16(6), pp.R217-28.
- Hodgson, A. et al., 2011. Mre11 and Exo1 contribute to the initiation and processivity of resection at meiotic double-strand breaks made independently of Spo11. *DNA repair*, 10(2), pp.138–48.
- Holliday, R., 1964. A mechanism for gene conversion in fungi. *Genetical research*, 5(2), pp.282–304.
- Hollingsworth, N.M. & Ponte, L., 1997. Genetic interactions between HOP1, RED1 and MEK1 suggest that MEK1 regulates assembly of axial element components during meiosis in the yeast *Saccharomyces cerevisiae*. *Genetics*,

- 147(1), pp.33–42.
- Hollingsworth, N.M., Ponte, L. & Halsey, C., 1995. MSH5, a novel MutS homolog, facilitates meiotic reciprocal recombination between homologs in *Saccharomyces cerevisiae* but not mismatch repair. *Genes and Development*, 9(14), pp.1728–1739.
- Holm, P.B., 1977. The premeiotic DNA replication of euchromatin and heterochromatin in *Lilium longiflorum* (Thunb.). *Carlsberg Research Communications*, 42(4), pp.249–281.
- Holzen, T.M. et al., 2006. Tid1/Rdh54 promotes dissociation of Dmc1 from nonrecombinogenic sites on meiotic chromatin. *Genes & development*, 20(18), pp.2593–604.
- Hong, E.L., Shinohara, A. & Bishop, D.K., 2001. *Saccharomyces cerevisiae* Dmc1 protein promotes renaturation of single-strand DNA (ssDNA) and assimilation of ssDNA into homologous super-coiled duplex DNA. *The Journal of biological chemistry*, 276(45), pp.41906–12.
- Hopfner, K.-P. et al., 2002. The Rad50 zinc-hook is a structure joining Mre11 complexes in DNA recombination and repair. *Nature*, 418(6897), pp.562–566.
- Hopfner, K.P. et al., 2001. Structural biochemistry and interaction architecture of the DNA double-strand break repair Mre11 nuclease and Rad50-ATPase. *Cell*, 105(4), pp.473–485.
- Hopfner, K.P. et al., 2000. Structural biology of Rad50 ATPase: ATP-driven conformational control in DNA double-strand break repair and the ABC-ATPase superfamily. *Cell*, 101(7), pp.789–800.
- Humphries, N. et al., 2013. The Ecm11-Gmc2 complex promotes synaptonemal complex formation through assembly of transverse filaments in budding yeast. *PLoS genetics*, 9(1), p.e1003194.
- Hunter, N. & Kleckner, N., 2001. The Single-End Invasion: An Asymmetric Intermediate at the Double-Strand Break to Double-Holliday Junction Transition of Meiotic Recombination. *Cell*, 106(1), pp.59–70.
- Hustedt, N. & Durocher, D., 2017. The control of DNA repair by the cell cycle. *Nat Cell Biol*, 19(1), pp.1–9.
- Ivanov, E.L., Korolev, V.G. & Fabre, F., 1992. XRS2, a DNA repair gene of *Saccharomyces cerevisiae*, is needed for meiotic recombination. *Genetics*, 132(3), pp.651–664.
- Iwasaki, H. et al., 1991. *Escherichia coli* RuvC protein is an endonuclease that resolves the Holliday structure. *The EMBO journal*, 10(13), pp.4381–9.
- Jessop, L. et al., 2006. Meiotic chromosome synapsis-promoting proteins antagonize the anti-crossover activity of sgs1. *PLoS Genetics*, 2(9), pp.1402–

1412.

- Jiao, K., Salem, L. & Malone, R., 2003. Support for a meiotic recombination initiation complex: interactions among Rec102p, Rec104p, and Spo11p. *Molecular and cellular biology*, 23(16), pp.5928–38.
- Johzuka, K. & Ogawa, H., 1995. Interaction of Well and Rad50: Two Proteins Required for DNA Repair and Meiosis-Specific Double-Strand Break Formation in *Saccharomyces cerevisiae*. *Genetics*, 139(1), pp.1521–1532.
- Joshi, N. et al., 2009. Pch2 links chromosome axis remodeling at future crossover sites and crossover distribution during yeast meiosis. *PLoS genetics*, 5(7), p.e1000557.
- Kane, S.M. & Roth, R., 1974. Carbohydrate Metabolism During Ascospore Development in Yeast. , 118(1), pp.8–14.
- Karathia, H. et al., 2011. *Saccharomyces cerevisiae* as a Model Organism: A Comparative Study. *PloS one*, 16015.
- Katis, V.L. et al., 2004. Spo13 Facilitates Monopolin Recruitment to Kinetochores and Regulates Maintenance of Centromeric Cohesion during Yeast Meiosis. *Current Biology*, 14(2), pp.2183–2196.
- Kaur, H., DeMuyt, A. & Lichten, M., 2015. Top3-Rmi1 DNA single-strand decatenase is integral to the formation and resolution of meiotic recombination intermediates. *Molecular Cell*, 57(4), pp.583–594.
- Keelagher, R.E. et al., 2010. Separable roles for Exonuclease I in meiotic DNA double-strand break repair. *DNA Repair*, 10(2), pp.126–137.
- Keeney, S., 2008. Spo11 and the Formation of DNA Double-Strand Breaks in Meiosis. *Genome dynamics and stability*, 2, pp.81–123.
- Keeney, S., Giroux, C.N. & Kleckner, N., 1997. Meiosis-specific DNA double-strand breaks are catalyzed by Spo11, a member of a widely conserved protein family. *Cell*, 88(3), pp.375–84.
- Keeney, S. & Kleckner, N., 1995. Covalent protein-DNA complexes at the 5' strand termini of meiosis-specific double-strand breaks in yeast. *Proceedings of the National Academy of Sciences of the United States of America*, 92(24), pp.11274–8.
- Kemp, B. et al., 2004. A role for centromere pairing in meiotic chromosome segregation service A role for centromere pairing in meiotic chromosome segregation. , (617), pp.1946–1951.
- Kiburz, B.M. et al., 2005. The core centromere and Sgo1 establish a 50-kb cohesin-protected domain around centromeres during meiosis I. *Genes and Development*, 19(24), pp.3017–3030.

- Kim, J. et al., 2014. Meikin is a conserved regulator of meiosis-I-specific kinetochore function. *Nature*, 517(7535), pp.466–471.
- Kim, S.T. et al., 1999. Substrate specificities and identification of putative substrates of ATM kinase family members. *Journal of Biological Chemistry*, 274(53), pp.37538–37543.
- King, J.S. & Mortimer, R.K., 1990. A polymerization model of chiasma interference and corresponding computer simulation. *Genetics*, 126(4), pp.1127–1138.
- Kirkpatrick, D.T. et al., 2000. Decreased meiotic intergenic recombination and increased meiosis I nondisjunction in *exo1* mutants of *Saccharomyces cerevisiae*. *Genetics*, 156(4), pp.1549–1557.
- Kirmizis, A. et al., 2007. Arginine methylation at histone H3R2 controls deposition of H3K4 trimethylation. *Nature*, 449(7164), pp.928–932.
- Kitajima, T.S. et al., 2006. Shugoshin collaborates with protein phosphatase 2A to protect cohesin. *Nature*, 441(7089), pp.46–52.
- Kleckner, N. et al., 2004. A mechanical basis for chromosome function. *Proceedings of the National Academy of Sciences of the United States of America*, 101(34), pp.12592–12597.
- Kleckner, N. & Weiner, B.M., 1993. Potential advantages of unstable interactions for pairing of chromosomes in meiotic, somatic, and premeiotic cells. *Cold Spring Harbor symposia on quantitative biology*, 58, pp.553–65.
- Klein, F. et al., 1999. A central role for cohesins in sister chromatid cohesion, formation of axial elements, and recombination during yeast meiosis. *Cell*, 98(1), pp.91–103.
- Klutstein, M. & Cooper, J.P., 2014. The chromosomal courtship dance-homolog pairing in early meiosis. *Current Opinion in Cell Biology*, 26(1), pp.123–131.
- Kosaka, H., Shinohara, M. & Shinohara, A., 2008. Csm4-dependent telomere movement on nuclear envelope promotes meiotic recombination. *PLoS Genetics*, 4(9).
- Kugou, K. et al., 2009. Rec8 Guides Canonical Spo11 Distribution along Yeast Meiotic Chromosomes. *Molecular biology of the cell*, 20(1), pp.3064–3076.
- Kurdzo, E.L. & Dawson, D.S., 2015. Centromere pairing - tethering partner chromosomes in meiosis I. *FEBS Journal*, 282, pp.2445–2457.
- Kurzbauer, M.-T. et al., 2012. The recombinases DMC1 and RAD51 are functionally and spatially separated during meiosis in *Arabidopsis*. *The Plant cell*, 24(5), pp.2058–70.
- Lam, I. & Keeney, S., 2015. Mechanism and regulation of meiotic recombination

- initiation. *Cold Spring Harbor Perspectives in Biology*, 7(1).
- Lashkari, D. a et al., 1997. Yeast microarrays for genome wide parallel genetic and gene expression analysis. *Proceedings of the National Academy of Sciences of the United States of America*, 94(November), pp.13057–13062.
- Lee, B.H., Amon, A. & Prinz, S., 2002. Spo13 regulates cohesin cleavage. *Genes and Development*, 16(13), pp.1672–1681.
- Lee, B.I. et al., 1999. Expression specificity of the mouse exonuclease 1 (mExo1) gene. *Nucleic Acids Research*, 27(20), pp.4114–4120.
- Lemmens, B.B.L.G., Johnson, N.M. & Tijsterman, M., 2013. COM-1 Promotes Homologous Recombination during *Caenorhabditis elegans* Meiosis by Antagonizing Ku-Mediated Non-Homologous End Joining N. Bhalla, ed. *PLoS Genetics*, 9(2), p.e1003276.
- Lengsfeld, B.M. et al., 2007. Sae2 is an endonuclease that processes hairpin DNA cooperatively with the Mre11/Rad50/Xrs2 complex. *Molecular cell*, 28(4), pp.638–51.
- Leung, W.K. et al., 2015. The synaptonemal complex is assembled by a polySUMOylation-driven feedback mechanism in yeast. *Journal of Cell Biology*, 211(4), pp.785–793.
- Lewis, L.K. et al., 2004. Role of the Nuclease Activity of *Saccharomyces cerevisiae* Mre11 in Repair of DNA Double-Strand Breaks in Mitotic Cells. *Genetics*, 166(4), pp.1701–1713.
- Li, J., Hooker, G.W. & Roeder, G.S., 2006. *Saccharomyces cerevisiae* Mer2, Mei4 and Rec114 form a complex required for meiotic double-strand break formation. *Genetics*, 173(4), pp.1969–1981.
- Li, P. et al., 2015. Ndj1, a telomere-associated protein, regulates centrosome separation in budding yeast meiosis. *Journal of Cell Biology*, 209(2), pp.247–259.
- Li, P., Jin, H. & Yu, H.-G., 2014. Condensin suppresses recombination and regulates double-strand break processing at the repetitive ribosomal DNA array to ensure proper chromosome segregation during meiosis in budding yeast. *Molecular biology of the cell*, 25(19), pp.2934–47.
- Lichten, M. & Goldman, A.S.H., 1995. MEIOTIC RECOMBINATION HOTSPOTS. *Annual Review of Genetics*, 29, pp.423–444.
- Lieber, M.R., 1997. The FEN-1 family of structure-specific nucleases in eukaryotic dna replication, recombination and repair. *BioEssays*, 19(3), pp.233–240.
- Lim, H.S. et al., 2011. Crystal structure of the Mre11-Rad50-ATPγS complex: Understanding the interplay between Mre11 and Rad50. *Genes and*

- Development*, 25(10), pp.1091–1104.
- Limbo, O. et al., 2007. Ctp1 Is a Cell-Cycle-Regulated Protein that Functions with Mre11 Complex to Control Double-Strand Break Repair by Homologous Recombination. *Molecular Cell*, 28(1), pp.134–146.
- Lindgren, C.C., 1955. Non-Mendelian Segregation in a Single Tetrad of *Saccharomyces* Ascribed to Gene Conversion. *Science*, 121(April 1955), pp.605–607.
- Lindgren, C.C. & Lindgren, G., 1943. Selecting, Inbreeding, Recombining, and Hybridizing Commercial Yeasts. *J Bacteriol*, 46(5), pp.405–419.
- Liu, J., Wu, T.C. & Lichten, M., 1995. The location and structure of double-strand DNA breaks induced during yeast meiosis: evidence for a covalently linked DNA-protein intermediate. *Embo J*, 14(18), p.4599–608.
- Llano, E. et al., 2012. Meiotic cohesin complexes are essential for the formation of the axial element in mice. *Journal of Cell Biology*, 197(7), pp.877–885.
- Lo, Y.-H., Chuang, C.-N. & Wang, T.-F., 2014. Pch2 prevents Mec1/Tel1-mediated Hop1 phosphorylation occurring independently of Red1 in budding yeast meiosis. *PloS one*, 9(1), p.e85687.
- Longhese, M.P. et al., 2009. DNA double-strand breaks in meiosis: checking their formation, processing and repair. *DNA repair*, 8(9), pp.1127–38.
- De los Santos, T. et al., 2003. The MUS81/MMS4 endonuclease acts independently of double-holliday junction resolution to promote a distinct subset of crossovers during meiosis in budding yeast. *Genetics*, 164(1), pp.81–94.
- Louis, E.J., 2016. Historical evolution of laboratory strains of *saccharomyces cerevisiae*. *Cold Spring Harbor Protocols*, 2016(7), pp.585–593.
- Lynn, A., Soucek, R. & Börner, G.V., 2007. ZMM proteins during meiosis: Crossover artists at work. *Chromosome Research*, 15(5), pp.591–605.
- MacQueen, A.J. & Hochwagen, A., 2011. Checkpoint mechanisms: The puppet masters of meiotic prophase. *Trends in Cell Biology*, 21(7), pp.393–400.
- MacQueen, A.J. & Roeder, G.S., 2009. Fpr3 and Zip3 Ensure that Initiation of Meiotic Recombination Precedes Chromosome Synapsis in Budding Yeast. *Current Biology*, 19(18), pp.1519–1526.
- Maleki, S. et al., 2007. Interactions between Mei4, Rec114, and other proteins required for meiotic DNA double-strand break formation in *Saccharomyces cerevisiae*. *Chromosoma*, 116(5), pp.471–86.
- Malone, R.E. et al., 1991. Isolation of mutants defective in early steps of meiotic recombination in the yeast *Saccharomyces cerevisiae*. *Genetics*, 128(1),

- pp.79–88.
- Mancera, E. et al., 2008. High-resolution mapping of meiotic crossovers and non-crossovers in yeast. *Nature*, 454, pp.479–485.
- Manders, E.M.M., Kimura, H. & Cook, P.R., 1999. Direct imaging of DNA in living cells reveals the dynamics of chromosome formation. *Journal of Cell Biology*, 144(5), pp.813–821.
- Manfrini, N. et al., 2010. Processing of meiotic DNA double strand breaks requires cyclin-dependent kinase and multiple nucleases. *The Journal of biological chemistry*, 285(15), pp.11628–37.
- Manhart, C.M. & Alani, E., 2016. Roles for mismatch repair family proteins in promoting meiotic crossing over. *DNA Repair*, 38, pp.84–93.
- Marko, J.F. & Siggia, E.D., 1997. Polymer models of meiotic and mitotic chromosomes. *Molecular Biology of the Cell*, 8(11), pp.2217–2231.
- Martínez-Pérez, E. et al., 1999. Homologous chromosome pairing in wheat. *Journal of cell science*, 112 (Pt 1, pp.1761–1769.
- Martini, E. et al., 2006. Crossover Homeostasis in Yeast Meiosis. *Cell*, 126(2), pp.285–295.
- de Massy, B., 2013. Initiation of meiotic recombination: how and where? Conservation and specificities among eukaryotes. *Annual review of genetics*, 47, pp.563–99.
- de Massy, B., Rocco, V. & Nicolas, A., 1995. The nucleotide mapping of DNA double-strand breaks at the CYS3 initiation site of meiotic recombination in *Saccharomyces cerevisiae*. *The EMBO journal*, 14(18), pp.4589–4598.
- Matos, J. & West, S.C., 2014. Holliday junction resolution: Regulation in space and time. *DNA Repair*, 19(100), pp.176–181.
- Matsuoka, S. et al., 2007. ATM and ATR substrate analysis reveals extensive protein networks responsive to DNA damage. *Science*, 316(5828), pp.1160–1166.
- McGovern, P.E. et al., 1996. Neolithic resinated wine. *Nature*, 381(6582), pp.480–481.
- McKee, A.H.Z. & Kleckner, N., 1997. A general method for identifying recessive diploid-specific mutations in *Saccharomyces cerevisiae*, its application to the isolation of mutants blocked at intermediate stages of meiotic prophase and characterization of a new gene SAE2. *Genetics*, 146(3), pp.797–816.
- Mckim, K.S. & Hayashi-hagihara, A., 1998. mei-W68 in *D.Melanogaster* encodes a Spo11 homolog: evidence that the mechanism for initiating meiotic

- recombination is conserved. *Genes & Development*, pp.2932–2942.
- McMahill, M.S., Sham, C.W. & Bishop, D.K., 2007. Synthesis-dependent strand annealing in meiosis M. Lichten, ed. *PLoS Biology*, 5(11), pp.2589–2601.
- McPherson, J.P. et al., 2004. Involvement of mammalian Mus81 in genome integrity and tumor suppression. *Science*, 304(5678), pp.1822–1826.
- Medhi, D., Goldman, A.S.H. & Lichten, M., 2016. Local chromosome context is a major determinant of crossover pathway biochemistry during budding yeast meiosis. *eLife*, 5, pp.1–48.
- Menees, T.M., Ross-MacDonald, P.B. & Roeder, G.S., 1992. MEI4, a meiosis-specific yeast gene required for chromosome synapsis. *Molecular and cellular biology*, 12(3), pp.1340–1351.
- Meussdoerffer, F.G., 2009. *A Comprehensive History of Beer Brewing*,
- Michaelis, C., Ciosk, R. & Nasmyth, K., 1997. Cohesins: Chromosomal proteins that prevent premature separation of sister chromatids. *Cell*, 91(1), pp.35–45.
- Mieczkowski, P.A., Fikus, M.U. & Ciesla, Z., 1997. Characterization of a novel DNA damage-inducible gene of *Saccharomyces cerevisiae*, DIN7, which is a structural homolog of the RAD2 and RAD27 DNA repair genes. *Molecular and General Genetics*, 253(6), pp.655–665.
- Milman, N., Higuchi, E. & Smith, G.R., 2009. Meiotic DNA double-strand break repair requires two nucleases, MRN and Ctp1, to produce a single size class of Rec12 (Spo11)-oligonucleotide complexes. *Molecular and Cellular Biology*, 29(22), pp.5998–6005.
- Mimitou, E.P. & Symington, L.S., 2009. DNA end resection: many nucleases make light work. *DNA repair*, 8(9), pp.983–95.
- Mimitou, E.P. & Symington, L.S., 2008. Sae2, Exo1 and Sgs1 collaborate in DNA double-strand break processing. *Nature*, 455(7214), pp.770–4.
- Mitchell, a P., Driscoll, S.E. & Smith, H.E., 1990. Positive control of sporulation-specific genes by the IME1 and IME2 products in *Saccharomyces cerevisiae*. *Molecular and cellular biology*, 10(5), pp.2104–2110.
- Mitchell, M.B., 1955. ABERRANT RECOMBINATION OF PYRIDOXINE MUTANTS OF *Neurospora*. *Proceedings of the National Academy of Sciences of the United States of America*, 41(4), pp.215–220.
- Miura, T., Shibata, T. & Kusano, K., 2013. Putative antirecombinase Srs2 DNA helicase promotes noncrossover homologous recombination avoiding loss of heterozygosity. *Proceedings of the National Academy of Sciences of the United States of America*, 110(40), pp.16067–72.
- Möckel, C. et al., 2012. ATP driven structural changes of the bacterial Mre11:Rad50

- catalytic head complex. *Nucleic Acids Research*, 40(2), pp.914–927.
- Mok, J. et al., 2010. Deciphering protein kinase specificity through large-scale analysis of yeast phosphorylation site motifs. *Science signaling*, 3(109), p.ra12.
- Moreau, S., Morgan, E.A. & Symington, L.S., 2001. Overlapping functions of the *Saccharomyces cerevisiae* Mre11, Exo1 and Rad27 nucleases in DNA metabolism. *Genetics*, 159(4), pp.1423–1433.
- Morin, I. et al., 2008. Checkpoint-dependent phosphorylation of Exo1 modulates the DNA damage response. *The EMBO journal*, 27(18), pp.2400–10.
- Mortimer, R.K. & Johnston, J.R., 1986. Genealogy of principal strains of the yeast genetic stock center. *Genetics*, 113(1), pp.35–43.
- Murakami, H. & Keeney, S., 2014. Temporospatial coordination of meiotic dna replication and recombination via DDK recruitment to replisomes. *Cell*, 158(4), pp.861–873.
- Nakada, D., Matsumoto, K. & Sugimoto, K., 2003. ATM-related Tel1 associates with double-strand breaks through an Xrs2-dependent mechanism. *Genes and Development*, 17(16), pp.1957–1962.
- Nasmyth, K., 2001. Disseminating the Genome: Joining, Resolving, and Separating Sister Chromatids During Mitosis and Meiosis. *Annual Review of Genetics*, 35(1), pp.673–745.
- NCBI Blast, ., 2016. NCBI Blast:hExo1 and scExo1. Available at: <https://blast.ncbi.nlm.nih.gov/Blast.cgi> [Accessed April 7, 2017].
- Neale, M.J. et al., 2002. Wild-type levels of Spo11-induced DSBs are required for normal single-strand resection during meiosis. *Molecular cell*, 9(4), pp.835–46.
- Neale, M.J., Pan, J. & Keeney, S., 2005. Endonucleolytic processing of covalent protein-linked DNA double-strand breaks. *Nature*, 436(7053), pp.1053–7.
- NEB, Double Digest Finder | NEB. Available at: <https://www.neb.com/tools-and-resources/interactive-tools/double-digest-finder> [Accessed May 13, 2017].
- Newnham, L. et al., 2010. The synaptonemal complex protein, Zip1, promotes the segregation of nonexchange chromosomes at meiosis I. *Proceedings of the National Academy of Sciences of the United States of America*, 107(2), pp.781–5.
- Nicolette, M.L. et al., 2010. Mre11-Rad50-Xrs2 and Sae2 promote 5' strand resection of DNA double-strand breaks. *Nature structural & molecular biology*, 17(12), pp.1478–85.
- Nimonkar, A. V. et al., 2011. BLM-DNA2-RPA-MRN and EXO1-BLM-RPA-MRN

- constitute two DNA end resection machineries for human DNA break repair. *Genes and Development*, 25(4), pp.350–362.
- Nishant, K.T. & Rao, M.R.S., 2006. Molecular features of meiotic recombination hot spots. *BioEssays*, 28(1), pp.45–56.
- Niu, H. et al., 2007. Mek1 kinase is regulated to suppress double-strand break repair between sister chromatids during budding yeast meiosis. *Molecular and cellular biology*, 27(15), pp.5456–67.
- Niu, H. et al., 2005. Partner Choice during Meiosis Is Regulated by Hop1-promoted Dimerization of Mek1 Hengyao. *Molecular biology of the cell*, 16(2), pp.5804–5818.
- Niu, H. et al., 2009. Regulation of meiotic recombination via Mek1-mediated Rad54 phosphorylation. *Molecular cell*, 36(3), pp.393–404.
- Obeso, D. & Dawson, D.S., 2010. Temporal characterization of homology-independent centromere coupling in meiotic prophase. *PLoS ONE*, 5(4).
- Obeso, D., Pezza, R.J. & Dawson, D., 2014. Couples, Pairs, and Clusters: Mechanisms and Implications of Centromere Associations in Meiosis. *Chromosoma*, 123(0), pp.43–55.
- Ogawa, T. et al., 1993. Similarity of the yeast RAD51 filament to the bacterial RecA filament. *Science (New York, N.Y.)*, 259(5103), pp.1896–1899.
- Oh, S.D. et al., 2007. BLM Ortholog, Sgs1, Prevents Aberrant Crossing-over by Suppressing Formation of Multichromatid Joint Molecules. *Cell*, 130(2), pp.259–272.
- Ohta, K. et al., 1998. Mutations in the MRE11, RAD50, XRS2, and MRE2 genes alter chromatin configuration at meiotic DNA double-stranded break sites in premeiotic and meiotic cells. *Proc Natl Acad Sci U S A*, 95(2), pp.646–651.
- Orans, J. et al., 2011. Structures of human exonuclease I DNA complexes suggest a unified mechanism for nuclease family. *Cell*, 145(2), pp.212–223.
- Osman, F. et al., 2003. Generating crossovers by resolution of nicked Holliday junctions: A role for Mus81-Eme1 in meiosis. *Molecular Cell*, 12(3), pp.761–774.
- Padmore, R., Cao, L. & Kleckner, N., 1991. Temporal comparison of recombination and synaptonemal complex formation during meiosis in *S. cerevisiae*. *Cell*, 66(6), pp.1239–1256.
- Page, S.L. & Hawley, R.S., 2001. c(3)G encodes a *Drosophila* synaptonemal complex protein. *Genes & development*, 15(23), pp.3130–43.
- Page, S.L. & Hawley, R.S., 2003. Chromosome choreography: the meiotic ballet.

- Science (New York, N.Y.)*, 301(5634), pp.785–789.
- Pan, J. et al., 2011. A hierarchical combination of factors shapes the genome-wide topography of yeast meiotic recombination initiation. *Cell*, 144(5), pp.719–731.
- Panizza, S. et al., 2011. Spo11-Accessory Proteins Link Double- Strand Break Sites to the Chromosome Axis in Early Meiotic Recombination. *Cell*, 146(3), pp.372–383.
- Pasteur, L., 1872. Nouvelles expériences pour démontrer que le germe de la levure qui fait le vin provient de l'extérieur des grains de raisin. *CR Searces Acad. Sci. Paris*, 75, pp.781–793.
- Paull, T.T. & Gellert, M., 1999. Nbs1 potentiates ATP-driven DNA unwinding and endonuclease cleavage by the Mre11/Rad50 complex. *Genes & development*, 13(10), pp.1276–88.
- Paulson, J.R. & Laemmli, U.K., 1977. The structure of histone-depleted metaphase chromosomes. *Cell*, 12(3), pp.817–828.
- Pecina, A. et al., 2002. Targeted stimulation of meiotic recombination. *Cell*, 111(2), pp.173–184.
- Penedos, A. et al., 2016. Correction: Essential and checkpoint functions of budding yeast ATM and ATR during meiotic prophase are facilitated by differential phosphorylation of a meiotic adaptor protein, Hop1. *PLoS ONE*, 11(4), pp.1–17.
- Petronczki, M. et al., 2006. Monopolar Attachment of Sister Kinetochores at Meiosis I Requires Casein Kinase 1. *Cell*, 126(6), pp.1049–1064.
- Petukhova, G., Stratton, S. & Sung, P., 1998. Catalysis of homologous DNA pairing by yeast Rad51 and Rad54 proteins. *Nature*, 393(6680), pp.91–4.
- Prieler, S. et al., 2005. The control of Spo11 ' s interaction with meiotic recombination hotspots. *Genes & development*, 19, pp.255–269.
- Primig, M. et al., 2000. The core meiotic transcriptome in budding yeasts. *Nature genetics*, 26(4), pp.415–23.
- Prinz, S., Amon, A. & Klein, F., 1997. Isolation of COM1, a new gene required to complete meiotic double- strand break-induced recombination in *Saccharomyces cerevisiae*. *Genetics*, 146(3), pp.781–795.
- Puddu, F. et al., 2015. Synthetic viability genomic screening defines Sae2 function in DNA repair. *The EMBO journal*, 34(11), pp.1509–22.
- Qiu, J. et al., 1999. Human Exonuclease 1 Functionally Complements Its Yeast Homologues in DNA Recombination, RNA Primer Removal, and Mutation

- Avoidance*. *The Journal of biological chemistry*, 274(25), pp.17893–17900.
- Rabitsch, K.P. et al., 2001. A screen for genes required for meiosis and spore formation based on whole-genome expression. *Current Biology*, 11(13), pp.1001–1009.
- Ralsler, M. et al., 2012. The *Saccharomyces cerevisiae* W303-K6001 cross-platform genome sequence: insights into ancestry and physiology of a laboratory mutt. *Open biology*, 2(8), p.120093.
- Rattray, A.J. et al., 2001. Fidelity of mitotic double-strand-break repair in *Saccharomyces cerevisiae*: A role for SAE2/COM1. *Genetics*, 158(1), pp.109–122.
- Raymond, W.E. & Kleckner, N., 1993. RAD50 protein of *S.cerevisiae* exhibits ATP-dependent DNA binding. *Nucleic Acids Research*, 21(16), pp.3851–3856.
- Resnick, M.A., 1976. The repair of double-strand breaks in DNA: A model involving recombination. *Journal of Theoretical Biology*, 59(1), pp.97–106.
- Ribeiro, J. et al., 2016. RPA homologs and ssDNA processing during meiotic recombination. *Chromosoma*, 125(2), pp.265–276.
- Rockmill, B. et al., 1995. Roles for two RecA homologs in promoting meiotic chromosome synapsis. *Genes & development*, 9(21), pp.2684–95.
- Rockmill, B. & Roeder, G.S., 1991. A meiosis-specific protein kinase homolog required for chromosome synapsis and recombination. *Genes & Development*, 5(12b), pp.2392–2404.
- Rockmill, B. & Roeder, G.S., 1990. Meiosis in asynaptic yeast. *Genetics*, 126(3), pp.563–574.
- Rockmill, B. & Roeder, G.S., 1998. Telomere-mediated chromosome pairing during meiosis in budding yeast. *Genes and Development*, 12(16), pp.2574–2586.
- Roeder, G.S. & Bailis, J.M., 2000. The pachytene checkpoint. *Trends in genetics : TIG*, 16(9), pp.395–403.
- Romanienko, P.J. & Camerini-Otero, R.D.D., 2000. The mouse Spo11 gene is required for meiotic chromosome synapsis. *Molecular cell*, 6(5), pp.975–987.
- Roy, B. & Hecht, S.M., 2014. Hairpin DNA sequences bound strongly by bleomycin exhibit enhanced double-strand cleavage. *Journal of the American Chemical Society*, 136(11), pp.4382–93.
- Rubin-Bejerano, I. et al., 1996. Induction of meiosis in *Saccharomyces cerevisiae* depends on conversion of the transcriptional repressor Ume6 to a positive regulator by its regulated association with the transcriptional activator Ime1. *Molecular and cellular biology*, 16(5), pp.2518–26.

- Salah, S. & Nasmyth, K., 2002. Destruction of the securin Pds1p occurs at the onset of anaphase during both meiotic divisions in yeast. *Chromosoma*, 109(1-2), pp.27-34.
- Sarbajna, S. & West, S.C., 2014. Holliday junction processing enzymes as guardians of genome stability. *Trends in Biochemical Sciences*, 39(9), pp.409-419.
- Sartori, A.A. et al., 2007. Human CtIP promotes DNA end resection. *Nature*, 450(7169), pp.509-514.
- Sasanuma, H. et al., 2007. Meiotic association between Spo11 regulated by Rec102, Rec104 and Rec114. *Nucleic Acids Research*, 35(4), pp.1119-1133.
- Sasanuma, H. et al., 2013. Remodeling of the Rad51 DNA strand-exchange protein by the Srs2 helicase. *Genetics*, 194(4), pp.859-872.
- Schacherer, J. et al., 2007. Genome-wide analysis of nucleotide-level variation in commonly used *Saccharomyces cerevisiae* strains. *PLoS ONE*, 2(3), pp.1-7.
- Scherthan, H. et al., 1996. Centromere and telomere movements during early meiotic prophase of mouse and man are associated with the onset of chromosome pairing. *Journal of Cell Biology*, 134(5), pp.1109-1125.
- Schiestl, R.H. & Prakash, S., 1990. RAD10, an excision repair gene of *Saccharomyces cerevisiae*, is involved in the RAD1 pathway of mitotic recombination. *Molecular and cellular biology*, 10(6), pp.2485-91.
- Schmekel, K. et al., 1993. The central region of the synaptonemal complex in *Blaps cribrosa* studied by electron microscope tomography. *Chromosoma*, 102(10), pp.669-81.
- Schwacha, A. & Kleckner, N., 1995. Identification of double holliday junctions as intermediates in meiotic recombination. *Cell*, 83(5), pp.783-791.
- Schwacha, A. & Kleckner, N., 1997. Interhomolog bias during meiotic recombination: Meiotic functions promote a highly differentiated interhomolog-only pathway. *Cell*, 90(6), pp.1123-1135.
- Schwacha, a & Kleckner, N., 1994. Identification of joint molecules that form frequently between homologs but rarely between sister chromatids during yeast meiosis. *Cell*, 76(1), pp.51-63.
- Serrentino, M.E. et al., 2013. Differential Association of the Conserved SUMO Ligase Zip3 with Meiotic Double-Strand Break Sites Reveals Regional Variations in the Outcome of Meiotic Recombination J. Sekelsky, ed. *PLoS Genetics*, 9(4), p.e1003416.
- Sharples, G.J. & Leach, D.R.F., 1995. Structural and functional similarities between the SbcCD proteins of *Escherichia coli* and the RAD50 and MRE11 (RAD32) recombination and repair proteins of yeast. *Molecular Microbiology*, 17(6),

- pp.1215–1217.
- Shinohara, A., Ogawa, H. & Ogawa, T., 1992. Rad51 protein involved in repair and recombination in *S. cerevisiae* is a RecA-like protein. *Cell*, 69(3), pp.457–70.
- Shinohara, M. et al., 2008. Crossover assurance and crossover interference are distinctly regulated by the ZMM proteins during yeast meiosis. *Nature genetics*, 40(3), pp.299–309.
- Shinohara, M. et al., 2003. Crossover interference in *Saccharomyces cerevisiae* requires a TID1/RDH54- and DMC1-dependent pathway. *Genetics*, 163(4), pp.1273–86.
- Shinohara, M. et al., 2000. Tid1/Rdh54 promotes colocalization of rad51 and dmc1 during meiotic recombination. *Proceedings of the National Academy of Sciences of the United States of America*, 97(20), pp.10814–9.
- Shinohara, M. & Shinohara, A., 2013. Multiple Pathways Suppress Non-Allelic Homologous Recombination during Meiosis in *Saccharomyces cerevisiae*. D. T. Kirkpatrick, ed. *PLoS ONE*, 8(4), p.e63144.
- Shonn, M.A., McCarroll, R. & Murray, A.W., 2002. Spo13 protects meiotic cohesin at centromeres in meiosis I. *Genes and Development*, 16(13), pp.1659–1671.
- Smith, A. V. & Roeder, G.S., 1997. The yeast Red1 protein localizes to the cores of meiotic chromosomes. *Journal of Cell Biology*, 136(5), pp.957–967.
- Smith, G.R. et al., 2003. Fission Yeast Mus81·Eme1 Holliday Junction Resolvase Is Required for Meiotic Crossing over but Not for Gene Conversion. *Genetics*, 165(4), pp.2289–2293.
- Smith, H.E. & Mitchell, A.P., 1989. A transcriptional cascade governs entry into meiosis in *Saccharomyces cerevisiae*. *Molecular and Cellular Biology*, 9(5), pp.2142–2152.
- Sommermeier, V. et al., 2013. Spp1, a Member of the Set1 Complex, Promotes Meiotic DSB Formation in Promoters by Tethering Histone H3K4 Methylation Sites to Chromosome Axes. *Molecular Cell*, 49(1), pp.43–54.
- Souquet, B. et al., 2013. MEIOB Targets Single-Strand DNA and Is Necessary for Meiotic Recombination. *PLoS Genetics*, 9(9), p.e1003784.
- Soustelle, C. et al., 2002. Replication protein A is required for meiotic recombination in *Saccharomyces cerevisiae*. *Genetics*, 161(2), pp.535–547.
- Southern, J. a et al., 1991. Identification of an Epitope on the P-Proteins and V-Proteins of Simian-Virus 5 That Distinguishes between 2 Isolates with Different Biological Characteristics. *Journal of General Virology*, 72(1991), pp.1551–1557.
- Stahl, F., 1996. Meiotic recombination in yeast: Coronation of the double-strand-

- break repair model. *Cell*, 87(6), pp.965–968.
- Stefanini, I. et al., 2015. Social wasps are a *Saccharomyces* mating nest. *Proceedings of the National Academy of Sciences*, 113(60 d), pp.2–6.
- Steiner, W.W., Schreckhise, R.W. & Smith, G.R., 2002. Meiotic DNA breaks at the *S. pombe* recombination hot spot M26. *Molecular Cell*, 9(4), pp.847–855.
- Steininger, S. et al., 2009. A novel function for the Mre11-Rad50-Xrs2 complex in base excision repair. *Nucleic Acids Research*, 38(6), pp.1853–1865.
- Stewart, M.N. & Dawson, D.S., 2004. Potential Roles for Centromere Pairing in Meiotic Chromosome Segregation. *Cell Cycle*, 3(10).
- Storlazzi, A. et al., 2003. Meiotic double-strand breaks at the interface of chromosome movement, chromosome remodeling, and reductional division. *Genes and Development*, 17(21), pp.2675–2687.
- Subramanian, V. V & Hochwagen, A., 2015. The Meiotic Checkpoint Network : Step-by-Step through Meiotic Prophase.
- Sun, X. et al., 2003. Sequence analysis of a functional *Drosophila* centromere. *Genome Research*, 13(2), pp.182–194.
- Sutton, W.S., 1903. The Chromosomes in Heredity. *Biological Bulletin*, 4(5), pp.231–251.
- Svendsen, J.M. et al., 2009. Mammalian BTBD12/SLX4 Assembles A Holliday Junction Resolvase and Is Required for DNA Repair. *Cell*, 138(1), pp.63–77.
- Sym, M., Engebrecht, J.A. & Roeder, G.S., 1993. ZIP1 is a synaptonemal complex protein required for meiotic chromosome synapsis. *Cell*, 72(3), pp.365–78.
- Symington, L.S., 2014. End resection at double-strand breaks: Mechanism and regulation. *Cold Spring Harbor Perspectives in Biology*, 6(8).
- Szankasi, P. & Smith, G.R., 1992. A DNA exonuclease induced during meiosis of *Schizosaccharomyces pombe*. *Journal of Biological Chemistry*, 267(5), pp.3014–3023.
- Szankasi, P. & Smith, G.R., 1995. A role for exonuclease I from *S. pombe* in mutation avoidance and mismatch correction. *Science (New York, N.Y.)*, 267(5201), pp.1166–9.
- Szostak, J.W. et al., 1983. The double-strand-break repair model for recombination. *Cell*, 33(1), pp.25–35.
- Tang, S. et al., 2015. Pervasive and essential roles of the top3-rmi1 decatenase orchestrate recombination and facilitate chromosome segregation in meiosis. *Molecular Cell*, 57(4), pp.607–621.

- Terentyev, Y. et al., 2010. Evidence that MEK1 positively promotes interhomologue double-strand break repair. *Nucleic acids research*, 38(13), pp.4349–60.
- Tishkoff, D.X. et al., 1997a. Identification and characterization of *Saccharomyces cerevisiae* EXO1, a gene encoding an exonuclease that interacts with MSH2. *Proceedings of the National Academy of Sciences*, 94(14), pp.7487–7492.
- Tishkoff, D.X. et al., 1997b. Identification and characterization of *Saccharomyces cerevisiae* EXO1, a gene encoding an exonuclease that interacts with MSH2. *Proceedings of the National Academy of Sciences of the United States of America*, 94(14), pp.7487–92.
- Tishkoff, D.X. et al., 1998. Identification of a human gene encoding a homologue of *Saccharomyces cerevisiae* EXO1, an exonuclease implicated in mismatch repair and recombination. *Cancer Research*, 58(22), pp.5027–5031.
- Tjio, J.H. & Levan, A., 1956. The Chromosome Number of Man. *Hereditas*, 42, pp.1–6.
- Toledo, L.I. et al., 2013. ATR Prohibits Replication Catastrophe by Preventing Global Exhaustion of RPA. *Cell*, 155(5), pp.1088–1103.
- Tomimatsu, N. et al., 2014. Phosphorylation of EXO1 by CDKs 1 and 2 regulates DNA end resection and repair pathway choice. *Nature communications*, 5, p.3561.
- Toth, A. et al., 2000. Functional Genomics Identifies Monopolin: A Kinetochores Protein Required for Segregation of Homologs during Meiosis I Attila To. *Cell*, 103, pp.1155–1168.
- Tran, P.T. et al., 2004. EXO1-A multi-tasking eukaryotic nuclease. *DNA Repair*, 3(12), pp.1549–1559.
- Traven, A. & Heierhorst, J., 2005. SQ/TQ cluster domains: Concentrated ATM/ATR kinase phosphorylation site regions in DNA-damage-response proteins. *BioEssays*, 27(4), pp.397–407.
- Trelles-Sticken, E., Dresser, M.E. & Scherthan, H., 2000. Meiotic Telomere Protein Ndj1p Is Required for Meiosis-specific Telomere Distribution, Bouquet Formation and Efficient Homologue Pairing. *J.Cell Biol.*2000.Oct.2.;151.(1):95.-106., 151(1), pp.95–106.
- Trujillo, K.M. et al., 1998. Nuclease activities in a complex of human recombination and DNA repair factors Rad50, Mre11, and p95. *Journal of Biological Chemistry*, 273(34), pp.21447–21450.
- Trujillo, K.M. & Sung, P., 2001. DNA Structure-specific Nuclease Activities in the *Saccharomyces cerevisiae* Rad50-Mre11 Complex. *Journal of Biological Chemistry*, 276(38), pp.35458–35464.

- Tsubouchi, H., Argunhan, B. & Tsubouchi, T., 2016. Shaping meiotic chromosomes with SUMO: a feedback loop controls the assembly of the synaptonemal complex in budding yeast. *Microbial Cell*, 3(3), pp.126–128.
- Tsubouchi, H. & Ogawa, H., 2000. Exo1 roles for repair of DNA double-strand breaks and meiotic crossing over in *Saccharomyces cerevisiae*. *Mol Biol Cell*, 11(7), pp.2221–2233.
- Tsubouchi, H. & Roeder, G.S., 2006. Budding yeast Hed1 down-regulates the mitotic recombination machinery when meiotic recombination is impaired. *Genes and Development*, 20(13), pp.1766–1775.
- Tsubouchi, T. & Roeder, G.S., 2005. A Synaptonemal Complex Protein Promotes Homology-Independent Centromere Coupling. *Science*, 308(5723).
- Tsukamoto, Y., 2004. Xrs2p Regulates Mre11p Translocation to the Nucleus and Plays a Role in Telomere Elongation and Meiotic Recombination. *Molecular Biology of the Cell*, 16(2), pp.597–608.
- Tung, K.S., Hong, E.J. & Roeder, G.S., 2000. The pachytene checkpoint prevents accumulation and phosphorylation of the meiosis-specific transcription factor Ndt80. *Proc Natl Acad Sci U S A*, 97(22), pp.12187–12192.
- Usui, T., Ogawa, H. & Petrini, J.H.J., 2001. A DNA damage response pathway controlled by Tel1 and the Mre11 complex. *Molecular Cell*, 7(6), pp.1255–1266.
- Viera, A. et al., 2007. Condensin I reveals new insights on mouse meiotic chromosome structure and dynamics. *PLoS ONE*, 2(8).
- Villarreal, D.D. et al., 2012. Microhomology Directs Diverse DNA Break Repair Pathways and Chromosomal Translocations. *PLoS Genetics*, 8(11), p.e1003026.
- Villeneuve, A.M. & Hillers, K.J., 2001. Whence meiosis? *Cell*, 106(6), pp.647–650.
- De Vries, F.A.T. et al., 2005. Mouse Sycp1 functions in synaptonemal complex assembly, meiotic recombination, and XY body formation. *Genes and Development*, 19(11), pp.1376–1389.
- Wang, B.-D.D. et al., 2005. Condensin binding at distinct and specific chromosomal sites in the *Saccharomyces cerevisiae* genome. *Mol Cell Biol*, 25(16), pp.7216–7225.
- Wassarman, P.M. & Fujiwara, K., 1978. Immunofluorescent anti-tubulin staining of spindles during meiotic maturation of mouse oocytes in vitro. *Journal of cell science*, 29, pp.171–188.
- Watanabe, Y. & Nurse, P., 1999. Cohesin Rec8 is required for reductional chromosome segregation at meiosis. *Nature*, 400(6743), pp.461–4.

- Weiner, B.M. & Kleckner, N., 1994. Chromosome pairing via multiple interstitial interactions before and during meiosis in yeast. *Cell*, 77(7), pp.977–991.
- Wellinger, R.J. & Zakian, V.A., 2012. Everything you ever wanted to know about *Saccharomyces cerevisiae* telomeres: Beginning to end. *Genetics*, 191(4), pp.1073–1105.
- White, J.H., Lusnak, K. & Fogel, S., 1985. Mismatch-specific post-meiotic segregation frequency in yeast suggests a heteroduplex recombination intermediate. *Nature*, 315(6017), pp.350–352.
- Williams, G.J. et al., 2011. ABC ATPase signature helices in Rad50 link nucleotide state to Mre11 interface for DNA repair. *Nature structural & molecular biology*, 18(4), pp.423–431.
- Williams, R.M. et al., 2002. The Ume6 regulon coordinates metabolic and meiotic gene expression in yeast. *Proceedings of the National Academy of Sciences of the United States of America*, 99(21), pp.13431–13436.
- Williamson, D.H. et al., 1983. The timing of the S phase and other nuclear events in yeast meiosis. *Experimental cell research*, 145(1), pp.209–17.
- Wold, M.S. & Kelly, T., 1988. Purification and characterization of replication protein A, a cellular protein required for in vitro replication of simian virus 40 DNA. *Proceedings of the National Academy of Sciences of the United States of America*, 85(8), pp.2523–7.
- Wu, H.-Y., Ho, H. & Burgess, S.M., 2010. Mek1 kinase governs outcomes of meiotic recombination and the checkpoint response. *Current biology: CB*, 20(19), pp.1707–1716.
- Wu, P.Y.J. & Nurse, P., 2014. Replication Origin Selection Regulates the Distribution of Meiotic Recombination. *Molecular Cell*, 53(4), pp.655–662.
- Wu, T.C. & Lichten, M., 1994. Meiosis-induced double-strand break sites determined by yeast chromatin structure. *Science (New York, N.Y.)*, 263(5146), pp.515–8.
- Xu, L. et al., 1995. NDT80, a meiosis-specific gene required for exit from pachytene in *Saccharomyces cerevisiae*. *Molecular and cellular biology*, 15(12), pp.6572–81.
- Y Ip, S.C. et al., 2008. Identification of Holliday junction resolvases from humans and yeast. *Nature*, 456(7220), pp.357–361.
- Yu, H.G. & Koshland, D.E., 2003. Meiotic condensin is required for proper chromosome compaction, SC assembly, and resolution of recombination-dependent chromosome linkages. *Journal of Cell Biology*, 163(5), pp.937–947.
- Zakharyevich, K. et al., 2012. Delineation of Joint Molecule Resolution Pathways in

- Meiosis Identifies a Crossover-Specific Resolvase. *Cell*, 149(2), pp.334–347.
- Zakharyevich, K. et al., 2010. Temporally and biochemically distinct activities of Exo1 during meiosis: double-strand-break resection and resolution of double-Holliday Junctions. *Molecular cell*, 40(6), pp.1001–1015.
- Zanders, S. et al., 2011. Pch2 modulates chromatid partner choice during meiotic double-strand break repair in *Saccharomyces cerevisiae*. *Genetics*, 188(3), pp.511–21.
- Zhang, L. et al., 2011. Meiotic double-strand breaks occur once per pair of (sister) chromatids and, via Mec1/ATR and Tel1/ATM, once per quartet of chromatids. *Proceedings of the National Academy of Sciences of the United States of America*, 108(50), pp.20036–41.
- Zickler, D. & Kleckner, N., 1999. Meiotic chromosomes: integrating structure and function. *Annual review of genetics*, 33(1), pp.603–754.
- Zickler, D. & Kleckner, N., 1998. The leptotene-zygotene transition of meiosis. *Annual Review of Genetics*, 32(1), pp.619–697.